

COMPLEXES WITH ALIPHATIC OXIMES, KETONES AND AMINES

A THERMODYNAMIC STUDY

A thesis presented for the degree of  
Doctor of Philosophy in Chemistry  
in the University of Canterbury,  
Christchurch, New Zealand.

by

G.R. HEDWIG

1972

ACKNOWLEDGEMENTS

I am grateful to Dr H.K.J. Powell for advice and encouragement throughout this work.

I would like to express my thanks to the technical staff of the Chemistry Department, and particularly to Mr R. Hooper, who designed and built the electronic equipment shown in Appendix A.

I acknowledge the award of a University Grants Committee Post-Graduate Scholarship.

G.R. Hedwig  
June 1972

### ABSTRACT

The thesis describes the preparation of the  $\beta$ -amino-ketone ligand 4,4,9,9-tetramethyl-5,8-diazadodecane-2,11-dione (1) and of the derived diamine-dioxime and tetraamine ligands.

Thermodynamic data are reported for complex formation of these ligands, and an analogous tetraamine, with protons and copper(II) ions.

For the protonation reactions, data are interpreted in terms of the structure of the ligands. The thermodynamic data for the formation of the copper complexes indicate that the donor strength of the functional groups is in the order

amine >> oxime >> ketone.

## CONTENTS

	<u>Page</u>
CHAPTER 1    Introduction	
1.1    Preface	1
1.2    Complex Formation in Aqueous Solution	3
1.3    This Work	16
CHAPTER 2    Experimental	
2.1    Preparation of the Ligands	18
2.2    Preparation of Solutions	22
2.3    Glassware	24
2.4    pH Measurements	25
2.5    The Design of an Isothermal Titration Calori- meter	28
2.6    Spectrophotometric Instruments	43
CHAPTER 3    The Calibration of the pH Meter as a Hydrogen Ion Concentration Probe	
3.1    pH(S) of the Standard Solutions	45
3.2    Hydrogen Ion Concentration	46
3.3    Choice of Concentration Quotients	47
3.4    Results and Calculations	49
3.5    Discussion	54
3.6    Summary and General Comments	60



CHAPTER 4	Calculation of Equilibrium Constants from pH Titration Data	
4.1	Calculation of the Protonation Equilibrium Constants	61
4.2	Calculation for the Ligands of the Stability Constants for the Copper Complexes	71
CHAPTER 5	Calculation of Enthalpy Data	
5.1	Calculation of $\Delta H_1$ for the Protonation of hm-3,2,3-tet	74
5.2	Calculation of the $\Delta H_1$ for the Diamine-Dioxime Protonation	78
5.3	Calculation of the Enthalpy Changes for the Formation of the Copper(II)/Diamine-Dioxime Complexes	78
5.4	Calculations in the Experimental Determination of $(\Delta H_1 + \Delta H_2)$ for the Copper/Diamine-Dioxime System	81
5.5	Calculation of the Enthalpy Change for the Formation of the Copper Complexes of 3,2,3-tet	83
5.6	Calculation of the Enthalpy Change for the Copper (hm-3,2,3-tet) Complex	86

CHAPTER 6	Protonation of the Ligands	
6.1	Protonation of the Diamine-Dioxime Ligand	88
6.2	Protonation of the Tetraamines 3,2,3-tet and hm-3,2,3-tet	110
6.3	Protonation of the Diamine-Diketone Ligand	121
CHAPTER 7	Formation of Copper(II) Complexes with the Ligands	
7.1	Formation of Copper Complexes with 3,2,3-tet and hm-3,2,3-tet	126
7.2	Formation of Copper Complexes with the Diamine-Dioxime Ligand	146
7.3	Formation of the Copper Complex with the Diamine-Diketone Ligand	165
7.4	Copper Complexes - A Brief Summary	170
Appendix A		
Appendix B		
Appendix C		
Appendix D		
Appendix E		
Appendix F		
References		

## CHAPTER 1

### INTRODUCTION

#### 1.1 PREFACE

The condensation reaction of  $\text{Ni(en)}_3(\text{ClO}_4)_2$  with acetone yields as one product the nickel complex of the cyclic tetradentate ligand hexamethyl-1,4,8,11-tetraazacyclotetradecadiene (B) which exists in cis and trans (diene) isomeric forms<sup>1</sup>. The trans form (1) is shown in Fig. 1.1. The hydrolysis of a solution of the ligand B (cis) yields a diamine-diketone ligand, 4,4,9,9-tetramethyl-5,8-diazadodecane-2,11-dione (2) (Fig. 1.1) which can be isolated as a dihydroperchlorate salt<sup>2</sup>. The reaction of the ligand B (cis) with aqueous hydroxylamine gives a diamine-dioxime ligand<sup>3</sup> 4,4,9,9-tetramethyl-5,8-diazadodecane-2,11-dione dioxime (3). Sodium-in-alcohol reduction of the ligand (3) gives the methyl substituted linear tetraamine ligand<sup>4</sup>, 2,11-diamino-4,4,9,9-tetramethyl-5,8-diazadodecane (4). (Fig. 1.1).

The ligands (2), (3) and (4) are structurally similar, the only difference being the changes in the two terminal functional groupings. This thesis involves a thermodynamic study ( $\Delta G$ ,  $\Delta H$  and  $\Delta S$ ) of complex formation by these ligands and the related tetraamine 1,2-bis(3'-aminopropylamino) ethane (5) with copper (II) and protons in aqueous solution.

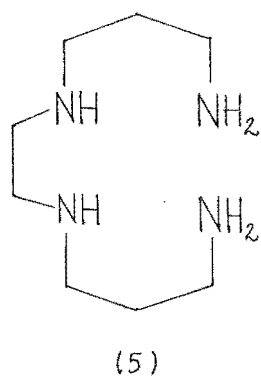
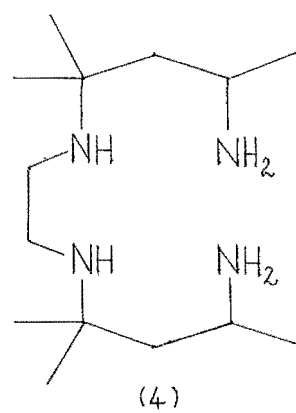
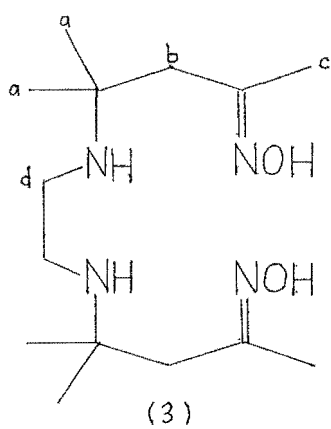
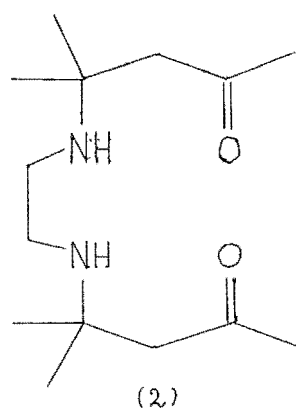
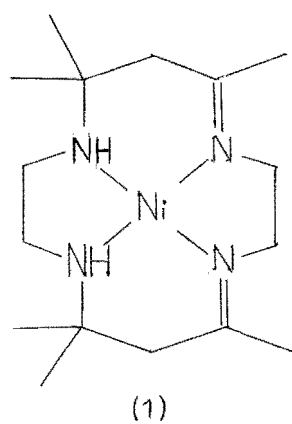


**Fig 1.1**

There are comparatively few thermodynamic data for complex formation of ligands containing oxime groups<sup>5</sup>. The complex formation of vic-dioximes<sup>6,7</sup> and related analytical reagents has been studied but generally in dioxan-water mixtures<sup>6</sup>. Murmann and co-workers have determined the energetics for complex formation by a number of amine substituted aliphatic  $\alpha$ -amine oximes<sup>8</sup> in aqueous solution.

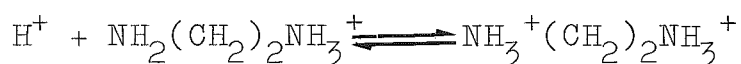
No thermodynamic data appear to be available<sup>5</sup> for complex formation with ligands analogous to (2) in Fig. 1.1. However, there has been considerable work on complex formation with  $\beta$ -diketones<sup>9</sup> (e.g. acetylacetone) and  $\beta$ -iminoketones<sup>10,11,12</sup>.

Since the pioneering work of Bjerrum<sup>13</sup> complex formation by amines has received much attention although most data are for mono and diamine ligands<sup>5</sup>.

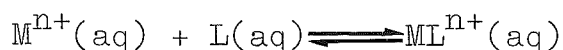
In relation to this work, the stability constants for some complexes with 1,3-bis(3'-aminopropylamino)propane(tripen) have been reported<sup>14</sup> and more recently those for some complexes with N,N'-bis(2-aminoethyl)-1,3-propanediamine (2,3,2-tet) were reported<sup>15</sup>. However, enthalpy data for polyamines is scarce and to date the only available data for linear tetraamines is for the ligand 1,2-bis(2'-aminoethylamino)ethane(trien)<sup>16</sup>.

## 1.2 COMPLEX FORMATION IN AQUEOUS SOLUTION

A complex may be defined as a species formed by the association of two or more simpler species each capable of independent existence in solution<sup>17</sup>. Complex formation can occur between species of like or unlike charges and also between charged and neutral species. The reactions



are examples of complex formation. Each complex has a certain stability which describes the amount of association which occurs in a solution containing species in equilibrium. Quantitatively the stability is determined by an equilibrium constant, e.g. for a reaction



$$K = \frac{\{\text{ML}\}^*}{\{\text{M}\}\{\text{L}\}} = \frac{[\text{ML}]}{[\text{M}] \cdot [\text{L}]} \cdot \frac{\gamma_{\text{ML}}}{\gamma_{\text{M}} \cdot \gamma_{\text{L}}} = K_c \cdot \frac{\gamma_{\text{ML}}}{\gamma_{\text{M}} \cdot \gamma_{\text{L}}} \quad 1.1$$

where { } denotes the activity of the species and  $\gamma_i$  is the activity coefficient which relates the concentration to the activity. For a particular equilibrium, the magnitude of the constant will depend on the units used to express the

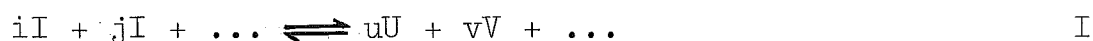
---

\* Charges are omitted from the symbols used.

concentrations of the species involved. Only when the concentrations are expressed on the mole fraction scale will the equilibrium constant be dimensionless (see section 1.2.3).

### 1.2.1 Free Energy Changes

For a reaction



the change in free energy of the system is expressed

$$dG = -SdT + VdP + \sum \mu_X dn_X$$

where  $\mu_X$  is the partial molal free energy or the chemical potential of species X, and S, T, V, P and n have their usual meanings<sup>18</sup>. The chemical potential is a differential expression, thus only the difference in the chemical potential between two states can be determined. It is usual to express the chemical potential  $\mu_X$  for a component in solution with respect to the chemical potential in some hypothetical standard state<sup>19</sup>  $\mu_X^0$ ,

$$\mu_X = \mu_X^0 + RT \ln a_X$$

where  $a_X$  is the activity of component X. (In the standard state  $a_X$  is unity. The standard state is often defined as a hypothetical solution of unit activity which possesses the

properties of an infinitely dilute solution).

For reaction I at constant temperature and pressure

$$\begin{aligned}\Delta G &= u\mu_u + v\mu_v + \dots - i\mu_i - j\mu_j \dots \\ &= \Delta G^\circ + RT \ln \frac{a_u^u a_v^v \dots}{a_i^i a_j^j \dots}\end{aligned}$$

where  $\Delta G^\circ$  is the free energy change when the substances are in their standard states. When reaction I is at equilibrium  $\Delta G = 0$  hence

$$\Delta G^\circ = -RT \ln \left( \frac{a_u^u a_v^v \dots}{a_i^i a_j^j \dots} \right) = -RT \ln K^\circ$$

where  $K^\circ$  is the equilibrium constant for the reaction. Thus the free energy change can be calculated if the equilibrium constant  $K^\circ$  can be determined.

Concentrations of species are more readily attained than are their activities. One approach for the calculation of thermodynamic equilibrium constants is to use the constant ionic strength method.

#### Control of activity coefficients using a constant ionic medium

The concept of ionic strength was introduced by Lewis and Randall<sup>20</sup> who stated, "in dilute solutions, the activity coefficient of a given strong electrolyte is the same in all solutions of the same ionic strength". It follows from equation 1.1 that  $K_c$  is related to  $K$  by a function of the ionic strength, i.e.



$$K = F(I) \cdot K_c.$$

The concentration quotients  $K_c$  are usually calculated from studies in solutions containing relatively large concentrations of an inert electrolyte and are valid only for the medium used. The choice of the background inert electrolyte is important. The ions must not form insoluble species with the reactants under study and if the ions of the background electrolyte are associated with the reactant species then it is necessary that at least the composition of the associated species remains constant throughout a series of experiments<sup>21</sup>.

Sodium chloride was used as the background electrolyte for this work. The main reason for the choice of NaCl was because the concentration quotients for the protonation of ethylenediamine, used for the electrode calibration (see Chapter 3), were determined in NaCl.

#### Determination of thermodynamic equilibrium constants

The thermodynamic equilibrium constant  $K^0$  can be obtained by extrapolating concentration quotients, determined at a number of ionic strengths, to infinite dilution ( $I = 0$ )

$$\text{i.e.} \quad \log K^0 = \lim_{I \rightarrow 0} (\log K_c + f(I))$$

where  $K_c$  is the concentration quotient and  $f(I)$  is a function of the ionic strength. The usual approach<sup>22</sup> is to make use of the extended form of the Debye-Huckel equation,

$$\log \gamma_{\pm} = - \frac{Az_1z_2\sqrt{I}}{1+B\sqrt{I}} + c'.I$$

where A and B are the Debye-Huckel parameters<sup>23</sup> and c is a small parameter. The value of  $K^0$  can be obtained graphically from

$$\log K^0 = \log K_c - \frac{Az^2\sqrt{I}}{1+B\sqrt{I}} - c.I$$

where  $\log K_c - \frac{Az^2\sqrt{I}}{1+B\sqrt{I}}$  is plotted against I, and  $\log K_c = \log K^0$  at  $I = 0$ . Generally the ionic strength function is adjusted so that the plot is linear and of a small slope. While this approach is purely empirical it eliminates the uncertainties due to extrapolations of highly curved functions<sup>24</sup> such as  $\log K_c$  against I or  $I^{\frac{1}{2}}$ . This graphical approach for the determination of  $\log K^0$  is used in this work.

### 1.2.2 Enthalpy Changes in Complex Formation

From the equation 1.2 ,

$$\Delta G^0 = \Delta H^0 - T\Delta S^0 , \quad 1.2$$

$$\Delta S^0 = - \left( \frac{\partial(\Delta G^0)}{\partial T} \right)_P$$

and on substituting back into equation 1.2

$$\left( \frac{\partial(\Delta G^0)}{\partial T} \right)_P = \frac{\Delta G^0 - \Delta H^0}{T} .$$

An alternative expression is

$$\left[ \frac{\partial}{\partial T} \left( \frac{\Delta G^\circ}{T} \right) \right]_P = \frac{-\Delta H^\circ}{T^2}$$

and as  $\Delta G^\circ = -RT \ln K^\circ$

$$\frac{\partial}{\partial T} (\ln K^\circ) = \frac{\Delta H^\circ}{RT^2} \quad 1.3$$

at constant pressure. Therefore the enthalpy change for a particular reaction can be determined from the temperature variation of the equilibrium constant. This approach requires the knowledge of accurate equilibrium constants over a wide temperature range. Without extreme care  $\Delta H^\circ$  and  $\Delta S^\circ$  values determined using the van't Hoff isochore (equation 1.3) are of little use. A far superior method is to measure the enthalpy change by direct calorimetric methods. The advent of thermistors has enabled accurate (errors  $< 0.5\%$ ) determinations of the enthalpy changes by direct calorimetric methods. Many different designs of calorimeters<sup>25-29</sup> have been used to determine the enthalpy changes for a variety of complex formation reactions.

#### Effect of ionic strength on $\Delta H$

The enthalpy changes for many complex formation reactions are determined in the presence of a background electrolyte. The standard enthalpy change  $\Delta H^\circ$  can be determined either by a short extrapolation to  $I = 0$  using enthalpy data at a number of ionic strengths or by applying a small correction to the enthalpy change valid for a

particular ionic strength. From the van't Hoff isochore,

$$\frac{\partial}{\partial T} (\ln K_c + \sum_i \ln \gamma_i) = \frac{\Delta H^0}{RT^2} \quad 1.3$$

where  $K_c$  is the concentration quotient and  $\sum_i \ln \gamma_i$  is the algebraic sum of the activity coefficients of the reactants and products in equilibrium. Rearranging equation 1.3

$$\Delta H^0 = RT^2 \frac{\partial}{\partial T} (\ln K_c) + RT^2 \frac{\partial}{\partial T} (\sum_i \ln \gamma_i)$$

thus

$$\Delta H^0 = \Delta H_c + RT^2 \frac{\partial}{\partial T} (\sum_i \ln \gamma_i) \quad 1.4$$

By differentiating an extended form of the Debye-Huckel equation,<sup>30</sup>

$$\frac{\partial}{\partial T} (\log \gamma_i) = 2 \times 10^{-3} \cdot \log \gamma_i$$

and substituting into equation 1.4

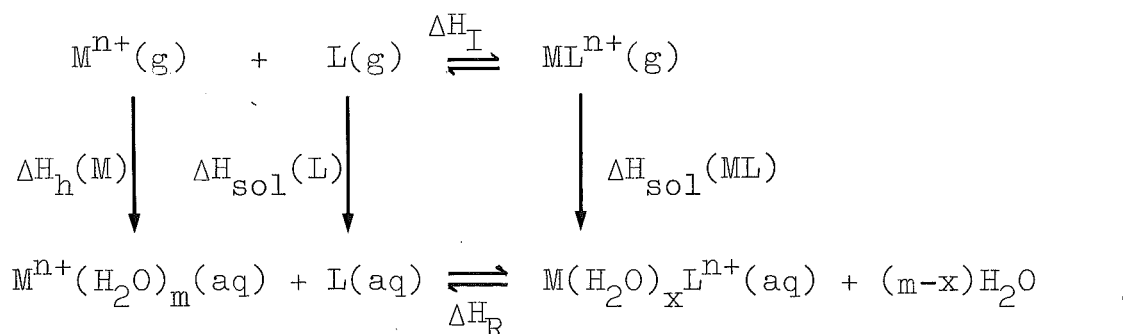
$$\Delta H^0 = \Delta H_c + RT^2 (\sum_i z_i^2) \cdot 2 \times 10^{-3} \cdot \log \gamma_i$$

where  $\Delta H_c$  is the enthalpy change at the particular ionic strength and  $\sum_i z_i^2$  is the algebraic sum of the charge on the ions in the equilibrium and  $\log \gamma_i$  is calculated using a Debye-Huckel expression<sup>31</sup>. For example, for the reaction  $H^+ + A \rightleftharpoons HA^+$   $\sum_i z_i^2 = 0$ , thus  $\Delta H^0 \simeq \Delta H_c$  while for the reaction  $HA^+ + H^+ \rightleftharpoons H_2A^{2+}$ , the correction to convert  $-\Delta H_c$  to  $-\Delta H^0$  is  $-0.83 \text{ kJ mol}^{-1}$ .

### Enthalpy cycle

The enthalpy change for a particular reaction is the property most directly related to the changes in the number and strength of chemical bonds. The enthalpy change for a reaction in aqueous solution is composed of two parts, (i) an internal part  $\Delta H_I$  where contributions to  $\Delta H$  arise from interactions that are independent of the environment and (ii) an environmental part  $\Delta H_E$  which results from inter-molecular interactions between the solvent and the molecules and ions taking part in the reaction. These changes can be related using an enthalpy cycle<sup>32</sup>.

Consider the reaction between a metal ion  $M^{n+}$  and a neutral molecule L to form a complex  $ML^{n+}$ . The enthalpy cycle can be represented



Using Hess's law,

$$\Delta H_I = \Delta H_R + \Delta H_h(M) - \Delta H_{sol}(L) - \Delta H_{sol}(ML)$$

where  $\Delta H_R$  is the enthalpy change for the reaction in aqueous solution (experimental quantity),  $\Delta H_h$  is the enthalpy of hydration of the  $M^{n+}$  ion and  $\Delta H_{sol}(X)$  is the enthalpy of

solution of the species X. The enthalpy of reaction  $\Delta H_R = \Delta H_I + \Delta H_E$  and the environmental enthalpy change is given by

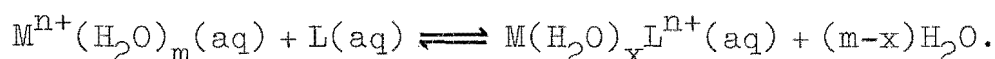
$$\Delta H_E = \Delta H_{sol}(ML) - \Delta H_h(M) - \Delta H_{sol}(L).$$

Thus, to calculate  $\Delta H_I$  (which will incorporate the coordinate bond energy and any crystal field stabilisation energy of the complex ML)  $\Delta H_E$  has to be determined. Metal ion hydration energies can be calculated<sup>33</sup> and for some ligands  $\Delta H_{sol}(L)$  can be determined<sup>34</sup>, but  $\Delta H_{sol}(ML)$  is not readily estimated. However, for a series of complexes with a given L reasonable assumptions about the variation of  $\Delta H_{sol}(ML)$  can be made, and thus changes in  $\Delta H_I$  for the series can be discussed<sup>33</sup>. Because of the uncertainty in the estimation of  $\Delta H_{sol}(ML)$ , reference of aqueous solution thermodynamic data to the gas phase has not generally been attempted.

### 1.2.3 Entropy Changes for Complex Formation

The role of the solvent is of paramount importance in the rationalisation of entropy changes in most complex formation reactions. Ions in aqueous solution order water molecules in their co-sphere due to the polarisation of the water molecules by the charge on the ion.

Consider the reaction



Contributions to the observed entropy change arise from a number of effects.

(i) The liberation of water molecules from the inner coordination sphere of the metal ion M which will cause a positive entropy change.

(ii) Changes in the solvent ordering ability of the 'free' and coordinated metal ion. In the complex the ligand will shield the solvent from the effect of the charge on the metal ion; the solvent is generally less ordered around the complex ion than in the free metal ion<sup>35</sup>. This difference will make a positive contribution to the overall entropy change. The uncoordinated ligand will also possess a hydration sphere, due to dipole-dipole interactions. On coordination there will be a small positive entropy contribution due to the 'release' of this hydration sphere.

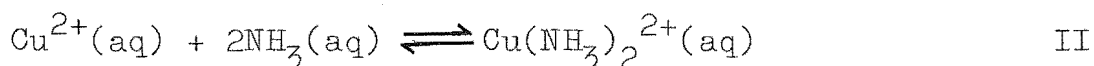
(iii) Contributions arising from the changes in the number of degrees of freedom (rotational, vibrational and translational) of the ligand L on coordination to the metal ion M (a loss of translational entropy and changes in the rotational and vibrational modes). These changes are collectively termed configurational entropy changes and will make a negative contribution to the overall entropy change.

Entropy changes are generally calculated using the Gibbs-Helmholtz equation (1.2) once the free energy and enthalpy changes have been experimentally determined.

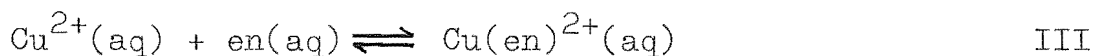
### Cratic Entropy and the Chelate Effect

From the equation  $\Delta G^\circ = -RT \ln K^\circ$ , the magnitude of the free energy change will depend on the units used to calculate the equilibrium constant  $K^\circ$ . As outlined by Gurney<sup>36</sup>, the free energy change for a reaction can be expressed in terms of a unitary part, which is calculated from a dimensionless equilibrium constant, and a cratic part which is associated with the change in the number of solute species. It is important, when comparing free energy changes (and entropy changes as  $\Delta H^\circ$  has no cratic contribution), to consider the changes that arise from both the unitary and cratic terms.

Consider the two reactions



and



The thermodynamic data for these reactions are shown in Table 1.1. The unitary entropy  $\Delta S^1$  ( $\Delta S^1 = \Delta S - \Delta n R \ln 55.5$  where  $\Delta n$  is the number of moles of products minus the moles of reactants) is also shown in Table 1.1.



Table 1.1

<u>Reaction</u>	<u><math>\Delta G</math> kcal mol<sup>-1</sup></u>	<u><math>\Delta H</math> kcal mol<sup>-1</sup></u>	<u><math>\Delta S</math> cal mol<sup>-1</sup>K<sup>-1</sup></u>	<u><math>\Delta S^\dagger</math> cal<sup>-1</sup>mol<sup>-1</sup>K<sup>-1</sup></u>
II	-10.7	-12.0	-4.4	11.6
III	-15.0	-14.6	1.3	9.3

Data from H.A. Bent, J. Phys. Chem., 60, 123 (1956)

---

The chelate effect (the extra stability of a metal ion complex with a bidentate ligand compared with that complex containing an equivalent number of monodentate ligands) is generally attributed as being largely due to the difference in the entropy terms<sup>37</sup>. However, the data in Table 1.1 indicate that when the cratic terms for the reactions II and III are considered the magnitude of the chelate effect is substantially reduced<sup>38</sup>.

#### Statistical Entropy

There can be a contribution to the entropy change from statistical factors. These are best considered by reference to a specific example. Consider the protonation of ethylenediamine. For the first stepwise protonation there are two possible sites of protonation and only one possible site of deprotonation. Thus  $\Delta S_1$  has a statistical contribution of  $+R\ln 2$ . For the second stepwise protonation there is only one possible site of protonation and two possible positions of deprotonation, thus there is a contribution to  $\Delta S_2$  of  $-R\ln 2$ .

#### 1.2.4 Crystal Field Stabilisation Energy (CFSE)

The ligand field theory considers only the effects of the electrostatic field of the ligands upon the partially filled d orbitals of the metal ion<sup>39</sup>. In an octahedral field, the d orbitals of the metal ion are split into an upper  $e_g$  group and a lower  $t_{2g}$  group with an energy difference  $\Delta_o$ . Preservation of the 'centre of gravity' of the set of levels<sup>40</sup> requires that the energy of the  $e_g$  set is raised by  $3/5 \Delta_o$  and the  $t_{2g}$  set is lowered by  $2/5 \Delta_o$ , relative to a spherically symmetrical field. Now the resulting CFSE, which depends on the distribution of electrons between the levels, is given by

$$\text{CFSE}(\text{octa.}) = \Delta_o \left( -\frac{2}{5} n_{t_{2g}} + \frac{3}{5} n_{e_g} \right)$$

where  $n$  is the number of electrons in the  $t_{2g}$  and  $e_g$  levels.

For the enthalpies of hydration of the first row transition metal ions, in the absence of CFSE,  $\Delta H^{\circ}_{\text{hyd}}$  would be expected to vary smoothly with increase in the atomic number and decrease in radius<sup>41</sup>. Experimentally this was not observed<sup>41</sup>. However, when corrections for CFSE were applied the values did fall on the predicted smooth curve.

When the octahedral field is tetragonally distorted further splitting in the energy levels occurs (see section 7.1.3) which results in an overall lowering of the energy of the system as predicted by Jahn and Teller<sup>42</sup> for certain d orbital populations, e.g.  $d^9$ , Cu(II). The CFSE will be greater than predicted by the expression above for an

octahedral field.

### 1.3 THIS WORK

The aim of this thesis was to study the effect of ketone, amine and oxime functional groups in the stability of the complexes with copper (II) ions and protons, in aqueous solution.

The techniques used to calculate the stability constants of the copper complexes and the basicity constants for each ligand required the knowledge of hydrogen ion concentrations. This work incorporated a detailed study on the calibration of a pH meter as a hydrogen ion concentration probe. The method and results of this calibration are discussed in Chapter 3.

The enthalpy changes for the formation of the complexes were determined by direct calorimetric methods. An incremental titration calorimeter of the isothermal jacket type was designed and constructed and is described in Chapter 2.

The equilibrium constants were calculated from the  $p[H^+]$  data by the method of least squares using computer programs\*. These calculations and a comparison of some results using computer and graphical techniques are discussed in Chapter 4. The enthalpy data were also calculated using computer programs. These calculations are discussed in

---

\*The spelling program has been used instead of programme when referred to computers.

Chapter 5. Listings of the computer programs used are shown in Appendix D.

The results and discussion are reported in two sections. The protonation of the ligands is discussed in Chapter 6 and the copper complexes with the ligands are discussed in Chapter 7.

## CHAPTER 2

### EXPERIMENTAL

#### 2.1 PREPARATION OF THE LIGANDS

##### 2.1.1 4,4,9,9-Tetramethyl-5,8-diazadodecane-2,11-dione Dioxime (Fig. 1.1 (3))

5,7,7,12,12,14-Hexamethyl-1,4,8,11-tetraazacyclotetradecane-4,14-diene nickel(II) perchlorate (prepared by the method of Curtis et al.<sup>1</sup>) (25 g) was stirred with KCN (10 g) in dry methanol until dissolved. Ether (250 ml) was added to precipitate  $\text{KClO}_4$  and  $\text{K}_2\text{Ni}(\text{CN})_4$  and the mixture was filtered with suction. A solution of hydroxylamine hydrochloride (17 g) in a mixture of water (50 ml) and methanol (100 ml) was added to the filtrate and the resulting solution was buffered to pH ca. 9 with NaOH (2 M). The solution was set aside in a stoppered flask for four days and then evaporated without heating. The white product was collected by vacuum filtration and recrystallised from benzene by Soxhlet extraction. (Found: C, 58.8; H, 10.4; N, 19.4%. Calculated for  $\text{C}_{14}\text{H}_{30}\text{N}_4\text{O}_2$ : C, 58.7; H, 10.5; N, 19.6%.)

##### 2.1.2 4,4,9,9-Tetramethyl-5,8-diazadodecane-2,11-dione Dioxime Dihydrochloride ( $\alpha.2\text{HCl}$ )

The isomeric oxime mixture (1 g) was warmed with isopropanol (ca. 100 ml) and 0.70 ml of conc. HCl (mole

ratio of ligand: acid of 1:2). Ether was carefully added until a permanent cloudiness appeared. The product separated on standing, and was recrystallised from isopropanol and ether. (Found: C, 46.2; H, 9.0; N, 15.6. Calculated for  $C_{14}H_{32}N_4O_2Cl_2$  C, 46.8; H, 8.9; N, 15.6%).

2.1.3 4,4,9,9-Tetramethyl-5,8-diazadodecane-2,11-dione  
Dioxime Dihydrobromide

The isomeric mixture (1.5 g) was warmed with isopropanol (~ 50 ml) and 1.22 ml of conc. HBr. The solution was filtered and ether was carefully added until a permanent cloudiness appeared. The resulting solution was chilled in an ice-bath. The product was collected after approximately one hour. Yield 1.85 g, 79%. (Found: C, 37.30; H, 7.23; N, 12.28. Calculated for  $C_{14}H_{32}N_4O_2Br_2$  C, 37.50; H, 7.14; N, 12.5%.)

2.1.4 4,4,9,9-Tetramethyl-5,8-diazadodecane-2,11-dione  
Dioxime Dihydroperchlorate ( $\gamma.2HClO_4$ )

The isomeric oxime mixture (0.8 g) was dissolved in 20 ml of ethanol and 8 ml of water. After filtering, 60%  $HClO_4$  (0.60 ml) was added. White needles separated on standing. (Found: C, 35.6; H, 6.8; N, 11.5. Calculated for  $C_{14}H_{32}Cl_2N_4O_{10}$  C, 34.5; H, 6.6; N, 11.5%.)

2.1.5 4,4,9,9-Tetramethyl-5,8-diazadodecane-2,11-dione  
Dihydroperchlorate (Fig. 1.1(2))

5,7,7,12,12,14-Hexamethyl-1,4,8,11-tetracyclotetradecane 4,14 diene-nickel(II) perchlorate (10 g) was stirred with 4 g of KCN in dry methanol (140 ml) until the crystals had dissolved.  $\text{KClO}_4$  and  $\text{K}_2\text{Ni}(\text{CN})_4$  were precipitated with ether (100 ml). The solution was evaporated without heating until the volume was approximately 50 ml. Dilute  $\text{HClO}_4$  (140 ml of 1:6 conc. acid:water) was added to the solution and the product, which formed immediately, was filtered with suction. The product was washed with aqueous methanol and ether. (Found: C, 36.52; H, 6.5; N, 6.5. Calculated for  $\text{C}_{14}\text{H}_{20}\text{Cl}_2\text{O}_{10}\text{N}_2$ : C, 36.8; H, 6.6; N, 6.1%.) Molecular weight as determined by potentiometric titration with standard NaOH was  $458 \pm 2$ . Calculated for  $\text{C}_{14}\text{H}_{20}\text{Cl}_2\text{O}_{10}\text{N}_2$  457.

2.1.6 1,5,8,12-Tetraazadodecane (3,2,3-tet) (Fig. 1.1(5))

1,3-diaminopropane (67 ml, 0.81 mole) was added to a cold constantly stirred solution of 1,2-dibromoethane (13 ml, .15 mole) in ethanol (50 ml). After refluxing (1.5 hr) solid KOH (40 g) was slowly added and the mixture further refluxed for one hour. The unreacted KOH and KBr were precipitated by the addition of ether (50 ml) and removed by filtration. Unreacted reagent was distilled from the filtrate and the product was twice fractionally distilled

under  $N_2$  and at reduced pressure. The fraction was collected at  $124-26^\circ C$  at ca. 0.3 mmHg. The purity as determined from potentiometric titrations with standard NaOH was  $99.1 \pm 0.8\%$ .

A sample of ligand.4HBr was prepared from a portion of the tetraamine. (Found: C, 19.5; H, 5.0; N, 11.0. Calculated for  $C_8H_{26}N_4Br_4$ : C, 19.3; H, 5.2; N, 11.2%.)

#### 2.1.7 2,11-Diamino-4,4,9,9-Tetramethyl-5,8-diazadodecane Dihydroperchlorate (Fig. 1.1(4)) (hm-3,2,3-tet)

The product was prepared by a sodium in amyl alcohol reduction of 4,4,9,9-tetramethyl-5,8-diazadodecane-2,11-dione dioxime and isolated by the addition of  $HClO_4$  to pH ca. 8.5. The sample used in this study was prepared by M. Burgess<sup>4</sup>. This sample was recrystallised from hot water. (Found: C, 36.7; H, 8.0; N, 12.2. Calculated for  $C_{14}H_{36}N_4Cl_2O_8$ : C, 36.6; H, 7.8; N, 12.2%.) Analysis by potentiometric titration gave a molecular weight of  $458 \pm 2$ . The calculated molecular weight for  $C_{14}H_{36}N_4Cl_2O_8$  is 459.

#### 2.1.8 Materials for Electrode Calibration (Chapter 3)

Ethylenediammonium chloride was recrystallised from water/propan-2-ol. (Found: C, 18.17; H, 7.53. Calculated for  $C_2H_{10}N_2Cl_2$ : C, 18.25; H, 7.52%.)

AnalaR grade acetic acid and sodium acetate were used without purification.



## 2.2 PREPARATION OF SOLUTIONS

All solutions were prepared using freshly boiled distilled water. The boiled water, while cooling, was protected from contamination by atmospheric carbon dioxide by bubbling  $N_2$  through the solution. The pH of the 'degassed' ( $CO_2$  free) water was generally in the range 6.6-7.1.

### 2.2.1 Sodium Hydroxide

Sealed containers of Hopkin and Williams 'AnalaR' sodium hydroxide pellets were used in the preparation of stock solutions. The pellets were washed two or three times with portions of 'degassed' distilled water prior to their addition to a well stoppered Pyrex flask containing  $CO_2$  free water. All sodium hydroxide solutions were prepared just prior to their use and were replaced regularly. The solutions were standardised ( $\pm 0.1-2\%$ ) by potentiometric titration against a solution of dried B.D.H. 'AnalaR' potassium hydrogen phthalate.

### 2.2.2 Sodium Chloride

A stock 1 M solution of sodium chloride was prepared by dissolving a known weight of B.D.H. 'AnalaR' sodium chloride in degassed distilled water. The concentration of this solution was periodically checked by gravimetric analysis of the chloride ion as silver chloride<sup>43</sup>.

### 2.2.3 Hydrochloric Acid

Stock hydrochloric acid solutions were prepared from B.D.H. AnalaR concentrated reagent by dilution with degassed distilled water. Solutions were standardised ( $\pm 0.3$ - $0.4\%$ ) by potentiometric titrations against standard solutions of recrystallised 'Fluka' Tris-(hydroxymethyl)-aminomethane (THAM) or against standard sodium hydroxide.

### 2.2.4 Copper Chloride

A stock copper chloride solution was prepared using B.D.H. AnalaR reagent. A sample of this reagent was dissolved in degassed water and filtered into a standard volumetric flask containing a known amount of HCl. The concentration of copper was determined by gravimetric analysis as copper salicylaldoximate<sup>43</sup> or by complexometric titration with standard EDTA using murexide as an indicator<sup>44</sup>.

### 2.2.5 Preparation of the N.B.S. Standard Buffer Solutions

B.D.H. AnalaR chemicals were used in the preparation of the standard buffers. With the exception of the carbonate buffer, all the standard buffers used in this work were prepared by the methods outlined by Bates<sup>45</sup>. The carbonate secondary standard was prepared by the method of Alner et al.<sup>46</sup>.

### 2.3 GLASSWARE

A-grade glassware was used where available. All pipettes were calibrated from the weight of water discharged at a known temperature using published density data<sup>60</sup>. The tolerances for standard flasks used were those given by Vogel<sup>47</sup>.

#### 'Agla' micrometer glass syringe

For pH and calorimetric titrations, the titrant was added using an 'Agla' Micrometer syringe (Burroughs Wellcome and Co.). It consists of a specially made and calibrated all glass syringe attached by a holder to a micrometer screw gauge which operates the plunger. The total delivery from the syringe is 0.5 ml and the readability of the screw gauge is  $\pm 0.0001$  ml.

The calibration was checked by dispensing increments of  $\alpha$ -bromonaphthalene which has a low vapour pressure at room temperature<sup>48</sup>. The delivery was found to be uniform along the syringe. From the weights of the four 0.10 ml increments dispensed the average volume was 0.099976 ml, i.e. a difference from the reading on the micrometer of 0.02%. A second 'Agla' syringe gave a difference of 0.06%.

## 2.4 pH MEASUREMENTS

### 2.4.1 pH Meter and Electrodes

All pH measurements were made using a Beckman 101901 Research pH meter of readability 0.0005 pH units (or .05 mv), coupled with a Beckman E<sub>2</sub> glass electrode of type 39004 and a Beckman calomel reference electrode of type 39071. In an alkaline solution, where the hydrogen ion concentration is low, glass electrodes may respond to any alkali metal ions present, thus imparting an error to the pH measurement<sup>49</sup>. The Beckman E<sub>2</sub> electrode shows minimum deviation due to sodium ions in alkaline solution<sup>50</sup>. The Beckman reference electrode has a carborundum frit junction through which saturated KCl diffuses. The rate of diffusion, which was determined from flame photometric measurements, was found to increase the ionic strength of a test solution by ca. 0.003 M/hour. Attempts were made to reduce this flow by placing a glass sleeve with a capillary outlet around the calomel electrode. A variety of different media were tried in the sleeve: agar-KCl mixtures (containing KCl concentrations of 0.1 m, 1 m or a saturated solution); KCl (satd, 1 m, 0.1 m); or test solution. However in each case either unstable or irreproducible EMF readings resulted.

#### 2.4.2 pH Titration Cell

The pH titration cell as shown in Fig. 2.1 is based on the design described by Perrin<sup>51</sup>. The cell consists of two double walled glass jackets (a and b), through which thermostatted water is passed. The temperature of this water was controlled at  $25.0 \pm 0.10^{\circ}\text{C}$  by a Tecam Tempunit. The two jackets were joined by a PVC plug (c) which was rigidly joined to the upper jacket and which fitted firmly into jacket b. A thin metal plate, which was earthed, was fixed to the underneath face of the PVC plug. The glass and calomel electrodes were mounted in the upper jacket and enclosed by the PVC lid (d).

The titrant was added from an 'Agla' micrometer glass syringe (see 2.3 ) through a fine vinyl tube and a stainless steel tube (25 gauge). The vinyl and stainless steel tubing were permanently fixed to a removable glass tube(e). When the steel tube was placed with the tip under the surface of the test solution there was no noticeable diffusion of the titrant.

Nitrogen could be passed over the surface, or through the test solution by way of the glass tube (f). The gas was bubbled through a 6 M solution of NaOH and then saturated with water vapour at  $25^{\circ}\text{C}$ , before entering the cell.

Stirring of the test solution was effected by a magnetic stirrer with a small teflon covered magnetic

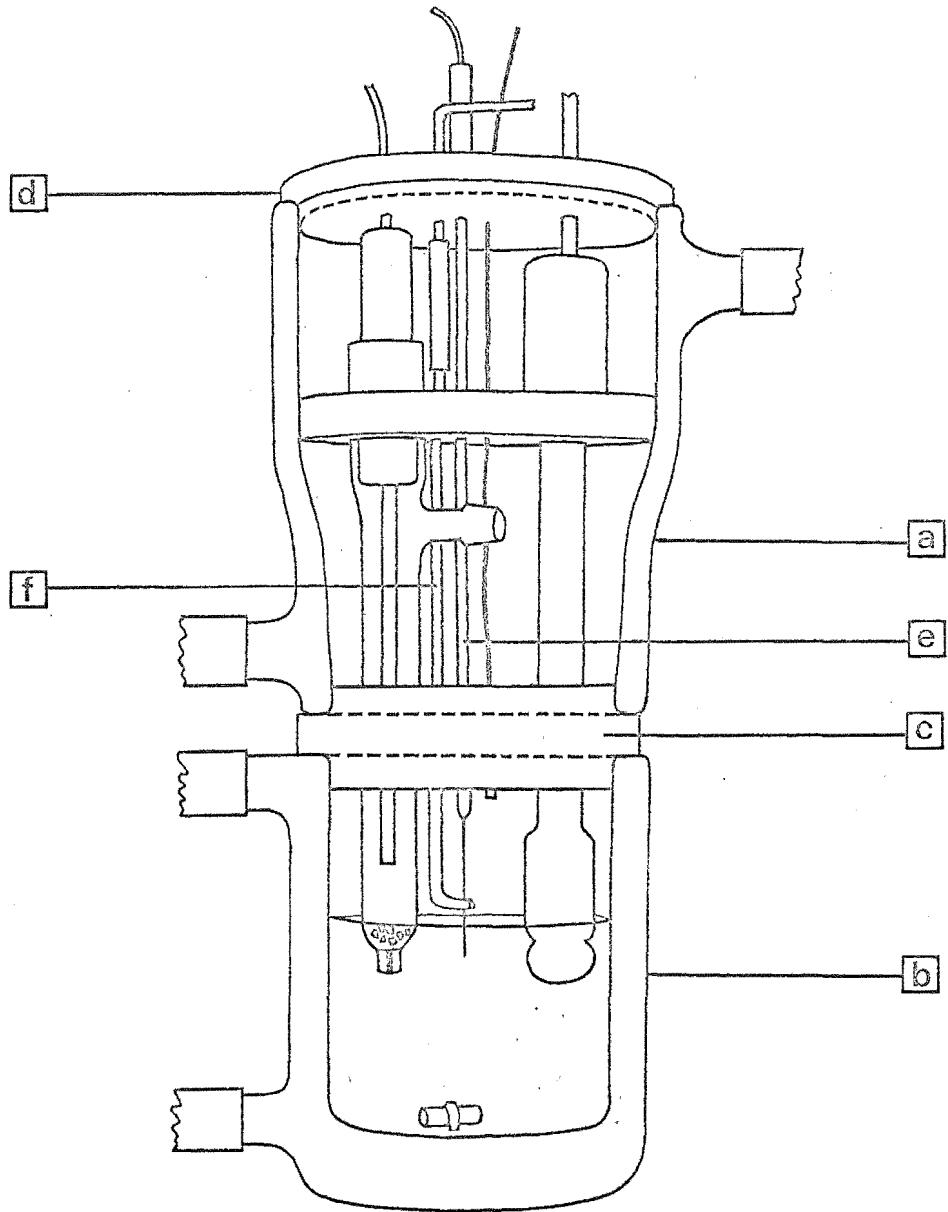


Fig 2.1

follower placed in the test solution. The moving magnetic field had no observable effect on the pH measurements. The difference between the pH of a test solution measured with and without stirring was  $< 0.002$  pH units.

#### 2.4.3 Procedure for pH Measurements

The electrodes and the lower glass jacket were firstly washed with distilled water then dried with absorbent tissue. A portion of the test solution, which had been stored at  $25^{\circ}\text{C}$ , was then added to the cell. The measured pH was found to drift for a short period. The reading became stable after five to eight minutes. For each pH measurement (after the initial measurement) during a pH titration, equilibration was obtained within two minutes.

Before any set of pH measurements the assembly was standardised using the 1:1 phosphate buffer (pH(S) 6.865 at  $25^{\circ}\text{C}$ ). The response of at least one of the other NBS primary standard buffers, potassium hydrogen phthalate or the borax buffer, was then checked. After a set of measurements, drifts in the standardisation were checked by the measurement of the 1:1 phosphate standard; the change in the phosphate reading was usually less than  $.003$  pH units after a set of measurements taking about one hour.

#### 2.4.4 Reproducibility of pH Measurements

For the pH measurement of a standard buffer the reproducibility was always within  $\pm 0.002$ , generally within

$\pm 0.001$ . The reproducibility of data obtained from the buffer regions of titrations was generally  $\pm 0.003$  pH units. The effect of slight errors in the volume of titrant added caused data in the end point regions of a titration curve to be subjected to a higher uncertainty.

#### Calibration of the electrode pair

The calibration of the pH assembly as a hydrogen ion concentration probe is described in Chapter 3.

## 2.5 THE DESIGN OF AN ISOTHERMAL JACKET TITRATION CALORIMETER

### 2.5.1 General Remarks on Calorimeter Design

The ionic strength used in the equilibrium constant studies was predominantly 0.10 M (NaCl). To maintain this constant ionic strength in the calorimeter it was necessary to have a relatively low concentration of the compound studied. Also, one of the compounds studied (oxime) was only sparingly soluble in aqueous solution above pH 9.5. To obtain a reasonable number of calorimetric points per titration it was necessary to measure heat changes of ca. 10J with a reasonable degree of accuracy. The calorimeter was designed with these points in mind.

The calculation of the enthalpy change for a particular reaction requires firstly a knowledge of the extent to which the reaction has occurred and secondly a measure of the heat evolved or absorbed. This heat change causes a change in



temperature of the calorimetric solution, which is measured. When heat is evolved or absorbed heat exchange between the calorimeter and jacket will occur. If the heat exchange due to convection can be neglected<sup>52</sup>, and if the thermal head is not too large, then the heat exchange is given by Newton's Law of Cooling

$$dT/dt = k(T_o - T) + w \text{ deg.min}^{-1} \quad ,$$

where  $k(\text{min}^{-1})$  is Newton's cooling coefficient,  $T_o$  is the jacket temperature,  $T$  is the temperature of the inner vessel and contents (considered at a uniform temperature) and  $w$  is the combined heat effect due to stirring and Joule heating. To keep the heat loss small either  $k$ , or the thermal heat, or both are kept small. The ultimate design of an isothermal jacket calorimeter is one where  $k$  is small and becomes constant within a very short period after the energy input<sup>53</sup>. Tests on the final calorimeter design (see 2.5.2) for a heat input of ca. 30J gave  $k$  as ca.  $6 \times 10^{-3} \text{ min}^{-1}$  and the time of 'equilibration' of approximately seven minutes. The use of a metal calorimeter inner vessel led to a shorter time of 'equilibration' but a higher  $k$  value and thus had no advantage over the glass vessel. The use of a PVC lid for the inner vessel gave an increased time of equilibration, which supports the comment of Tyrrell and Beezer<sup>54</sup> that a calorimeter with an indeterminate boundary will show  $k$  values

which tend only slowly to a constant limiting value.

The effect of heat changes due to evaporation has been discussed by Johanasson<sup>26</sup>. Contributions to the overall heat changes from this effect were made negligible by having a small vapour space over the surface of the calorimetric liquid.

Thermistors have been widely used as sensors for calorimetry<sup>25-29</sup>. Their use has distinct advantages over the previously used resistance thermometers and multi-junction thermocouples; they are small, have a rapid response to temperature changes and a high sensitivity. A thermistor was used as a temperature sensor in this work.

The usual and most convenient heat capacity determinations require the measurement of an electrical energy input and of the resulting temperature change. The fundamental quantities in measuring electrical energy are potential difference, resistance and time; if  $V$  is the potential difference across a resistance  $R$  for a time  $t$  then the energy dissipated in the resistance is  $Q = V^2 t / R$ .

The standard design of heater circuit<sup>55</sup> was adopted for this calorimeter. Several designs of heaters were tried. A heater coil immersed in silicon oil inside a thin walled glass tube led to heat losses along the tube to the calorimeter lid. This effect was also observed by Johansson<sup>26</sup> using a similar type of heater. A heater coil inside a small metal

thimble at the end of a glass tube did not prove as satisfactory as the final design (see 2.5.2).

## 2.5.2 Description of the Calorimetric System

### The calorimeter

An outline of the calorimeter is shown in Fig. 2.2. The calorimeter consisted of an outer brass can (1) and lid (2) and an inner thin walled glass vessel (3) with a light brass lid (4). The glass vessel was silvered on the outer wall and covered with a layer of very thin reflecting tin foil. A threaded brass ring was sealed with epoxy resin glue (Araldite AW106 and HU 953U) to the rim of the glass. The underneath face of the inner brass lid (4) was coated with a layer of polyurethane enamel. Care was taken to ensure that the threaded brass ring was also well insulated from the test solution in the calorimeter. The maximum capacity of the inner glass vessel was approximately 110 ml. The two lids (2) and (4) were permanently joined by a short nylon shaft through which the hollow glass stirrer shaft (5) passed. The outer lid (2) was permanently fastened to a tufnal disc (6) by way of three connecting tubes; a central brass tube through which the stirrer shaft passed and two other tubes (7) and (8) which carried the leads to the heater (9) and thermistor (10), and the tubes to the cooler (11). The calorimeter solution was stirred by means of a glass propeller stirrer (5) which was connected to a

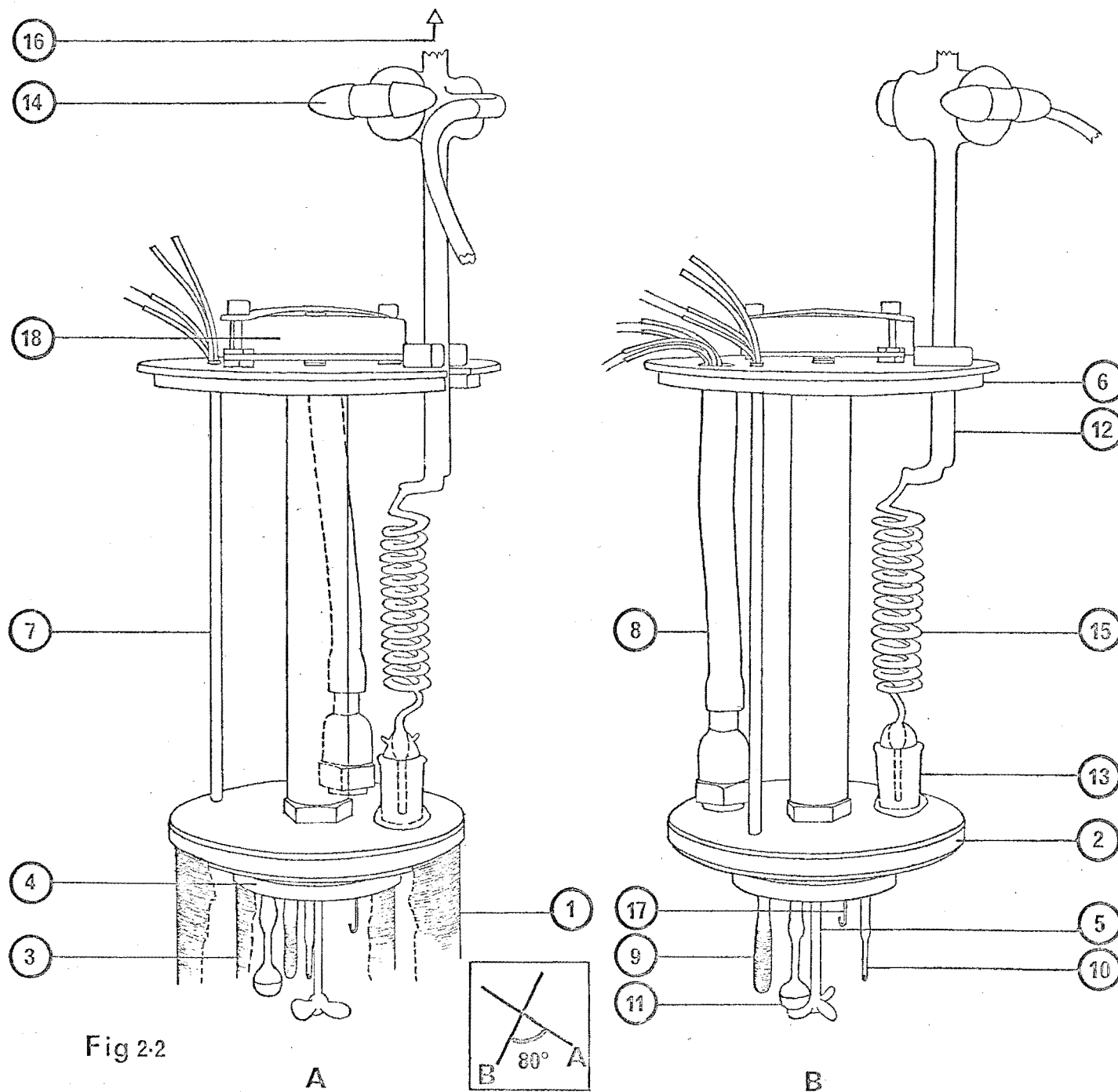


Fig 2-2

synchronous motor (18) (Phillips type AU 5100/22, 250 rev/min) mounted on the wooden disc (6). The adequacy of the stirring was checked by observing the flow patterns when a few crystals of  $\text{KMnO}_4$  were added to water in the inner glass vessel.

The cooler (11) consisted of a thin walled glass tube connected to the inner lid (4) by a small PVC plug, and with a small bulb at the lower end. The bulb contained about 0.2 ml of water. Two vinyl tubes were sealed to the cooler tube, one of which passed down the centre of the tube to a depth just above the surface of the water. Cooling was effected by passing air (at room temperature) over the surface of the water by connecting the other tube to a water pump.

The heater (9) consisted of a thin walled glass tube which was also connected to the inner lid by a small PVC plug. Cotton-covered manganin wire was wound around the outside of the lower half of this tube. The manganin wire was insulated from the solution by a thin coating of Araldite. The ends of the manganin wire were soldered to four copper wire leads which connected the heater to the heating circuit and to the potentiometer (see Fig. 2.4). The resistance of the heater was  $37.45 \pm 0.01\Omega$  at  $25^\circ\text{C}$  (see section on Electrical Calibration below).

Fig. 2.3 shows the probes of the calorimeter in more detail.

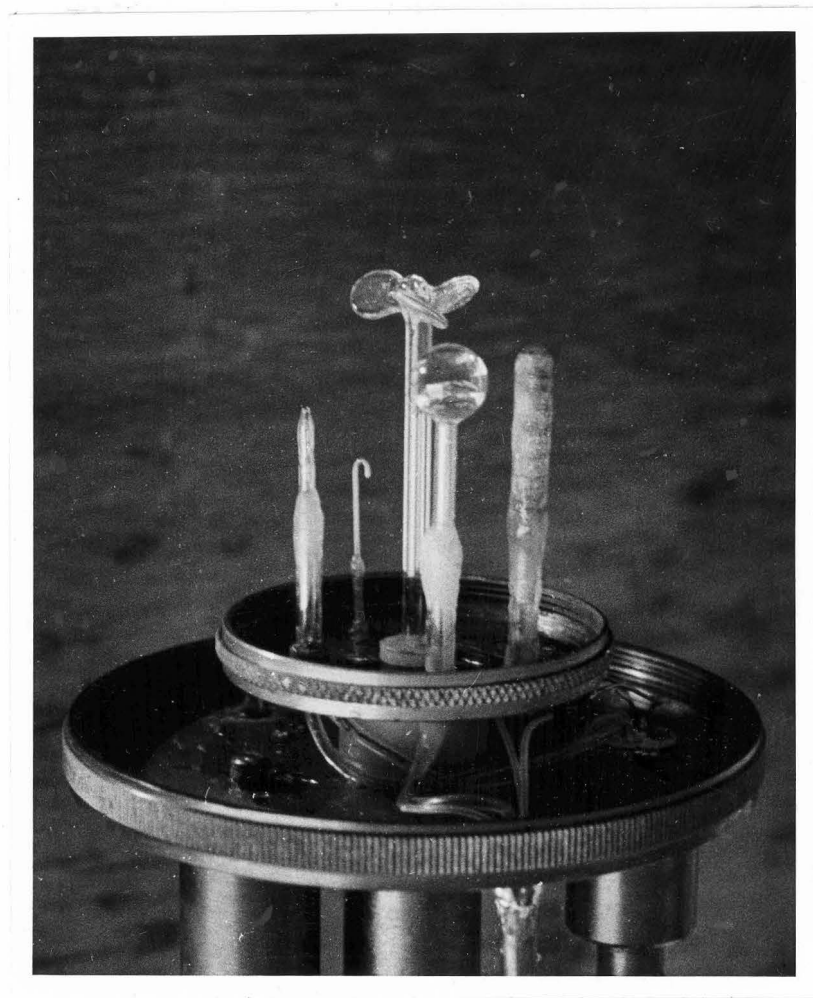


Fig 2.3

The titrant addition assembly consisted of a glass tube (12) which was held in position by a spring clip mounted on the disc (6) and by a quickfit B12 joint (13) mounted on the lid of the calorimeter (2). The glass tube was joined to a thin walled glass spiral (15) of total volume ca. 0.9 ml, which enabled efficient thermostating of the titrant solution. The three-way tap (14) enabled the 'Agla' micrometer glass syringe (16) (see 2.3) to be refilled from a titrant reservoir. A short section of flexible vinyl tubing joined the end of the glass titrant line to a fine (ca. 25 gauge) J shaped glass tube (17). The titrant line could be readily dismantled for cleaning.

#### Temperature Measurement

The temperature of the solution inside the calorimeter was measured using a single NTC thermistor (Phillips type 2322 627 11103) which had a resistance of  $8950\Omega$  at  $25^{\circ}\text{C}$ . With this type of thermistor, the semiconducting head is sealed into a small glass tube by the manufacturer. This thermistor tube was joined to a short length of glass tubing which was fixed to the lid (4) by a small PVC plug. Two thread-like constantan wires connected the thermistor to the AC bridge.

A linear relationship was found between thermistor resistance and temperature over a  $0.4^{\circ}\text{C}$  temperature range ( $24.9$ - $25.3^{\circ}\text{C}$ ). The temperature coefficient of resistance was  $368 \pm 5 \Omega/^{\circ}\text{C}$ .

The thermistor was incorporated into an AC transformer bridge (see Appendix A), the output of which was rectified and fed to a Honeywell Electronik 194 Lab/Test Recorder, the chart of which constituted a temperature scale. The AC bridge was operated at a R.M.S. voltage of ca. 0.1-0.2 V.

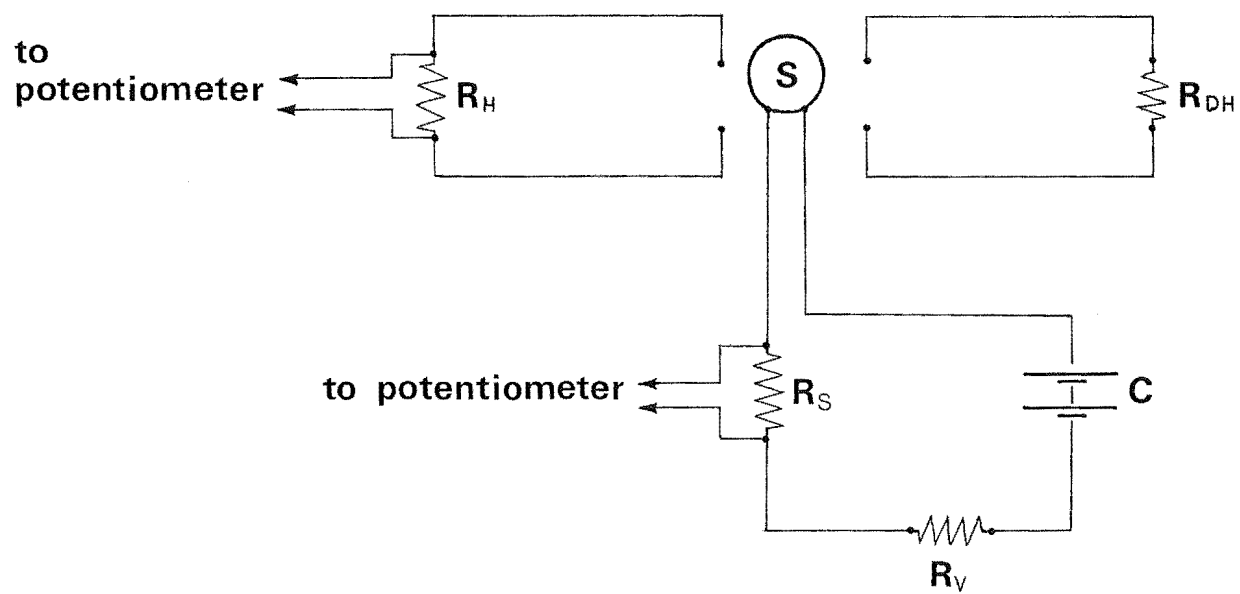
#### Electrical Calibration System

The heater circuit for the calibration of the heat capacity of the calorimeter and its contents is shown in Fig. 2.4. The current passing through the heater was determined by measuring the potential difference across a precision resistor ( $R_S$ ) in series with the heater. The resistance of the heater ( $R_H$ ) was calculated from the potential difference across the heater and from the potential difference across the precision resistor ( $R_S$ ). The switch (S) enabled the cells (C) to be discharged through a dummy heater ( $R_{DH}$ ).

The current through the heater could be varied by altering the total resistance in the circuit by the insertion of precision resistors ( $R_V$ ).

All voltage measurements were made using a Cambridge Slide Wire Potentiometer, type 44244/3 (readability of 0.001mV), Muirhead standard cell and a sensitive galvanometer (H. Tinsley & Co. type SR4/45). The voltages recorded using this potentiometric set up were checked for systematic errors by measuring a particular voltage using the





$$R_S = 10.0 \, \Omega \, (\pm 0.1\%)$$

Fig. 2-4 Calorimetric heater circuit

potentiometer and also using a Marconi Differential D.C. Voltmeter type TF2606. The agreement between the two measurements was well within the experimental error.

The precision resistors used in the heater circuit were H.W. Sullivan non-reactive resistances, tolerance  $\pm 0.1\%$  and ERG precision wire-wound resistors, tolerance  $\pm 0.05\%$ .

The heating time was determined as the time between the switching on and switching off of a microswitch operated by a synchronous motor driven cam. During this time the current was switched from the dummy heater to the calorimeter heater. The heating time was determined as  $63.70 \pm 0.03$  seconds by using a Levell Universal counter-timer type TM51B. The time was determined as the mean of a number of measurements made at different times during a normal working day. The error is expressed as the standard deviation of a measurement from the mean.

#### Thermostat Bath

The calorimeter was immersed in a water bath containing approximately 55 l of water. The temperature of the water was controlled to better than  $\pm 0.001^{\circ}\text{C}$  by the controller described in Appendix A. The temperature of the bath was measured using a mercury in glass thermometer which was graduated in hundredths of a degree Centigrade. The thermometer was calibrated using a Pt resistance thermometer and a Rosemount Eng. Co. Ltd Precision Comparison Bridge Model VLF 51A.

### 2.5.3 Procedure for Operation of the Calorimeter

The titrant line was filled with the titrant solution at room temperature, the J tip being filled to such a position which allowed for the volume expansion of the solution in the glass spiral (ca. 0.90 ml) when the calorimeter was immersed in the thermostat bath; 0.0005 ml for a change from room temperature (ca. 23°C) to bath temperature.

The calorimetric test solution, which had been stored at 25°C in a thermostat bath, was added to the inner glass vessel at room temperature using a pipette calibrated at 25°C. The assembled calorimeter was placed into the water bath and the stirrer started. Additional heating (or occasionally cooling) was then applied, using the calorimetric heater (or cooler), to bring the temperature of the calorimetric solution to approximately that of the thermostat bath. This temperature was previously measured by placing the thermistor in the thermostat bath. The assembly was then left to come to thermal equilibrium (ca. one to two hours).

The recorder trace of a typical calorimetric run is shown in Fig. 2.5. The AC bridge was in balance when the recorder pen was at the position marked (1). The chart paper advanced at 1 division (ca. 2 mm) in 19 sec. (stop-watch). Before a run the temperature of the calorimeter and contents was adjusted so that the solution was heating at



ca. 0.03  $\Omega$ /min. (see Fig. 2.5). At the start of a run the resistance of the decade box was adjusted so that the bridge was in balance and the capacitance balance was checked. The resistance was then adjusted so that the bridge was out of balance and the trace was started (2). The recorder chart was calibrated in lateral divisions/ohm by noting the effect of a large (ca. 0.60 $\Omega$ ) resistance change (3) in one arm of the bridge (decade box). The usual working sensitivity was ca. 12 chart divisions for a 0.1 $\Omega$  change in thermistor resistance. This sensitivity corresponds to ca.  $2 \times 10^{-5}$   $^{\circ}\text{C}$ /chart division. The fore period trace was followed for about 5 minutes, which was sufficient time to give a well defined straight line. Heat was then applied using the calorimeter heater (or in the case of a reaction titrant was added) and this effected a deflection on the chart (4). At the end of the heating (or reaction) period the bridge was adjusted to a position near balance and the resistance was recorded. The trace, which corresponds to a cooling curve, was then followed for about twenty minutes.

#### 2.5.4 Procedure for a Complete Calorimetric Titration

A typical calorimetric titration consisted of a number of runs as described. After the end of each individual run the calorimetric inner vessel and contents were cooled to a temperature close to that at the start of the previous run. After about ten minutes the next run was commenced.

Heat capacity calibrations were normally performed at the beginning, the middle and the end of a calorimetric titration. The heat capacity of any point in the titration was interpolated off a linear plot of  $Q_H/\Delta R$  (the calibration constant) against the total volume in the calorimeter.

#### 2.5.5 Calculation of the Resistance Change from Calorimetric Runs

The cooling curve trace in Fig. 2.5 shows a region (5) where trace is quite curved and a second region (6) where the plot is reasonably linear. Experimental determinations of the Newton's Law of Cooling coefficient showed that there is a considerable variation in this quantity over the region (5). However, in region (6), Newton's law of cooling is being obeyed to about 2%. The time of 'equilibrium' after a heat input of ca. 9J was thus about 6-7 minutes. This compares favourably with values for other calorimeters of this type<sup>56</sup>. The method used to obtain corrected resistance changes was to take linear extrapolations along the region (6) and the trace (2) to a time equal to half the time of the reaction period. The resistance readings at these points were subtracted to find the corrected resistance change. Exactly the same approach was used for the heat calibrations. Thus, as the two experiments were matched closely in terms of the magnitude of the heat input, the results can be directly compared to obtain the heat change for the reaction.

#### 2.5.6 Addition of the Titrant

The volume of titrant was added manually, at a constant rate, so that the time of addition was close to the time of heating in the heat capacity determinations, i.e. approximately one minute. After the increment was added the three way tap (see 2.5.2) was turned off. As all the titrant line was not the same temperature, the volume expansion of the portion of the titrant that was added into the thermostat bath caused a small additional amount to diffuse from the J tip into the calorimeter. Taking the average room temperature to be  $23^{\circ}\text{C}$  and an average increment to be 0.30 ml then the expansion of the titrant solution will cause 0.00015 ml to be ejected from the J tip. This is of the order of the error in dispensing the volume (see section 2.3).

#### 2.5.7 Effect of Adding the Titrant Without Stringent Temperature Control

Calorimeters of this type of design usually come to an equilibrium, i.e. when the heat losses are balanced by Joule heating and the heat of stirring, at a temperature slightly above that of the thermostat bath. For this calorimeter, where the rate of stirring is not too great, the equilibrium position was  $0.010\text{--}0.015^{\circ}\text{C}$  above the bath temperature. If the titrant temperature is assumed to be as great as  $0.01^{\circ}\text{C}$  lower than that of the calorimeter solution then the resultant temperature change on the addition of

0.30 ml of titrant into 100 ml in the calorimeter can be calculated.

Let  $T$  be the final temperature of the calorimetric solution and consider both the titrant and calorimeter solution to be water then,

$$0.30(T - 25.000) = 100.0(25.010 - T)$$

solving for  $T$  gives  $T = 25.00997^{\circ}\text{C}$ , i.e. a temperature change of  $3 \times 10^{-5}^{\circ}\text{C}$ , i.e. approximately one chart division. Before an actual calorimetric run, the temperature of the contents was adjusted so that the initial trace was heating (see Fig. 2.5); at the start of a run the actual temperature difference between the titrant and the calorimetric solution was considerably less than  $0.01^{\circ}\text{C}$ . Therefore no corrections were applied to the  $\Delta R$  measurement, due to temperature differences between the titrant and calorimetric solution at the start of a run.

#### 2.5.8 Precision of the Calorimetric Measurements

The precision of the assembly was determined by many electrical calibrations. Some of the results obtained are shown in Table 2.1. The mean of the five values for the calorimetric solution of volume 99.34 ml is 1.198 and the standard deviation is 0.002. The precision of the instrument, as judged by the standard deviation, is therefore  $\pm 0.2\%$ .



TABLE 2.1

Calibration constants for the calorimeter at  $25.0 \pm 0.01^\circ\text{C}$

<u>Total Volume</u> (ml)	$\underline{Q}^b$ (J)	$\underline{\Delta R}^c$ (ohm)	$\underline{Q/\Delta R}^a$ (J ohm <sup>-1</sup> )
98.84	7.482 <sub>6</sub>	6.291	1.189
98.84	7.391 <sub>5</sub>	6.212	1.190
98.84	7.041 <sub>2</sub>	5.930	1.187
99.34	8.074 <sub>8</sub>	6.748	1.197
99.34	8.077 <sub>7</sub>	6.745	1.198
99.34	8.078 <sub>7</sub>	6.761	1.195
99.34	9.214 <sub>3</sub>	7.683	1.199
99.34	9.215 <sub>4</sub>	7.683	1.199

<sup>a</sup> The calibration constant for a given volume.

<sup>b</sup> Heat input (in Joules).

<sup>c</sup> Measured change in thermistor resistance.

### 2.5.9 Accuracy of the Calorimeter

The accuracy of the calorimeter was checked by comparing the enthalpy data for two standard reactions with the literature data for these reactions.

#### Heat of neutralisation of HCl and NaOH

98.84 ml of 0.034 NaOH was added to the calorimeter and the titrant line was filled with 0.5002 M HCl. Experimental results are given in Table 2.2, the enthalpy values in the last column refer to a state of infinite dilution. The heats of dilution of HCl, NaOH and NaCl were obtained from reference 57. The average value of the heat of ionisation of water  $\Delta H^\infty$  was  $-56.28 \pm 0.07 \text{ kJ mol}^{-1}$ , the error being expressed by the standard deviation. The precision, as judged by the standard deviation, was adequate, however the agreement of this value of  $\Delta H^\infty$  was not in particularly good agreement with the current literature values. A survey of data on the heat of neutralisation of strong acid and strong base at infinite dilution<sup>27</sup> shows that an average value would be ca.  $-55.8 \text{ kJ mol}^{-1}$ . A more recent determination by Grenthe, Ots and Ginstруп<sup>56</sup> gave a value of  $-55.84 \text{ kJ mol}^{-1}$ . The difference between the value determined in this study and the value of Grenthe is 0.8% which is just outside the total estimated experimental error (0.6%) in this work.

TABLE 2.2

Heat of neutralisation of NaOH by HCl at 25°C

$\frac{\text{Volume}^a}{(\text{ml})}$	$\frac{\text{Increment}}{\text{number}}$	$\frac{\text{Conc. HCl}}{\text{added (x } 10^3)} \frac{(\text{mol l}^{-1})}{(\text{mol l}^{-1})}$	$\frac{Q_H}{\Delta R_H}^b$	$\frac{\Delta R}{(\Omega)}$	$\frac{Q_{\text{react}}}{(\text{J})}$	$\frac{Q_{\text{corr}}^c}{(\text{J})}$	$\frac{-\Delta H_w^\infty}{(\text{kJ mol}^{-1})}$
0.280	1	1.408 <sub>9</sub>	1.192	6.746	8.041	7.376	56.23
0.280	2	1.405	1.196	6.727	8.045	7.880	56.26
0.280	3	1.401	1.200	6.694	8.033	7.868	56.17
0.280	4	1.397 <sub>9</sub>	1.204	6.690	8.055	7.890	56.33
0.280	5	1.393	1.207	6.675	8.057	7.892	56.34
0.280	6	1.389	1.212	6.649	8.055	7.890	56.33

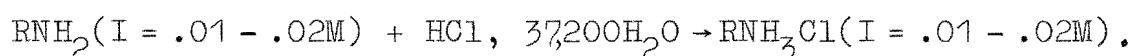
<sup>a</sup> Volume of 0.5002M HCl added.

<sup>b</sup> Calibration constant.

<sup>c</sup> Corrected for  $\Delta H^{\text{dil}}$  HCl and corrected to infinite dilution.<sup>57</sup>

### Enthalpy of protonation of TRIS with HCl

More recently, the reaction of tris(hydroxymethyl) aminomethane (TRIS) with hydrochloric acid has been used as a calorimetric standard reaction<sup>56,58</sup>. Data for this reaction are shown in Table 2.3. The mean and standard deviation of the eight determinations of the enthalpy of protonation was  $-47.83 \pm 0.05 \text{ kJ mole}^{-1}$ . This is the enthalpy change for the process



The heat change was corrected for the heat of dilution of HCl using the published data<sup>57</sup>. No corrections were made for the heat of neutralisation of the hydroxide ion in the alkaline TRIS buffer solution. This correction would be very small as the solution of TRIS was ca. 50% neutralised, at the start of the calorimetric titration, with HCl. Grenthe, Ots and Ginstrup<sup>56</sup> determined the enthalpy value for the neutralisation of TRIS as  $-47.44 \text{ kJ mol}^{-1}$  and Ojelund and Wadsö<sup>59</sup> recently obtained a value of  $-47.48 \pm 0.03 \text{ kJ mol}^{-1}$ . The difference between the value determined in this work and these literature values is 0.7%, which is again just greater than the estimated experimental percentage error of 0.6%.

TABLE 2.3

Enthalpy of protonation of TRIS at 25°C

<u>Volume</u> <sup>a</sup> (ml)	<u>Mmoles</u>	<u>QH/ΔR</u>	<u>ΔR</u> (Ω)	<u>Q<sub>react</sub></u> (J)	<u>Q<sub>corr</sub></u> <sup>b</sup> (J)	<u>-ΔH</u> (kJ mol <sup>-1</sup> )
0.330	0.16507	1.192	6.782	8.084	7.904	47.88
0.330	0.16507	1.198	6.730	8.062	7.882	47.75
0.330	0.16507	1.201	6.722	8.073	7.893	47.82
0.300	0.15006	1.208	6.077	7.341	7.177	47.83
0.300	0.15006	1.211	6.062	7.341	7.177	47.83
0.300	0.15006	1.216	6.043	7.348	7.184	47.87
0.300	0.15006	1.200	6.127	7.352	7.188	47.90
0.300	0.15006	1.195	6.136	7.332	7.168	47.77

<sup>a</sup> Volume of 0.5002M HCl added.

<sup>b</sup> Corrected for the heat of dilution of HCl. Values in Joules.

## 2.6 SPECTROPHOTOMETRIC INSTRUMENTS

All infrared spectra were recorded as nujol mulls using a Shimadzu IR 27G or a Perkin Elmer 337 spectrophotometer.

Electronic Absorption spectra were recorded with a Shimadzu MPS-50L spectrophotometer.

N.M.R. spectra were measured, with TMS as an internal (or external) reference, using a Varian A-60 spectrophotometer.

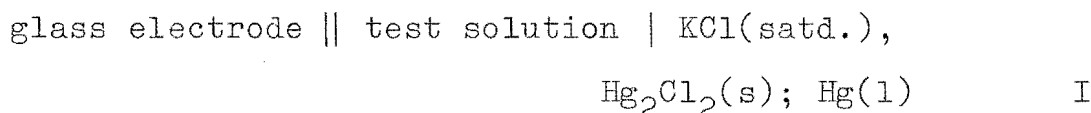
### Microanalyses

Carbon, Hydrogen and Nitrogen analyses were determined in the Microanalytical Laboratory, University of Otago.

### CHAPTER 3

#### THE CALIBRATION OF THE pH METER AS A HYDROGEN ION CONCENTRATION PROBE

The advances in instrumentation over the last few decades has enabled precise pH measurements to be made using commercial meters and electrodes. However, it is well known<sup>61</sup> that pH is essentially an empirical parameter and its interpretation in terms of hydrogen ion concentrations ( $[H^+]$ ) or activities ( $a_{H^+}$ ) involves assumptions associated with liquid junction potentials and single ion activity coefficients. The cell used in this work was



with an emf given by

$$E = E^{\circ} + E_{\text{as}} + E_{\text{LJ}} - \frac{RT}{F} \ln a_{H^+} \quad 3.1$$

where  $E_{\text{as}}$  is the asymmetry potential of the glass electrode,  $E_{\text{LJ}}$  is the liquid junction potential and  $E^{\circ}$  is the standard emf for the cell, which will equal the standard emf for the reference electrode in saturated KCl.

Most pH measurements using a cell of type I are made by incorporating the Operational Definition of  $\text{pH}^{62}$ , whereby the pH of an unknown solution X is related to the pH of some

standard solution S. From equation 3.1, when the unknown solution X is the test solution the cell emf is given by

$$E_X' = E^O + E_{as} + E_{LJ}' + \frac{2.303RT}{F} \cdot pH' \quad 3.2$$

and for the standard solution S

$$E_S = E^O + E_{as} + E_{LJ}^S + \frac{2.303RT}{F} pH(S) \quad 3.3$$

From equations 3.2 and 3.3

$$pH' = pH(S) - \frac{(E_{LJ}' - E_{LJ}^S) + (E_S - E_X')}{2.303RT/F} \quad 3.4$$

### 3.1 pH(S) OF THE STANDARD SOLUTIONS

The assignment of pH(S) values to a set of standard solutions was made on the basis of measurements in a cell without liquid junction using Pt, H<sub>2</sub> and Ag, AgCl electrodes<sup>63</sup>. The procedure used was to determine the quantity  $p(a_H \gamma_{Cl})$  for the standard buffer solution containing small concentrations of added chloride ion and then to evaluate the quantity  $p(a_H \gamma_{Cl})^O$ , the limit approached by  $p(a_H \gamma_{Cl})$  as the concentration of chloride ion approached zero,  $pa_H$  was then computed from  $p(a_H \gamma_{Cl})^O$  by using an extrathermodynamic assumption concerning the value of the hypothetical single ion activity coefficient for the chloride ion. The convention used to evaluate  $\log \gamma_{Cl}$  is known as the Bates-Guggenheim convention<sup>64</sup>. The standard buffer solutions were chosen for their reproducibility,



stability, buffer capacity and ease of preparation<sup>65</sup>. These standard buffer solutions set up a conventional activity scale which will closely approach but not equal a true thermodynamic activity scale.

From equation 3.4 the measured pH of the unknown solution, pH', will only approach the conventional activity scale if the term  $(E'_{LJ} - E^S_{LJ})$ , the residual liquid junction potential, is small. This residual liquid junction potential will be small if the standard and test solutions match each other closely in ionic strength, solution composition and pH. This will seldom be the case. For example, the majority of equilibrium constant measurements which involve determination of solution pH have been made on solutions with  $I = 1.0$  or  $0.10$  with respect to some background electrolyte<sup>5</sup>. The ionic strength of the buffers most commonly used for cell calibration, potassium hydrogen phthalate and sodium tetraborate have  $I = 0.053$  and  $0.02$  M respectively.

### 3.2 HYDROGEN ION CONCENTRATION

For equilibrium constant measurements the pH of the solution is often determined to give a measure of the hydrogen ion concentration  $[H^+]$ . An additional expression relating the hypothetical single ion activity coefficient for the hydrogen ion,  $\gamma_{H^+}$  is needed to convert the measured pH from the operational activity scale to a hydrogen ion

concentration,

$$\text{pH}' = \text{p}[\text{H}^+] - \log \gamma_{\text{H}^+} .$$

It is generally assumed that some simple equation (e.g. an extended Debye-Huckel equation or the Davies<sup>66</sup> equation) accurately defines  $\gamma_{\text{H}^+}$  for (probably) a mixed electrolyte solution and allows precise conversion of  $\text{pH}'$  to  $\text{p}[\text{H}^+]$ .

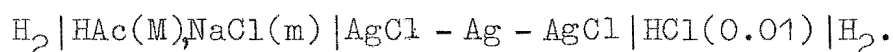
These assumptions concerning residual liquid junction potentials and single ion activity coefficients can be avoided by calibration of the cell against solutions of known  $[\text{H}^+]$  with the same ionic strength and ionic background as the test solutions.

The calibration of the cell I against solutions of known hydrogen ion concentration in the pH range 2 to 10.6 was made using dilute hydrochloric acid solutions, ethylenediamine/ethylenediammonium chloride and acetic acid/sodium acetate buffers all in NaCl medium. The hydrogen ion concentrations for the buffer solutions can be readily calculated from the solution composition and the concentration quotients for the buffer.

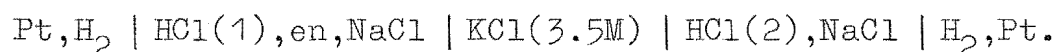
### 3.3 CHOICE OF CONCENTRATION QUOTIENTS

This calibration method requires the knowledge of accurate concentration quotients for the buffer systems. For acetic acid and ethylenediamine accurate quotients are

known at various ionic strengths and temperatures. The concentration quotients used for acetic acid were determined by Harned and Hickey<sup>67</sup> using an unbuffered cell without liquid junction,



The quotients for ethylenediamine were determined using a cell with liquid junction however, the experimental technique used was such that the effect of the unknown residual liquid junction potential was eliminated, so that reliable quotients were obtained<sup>68</sup>. The cell used was



II

The ionic strengths in the two half cells were kept equal, making the hypothetical single ion activity coefficient  $\gamma_{\text{H}^+}$  for each half cell solution approximately equal and giving similar liquid junction potentials at each liquid junction. For the cell II

$$E = \frac{RT}{F} \cdot \ln \frac{a_{\text{H}^+}(2)}{a_{\text{H}^+}(1)} + E_j \quad 3.5$$

where  $E_j$  is the contribution from the liquid junctions.

" The approximate concentration of hydrogen ion in the buffer was calculated from equation 3.5, assuming  $E_j = 0$  and  $\gamma_{\text{H}^+}(1) = \gamma_{\text{H}^+}(2)$ . This value was then used to calculate the

concentration quotient. Values of the concentration quotient were calculated from emf measurements at different fixed ratios of  $[H^+]_1/[H^+]_2$  and the data were extrapolated to zero concentration of buffer. Errors introduced by small differences in the activity coefficients and in the two liquid junction potentials were thus eliminated. Everett and Pinsent<sup>68</sup> determined constants at 0° to 60°, at 10° intervals, and ionic strengths from 0.07 to 0.30 M. The values for this study, interpolated for 25°C and  $I = 0.04$ , 0.10, 0.15 and 0.20M, are shown in Table 3.1. The  $k_A$  values for acetic acid are also shown in Table 3.1.

### 3.4 RESULTS AND CALCULATIONS

#### Internal Consistency of the N.B.S. Standard Buffers

The linearity and slope of the conventional activity scale set up by the N.B.S. buffers was checked by measuring the response of the primary and secondary standard buffers with respect to the 1:1 phosphate buffer. The NBS primary standards are internally consistent for cells with and without junction<sup>70</sup> when a Pt,  $H_2$  electrode is used. However, small deviations of 0.005 - 0.02 pH were found when a representative selection of glass electrodes were compared with the  $H_2$  electrode in certain buffer solutions<sup>71</sup>.

Using cell I the carbonate, borax, tetroxalate buffers and the  $HCl/KCl$  solution gave pH' values in agreement with the pH(S) tabulated by Bates<sup>72</sup> to within  $\pm 0.003$ pH. However,

TABLE 3.1

Interpolated  $k_i$  values for 1,2-diaminoethane and  
interpolated  $k_A$  values for acetic acid, each at  
25°C and  $I = 0.20, 0.15, 0.10, 0.04$  M, NaCl media.

<u>I</u>	1,2-Diaminoethane <sup>a</sup>		Acetic Acid <sup>b</sup>
	<u>Log <math>k_1</math></u>	<u>Log <math>k_2</math></u>	<u><math>k_A \times 10^5</math> (moles.litre<sup>-1</sup>)</u>
0.20	9.996 ± 0.003	7.189 ± 0.003	3.090 ± 0.005
0.15	9.970 ± 0.003	7.152 ± 0.003	2.975 ± 0.005
0.10	9.960 ± 0.003	7.105 ± 0.003	2.809 ± 0.005
0.04	9.941 ± 0.005	7.027 ± 0.005	2.489 ± 0.005

<sup>a</sup> From reference 68

<sup>b</sup> From reference 69

for the 0.05 M potassium hydrogen phthalate and the saturated potassium hydrogen tartrate there were small discrepancies (phthalate,  $\text{pH}'$  4.026,  $\text{pH}(\text{S})$  4.008; tartrate,  $\text{pH}'$  3.570,  $\text{pH}(\text{S})$  3.557).

#### HCl/NaOH Titrations

The pH titration technique was described in section 2.4. Data from the titrations of NaOH against hydrochloric acid/sodium chloride solutions at  $I = 0.20 \text{ M}$ ,  $0.10 \text{ M}$  and  $0.04 \text{ M}$  are given in Table 3.2. Values of  $\text{p}[\text{H}^+]$  were calculated from the analytical concentrations of acid and alkali, assuming complete dissociation. Near the end point in the titration, readings became progressively less stable and data at  $\text{pH}' > 4$  were not considered. A plot of  $\text{pH}'$  against  $\text{p}[\text{H}^+]$  was linear in the range  $\text{pH}' = 2$  to  $3$ . However, as the  $\text{pH}'$  values increased further the plot became curved; the data tended to larger  $\frac{\text{pH}'}{\text{p}[\text{H}^+]}$  values at the  $\text{pH}'$  approached  $3.5$  as observed by McBryde<sup>73</sup>.

#### Acetic Acid/NaOH Titrations

Data from the titrations of standard sodium hydroxide against acetic acid/sodium chloride solutions at total ionic strengths of  $I = 0.20$ ,  $0.10$  and  $0.04 \text{ M}$  are shown in Table 3.3. Only data from the most buffered region of the titration curve ( $\text{pK}_A \pm 0.7$ ) were considered. The hydrogen ion concentration  $[\text{H}^+]$  at each titration point was calculated from

TABLE 3.2

pH' and p[H<sup>+</sup>] values from HCl/NaOH titrations in  
NaCl media at I = 0.20, 0.10 and 0.04 M

<u>I = 0.20 M</u>			<u>I = 0.10 M</u>			<u>I = 0.04 M</u>		
pH' <sup>a</sup>	p[H <sup>+</sup> ]	Δ <sup>b</sup>	pH'	p[H <sup>+</sup> ]	Δ	pH'	p[H <sup>+</sup> ]	Δ
2.083	2.016	.067	2.133	2.061	0.072	2.084	2.016	.068
2.150	2.081	.069	2.187	2.115	0.072	2.151	2.081	.070
2.256	2.185	.071	2.250	2.177	0.073	2.254	2.185	.069
2.321	2.248	.073	2.320	2.247	0.073	2.317	2.248	.069
2.395	2.322	.073				2.393	2.322	.071
2.485	2.410	.075				2.480	2.410	.070
2.597	2.521	.076				2.589	2.521	.068
2.750	2.671	.079				2.741	2.671	.070
						2.970	2.899	.071

<sup>a</sup> pH' = pH (measured)

<sup>b</sup> Δ = pH' - p[H<sup>+</sup>].

TABLE 3.3

pH', p[H<sup>+</sup>] and pH'' data from acetic acid<sup>a</sup>-NaOH titrations  
in NaCl media at I = 0.20, 0.10 and 0.04 M

<u>I = 0.20 M</u>			<u>I = 0.10 M</u>			<u>I = 0.04 M</u>		
pH', <sup>b</sup>	pH'' <sup>c</sup>	p[H <sup>+</sup> ]	pH'	pH''	p[H <sup>+</sup> ]	pH'	pH''	p[H <sup>+</sup> ]
3.877	3.855	3.789	3.913	3.887	3.826	3.814	3.792	3.722
4.000	3.979	3.915	4.039	4.020	3.954	3.963	3.942	3.876
4.110	4.090	4.026	4.149	4.129	4.066	4.090	4.070	4.005
4.209	4.189	4.126	4.249	4.229	4.166	4.201	4.181	4.119
4.301	4.283	4.219	4.428	4.413	4.346	4.301	4.282	4.220
4.388	4.371	4.306	4.594	4.577	4.512	4.480	4.462	4.402
4.472	4.454	4.389	4.758	4.743	4.656	4.564	4.548	4.487
4.636	4.619	4.553	4.841	4.826	4.761	4.646	4.629	4.569
4.719	4.702	4.635	4.929	4.915	4.850	4.810	4.794	4.733
4.894	4.880	4.808	5.025	5.010	4.945	4.986	4.970	4.909

<sup>a</sup> Initial concentration of acetic acid I = 0.20 and 0.10,  
9.285 x 10<sup>-3</sup> M; I = 0.04, 9.236 x 10<sup>-3</sup> M.

<sup>b</sup> pH' = pH (measured.)

<sup>c</sup> pH'' = pH' + correction for non-linear response to NBS buffers.



$$\begin{aligned}
 K_A &= \frac{[\text{CH}_3\text{COO}^-][\text{H}^+]}{[\text{CH}_3\text{COOH}]} \\
 &= \frac{(C_S + [\text{H}^+] - K_W/[\text{H}^+]) \cdot [\text{H}^+]}{(C_a - C_S - [\text{H}^+] + K_W/[\text{H}^+])}
 \end{aligned}
 \tag{3.6}$$

where  $C_a$  is the initial concentration of acetic acid,  $C_S$  is the concentration of sodium acetate (added NaOH) and  $K_W$  is the ionic product for water in NaCl solution at a given ionic strength<sup>74</sup>. The term  $K_W/[\text{H}^+]$ , a correction for the hydrolysis of acetate ion, was approximated to  $K_W/\text{antilog}(-\text{pH}')$  and the resultant quadratic equation in  $[\text{H}^+]$  from equation 3.6 was solved to give  $\text{p}[\text{H}^+]$  at each point in the titration curve buffer region.

#### Ethylenediammonium Chloride/NaOH Data

Data from the titrations of NaOH against solutions of ethylenediammonium chloride/sodium chloride solutions at  $I = 0.20, 0.15, 0.10$  and  $0.04$  M are given in Table 3.4.

Experimental data were used from the most buffered regions, extending from pH 6.7 to 8.0 and from 9.0 to 10.6. The mass balance equations for  $T_B$  and  $T_H$  are

$$T_B = [B] + [BH^+] + [BH_2^{2+}] \tag{3.7}$$

$$T_H + [\text{OH}^-]' = [\text{H}^+] + [BH^+] + 2[BH_2^{2+}] \tag{3.8}$$

where  $[\text{OH}^-]'$  is the concentration of hydroxide ion formed by hydrolysis of the ethylenediamine (B). Using the protonation

TABLE 3.4

pH' and p[H<sup>+</sup>] values from 1,2-diaminoethane dihydrochloride -  
NaOH titrations in NaCl media<sup>a</sup> at  
I = 0.20, 0.15, 0.10 and 0.04 M

<u>I = 0.20</u>				<u>I = 0.15</u>			
Vol. <sup>b</sup>	pH'	p[H <sup>+</sup> ]	Δ <sup>c</sup>	Vol.	pH'	p[H <sup>+</sup> ]	Δ
.050	7.016	6.956	.060	.040	6.836	6.774	.062
.060	7.147	7.089	.058	.060	7.108	7.052	.056
.070	7.276	7.217	.059	.080	7.366	7.309	.057
.080	7.406	7.346	.060	.090	7.501	7.445	.056
.090	7.541	7.481	.060	.100	7.651	7.595	.056
.100	7.692	7.632	.060	.120	8.055	8.000	.055
.160	9.368	9.327	.041	.160	9.351	8.304	.047
.170	9.535	9.500	.035	.170	9.524	9.478	.046
.180	9.675	9.642	.033	.180	9.667	9.621	.046
.190	9.800	9.767	.033	.190	9.790	9.746	.044
.200	9.912	9.880	.032	.200	9.903	9.861	.042
.210	10.017	9.986	.031	.210	10.008	9.969	.039
.220	10.118	10.087	.031	.230	10.209	10.172	.037
.230	10.215	10.185	.030				

Table 3.4 (contd.)

<u>I = 0.10</u>				<u>I = 0.04</u>			
Vol.	pH'	p[H <sup>+</sup> ]	$\Delta$	Vol.	pH'	p[H <sup>+</sup> ]	$\Delta$
.030	6.634	6.571	.063	.030	6.547	6.483	.064
.040	6.798	6.740	.058	.040	6.710	6.651	.059
.050	6.942	6.886	.056	.050	6.852	6.796	.056
.060	7.075	7.021	.054	.060	6.983	6.929	.054
.070	7.204	7.151	.053	.080	7.237	7.187	.050
.080	7.337	7.284	.053	.100	7.525	7.475	.050
.090	7.475	7.424	.051	.120	7.938	7.890	.048
.100	7.633	7.582	.051	.140	8.748	8.704	.044
.150	9.176	9.142	.034	.160	9.326	9.285	.041
.160	9.394	9.355	.039	.180	9.645	9.605	.040
.170	9.561	9.521	.040	.190	9.772	9.733	.039
.180	9.701	9.660	.041	.200	9.887	9.850	.037
.190	9.825	9.785	.040	.220	10.102	10.068	.034
.200	9.938	9.899	.039	.240	10.310	10.278	.032
.210	10.047	10.008	.039				
.220	10.151	10.113	.038				
.230	10.253	10.216	.037				
.240	10.354	10.317	.037				

- <sup>a</sup> Initial volume of 1,2-diaminoethane dihydrochloride/NaCl solution 49.90 ml. Initial concentration of 1,2-diaminoethane dihydrochloride  $2.977 \times 10^{-3} \text{M}$  (I = 0.20, 0.15M),  $2.961 \times 10^{-3} \text{M}$  (I = 0.10M) and  $2.972 \times 10^{-3} \text{M}$  (I = 0.04M).
- <sup>b</sup> Volume (ml) of NaOH titre, concentration 1.098M (I = 0.20, 0.15 and 0.04M) and 1.114M (I = 0.10M).
- <sup>c</sup>  $\Delta = \text{pH}' - \text{p}[\text{H}^+]$ .

constant quotients

$$k_1 = \frac{[BH^+]}{[B] \cdot [H^+]} \quad \text{and} \quad k_2 = \frac{[BH_2^{2+}]}{[BH^+] \cdot [H^+]}$$

and equations 3.7 and 3.8, a cubic equation 3.9 was derived

$$\begin{aligned} k_1 k_2 [H^+]^3 + (k_1 k_2 (2T_B - T_H - [OH^-]') + k_1) [H^+]^2 \\ + (k_1 (T_B - T_H - [OH^-]' + 1) [H^+] \\ - (T_H + [OH^-]')) = 0 \end{aligned} \quad 3.9$$

This equation was solved by the Newton-Rapson method<sup>75</sup> using the experimental value, antilog (-pH'), as an approximate solution for  $[H^+]$ . An alternative treatment was to form a quadratic equation 3.10

$$C(1 + k_1 [H^+] + k_1 k_2 [H^+]^2) = T_B(k_1 [H^+] + 2k_1 k_2 [H^+]^2) \quad 3.10$$

where  $C = T_H + [OH^-]' - [H^+]$ . For the term C,  $[H^+]$  was initially estimated from the experimental pH' value. The quadratic equation was solved for  $[H^+]$  and an iterative procedure used to obtain improved values of  $[H^+]$ . Both calculation procedures gave identical results.

#### Graphical Plots of pH' Against p[H<sup>+</sup>]

For the separate systems HCl/NaOH, acetic acid/NaOH and ethylenediammonium chloride/NaOH the plots of pH' against p[H<sup>+</sup>] were colinear for each ionic strength, within the experimental error. Also a plot of pH' against p[H<sup>+</sup>] gave a

straight line for the hydrochloric acid data and the two sets of ethylenediamine/hydrochloric acid data.

The acetic acid data did not lie on this line. However, the deviation was consistent with that for the NBS standard buffers in this same pH region, and correction of data for the non-linear response to the NBS standards gave data ( $\text{pH}''$ , Table 3.3) which lay on the straight line.

A linear least squares analysis of the pH data using an equation of the form  $\text{pH}' = M\text{p}[\text{H}^+] + C$  gave the following results.

For 70 data points from the hydrochloric and ethylenediamine sets

$$M = 0.9953 \pm 0.0002, C = 0.086 \pm 0.002$$

and  $\sigma$ , the standard deviation of  $\text{pH}'$  values from the computed curve, was 0.005 pH.

For 100 data points containing the  $\text{pH}''$  acetic acid data

$$M = 0.9951 \pm 0.0003, C = 0.088 \pm 0.002, \quad \sigma = 0.005$$

For 100 data points containing the  $\text{pH}'$  acetic acid data

$$M = 0.9932 \pm 0.0003, C = 0.106 \pm 0.002, \quad \sigma = 0.011.$$

Thus, for each ionic strength the experimental data for HCl and buffer solutions are colinear with approximately unit slope,  $\text{pH}' = 0.9953 \text{p}[\text{H}^+] + 0.086$ ,  $\sigma(\text{pH}') = 0.005$ .

### 3.5 DISCUSSION

From equation 3.4 any deviation of a pH measurement, pH', from the conventional activity scale set up by the standard buffers results from the term

$$- \frac{(E'_{LJ} - E^S_{LJ})}{2.303RT/F} .$$

If it is assumed that the conventional activity scale is equivalent to a true thermodynamic activity scale then

$$pH' = p[H^+] - \log \gamma_{H^+} - \frac{(E'_{LJ} - E^S_{LJ})}{2.303RT/F} .$$

If  $\log \gamma_{H^+}$  and  $(E'_{LJ} - E^S_{LJ})$  are functions of the ionic strength, under the conditions used in the titrations, then plots of pH' against  $p[H^+]$  at different ionic strengths should be parallel and with a separation

$$\Delta \left[ - \frac{(E'_{LJ} - E^S_{LJ})}{2.303RT/F} - \log \gamma_{H^+} \right]$$

where  $\Delta$  refers to the change in the quantity in brackets, from one ionic strength to another. The results above show that the plots are parallel and coincident within experimental error. This result implies that the rate of change of the residual liquid junction potential with ionic strength is approximately compensated by the rate of change of  $\log \gamma_{H^+}$  with ionic strength.

The observed slope and intercept for  $\text{pH}' = (\text{slope})\text{p}[\text{H}^+] + \text{intercept}$  agree well with the data published by McBryde<sup>73</sup> for dilute HCl solutions (slope 0.990, 0.994, 0.995 and intercept 0.088, 0.105, 0.097 at  $I = 0.05, 0.10$  and  $0.20$  M respectively, NaCl medium). The non-unit slope implies that the operational activity coefficient, defined by  $-\log \gamma_{\text{H}^+}' = \text{pH}' - \text{p}[\text{H}^+]$ , must vary with the solution pH, i.e.

$$-\log \gamma_{\text{H}^+}' = \frac{(E_{\text{LJ}}' - E_{\text{LJ}}^{\text{S}})}{2.303RT/F}$$

varies with the solution pH. This implies that  $\gamma_{\text{H}^+}'$  or  $\Delta E_{\text{LJ}}$ , the residual liquid junction potential or both of these quantities are a function of the solution pH.

For the pH range 2-3, the activity coefficients of HCl in an HCl/NaCl solution at a constant total ionic strength of  $0.10$  M varies little with HCl concentration<sup>76</sup>. However, it is predicted that the liquid junction potential for the junction solution/KCl(sat.) will vary with solution pH<sup>77</sup>. (It is also expected to be a function of ionic strength and the nature of the ions<sup>78</sup>.) For solutions of high acidity or alkalinity, the ions  $\text{H}_3\text{O}^+$  and  $\text{OH}^-$ , which have high mobilities compared with most other ions<sup>79</sup>, will make significant contributions to the liquid junction potential.

Bates et al.<sup>80</sup> compared the  $\text{p}a_{\text{H}}$  value for a number of buffer solutions and solutions of strong and weak acids and

bases with the pH obtained from a cell with liquid junction. Their results showed that the liquid junction potentials were indeed larger at either ends of the pH scale but there appeared to be no uniformity of sign or magnitude of these potentials.

#### Use of the Calibration Curve

For each ionic strength the standard solutions used for calibration contains a low concentration of the buffer (0.003 to 0.009 M) compared with the background electrolyte (.04 to 0.20 M). If the test solution is of a similar composition then it can be assumed that at the same ionic strength and pH the standard and test solution will generate the same liquid junction potential in the cell.

If the same NBS buffer is used to standardise the assembly both for the calibration titrations and for the test solution measurement then the residual liquid junction potentials for the two solutions will be identical. Also, for the test solution and the calibration solution  $\gamma_{H^+}(\text{standard}) = \gamma_{H^+}(\text{test})$  for a given ionic strength thus, standard and test solutions with the same pH' have the same value of  $p[H^+]$ .

Any set of pH' data from titrations were generally converted to  $p[H^+]$  values within the various computer programs (see Appendix D) using the equation

$$pH' = 0.9953 p[H^+] + 0.086.$$



pH' data in the pH range 3 - 5.5 were converted to  $p[H^+]$  values using a plotted calibration curve (a plot of pH' against  $p[H^+]$ ).

#### Previous Work on Electrode Calibration

Strong acid - strong base titrations have often been used for electrode calibration<sup>81,73,82</sup> although their use is restricted to narrow pH ranges. Recently McBryde<sup>83</sup> has extended the calibration of the pH meter assembly into the alkaline region. His results show that the values of  $\Gamma_H$  (a quantity relating  $H = 10^{-pH}$  to the true hydrogen ion concentration  $[H^+]$ ) measured in acidic solution agree well with that value calculated from measurements in alkaline solution.

Acetic acid/sodium acetate buffer solutions have previously been used to calibrate cells containing glass and calomel electrodes<sup>84,85</sup> although no experimental details have been given. Perrin and Childs<sup>86</sup> treated a quantity  $F$  ( $pH' = p[H^+] + \log F$ ) as an adjustable parameter in applying a least-squares program to the results of pH titrations for the determination of acidity constants.

The uncertainty associated with liquid junction potentials can be eliminated by using a Ag, AgCl reference electrode<sup>73</sup>, however, the use of such a cell is more restrictive than a cell of type I (e.g. a ligand bromide salt could not readily be studied).

Earlier Powell and Curtis<sup>87</sup> used the ethylenediamine/HCl system for the calibration of a pH assembly. Their plots of pH' against  $p[H^+]$  were parallel and colinear for the various ionic strengths studied (used  $NaClO_4/Ba(ClO_4)_2$  media).

#### Use of Single Ion Activity Coefficients

A more commonly used approach for the conversion of the measured pH to a concentration value is to assume that the measured pH corresponds to an activity  $pa_H$  and then use an estimation of the hypothetical single ion activity coefficient  $\gamma_{H^+}$  to convert  $pa_H$  to  $p[H^+]$ . For a mixed electrolyte system, the  $\gamma_{H^+}$  value will be dependent on all the specific ionic interactions in solution as related in the Guggenheim equation<sup>88</sup>. This equation is seldom used for mixed electrolytes as the values of the interaction coefficients in the mixture are usually not known. Commonly the empirical Davies equation is used.

$$-\log \gamma_{H^+} = Az_+^2 \left( \frac{\sqrt{I}}{1+\sqrt{I}} - \beta I \right)$$

where  $\beta = 0.30$ . Using this equation, the mean activity coefficients of a large number of 1:1 and 1:2 electrolytes agree to within 2% of the experimental values<sup>89</sup>. Use of this equation for a cell with liquid junction incorrectly implies an equality

$$-\log \gamma_{H^+}(\text{Davies}) = -\log \gamma_{H^+} - \frac{E'_{LJ} - E^S_{LJ}}{2.303RT/F} = pH' - p[H^+]$$

and can give erroneous estimates of  $p[H^+]$  in solution. This point is illustrated in Table 3.5 where  $(pH' - p[H^+])$ , the operational activity coefficient, is compared with  $-\log \gamma_{H^+}$  (Davies) for solutions of different pH and ionic strength. Kielland<sup>90</sup> has estimated values of ion size parameters of a large number of inorganic and organic ions from data on mobilities, ionic radii and hydration numbers. Using his suggested value of  $9 \text{ \AA}$  for  $H^+$  ion and using the Debye-Huckel expression

$$-\log \gamma_i = \frac{A z_i^2 \sqrt{I}}{1 + \rho \sqrt{I}} \quad \rho = Ba^0,$$

where A and B are functions of medium and temperature<sup>23</sup> and  $a^0$  is the ion size parameter, the values for  $-\log \gamma_{H^+}$  at 0.20, 0.10 and 0.04 M ionic strength are  $-\log \gamma_{H^+} = 0.081$ , 0.065 and 0.052 respectively. These results are in somewhat better agreement with the operational activity coefficients in Table 3.5.

These empirical calculations serve to illustrate that assumptions involving single ion activity coefficients of the hydrogen ion for use in converting measured pH values to hydrogen ion concentrations can be avoided by calibrating the pH assembly directly using solutions, preferably buffer solutions, of known hydrogen ion concentrations.

The difference between the effect of the Davies equation and the  $pH'/p[H^+]$  calibration curve in applying corrections

TABLE 3.5

Comparison of the operational activity coefficient

$\gamma_{H^+}^{\dagger}$  and empirical (Davies equation) activity

coefficient for the cell glass electrode //

solution / KCl(satd),  $Hg_2Cl_2$ ; Hg.  
(NaCl medium)

pH <sup>†</sup>	I	$-\log \gamma_{H^+}^{\dagger}$	$-\log \gamma_{H^+}^{\dagger}(\text{Davies})$
9.800	0.20	.033	0.124
7.276	0.20	.059	0.124
4.090	0.20	.064	0.124
9.938	0.10	.039	0.105
7.337	0.10	.053	0.105
4.134	0.10	.068	0.105
9.887	0.04	.037	0.077
7.237	0.04	.050	0.077
3.942	0.04	.066	0.077

TABLE 3.6

Log  $k_i$  values for the protonation of 1,5,8,12-tetraazadodecane in NaCl media

I(m/l)	log $k_1$		log $k_2$	
	$\text{pH}'/\text{p}[\text{H}^+]\text{calib.}^a$	Davies eqtn. <sup>b</sup>	$\text{pH}'/\text{p}[\text{H}^+]\text{calib.}$	Davies eqtn.
0.20	$10.62 \pm 0.03^c$	$10.25 \pm 0.02$	$9.82 \pm 0.02$	$9.84 \pm 0.02$
0.15	$10.57 \pm 0.03$	$10.29 \pm 0.02$	$9.79 \pm 0.02$	$9.80 \pm 0.02$
0.10	$10.53 \pm 0.03$	$10.33 \pm 0.02$	$9.77 \pm 0.02$	$9.76 \pm 0.02$
0.04	$10.50 \pm 0.02$	$10.37 \pm 0.02$	$9.69 \pm 0.02$	$9.68 \pm 0.02$
0.00	$10.46^{d\pm} 0.03$	$10.42^{d\pm} 0.03$	$9.51^{e\pm} 0.02$	$9.50^{e\pm} 0.02$

I(m/l)	log $k_3$		log $k_4$	
	$\text{pH}'/\text{p}[\text{H}^+]\text{calib.}$	Davies eqtn.	$\text{pH}'/\text{p}[\text{H}^+]\text{calib.}$	Davies eqtn.
0.20	$8.41 \pm 0.02$	$8.31 \pm 0.02$	$5.76 \pm 0.03$	$5.67 \pm 0.03$
0.15	$8.36 \pm 0.02$	$8.26 \pm 0.02$	$5.65 \pm 0.02$	$5.60 \pm 0.02$
0.10	$8.30 \pm 0.02$	$8.23 \pm 0.02$	$5.59 \pm 0.02$	$5.55 \pm 0.02$
0.04	$8.12 \pm 0.02$	$8.08 \pm 0.02$	$5.34 \pm 0.03$	$5.33 \pm 0.03$
0.00	$7.81^{f\pm} 0.02$	$7.79^{f\pm} 0.02$	$4.86^{g\pm} 0.03$	$4.90^{g\pm} 0.03$

<sup>a</sup> From the application of the  $\text{pH}'/\text{p}[\text{H}^+]$  calibration curve.<sup>b</sup> From the application of the Davies equation for single ion activity coefficients.<sup>c</sup> All errors estimated as the standard deviation from a number of independent determinations.<sup>d</sup> From a plot of log  $k_1$  vs. I.<sup>e</sup> From a plot of log  $k_2 - I^{1/2}/(1+I^{1/2})$  vs I.<sup>f</sup> From a plot of log  $k_3 - 2I^{1/2}/(1+I^{1/2})$  vs I.<sup>g</sup> From a plot of log  $k_4 - 3I^{1/2}/(1+I^{1/2})$  vs I.

to the  $\text{pH}'$  values is appreciated by comparing the protonation constants for the compound 1,5,8,12-tetraazadodecane (3,2,3-tet) when the  $\text{p}[\text{H}^+]$  values were obtained by the two different methods. (The titration data are shown in Table 6.11 and the method of calculation of the constants is described in Chapter 4). The data in Table 3.6 show that large differences in the protonation constants do occur. The magnitudes of these differences vary as  $I$  varies and, as expected, these changes correlate with the differences between the operational and the Davies activity coefficient in Table 3.5.

### 3.6 SUMMARY AND GENERAL COMMENTS

The important features of this calibration method are

- (i) The  $\text{p}[\text{H}^+]$  values are obtained independent of the set of standard solutions (NBS, British Standards etc.) used to standardise the pH meter.
- (ii) No empirical expression is required for  $\gamma_{\text{H}^+}$ .
- (iii) The method uses buffer solutions thus, precise  $\text{pH}'$  data are readily obtained.
- (iv) The method is reasonably rapid and once completed for any one electrode system the calibration need only be checked by comparing the response of the standard buffers with that when the calibration was performed.

## CHAPTER 4

### CALCULATION OF EQUILIBRIUM CONSTANTS FROM pH TITRATION DATA

#### 4.1 CALCULATION OF THE PROTONATION EQUILIBRIUM CONSTANTS OF THE LIGANDS

For each of the ligands used in this study, the (vol. of NaOH, pH) data were obtained from titrations of a solution of the ligand, acid and background electrolyte (NaCl) using the procedure outlined in section 2.4. The experimentally measured pH was converted to a hydrogen ion concentration  $p[H^+]$  as outlined in Chapter 3.

##### 4.1.1 Calculation of the Secondary Concentration Variable $\bar{n}$

This calculation is described for the base 3,2,3-tet. The procedure adopted for the other ligands was identical, although the equations derived were obviously slightly different in two cases (oxime and ketone).

At each point during a titration there are equilibria among the species  $L$ ,  $H^+$ ,  $HL^+$ ,  $H_2L^{2+}$ ,  $H_3L^{3+}$ ,  $H_4L^{4+}$  in solution:

$$k_1 = \frac{[HL]}{[H][L]} \quad k_2 = \frac{[H_2L]}{[H][HL]} \quad k_3 = \frac{[H_3L]}{[H][H_2L]} \quad k_4 = \frac{[H_4L]}{[H][H_3L]}$$

The charges have been omitted for clarity. The mass balance equations for  $T_L$ , the total concentration of base and  $T_H$ ,

the total concentration of dissociable hydrogen ions are;

$$T_L = [L] + [HL] + [H_2L] + [H_3L] + [H_4L] \quad 4.1$$

and

$$T_L = [H] + [HL] + 2[H_2L] + 3[H_3L] + 4[H_4L] - [OH] \quad 4.2$$

where  $[L]$  and  $[H]$  are the concentration of free base and the concentration of hydrogen ions respectively. The term  $[OH]$ , the concentration of hydroxide ion, arises from hydrolysis reactions of the type  $H_nL^{n+} + H_2O \rightleftharpoons H_{n+1}L^{(n+1)+} + OH^-$ .

The secondary concentration variable<sup>91</sup>  $\bar{n}$ , which defines the degree of protonation of the system, is the average number of protons attached per base. This definition implies

$$\bar{n} = \frac{T_H - [H] + [OH]}{T_L} \quad 4.3$$

i.e.  $\bar{n}$  is equal to the total concentration of coordinated protons divided by the concentrations of available ligand.

From equations 4.1, 4.2 and 4.3

$$\begin{aligned} \bar{n} &= \frac{T_H - [H] + [OH]}{T_L} \\ &= \frac{[HL] + 2[H_2L] + 3[H_3L] + 4[H_4L]}{[L] + [HL] + [H_2L] + [H_3L] + [H_4L]} \end{aligned} \quad 4.4$$

Now incorporating the equilibrium expressions into equation 4.4

$$\bar{n} = \frac{\beta_1[H] + 2\beta_2[H]^2 + 3\beta_3[H]^3 + 4\beta_4[H]^4}{1 + \beta_1[H] + \beta_2[H]^2 + \beta_3[H]^3 + \beta_4[H]^4} \quad 4.5$$



where  $\beta_i = \prod_{j=1}^i k_j$ . In general, equation 4.5 is expressed as

$$\bar{n} = \frac{\sum_{n=0}^N n \beta_n [H]^n}{\sum_{n=0}^N \beta_n [H]^n} \quad 4.6$$

where N is the total number of stepwise protonations and  $\beta_0 = 1$ .

The calculation of  $\bar{n}$  using equation 4.4 is easily, though laboriously, achieved with the aid of a desk calculator. A short Fortran computer program, FORM (see Appendix D) was written to perform the repetitive calculations of  $\bar{n}$  from titration data.

#### 4.1.2 Bjerrum's Half- $\bar{n}$ Method

This method for the calculation of the equilibrium constants from the secondary concentration variable  $\bar{n}$ , along with the conditions for its use, have recently been discussed by both Sen<sup>92</sup> and by Schröder<sup>93</sup>. An outline of the method as applied to 3,2,3-tet is as follows.

Equation 4.5 can be rearranged to give an expression for each  $k_i$  in terms of  $\bar{n}$ ,  $[H]$  and the other three equilibrium constants. By assuming that only one equilibrium is important at any  $\bar{n} = n - \frac{1}{2}$  ( $n$  an integer,  $1 \leq n \leq 4$ ), then approximate values of the constants are obtained from the  $p[H^+]$  value at  $\bar{n} = n - \frac{1}{2}$ , i.e.

$$k_n = \left( \frac{1}{[H]} \right)_{\bar{n} = n - \frac{1}{2}} \quad 4.7$$

The values of  $p[H^+]$  at the particular  $\bar{n}$  values were interpolated from the formation curve (a plot of  $\bar{n}$  against  $p[H^+]$ ).

The rearranged equations for 3,2,3-tet are

$$\begin{aligned}
 k_4 &= \left( \frac{1}{[H]} \right)_{\bar{n}=3.5} \left( \frac{7}{k_1 k_2 k_3 [H]^3} + \frac{5}{k_2 k_3 [H]^2} + \frac{3}{k_2 [H]} + 1 \right) \\
 k_3 &= \left( \frac{1}{[H]} \right)_{\bar{n}=2.5} \left( \frac{5 + 3k_1 [H] + k_1 k_2 [H]^2}{k_1 k_2 [H]^2 + 3k_1 k_2 k_4 [H]^3} \right) \\
 k_2 &= \left( \frac{1}{[H]} \right)_{\bar{n}=1.5} \left( \frac{3 + k_1 [H]}{k_1 [H] + 3k_2 k_1 [H]^2 + 5k_4 k_3 k_1 [H]^3} \right) \\
 k_1 &= \left( \frac{1}{[H]} \right)_{\bar{n}=0.5} \left( \frac{1}{1 + 3k_2 [H] + 5k_3 k_2 [H]^2 + 7k_4 k_3 k_2 [H]^3} \right)
 \end{aligned} \tag{4.8}$$

If the ratio of successive constants  $\frac{k_n}{k_{n+1}} > 10^4$  then  $k_n$  is accurately expressed by equation 4.7. However, a successive approximations method must be used for ratios less than  $10^4$ .

Improved values of  $k_1, k_2, k_3$  and  $k_4$  are calculated from equations 4.8. These values are then resubstituted and further improved constants obtained. The process is repeated until convergence is obtained. Convergence can be slow if the magnitude of successive constants is similar.

This method for the calculation of  $k_1$  only uses  $N$  sets of data for the calculation of the  $N$  constants, which is not a recommended approach. The process can also be tedious, especially when convergence is not rapid and  $N$  is greater than two. The results of a Bjerrum calculation on a set of

data for 3,2,3-tet are given in Table 4.3 (see section 4.1.5).

#### 4.1.3 Graphical Methods

Before the advent of computers, graphical solution techniques were widely used for the calculation of concentration equilibrium constants<sup>17,94</sup>. Graphical methods are preferable to direct solution using methods similar to 4.1.2 because more data can be considered simultaneously and the effect of experimental errors is more readily assessed.

Graphical methods were not widely used in this work. A graphical method described by Rossotti<sup>95</sup> was tried on one set of  $(\bar{n}, p[H^+])$  data for 3,2,3-tet as a comparison with the widely used approach described in 4.1.4.

Equation 4.5 can be rearranged

$$\bar{n} + (\bar{n}-1)\beta_1[H] + (\bar{n}-2)\beta_2[H]^2 + (\bar{n}-3)\beta_3[H]^3 + (\bar{n}-4)\beta_4[H]^4 = 0$$

dividing by  $k_1(\bar{n}-2)[H]^2$

$$\frac{\bar{n}}{(\bar{n}-2)[H]^2} \cdot \frac{1}{k_1} + \frac{(\bar{n}-1)}{(\bar{n}-2)[H]} + k_2 + \left( \frac{\sum_{n=3}^4 (\bar{n}-n)\beta_n[H]^n}{k_1(\bar{n}-2)[H]^2} \right) = 0$$

If the term in brackets is small compared with the other terms, then a linear plot of  $\frac{-(\bar{n}-1)}{(\bar{n}-2)[H]}$  against  $\frac{\bar{n}}{(\bar{n}-2)[H]^2}$  would yield  $k_2$  as the intercept and  $\frac{1}{k_1}$  as the slope. The values of  $k_1$  and  $k_2$  obtained are given in Table 4.3.

These values were substituted into a rearranged form of equation 4.5 and  $\beta_3$  and  $\beta_4$  calculated. Let

$$C = \bar{n} + (\bar{n}-1)\beta_1[H] + (\bar{n}-2)\beta_2[H]^2$$

then

$$C - (\bar{n}-3)\beta_3[H]^3 + (\bar{n}-4)\beta_4[H]^4 = 0.$$

Dividing by C

$$1 + \frac{(\bar{n}-3)[H]^3}{C} \cdot \beta_3 + \frac{(\bar{n}-4)[H]^4}{C} \cdot \beta_4 = 0$$

thus when  $\beta_3 = 0$ ,  $\beta_4 = -1/\left(\frac{(\bar{n}-4)}{C}[H]^4\right)$  and when  $\beta_4 = 0$ ,

$\beta_3 = -1/\left(\frac{(\bar{n}-3)}{C}[H]^3\right)$ . The lines joining the points  $(0, \frac{-C}{(\bar{n}-4)[H]^4})$  and  $(\frac{-C}{(\bar{n}-3)[H]^3}, 0)$  for any given  $(\bar{n}, [H])$

should all intersect at a point  $(\beta_3, \beta_4)$ , thus  $\beta_3$  and  $\beta_4$  can be calculated. In practice the lines intersect in a region, which gives an estimate on the uncertainty in the calculation of  $\beta_3$  and  $\beta_4$ . The constants, and uncertainties, estimated using this graphical method are given in Table 4.3.

A graphical method suggested by Scatchard<sup>96</sup> was applied to the same  $(\bar{n}, p[H^+])$  data as used above. A function Q is defined

$$Q = \frac{\bar{n}}{(4-\bar{n})[H]} = \frac{k_1 + 2k_1k_2[H] + 3k_1k_2k_3[H]^2 + 4k_1k_2k_3k_4[H]^3}{4 + 3k_1[H] + 2k_1k_2[H]^2 + k_1k_2k_3[H]^3}$$

Now in the limit, as  $H \rightarrow 0$ ,  $Q \rightarrow \frac{k_1}{4}$  and in the limit as  $H \rightarrow \infty$  and  $\bar{n} \rightarrow 4$ ,  $Q \rightarrow 4k_4$ . From a plot of  $\log Q$  against  $\bar{n}$ , from the limits  $\bar{n} \rightarrow 0$  and  $\bar{n} \rightarrow 4$ , estimates of  $k_1$  and  $k_4$  are obtained. This approach should only be regarded as

approximate due to the difficulty in obtaining accurate  $\bar{n}$  data as  $\bar{n}$  tends to both 4 and 0. Estimates of these two parameters are shown in Table 4.3.

#### 4.1.4 Least Squares Method

In principle,  $N$  simultaneous equations of the type equation 4.6 are necessary to solve for the  $N$  unknowns  $\beta_1 \dots \beta_N$ . However, as the measured variables  $\bar{n}$  and  $[H^+]$  are subject to error a better approach is to obtain  $m$  sets of values  $(\bar{n}, [H^+])$   $m > N$  and use a least squares analysis. The algebra of this process is outlined in Appendix C. This method for the calculation of stability and basicity constants has been extensively used by many workers over the last decade<sup>97,98</sup>. The least squares method was used throughout this work.

For the calculation of the basicity constants of the ligands, equation 4.6 was used. The LHS (termed  $F_o$ ) is readily calculated from the analytical concentrations and the hydrogen ion concentration and has an uncertainty  $\sigma$ , the standard deviation of the measurement  $F_o$ . The RHS (termed  $F_c(x,y)$ ) is a function of the hydrogen ion concentration and the unknown parameters  $k_1, k_2 \dots k_N$ . The least squares procedure varies the unknown parameters so as to minimise the error square sum

$$M(x,y) = \sum_i^n w_i ((F_o)_i - (F_c(x,y))_i)^2 \quad 4.7$$

where the weighting factor  $w_i = 1/\sigma_i^2$ .

A description and a listing of the least squares program ORGLS used in this work is given in Appendix D.

### Weighting Procedure

Weighting of the data in a least squares analysis should be incorporated to allow for the variation of  $\sigma_i$ , the standard deviation of the  $i^{\text{th}}$  observation. If there is a variation in  $\sigma_i$  throughout a particular set of data then the use of unit weights (i.e. all the data is considered of equal weight) is likely to produce a bias in the calculated parameters. Care in the use of a particular weighting procedure is also needed for an accurate estimation of the uncertainties of the parameters<sup>99</sup>. In the calculation of the basicity constants of the ligand, the least squares process minimised  $\sum(\bar{n}_{\text{obs}} - \bar{n}_{\text{calc}})^2$ . An estimation of  $\sigma_{\bar{n}_{\text{obs}}}$  can be calculated from the terms contributing to the expression for  $\bar{n}$ ,

$$\bar{n} = \frac{T_H - [H] + K_w/[H]}{T_L}$$

The uncertainties in  $T_H$  and  $T_L$  will be constant throughout a titration. The term  $[H]$  is small compared with  $T_H$  therefore the uncertainty in  $[H]$  has a negligible effect on  $\bar{n}$  and can thus be disregarded. However, when  $[H]$  is small ( $\text{pH} > 10$ ) the term  $K_w/[H]$  makes an important contribution to  $\bar{n}$  and under these conditions  $\bar{n}$  is a non-linear function of  $[H]$ .

Below  $\text{pH} \sim 10$  the contributions from the hydrolysis term are small and  $\sigma_{\bar{n}}$  will be approximately constant. Under these conditions the  $\bar{n}$  data may be weighted at unity.

The general equation for the propagation of variance, assuming no correlation between the  $x_i$  is given by<sup>100,101</sup>

$$\sigma_y^2 = \sum_i \sigma_{x_i}^2 \left( \frac{\partial y}{\partial x_i} \right)^2 \quad \text{where } y = f(x_i).$$

Applying this equation to the expression for  $\bar{n}$

$$\sigma_{\bar{n}}^2 = \sigma_{[H]}^2 \left( \frac{\partial(\bar{n})}{\partial[H]} \right)^2 + C^2$$

where  $C$  is a term which incorporates the estimated standard deviations of  $T_H$  and  $T_L$ ; this term will be approximately constant throughout a titration. Differentiating  $\bar{n}$  with respect to  $[H]$

$$\sigma_{\bar{n}}^2 = \left( -\frac{1}{T_L} \right)^2 \left( 1 + \frac{K_w}{[H]^2} \right)^2 \sigma_{[H]}^2 + C^2 \quad 4.9$$

Thus an estimation of  $\sigma_{\bar{n}}$  can be obtained from this equation.

An alternative approach was to calculate  $\sigma_{\bar{n}}$  directly for each titration point, by using experimental  $\bar{n}$  data from a number of titrations under the same conditions.

The basicity constants for hm-3,2,3-tet were calculated using different weighting procedures. Thirtynine data points in the range  $\bar{n} = 3.8 - \bar{n} = 0.5$  were used in the calculations. A comparison of the results is shown in Table 4.1.

TABLE 4.1

A comparison of the basicity constants for  
hm-3,2,3-tet calculated using different  
weighting procedures

<u>weighting</u>	<u>log k<sub>1</sub></u>	<u>log k<sub>2</sub></u>	<u>log k<sub>3</sub></u>	<u>log k<sub>4</sub></u>
unit weights	11.10 <sub>5</sub>	10.06 <sub>0</sub>	7.61 <sub>4</sub>	4.90 <sub>3</sub>
cal. $\bar{\sigma}_{\bar{n}}$ directly <sup>a</sup>	11.11 <sub>8</sub>	10.05 <sub>5</sub>	7.61 <sub>4</sub>	4.90 <sub>3</sub>
using eqn. 4.8 <sup>b</sup>	11.11 <sub>6</sub>	10.05 <sub>5</sub>	7.61 <sub>4</sub>	4.90 <sub>3</sub>
using eqn. 4.8 <sup>c</sup>	11.11 <sub>6</sub>	10.05 <sub>5</sub>	7.61 <sub>4</sub>	4.90 <sub>3</sub>

<sup>a</sup> From the consideration of the  $\bar{n}$  data from a number of reproducible titrations.

<sup>b</sup> C was estimated as 0.003 (from a consideration of the errors in  $T_H$  and  $T_L$ ).

<sup>c</sup> C was calculated from  $C = \frac{(T_{H_i} - [NaOH]) \cdot 0.3\%}{T_L}$

where  $T_{H_i}$  is the initial total acid concentration.



These results show that the effect of weighting only causes small changes in the magnitude of the constants. Other workers<sup>98</sup> have also reported that weighting only produces changes within the estimated uncertainty, when  $\bar{n}_{\text{obs}} - \bar{n}_{\text{calc}}$  is minimised in the least squares procedure. Perrin<sup>102</sup> also found that when differences in the analytical hydrogen ion concentration were minimised the effect of weighting was minimal. The weighting procedures did not produce large changes in the errors calculated by the program ORGLS. (For all the weighting schemes and for unit weights, the errors in the  $\log k_1$  values appeared to be underestimated.)

#### Testing of the Program ORGLS

The  $\bar{n}$ ,  $p[H^+]$  data and the basicity constants for 3,3'-diaminodipropylamine have been reported<sup>103</sup>. The basicity constants were obtained using Sillen's<sup>104</sup> procedure applied to selected data points (ten in number) as indicated by the authors. In their calculation procedure, the constants were varied so as to minimise the difference between the calculated and experimental EMF values. The reported  $(\bar{n}, p[H^+])$  data points were used to calculate the three basicity constants using ORGLS. Each  $\bar{n}$  observation was weighted as unity, thus the errors calculated by the program were not meaningful; no errors for the constants were assessed. A comparison between the constants obtained and the published values is shown in Table 4.2. The

TABLE 4.2

Computation (using ORGLS) of  $k_1$ ,  $k_2$  and  $k_3$  for 3,3'-  
diaminodipropylamine from published data

	<u><math>\log k_1</math></u>	<u><math>\log k_2</math></u>	<u><math>\log k_3</math></u>
published constants:	$10.65 \pm 0.02$	$9.57 \pm 0.03$	$7.72 \pm 0.03$
from ORGLS:	$10.65_4$	$9.56_7$	$7.71_7$

Residuals from the final refinement cycle of ORGLS

<u><math>\bar{n}_{\text{obs}}</math></u>	<u><math>10^3(\bar{n}_{\text{obs}} - \bar{n}_{\text{calc}})</math></u>
2.657	-0.109
2.487	0.375
2.316	-0.308
1.818	0.303
1.659	-0.713
1.507	0.118
1.224	0.405
0.706	-0.079
0.575	-0.079
0.476	0.016

TABLE 4.3

A comparison of basicity constants calculated  
using different methods.

	<u>Graphical</u> <sup>a</sup>		<u>Least Squares</u> <sup>a</sup>
	Scatchard	Rossotti	
log $k_1$ :	10.7 $\pm$ 0.15	10.54 $\pm$ 0.02	10.58 $\pm$ 0.02
log $k_2$ :	-	9.85 $\pm$ 0.02	9.82 $\pm$ 0.02
log $k_3$ :	-	8.35 $\pm$ 0.06	8.41 $\pm$ 0.02
log $k_4$ :	5.82 $\pm$ 0.04	6.0 $\pm$ 0.1	5.76 $\pm$ 0.02

	<u>Bjerrum</u> <sup>b</sup>	<u>Least Squares</u> <sup>b</sup>
log $k_1$ :	10.33	10.34 $\pm$ 0.02
log $k_2$ :	9.77	9.77 $\pm$ 0.02
log $k_3$ :	8.25	8.24 $\pm$ 0.02
log $k_4$ :	5.53	5.56 $\pm$ 0.02

<sup>a</sup> Calculations performed on a data set not reported  
in this work.

<sup>b</sup> The data used is a different set to that used in a.

agreement between the sets of values is satisfactory.

#### 4.1.5 A Comparison of the Direct Solution, Graphical and Least Squares Methods

The basicity constants calculated using the three methods are compared in Table 4.3. All the  $\log k_1$  values have been rounded to two places of decimals. A comparison between the Bjerrum results and the least squares results shows favourable agreement. The least squares results would be considered the more accurate due to the use of all the available data. A comparison of the graphical and least squares results also shows favourable agreement. With the adopted Rossotti approach, errors in the calculations were accumulative; the first plot gave  $k_1$  and  $k_2$  but the second plot gave  $\beta_3$  and  $\beta_4$ , thus any errors in the estimation of  $k_1$  and  $k_2$  also contribute to the error in  $k_3$  and  $k_4$ . There is a large uncertainty on  $k_1$  determined by the Scatchard approach due to the difficulty in the extrapolation to  $\bar{n} \rightarrow 0$ . Data to  $\bar{n} = 3.8$  were used in the extrapolation to determine  $k_4$  and as the positive slope of the curve decreased as  $n \rightarrow 4$  the value of  $k_4$  could be more accurately assessed than could  $k_1$ .

#### 4.2 CALCULATION OF THE STABILITY CONSTANTS FOR THE COPPER COMPLEXES

The competitive complex formation technique involving hydrogen ions<sup>105</sup> was used for the study of the copper-ligand

complexes. The titration procedure used was to titrate a solution containing metal ions, ligand and acid with standard alkali. The approach used to calculate the stability constants for the copper complexes from the titration data depended on the number of complexes species formed.

For only one metal-ligand species the three mass balance equations for  $T_M$  (the total metal ion concentration),  $T_H$  and  $T_L$  contain three unknowns  $[L]$ ,  $[M]$  and the metal ligand stability constants, basicity constants for the ligand having been previously determined. For each titration point, the equations could be solved directly to give the stability constant of the complex.

For more than one metal-ligand species the equations for  $T_M$ ,  $T_L$  and  $T_H$  can no longer be solved directly to determine the unknown constants. The calculation approach adopted depended on the number and type of complexes present and whether their formation was concurrent. The least squares approach was used. The details of the calculations for the metal ligand stability constants for each ligand are discussed in the appropriate sections of Chapter 7.

## CHAPTER 5

### CALCULATION OF ENTHALPY DATA

The calculation of  $\Delta H$  for a reaction requires a knowledge of the extent to which the reaction has occurred and a measure of the heat changes for the reaction and any secondary reactions that may occur. For a reaction that goes to completion, the extent of reaction is determined by the number of moles of the reactant which is not in excess. However, for an equilibrium reaction (for example the protonation of an amine) a knowledge of the concentration quotient valid for the calorimetric conditions, and the 'position' of equilibrium, is required. When a batch calorimetric technique is used the extent of an equilibrium reaction is usually determined from the predetermined concentration quotient for the reaction and from the measured pH and stoichiometry of the calorimetric solution at the end of a run<sup>106</sup>. However, for titration calorimetry it is only possible to measure the  $p[H^+]$  at the end of a complete titration. A mathematical approach for the calculation of the extent of reaction for each titration point was adopted in this work.

# 5.1 CALCULATION OF $\Delta H_i$ FOR THE PROTONATION OF hm-3,2,3-tet AND 3,2,3-tet

## Solution Composition at Each Titration Point

Equation 3.6 as applied to these tetraamines can be rearranged to give

$$T_H = [H] - K_w/[H] + T_L \frac{\left( \sum_{n=1}^4 n \beta_n [H]^n \right)}{\left( \sum_{n=0}^4 \beta_n [H]^n \right)} \quad 5.1$$

where  $\beta_n = \prod_{i=1}^n k_i$ ,  $k_i$  being the concentration quotient for the stepwise protonation reaction  $LH_{i-1} + H = LH_i$ , and where  $\beta_0 = 1$ . This equation 5.1 can be further rearranged to give a polynomial in  $[H]$  of the form

$$f([H]) = a[H]^6 + b[H]^5 + c[H]^4 + d[H]^3 + e[H]^2 + f[H]^4 - K_w \quad 5.2$$

where the coefficients  $a$ ,  $b$ ,  $c$ ,  $d$ ,  $e$  and  $f$  are readily calculated from the terms  $\beta_i$ ,  $T_L$ ,  $T_H$  and  $K_w$ . This polynomial in  $[H]$  was solved using the Newton-Rapson method<sup>75</sup> which initially required an approximate solution for  $[H]$ .

For each titration point an approximation of  $\bar{n}$  was calculated assuming that the contributions from  $[H]$  and  $K_w/[H]$  were zero, i.e.  $\bar{n} = T_H/T_L$ . The value of  $p[H^+]$  corresponding to this value of  $\bar{n}$  was interpolated from a previously determined formation curve. This  $p[H^+]$  value was then used to calculate an improved value of  $\bar{n}$ ,

$\bar{n} = (T_H - [H] + K_w/[H])/T_L$ ; the graphical process was then repeated. The value of  $[H^+]$  was then used as an approximate solution to the polynomial 5.2. Only a few cycles of the Newton-Rapson process were required to obtain a convergent solution to within 0.0005 pH units.

The concentrations of the species  $LH_1$  at each titration point were calculated using this hydrogen ion concentration value from the Newton-Rapson process.

The calculated  $p[H^+]$  for the last titration point compared favourably ( $\pm 0.01$  pH) with the value calculated from the measured pH of the calorimetric solution at the end of a run.

These calculations were performed using a suitable computer program. A listing and sample output for this program, THERM, is shown in Appendix D.

#### Calculation of the Changes in the Concentrations of $LH_1$ between Successive Titration Points

For these tetraamine ligands, the stepwise enthalpy changes are  $L + H \rightleftharpoons LH, \Delta H_1$ ;  $LH + H \rightleftharpoons LH_2, \Delta H_2$ ;  $LH_2 + H \rightleftharpoons LH_3, \Delta H_3$ ;  $LH_3 + H \rightleftharpoons LH_4, \Delta H_4$ . On the addition of the titrant acid, the overall heat change  $Q$ , corrected for the secondary reactions, can be expressed in terms of these stepwise enthalpy changes

$$Q = r\Delta H_1 + s\Delta H_2 + t\Delta H_3 + u\Delta H_4$$



where  $r$ ,  $s$ ,  $t$  and  $u$  are respectively the number of mmoles of the species  $LH$ ,  $LH_2$ ,  $LH_3$  and  $LH_4$  formed at each titration increment, and  $Q$  is the corrected heat change expressed in Joules. The values of  $r$ ,  $s$ ,  $t$  and  $u$  were calculated as follows. On the addition of the titrant  $HCl$ , protonation of the ligand species will occur ( $\bar{n}$  will increase). The number of mmoles of  $LH$  formed ( $r$ ) was calculated from the difference between the number of mmoles of  $L$  before and after the addition of the titrant increment. Similarly, the number of mmoles of  $LH_2$  formed was calculated from the number of mmoles of  $LH$  before the increment of titrant  $(LH)_i$ , the value after the increment  $(LH)_f$  and the number of mmoles of  $LH$  that formed during the increment, i.e.

$$s = (LH)_i + r - (LH)_f.$$

Similar equations were used to calculate  $t$  and  $u$ ,

$$t = (LH_2)_i + s - (LH_2)_f \quad \text{and} \quad u = (LH_3)_i + t - (LH_3)_f.$$

(The value of  $u$  could also be calculated from the difference between the number of mmoles of  $LH_4$  before and after the titration increment).

These calculations were also performed using the program THERM. The heat changes were also corrected for the heat of neutralisation of  $OH^-$  using THERM. Having obtained the values of  $r$ ,  $s$ ,  $t$ ,  $u$  and a corrected  $Q$  value, the values

of  $\Delta H_i$  were calculated using a linear least squares method.

#### Least Squares Calculation of $\Delta H_i$

The general least squares program ORGLS (see Appendix D) was adapted for the calculation of the enthalpy changes for the stepwise protonation reactions. If

$$Q_{\text{calc}} = r\Delta H_1 + s\Delta H_2 + t\Delta H_3 + u\Delta H_4 \quad 5.3$$

then the least squares process varied the parameters  $\Delta H_i$  so as to minimise the error square sum

$$\sum_i^n w_i (Q_{\text{obs}} - Q_{\text{calc}})_i^2$$

where  $w_i$  is the weighting factor for the  $i^{\text{th}}$  measurement of  $Q_{\text{obs}}$ , the corrected heat change. The values of  $Q_{\text{calc}}$  (calculated using the parameters of best fit) for these tetraamine ligands are shown in the Tables 6.12 and 6.13.

#### Errors in the Enthalpy Changes

The weighting factor for each experimental  $Q$  value was estimated from the uncertainty in the determination of each value, the main contributions arising from the measured resistance change of the thermistor and from the uncertainty in the calorimeter calibration constant (see 2.5.8).

The errors in the enthalpy values were obtained from the diagonal term of the inverted matrix during the least squares analysis using ORGLS (see Appendix D). No correlation of the errors for the experimental heat change and the errors arising from the calculation of  $r, s, t$  and  $u$  was considered.

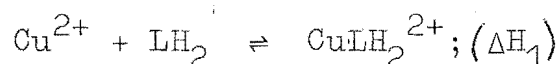
## 5.2 CALCULATION OF THE $\Delta H_1$ FOR THE DIAMINE-DIOXIME PROTONATION

The same procedure as outlined above for hm-3,2,3-tet and 3,2,3-tet was used to calculate the solution composition at each titration point, the changes in composition, and the enthalpy changes for the protonation of the diamine-dioxime.

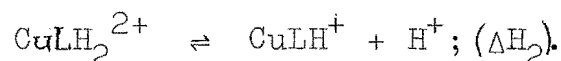
## 5.3 CALCULATION OF THE ENTHALPY CHANGES FOR THE FORMATION OF THE COPPER(II)/DIAMINE-DIOXIME COMPLEXES

### Solution Composition at Each Titration Point

For the copper diamine-dioxime complexes the enthalpies of complex formation are



and



For each point in the titration of the complex  $\text{CuLH}^+$  with HCl, three equations can be formulated. These are the two mass balance relationships

$$T_M = [\text{Cu}] + [\text{CuLH}_2] + [\text{CuLH}] \quad 5.4$$

and

$$T_L = [\text{LH}_2] + [\text{LH}_3] + [\text{LH}_4] + [\text{CuLH}_2] + [\text{CuLH}] \quad 5.5$$

where  $T_M$  and  $T_L$  are the total concentrations of metal ion and ligand present. The third equation is the electro-neutrality relationship,

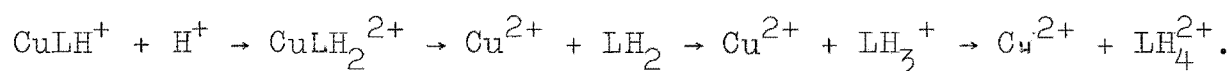
$$\begin{aligned}
& [\text{CuLH}^+] + 2[\text{Cu}^{2+}] + [\text{Na}^+] + [\text{H}^+] + [\text{LH}_3^+] + 2[\text{LH}_4^{2+}] + 2[\text{CuLH}_2^{2+}] \\
& = [\text{Cl}^-]_{\text{init}} + [\text{Br}^-] + [\text{OH}^-] + [\text{Cl}^-]_{\text{add}}
\end{aligned} \tag{5.6}$$

where  $[\text{Cl}]_{\text{init}}$  is the concentration of chloride ion in the solution which was added as  $\text{CuCl}_2$ , and  $[\text{Br}^-]$  is the concentration of bromide ion that was added as ligand dihydrobromide,  $[\text{Cl}^-]_{\text{add}}$  is the concentration of the chloride ion added as the titrant ( $\text{HCl}$ ) and  $[\text{Na}^+]$  is the concentration of  $\text{NaOH}$  added for the initial pH adjustment. As the concentration quotients for all the equilibria are known, equations 5.4 - 5.6 form a system of three nonlinear equations in the three unknowns  $[\text{H}]$ ,  $[\text{LH}_2]$  and  $[\text{Cu}]$ . These equations were solved using a successive approximations method. For a given value of  $[\text{H}]$ ,  $[\text{Cu}]$  and  $[\text{LH}_2]$  were calculated from equations 5.4 and 5.5. Equation 5.6 was then rearranged to give a cubic equation in  $[\text{H}]$  which was solved, using the Newton-Rapson method, to give an improved value for  $[\text{H}]$ . This improved value of  $[\text{H}]$  was then used to calculate improved values for  $[\text{LH}_2]$  and  $[\text{Cu}]$ . This complete process was then repeated until convergent values of  $[\text{H}^+]$ ,  $[\text{Cu}]$  and  $[\text{LH}_2]$  were obtained. The final values for these unknowns were checked for internal consistency with the equations 5.4 - 5.6. These values were then used to calculate the solution composition at each titration point. These calculations were performed using a suitable computer

program THERMOX (adapted from CUTHERM, see Appendix D).

### Calculation of the Changes in Composition Between Successive Titration Points

In the calorimetric titration the initial solution pH was adjusted so that  $\text{CuLH}^+$  was the predominant complexed species. The reaction scheme as titrant HCl was added to the calorimetric solution can be represented,



For each titration increment, the change in the number of mmoles of  $\text{CuLH}^+(\text{r})$  is simply the difference between the number of mmoles of the species before and after the titration increment. The enthalpy change for this process will be  $-\Delta\text{H}_2$ . The number of mmoles of the species  $\text{CuLH}_2^{2+}$  that decomposes (s) will be given by

$$s = (\text{CuLH}_2)_i + r - (\text{CuLH}_2)_f$$

where  $(\text{CuLH}_2)_i$  is the number of mmoles before the titration increment and  $(\text{CuLH}_2)_f$  is the number of mmoles after the increment. The enthalpy change for this process will be  $-\Delta\text{H}_1$ . Similarly the number of mmoles of  $\text{LH}_3^+$  (corr1) and  $\text{LH}_4^{2+}$  (corr2) formed will be given by

$$\text{corr1} = (\text{LH}_2)_i + s - (\text{LH}_2)_f \text{ and } \text{corr2} = (\text{LH}_3^+)_i + \text{corr1} - (\text{LH}_3^+)_f$$

(The symbols i and f have the same meaning as those used above for  $\text{CuLH}_2$ .)

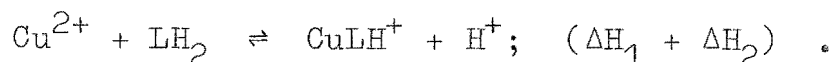
The overall heat change on reaction was corrected for protonation of the diamine-dioxime using the determined enthalpy data (section 6.1). The correction for the secondary hydrolysis reaction was zero for this titration.

These calculations and corrections of the heat change  $Q$  were incorporated into the program THERMOX. The results from this program are shown in Table 7.18.

The enthalpy changes  $\Delta H_1$  and  $\Delta H_2$  were calculated from a least squares analysis on the  $Q_{\text{corr}}$  (the heat change corrected for the protonations of the ligand)  $r$  and  $s$  data obtained from THERMOX. The  $Q_{\text{calc}}$  values from the least squares analysis are also reported in Table 7.18.

#### 5.4 CALCULATIONS IN THE EXPERIMENTAL DETERMINATION OF $(\Delta H_1 + \Delta H_2)$ FOR THE COPPER/DIAMINE-DIOXIME SYSTEM

For the titration of an alkaline solution ( $\text{pH} \sim 10$ ) of the ligand against copper chloride, the overall reaction was



For each titration point, equations 4.4 - 4.6 are still applicable but some simplifications can be made. From 4.4 and 4.5

$$T_L - T_M + [\text{Cu}] = [\text{LH}_2](1 + \beta_1[\text{H}]^2 + \beta_2[\text{H}]^2) \quad 5.7$$

Equation 5.6 can be rearranged to give

$$2[\text{Cu}^{2+}] + [\text{CuLH}^+] + 2[\text{CuLH}_2^{2+}] + [\text{Na}^+] + [\text{H}^+] + [\text{LH}_3^+] + 2[\text{LH}_4^{2+}]$$

$$= 2T_M + 2T_L + [\text{OH}^-] + \text{ACIDA}$$

which on the elimination of  $T_M$  gives

$$\text{ACIDA} + 2T_L - [\text{Na}] + K_w/[\text{H}] - [\text{H}] + [\text{CuLH}] = [\text{LH}_2](\beta_1[\text{H}] + 2\beta_2[\text{H}]^2)$$

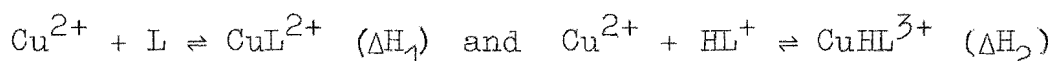
5.8

where ACIDA is the concentration of HCl added in the  $\text{CuCl}_2$  titrant. If it is initially assumed that  $[\text{Cu}] = 0$  and  $[\text{CuLH}] = T_M$  then the LHS of equation 5.8 can be readily calculated, assuming an approximate value for  $[\text{H}]$ , then from equations 5.8 and 5.7, on the elimination of  $[\text{LH}_2]$ , the resulting quadratic equation can be solved for a new value of  $[\text{H}]$ . This value is then used to calculate a new value for  $[\text{LH}_2]$  and also values for  $[\text{Cu}]$  and  $[\text{CuLH}]$ . The process is then repeated until convergence of the  $[\text{H}^+]$  values is obtained (usually a few cycles). The solution composition at each point in the titration was then calculated and the heat change was corrected for the protonation of the excess ligand. From the corrected heat change and the number of mmoles of  $\text{CuLH}^+$  formed, the  $(\Delta H_1 + \Delta H_2)$  value was calculated (see section 7.2).

## 5.5 CALCULATION OF THE ENTHALPY CHANGES FOR THE FORMATION OF THE COPPER COMPLEXES OF 3,2,3-tet

### Calculation of the Solution Composition at each Titration Point

For the determination of the enthalpy changes for the reactions



solutions made from the solid complex  $\text{Cu}(3,2,3\text{-tet})(\text{ClO}_4)_2$ <sup>107</sup> were titrated with HCl. The mass balance equations for  $T_M$ ,  $T_L$  and  $T_H$  for this system are

$$T_M = [\text{Cu}] + [\text{CuL}] + [\text{CuHL}] \quad 5.9$$

$$T_L = [\text{L}] + [\text{HL}] + [\text{H}_2\text{L}] + [\text{H}_3\text{L}] + [\text{H}_4\text{L}] + [\text{CuL}] + [\text{CuHL}] \quad 5.10$$

$$T_H = [\text{H}] + [\text{HL}] + 2[\text{H}_2\text{L}] + 3[\text{H}_3\text{L}] + 4[\text{H}_4\text{L}] + [\text{CuHL}] - K_w/[\text{H}] \quad 5.11$$

These three nonlinear equations in the unknowns  $[\text{H}]$ ,  $[\text{L}]$  and  $[\text{Cu}]$  were solved by a successive approximations method.

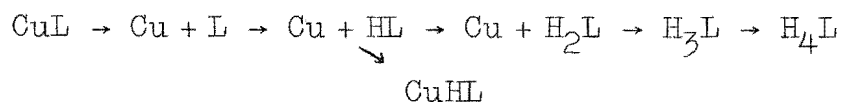
An approximate value for  $[\text{H}]$  at each calorimetric titration point was estimated from the titration curve of a pH titration of NaOH against a portion of the solution at the end of a calorimetric run. Given this value of  $[\text{H}]$  for each point, the quadratic equation in  $[\text{L}]$  formed on the elimination of  $[\text{Cu}]$  from equations 5.9 and 5.10 was solved to obtain a



value of [L]. This value was then substituted into equation 4.9 to calculate a value for [M]. These values of [M] and [L] were then substituted into equation 5.11, which was solved by the Newton-Rapson method to obtain an improved value for [H]. This value was then used to calculate improved values for both [L] and [M]. The complete process was repeated until convergence of the values was obtained. The final values for [H], [M] and [L] were then used to calculate the solution composition for the particular titration point. These calculations were performed using the computer program CUTHERM.

#### Calculation of the Changes in Solution Composition Between Successive Titration Points

The reaction scheme as the titrant acid is added to the CuL complex can be represented



The calculations of the changes in the number of mmoles of each species are as follows: The number of mmoles of CuL that decomposed (r) is simply the difference between the number of mmoles of the species before and after the titration increment. The enthalpy change for this process will be  $-\Delta H_1$ . For CuHL the number of mmoles formed (s) will be the difference between the final and initial values, the

enthalpy change for this process being  $+\Delta H_2$ . The number of mmoles of HL formed (corr1) is given by

$$\text{corr1} = r + (L)_i - (L)_f$$

where i and f have the meaning as described in section 4.3. Similarly the number of mmoles of  $H_2L$ ,  $H_3L$  and  $H_4L$  formed (corr2, corr3 and corr4 respectively) are given by the equations

$$\text{corr2} = (HL)_i + \text{corr1} - [(HL)_f + s]$$

$$\text{corr3} = (H_2L)_i + \text{corr2} - (H_2L)_f$$

$$\text{corr4} = (H_3L)_i + \text{corr3} - (H_3L)_f$$

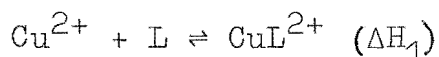
The heat of reaction Q was corrected for the heat of protonation of the ligand species using the corr1 - corr4 values and the enthalpies of protonation (section 6.2). These calculations were also incorporated into the program CUTHERM.

From the corrected heat changes and the corresponding r and s values for each titration increment,  $\Delta H_1$  and  $\Delta H_2$  were calculated using the linear least squares method. The results of the calculations using CUTHERM and results from the least squares analysis are shown in Tables 7.6 and 7.7.

## 5.6 CALCULATIONS OF THE ENTHALPY CHANGE FOR THE COPPER (hm-3,2,3-tet) COMPLEX

### Calculation of the Solution Composition at Each Titration Point

For the determination of the enthalpy change for



a solution of the ligand was titrated with copper chloride.

The mass balance equations for  $T_L$ ,  $T_M$  and  $T_H$  are

$$T_L = [\text{L}] + [\text{HL}] + [\text{H}_2\text{L}] + [\text{H}_3\text{L}] + [\text{H}_4\text{L}] + [\text{CuL}] \quad 5.12$$

$$T_M = [\text{Cu}] + [\text{CuL}] \quad 5.13$$

$$T_H = [\text{H}] + [\text{HL}] + 2[\text{H}_2\text{L}] + 3[\text{H}_3\text{L}] + 4[\text{H}_4\text{L}] - K_w/[\text{H}] \quad 5.14$$

From equations 5.12 and 5.13

$$T_L - T_M + [\text{Cu}] = [\text{L}] + [\text{HL}] + [\text{H}_2\text{L}] + [\text{H}_3\text{L}] + [\text{H}_4\text{L}] \quad 5.15$$

$[\text{Cu}]$  is initially set equal to zero; then the resulting polynomial in  $[\text{H}]$  formed on the elimination of  $[\text{L}]$  from equations 5.14 and 5.15 was solved for  $[\text{H}]$  using the Newton-Rapson procedure. (An initial  $p[\text{H}]$  value for each titration point was estimated from the value of  $\bar{n}_H$ ). Values of  $[\text{L}]$  and  $[\text{Cu}]$  were then calculated and the process was repeated until convergence of the  $[\text{H}]$  value was obtained. The final values of  $[\text{H}]$ ,  $[\text{L}]$  and  $[\text{Cu}]$  were then used to calculate the solution

composition at each point. These calculations were performed by a suitable adaption of the program CUTHERM.

#### Calculation of the Changes in Solution Composition

As there was only one complex formed, the enthalpy change  $\Delta H_1$  was calculated directly from the corrected heat change and from the change in the number of mmoles of the species  $\text{CuL}(r)$ , which is simply the difference between the number of mmoles of  $\text{CuL}$  after and before the titration increment. The number of mmoles of  $\text{HL}$  formed ( $\text{corr1}$ ) as the copper chloride titrant was added to the ligand plus acid solution was calculated from

$$\text{corr1} = (\text{L})_i - (r + (\text{L})_f)$$

Similarly the number of mmoles of  $\text{LH}_2$ ,  $\text{LH}_3$  and  $\text{LH}_4$  formed on the addition of titrant (termed  $\text{corr2}$ ,  $\text{corr3}$  and  $\text{corr4}$  respectively) were calculated from

$$\text{corr2} = (\text{HL})_i + \text{corr1} - (\text{HL})_f, \text{corr3} = (\text{H}_2\text{L})_i + \text{corr2} - (\text{H}_2\text{L})_f$$

and  $\text{corr4} = (\text{H}_3\text{L})_i + \text{corr3} - (\text{H}_3\text{L})_f$

where the symbols  $i$  and  $f$  have the same meaning as described previously (section 4.3). The heat of reaction was then corrected for the heat of protonation of the ligand species using the values  $\text{corr1}$  to  $\text{corr4}$  and the corresponding enthalpies of protonation. The correction for the secondary hydrolysis reaction was also made. The results of these calculations are shown in Table 7.2.

## CHAPTER 6

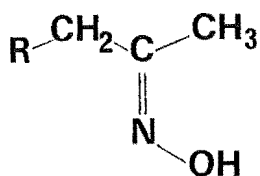
### PROTONATION OF THE LIGANDS

#### 6.1 PROTONATION OF THE DIAMINE-DIOXIME LIGAND

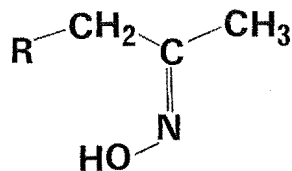
This diamine-dioxime ligand (Fig. 1.1) has two secondary amine groups for which protonation thermodynamic data have been determined. The nitrogen of an oxime function is found to be very weakly basic<sup>108</sup>; no attempt was made to measure the basicity constant for the oxime functions of this ligand. In addition to this basicity proton ionisation from the oxime function is likely. An estimate of the acidity of this oxime group has been determined.

##### 6.1.1 Oxime Isomerism

The reaction of hydroxylamine with aldehydes and unsymmetrical ketones often leads to the formation of two geometric isomers<sup>109</sup>. For the ketoxime in this study these isomeric forms are



syn (methyl)



anti (methyl)

Before the advent of NMR the Beckman rearrangement was used for the assignment of oxime configuration<sup>109</sup>. This

assignment was not always unequivocal due to the possible interconversion of isomers under rearrangement conditions<sup>110</sup>.

NMR studies have been extensively used for oxime structure elucidation<sup>111-114</sup>. A separate resonance has been observed for the protons on the  $\alpha$  carbons in syn and anti isomers of a number of ketoximes<sup>111</sup>. For a group  $\alpha\text{CH}_x-$  in isomeric syn and anti ketoximes the resonance separation  $\tau_{\text{CH}_x}(\text{syn}) - \tau_{\text{CH}_x}(\text{anti})$  can be somewhat solvent dependent<sup>111</sup>. In ketoximes the resonance separation is generally larger for the  $\alpha$ -methylene protons than for  $\alpha$ -methyl protons<sup>112</sup>. Also it has been generally accepted for ketoximes that both for an  $\alpha$ -methyl and an  $\alpha$ -methylene group the resonance at higher field strength is associated with a trans(OH) configuration<sup>111,112</sup>.

The exact nature of the anisotropic deshielding associated with the oxime is not known with certainty. From studies on the change in NMR spectra on protonation of the oxime nitrogen Saito and coworkers<sup>113</sup> concluded that the deshielding effect arises from the lone pair of electrons on the oxime nitrogen. However, there is considerable evidence<sup>112,114</sup> to support the proposal<sup>112</sup> that the deshield-effect arises from a proximity effect involving the oxime OH group.

For the diamine-dioxime ligand and the dihydro-chloride and dihydroperchlorate salts, IR and some NMR data

have been reported<sup>3</sup>. Further NMR data are shown in Table 6.1. For the ligand  $\text{LH}_2$  in  $\text{CF}_3\text{COOH}$  the splitting of the resonances for the  $\alpha$ -methyl and  $\alpha$ -methylene protons indicate the occurrence of two isomeric forms for the oxime function and furthermore, the resonance integral shows that the resonance at higher field for both the  $\alpha$ -methyl and  $\alpha$ -methylene protons is associated with the same oxime configuration. This was assigned as the anti isomer<sup>3</sup>. The NMR of  $\text{LH}_2 \cdot 2\text{HCl}$  in  $\text{CF}_3\text{COOH}$  showed isomeric purity and by comparison with the NMR data for  $\text{LH}_2$  a syn configuration was assigned (the  $\alpha$  isomer). Similarly, a comparison of the NMR of  $\text{LH}_2 \cdot 2\text{HClO}_4$  (termed  $\gamma$ ) in  $\text{CF}_3\text{COOH}$  with that for  $\text{LH}_2$  in the same solvent indicated the perchlorate salt was in the anti configuration. The solvent dependence on the resonance splitting, and on the chemical shift, can be seen from a comparison of the NMR data for  $\text{D}_2\text{O}/\text{CF}_3\text{COOH}$  solvent with that obtained in  $\text{D}_2\text{O}$  and  $\text{CF}_3\text{COOH}$  alone. It appears that the isomeric configurations are 'frozen' in  $\text{CF}_3\text{COOH}$  and isomerisation does occur for each isomer in aqueous  $\text{CF}_3\text{COOH}$ . This observation is consistent with that of Norris and Sternhell<sup>115</sup> who reported that the addition of  $\text{CF}_3\text{COOH}$  to dioxan solutions of some quinone monoximes slows the rate of syn-anti interconversion while aqueous solutions of  $\text{CF}_3\text{COOH}$  increase the isomerisation rate. The NMR for the dihydrobromide salt of the ligand in  $\text{D}_2\text{O}$  shows the existence of two isomeric forms. As for the

TABLE 6.1

NMR data for the diamine-dioxime ligand at ca. 30°C

<u>Chemical shifts<sup>x</sup> (and resonance integral<sup>y</sup> ratios)</u>					
<u>Compound</u>	<u>solvent</u>	<u>a<sup>z</sup></u>	<u>c</u>	<u>b</u>	<u>d</u>
LH <sub>2</sub>	CF <sub>3</sub> COOH	8.35	7.64, 7.54(2:1)	6.88, 6.73(2:1)	6.20
LH <sub>2</sub> .2HCl	CF <sub>3</sub> COOH	8.25	7.47	6.65	6.08
LH <sub>2</sub> .2HCl	50% D <sub>2</sub> O/CF <sub>3</sub> COOH	8.78, 8.74	8.20, 7.96(1.7:1)	7.52, 7.25(1.7:1)	6.70
LH <sub>2</sub>	D <sub>2</sub> O/CF <sub>3</sub> COOH	8.50, 8.47	7.95, 7.68(.75:1)	7.28, 6.97(.75:1)	6.44
LH <sub>2</sub> .2HCl	D <sub>2</sub> O	8.58	8.08	7.35	6.65
LH <sub>2</sub> .2HBr	D <sub>2</sub> O	8.59	8.08, 8.03(2:1)	7.36, 7.22(2:1)	6.66
LH <sub>2</sub> .2HClO <sub>4</sub>	CF <sub>3</sub> COOH	8.30	7.60	6.85	6.15
LH <sub>2</sub> .2HClO <sub>4</sub>	50% D <sub>2</sub> O/CF <sub>3</sub> COOH	8.50, 8.47	7.94, 7.68(.8:1)	7.27, 6.95(.8:1)	6.44

<sup>x</sup>  $\tau$  values in ppm relative to TMS.<sup>y</sup> Integral ratios are expressed as the ratio of the high field resonance integral to the low field integral.<sup>z</sup> The letters a,b,c,d refer to the protons as indicated in Fig. 1.1.



$\alpha$ -dihydrochloride the NMR spectrum was unchanged by the addition of small amounts of sodium chloride, sodium hydroxide or hydrochloric acid. It also appears (see Table 6.1) that if the NMR spectrum of  $\text{LH}_2 \cdot 2\text{HCl}$  in  $\text{D}_2\text{O}$  is still representative of a pure syn isomer then for  $\text{LH}_2 \cdot 2\text{HBr}$  the resonance for the  $\alpha$ -methyl and  $\alpha$ -methylene protons at higher fields are associated with a syn isomeric form of an oxime group. This is in contrast with the assignment in  $\text{CF}_3\text{COOH}$  and perhaps indicates the importance of solvent effects for this diamine-dioxime compound.

#### Rate of Isomerisation of the Oxime Function

Little quantitative information on the rate of isomerisation of oximes is available. A number of thermal and photochemical isomerisations of aromatic oximes have been studied<sup>116</sup>, from a preparative viewpoint. It has been suggested that acids, bases and some salts catalyse oxime isomerisation<sup>117</sup>.

On a macroscopic scale it appears that for the diamine-dioxime ligand isomerisation occurs readily in aqueous solution. As judged from visible absorption spectra, dissolution of the separate syn ( $\alpha \cdot 2\text{HCl}$  salt) or anti ( $\gamma \cdot 2\text{HClO}_4$ ) isomers with copper ions at the appropriate pH leads to the immediate formation of identical copper complexes (see Chapter 7). Also, the addition of dilute perchloric acid to a solution of  $\alpha \cdot 2\text{HCl}$  in water leads to

the immediate formation of  $\gamma.2\text{HClO}_4$ .

However, on the NMR time scale the identification of two oxime configurations in solvent  $\text{D}_2\text{O}$  indicates a slow rate of isomerisation.

No temperature dependent NMR studies were attempted.

### 6.1.2 Protonation of the Amine Nitrogens

#### Results

Data from the pH titrations of both  $\text{LH}_2.2\text{HCl}(\alpha)$  and  $\text{LH}_2.2\text{HClO}_4(\gamma)$  ligand solutions against NaOH are given in Tables 6.2 and 6.3. Only one titration from each set of reproducible titrations has been tabulated. The ligand solutions were prepared just prior to the commencement of a set of titrations, which were normally completed within about three hours. Within this period there was no observable hydrolysis of the oxime group (by pH measurement). For titrations of NaOH against the ligand  $\text{LH}_2(\alpha+\gamma)$  dissolved in HCl the experimental end points for the removal of one proton from the protonated ligand did not agree particularly well with the calculated values. This was probably due to incomplete dissolution of the sparingly water soluble  $\text{LH}_2$  ligand. These titration data were not used in the calculations of protonation constants.

The protonation of the diamine-dioxime ligand can be represented by the two stepwise equilibria

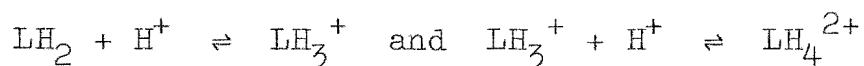


TABLE 6.2

Data from titrations of the diamine-dioxime ligand against standard NaOH at I = 0.10M (NaCl) an 25°C

Solid isomer:	$\alpha^a(\text{syn methyl})$			$\gamma^b(\text{anti methyl})$		
	Volume	$\bar{n}$	$p[H^+]$	Volume	$\bar{n}$	$p[H^+]$
	0.020	1.844	5.644	0.020	1.830	5.680
	0.030	1.770	5.842	0.030	1.750	5.881
	0.040	1.695	6.003	0.040	1.668	6.047
	0.050	1.620	6.148	0.050	1.586	6.196
	0.060	1.545	6.280	0.060	1.505	6.338
	0.070	1.469	6.411	0.070	1.422	6.478
	0.080	1.394	6.548	0.080	1.340	6.627
	0.090	1.318	6.687	0.090	1.258	6.793
	0.100	1.243	6.850	0.100	1.176	6.997
	0.110	1.168	7.050	0.110	1.094	7.280
	0.120	1.092	7.332	0.115	1.054	7.486
	0.125	1.055	7.529	0.120	1.013	7.742
	0.130	1.018	7.788	0.125	0.974	8.046
	0.135	0.982	8.068	0.130	0.936	8.307
	0.140	0.947	8.303	0.135	0.899	8.478
	0.145	0.913	8.481	0.140	0.862	8.622
	0.150	0.879	8.618	0.150	0.790	8.842
	0.160	0.812	8.828	0.160	0.720	9.007
	0.170	0.747	8.988	0.170	0.651	9.143
	0.180	0.683	9.121	0.180	0.586	9.264
	0.190	0.621	9.239	0.190	0.523	9.374
	0.200	0.562	9.346	0.200	0.463	9.473
	0.210	0.505	9.442	0.210	0.408	9.569
	0.220	0.453	9.537	0.220	0.358	9.659
	0.230	0.403	9.623	0.230	0.312	9.744
	0.240	0.358	9.706	0.240	0.271	9.823
	0.250	0.317	9.785			
	0.260	0.280	9.858			

<sup>a</sup> Composition of solution:  $T_L = 4.797 \times 10^{-4}M$ ,  $T_H = 9.593 \times 10^{-4}M$ ,  
[NaOH] = 0.1813M, initial volume = 49.94 ml.

<sup>b</sup> Composition of solution:  $T_L = 4.883 \times 10^{-4}M$ ,  $T_H = 9.765 \times 10^{-4}M$ ,  
[NaOH] = 0.1720, initial volume = 49.94 ml.

TABLE 6.3

Data<sup>a</sup> from titrations of the diamine-dioxime ligand  
against standard NaOH at 25°C

<u>I = 0.20 M</u>			<u>I = 0.15 M</u>			<u>I = 0.04 M</u>		
$\alpha$ isomer			$\gamma$ isomer			$\alpha$ isomer		
Volume	$\bar{n}$	p[H <sup>+</sup> ]	Volume	$\bar{n}$	p[H <sup>+</sup> ]	Volume	$\bar{n}$	p[H <sup>+</sup> ]
0.020	1.855	5.714	0.020	1.843	5.701	0.020	1.840	5.477
0.030	1.786	5.903	0.030	1.769	5.892	0.030	1.766	5.690
0.040	1.716	6.056	0.040	1.694	6.052	0.040	1.691	5.858
0.050	1.646	6.192	0.050	1.618	6.199	0.050	1.616	6.004
0.060	1.576	6.322	0.060	1.542	6.329	0.060	1.540	6.139
0.070	1.505	6.455	0.070	1.466	6.459	0.070	1.464	6.271
0.080	1.435	6.567	0.080	1.391	6.597	0.080	1.388	6.404
0.090	1.365	6.685	0.100	1.239	6.888	0.090	1.312	6.546
0.100	1.294	6.821	0.110	1.163	7.083	0.100	1.236	6.703
0.110	1.224	6.987	0.120	1.087	7.352	0.110	1.160	6.892
0.120	1.154	7.185	0.125	1.050	7.543	0.120	1.083	7.152
0.130	1.084	7.462	0.130	1.013	7.781	0.130	1.008	7.571
0.135	1.049	7.640	0.135	0.977	8.053	0.135	0.971	7.873
0.140	1.015	7.849	0.140	0.942	8.286	0.140	0.935	8.154
0.145	0.982	8.094	0.150	0.873	8.602	0.150	0.865	8.531

Table 6.3 (contd.)

<u>I = 0.20 M</u>			<u>I = 0.15 M</u>			<u>I = 0.04 M</u>		
$\alpha$ isomer			$\gamma$ isomer			isomer		
Volume	$\bar{n}$	p[H <sup>+</sup> ]	Volume	$\bar{n}$	p[H <sup>+</sup> ]	Volume	$\bar{n}$	p[H <sup>+</sup> ]
0.150	0.949	8.307	0.160	0.807	8.815	0.160	0.796	8.762
0.160	0.886	8.598	0.170	0.742	8.977	0.170	0.729	8.938
0.170	0.824	8.803	0.180	0.679	9.109	0.180	0.663	9.074
0.180	0.765	8.971	0.190	0.618	9.224	0.190	0.599	9.198
0.190	0.705	9.091	0.200	0.559	9.328	0.200	0.538	9.313
0.200	0.648	9.203	0.210	0.503	9.422	0.210	0.479	9.415
0.210	0.595	9.314	0.220	0.450	9.513	0.220	0.425	9.515
0.220	0.540	9.395	0.230	0.410	9.598	0.230	0.373	9.604
0.230	0.491	9.484	0.240	0.355	9.676	0.240	0.327	9.695
0.240	0.443	9.563	0.250	0.315	9.754	0.250	0.283	9.776
0.250	0.399	9.640	0.260	0.278	9.825			
0.260	0.358	9.713						
0.270	0.320	9.782						
0.280	0.286	9.847						

- <sup>a</sup> Composition of solution: I = 0.04M;  $T_L = 4.508 \times 10^{-4}M$ ,  
 $T_H = 9.016 \times 10^{-4}M$ , [NaOH] = 0.1720, initial volume = 49.94 ml.  
I = 0.15M;  $T_L = 4.524 \times 10^{-4}M$ ,  $T_H = 9.048 \times 10^{-4}M$ , [NaOH] = 0.1720M  
initial volume = 49.94 ml. I = 0.20M;  $T_L = 4.883 \times 10^{-4}M$ ,  
 $T_H = 9.765 \times 10^{-4}M$ , [NaOH] = 0.1720M, initial volume = 49.94 ml.

with concentration quotients given by

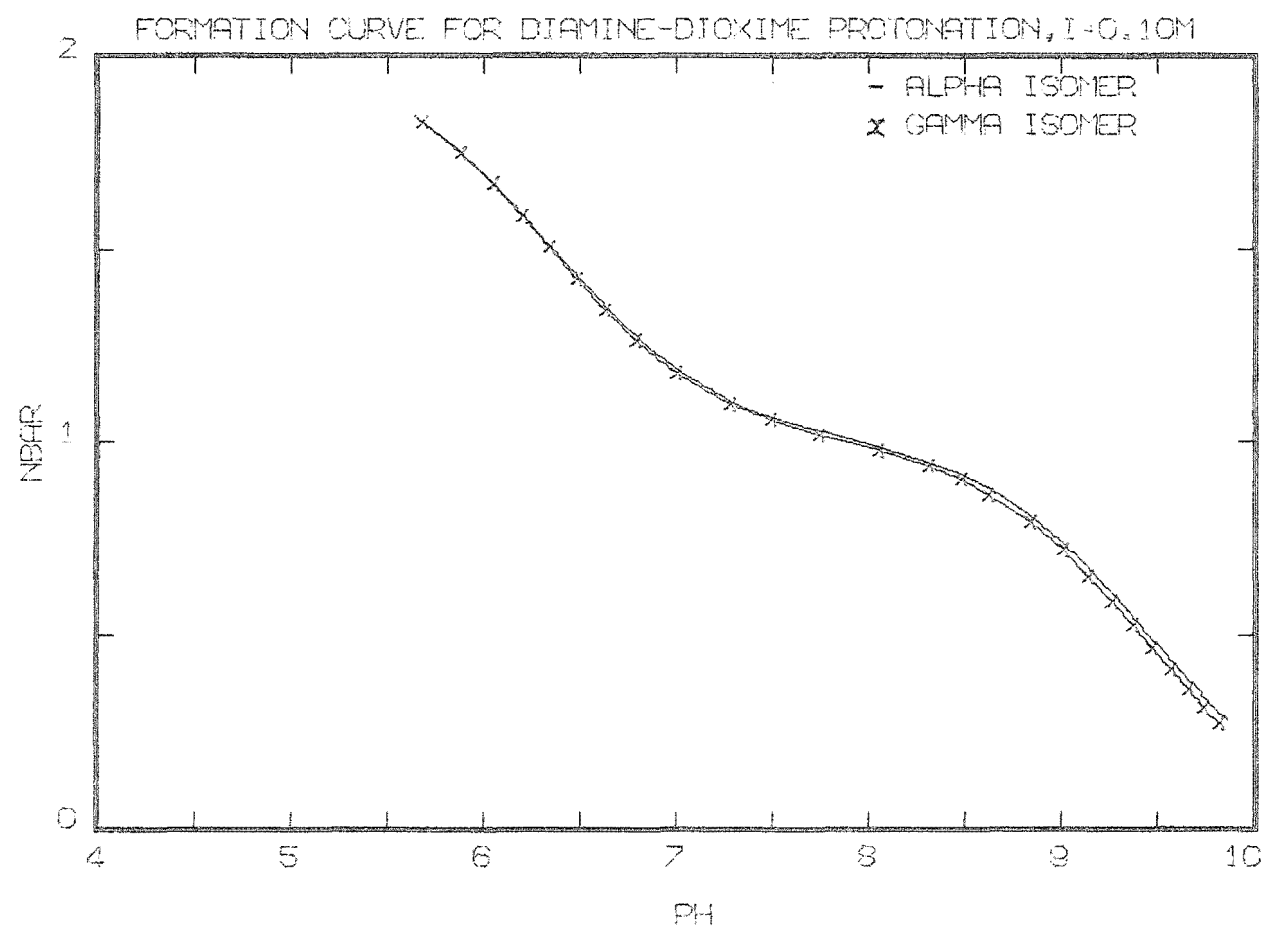
$$k_3 = \frac{[\text{LH}_3]}{[\text{LH}_2][\text{H}]} \quad \text{and} \quad k_4 = \frac{[\text{LH}_4]}{[\text{LH}_3][\text{H}]}$$

the charges having been omitted for clarity.

These quotients  $k_4$  and  $k_3$  were calculated from the pH titration data by the least squares method (see Chapter 4) and the results are given in Table 6.4. The uncertainties in the log  $k$  values were estimated from a consideration of the analytical errors involved in a titration and from the standard deviation in the log  $k$  value from a number of titrations, performed under identical conditions. The formation curves for the titration data (Table 6.2) at an ionic strength of 0.10 M for both the  $\text{LH}_2 \cdot 2\text{HCl}(\alpha)$  and  $\text{LH}_2 \cdot 2\text{HClO}_4(\gamma)$  isomers are shown in Fig. 6.1. These curves are almost superimposable in the region  $\bar{n} = 1.8$  to  $\bar{n} = 0.8$ , however in the  $\bar{n}$  range 0.8 - 0.2 a slight difference is apparent. This difference is reflected in the difference between the log  $k_3$  values for the  $\alpha$  and  $\gamma$  data (Table 6.4), although on consideration of the errors in the log  $k_3$  values this difference of 0.027 is not statistically significant.

Log  $k_n^0$  values were obtained from the extrapolation of a plot of log  $k_n$  against  $f(I)$  to  $I = 0$ , as described in Chapter 1. The extrapolations are shown in Fig. 6.2 and the results are recorded in Table 6.4.

**Fig 6-1**



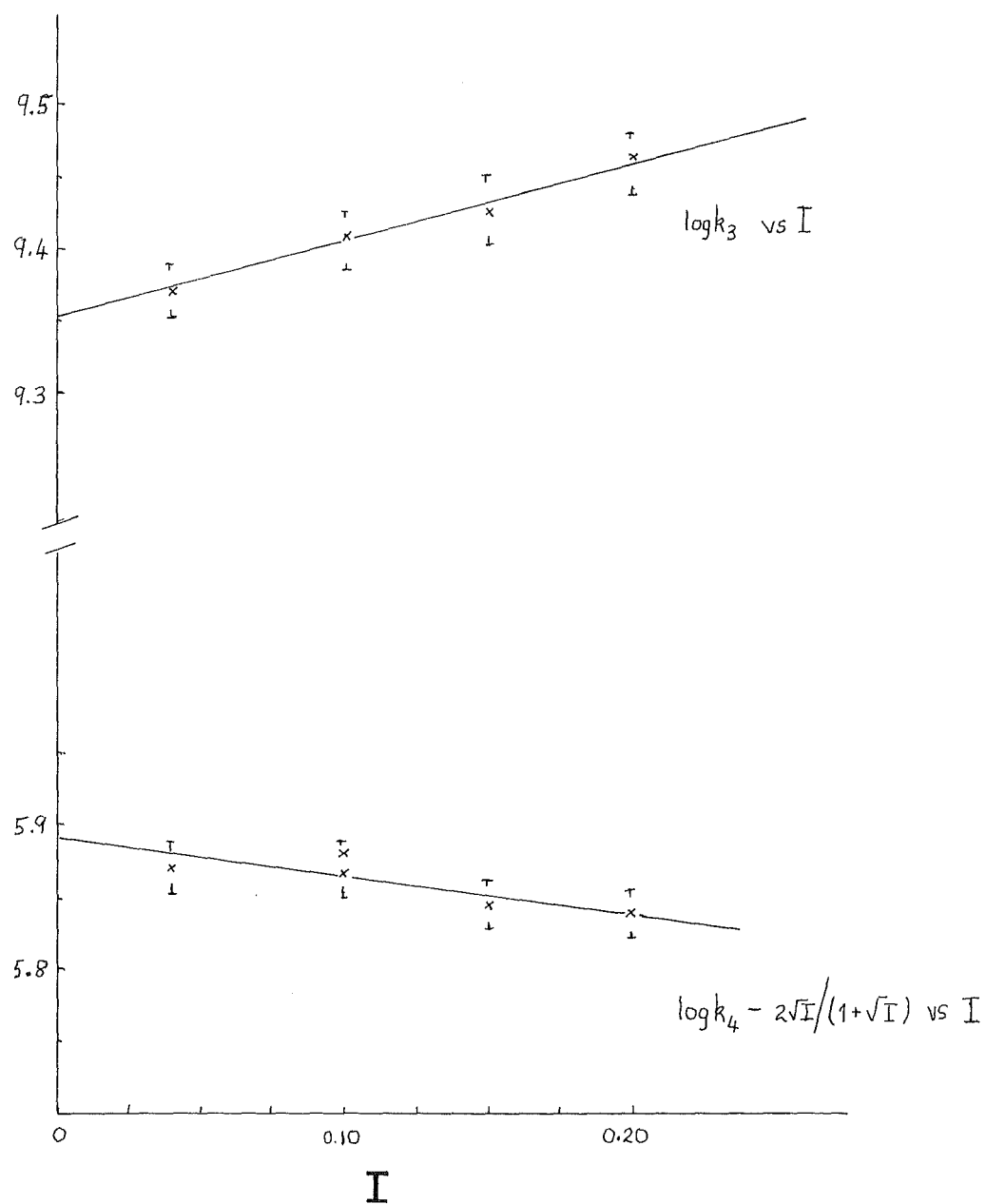


**Fig 6.2** Plots of  $\log k_n$  against  $I$  for diamine-dioxime protonation



TABLE 6.4

Protonation constants for the diamine-dioxine  
ligand at 25°C, NaCl solution

<u>Ionic strength</u>	<u>Isomer</u> <sup>a</sup>	<u>log k<sub>4</sub></u>	<u>log k<sub>3</sub></u>
0.20	α	6.45 <sub>7</sub> ± 0.02 <sup>c</sup>	9.46 <sub>5</sub> ± 0.02
0.15	γ	6.40 <sub>2</sub> ± 0.02	9.42 <sub>5</sub> ± 0.02
0.10	α	6.36 <sub>2</sub> ± 0.02	9.45 <sub>2</sub> ± 0.02
0.10	γ	6.34 <sub>7</sub> ± 0.02	9.40 <sub>7</sub> ± 0.02
0.04	α	6.20 <sub>2</sub> ± 0.02	9.37 <sub>0</sub> ± 0.02
0.00 <sup>b</sup>	-	5.89 ± 0.02	9.35 ± 0.02

<sup>a</sup> α denotes that the constants were derived from titrations using the α.2HCl salt; γ denotes γ2HClO<sub>4</sub> was used.

<sup>b</sup> Constants of I = 0 were obtained using an extrapolation procedure (see Fig. 6.2).

<sup>c</sup> Errors estimated as described in the text.

Data from the calorimetric titrations of solutions of the diamine-dioxime bromide salt and alkali, against standard HCl, are given in Table 6.5. The method used to calculate solution composition at each titration point is outlined in Chapter 5. The tabulated heat change  $Q_m$  is the measured heat change, corrected for the heat of dilution of HCl<sup>57</sup>. The stepwise enthalpies of protonation ( $LH_2 + H^+ \rightleftharpoons LH_3^+$ ,  $\Delta H_3$ ;  $LH_3^+ + H^+ \rightleftharpoons LH_4^{2+}$ ,  $\Delta H_4$ ) were calculated using the least squares procedure outlined in Chapter 5. The values of the calculated heat change ( $Q_{calc}$ ) from the least squares analyses are also given in Table 6.5. A comparison of each  $Q_{calc}$  value with the corresponding  $Q_{corr}$  value, the measured heat change  $Q_M$  corrected for the heat of neutralisation of hydroxide ion, indicates that the least squares refinement of the heat data was satisfactory. With the exception of one difference the  $Q_{corr} - Q_{calc}$  values are all less than 1% of  $Q_{corr}$ .

The enthalpy changes calculated from the least squares analysis were corrected to infinite dilution (as discussed in Chapter 1). These values, along with the corresponding free energy and entropy changes, are given in Table 6.6. The uncertainties in the enthalpy values were obtained from the least squares analysis (see Chapter 5) using weighted  $Q_{corr}$  values.

TABLE 6.5

Calorimetric results from the titration of diaminedioxime solutions against HCl, I = 0.10M, 25°C

Vol. <sup>a</sup> (ml)	p[H <sup>+</sup> ] <sup>b</sup>	$\bar{n}$	LH <sub>2</sub> <sup>c</sup> (mmol)	LH <sub>3</sub> <sup>+</sup> (mmol)	LH <sub>4</sub> <sup>2+</sup> (mmol)	$\Delta(LH_3)^d$ (mmol)	$\Delta(LH_4)$ (mmol)	Q <sub>M</sub> (J)	Q <sub>corr</sub> <sup>f</sup> (J)	Q <sub>calc</sub> <sup>g</sup> (J)	Run No. <sup>h</sup>
<u>Titration 1</u>											
0.300	10.001	0.204	0.39903	0.10227	0.00002						1
						0.15169	0.00020	6.604	5.923	6.007	
0.620	9.399	0.507	0.24733	0.25376	0.00023						1
						0.16439	0.00160	6.763	6.582	6.565	
0.950	8.709	0.838	0.08295	0.41655	0.00182						1
						0.08115	0.08211	6.616	6.570	6.512	
1.270	7.045	1.164	0.00179	0.41559	0.08394						1
						0.00156	0.16248	6.652	6.651	6.598	
1.590	6.364	1.491	0.00023	0.25467	0.24642						1
						0.00022	0.17394	6.990	6.990	7.005	
1.930	5.635	1.838	0.00001	0.08094	0.42036						1
<u>Titration 2</u>											
0.320	9.712	0.333	0.35937	0.17913	0.00008						2
						0.15782	0.00041	6.606	6.278	6.258	
0.640	9.187	0.627	0.20155	0.33654	0.00049						2
						0.15769	0.00428	6.541	6.422	6.408	
0.960	8.362	0.927	0.04386	0.48995	0.00477						2
						0.04269	0.12103	-	-	-	
1.280	6.865	1.231	0.00117	0.41161	0.12580						2
						0.00101	0.17329	6.981	6.980	7.010	
1.620	6.253	1.555	0.00017	0.23932	0.29909						2
						0.00016	0.17902	7.176	7.176	7.207	
1.970	5.452	1.888	0.00001	0.06046	0.47811						2

<sup>a</sup> Cumulative volume of 0.5128M HCl added at each titration point.<sup>b</sup> p[H<sup>+</sup>] values are calculated as described in Chapter 5.<sup>c</sup> Values are the number of mmoles of each species at each titration point.<sup>d</sup> Values tabulated are the changes in the no. of mmoles between successive titration points.<sup>f</sup> Q<sub>M</sub> (J) corrected for the neutralisation of OH<sup>-</sup> ion.<sup>g</sup> See text.<sup>h</sup> Titration 1; T<sub>L</sub> = 5.072 x 10<sup>-3</sup>M, T<sub>H</sub> = -0.686 x 10<sup>-3</sup>M, Initial volume = 98.84 mlTitration 2: T<sub>L</sub> = 5.449 x 10<sup>-3</sup>M, T<sub>H</sub> = 0.069 x 10<sup>-3</sup>M, Initial volume = 98.84 ml.

TABLE 6.6

Thermodynamic data for stepwise protonation of the  
diamine-dioxime ligand at 25°C at I = 0.0M

<u>Reaction</u>	<u>log k°</u>	<u>-ΔG°kJmol<sup>-1</sup></u>	<u>-ΔH°kJmol<sup>-1</sup></u>	<u>ΔS°Jmol<sup>-1</sup>K<sup>-1</sup></u>
$\text{LH}_2 + \text{H}^+ \rightleftharpoons \text{LH}_3^+$	$9.35 \pm 0.02$	$53.36 \pm 0.1$	$39.55 \pm 0.3$	$46.3 \pm 1.3$
$\text{LH}_3^+ + \text{H}^+ \rightleftharpoons \text{LH}_4^{2+}$	$5.89 \pm 0.02$	$33.61 \pm 0.1$	$39.39 \pm 0.3$	$-19.4 \pm 1.3$

Thermodynamic data for protonation of ethylenediamine  
and NN'-dimethylethylenediamine at 25°C and I = 0.00M

	<u>log k°</u>	<u>-ΔG°kJmol<sup>-1</sup></u>	<u>-ΔH°kJmol<sup>-1</sup></u>	<u>ΔS°Jmol<sup>-1</sup>K<sup>-1</sup></u>
$\text{NH}_2\text{CH}_2\text{CH}_2\text{NH}_2^a$	9.91	56.56	49.96	22.2
	(9.93)	(56.69)	(49.83)	(23.0)
	7.13	40.69	46.15	-18.3
	(6.86)	(39.16)	(46.36)	(-24.3)
$\text{MeNHCH}_2\text{CH}_2\text{NHMe}^b$	10.03 <sub>2</sub>	57.25	44.94	41.3
	6.79 <sub>5</sub>	38.78	39.02	-0.8

<sup>a</sup>Data from reference 124. Values in parenthesis from reference 87 and references therein.

<sup>b</sup>Log k° data from reference 119. ΔH data from reference 121 was corrected to infinite dilution as described in Chapter 1.

## Discussion

The oxime functional group and the amine group are well recognised as a hydrogen bonding acid and a hydrogen bonding base respectively<sup>118</sup>. Molecular models of the diamine-dioxime ligand show that for the  $\gamma$  (anti) configuration of the oxime group intramolecular hydrogen bonding between the oxime OH and the amine nitrogen, - OH ... N, is favourable while for the  $\alpha$  (syn) isomer no such hydrogen bonding appears possible. This implies that in the gas phase the first protonation constant ( $\log k_3$ ) for a  $\gamma$  isomer might be slightly smaller than that for an  $\alpha$  isomer.

The  $\log k$  values for the diamine-dioxime ligand protonation at  $I = 0.10$  M (see Table 6.4) obtained using the  $\alpha$  and the  $\gamma$  isomers were found to be equal, within the estimated experimental uncertainty. This suggests either that the protonation constants for the  $\alpha$  and  $\gamma$  isomers in aqueous solution are very similar, or that the rate of isomerisation is rapid (on the pH measurement time scale) and that the equilibrium isomer ratio of  $\alpha:\gamma$  is rapidly established. Other evidence supports rapid isomerisation (see section 7.2).

The free energy data in Table 6.6 show that there is a considerable reduction in the basicity of the amine nitrogens in the diamine-dioxime ligand compared with either ethylenediamine or N,N'-dimethylethylenediamine. This decrease is perhaps best discussed by separating out the effect due to

(i) the alkyl chains attached to the amine nitrogens, and (ii) the introduction of two oxime substituents onto the alkyl chain.

#### Effect of Alkyl Substituents

There are few thermodynamic data available for the protonation of N-alkyl substituted ethylenediamine compounds<sup>5</sup>. Näsanen<sup>119,120</sup> has determined thermodynamic protonation constants for a number of methyl and ethyl substituted ethylenediamines, however no enthalpy changes were determined. The enthalpy data for NN'-dimethyl-ethylenediamine protonation at  $I = 0.50$  ( $\text{KNO}_3$ ) have recently been reported<sup>121</sup>; these values, corrected to infinite dilution as described in Chapter 1 are shown in Table 6.6. The only other enthalpy data for some N substituted ethylenediamines were determined by Basolo and coworkers<sup>122</sup> using a non-calorimetric method. Their data for NN'-dimethyl-ethylenediamine is in considerable disagreement with that from reference 121.

It is well known that for a large number of primary n-alkyl monoamines the basicity does not uniformly increase with chain length but shows small fluctuations about a fixed value<sup>123,124</sup>. This is also true for a smaller number of secondary N-alkyl monoamines<sup>124</sup>. An inspection of the enthalpy and entropy changes shows that this approximately constant basicity arises from the compensation of the

$\Delta H^\circ$  and  $T\Delta S^\circ$  terms; as the chain length increases  $-\Delta H^\circ$  increases and  $\Delta S^\circ$  decrease. The usual explanation<sup>68,125</sup> for this effect is that 'hydrocarbon chain stiffening' occurs.

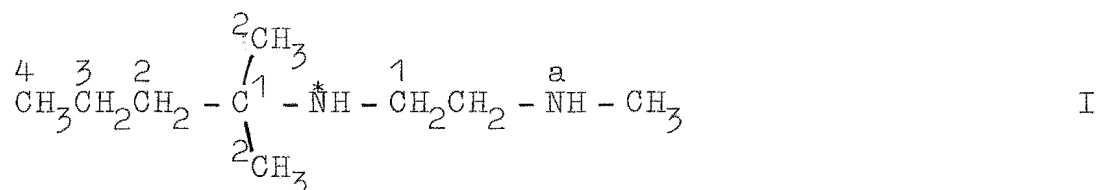
According to the electrostatic theory<sup>126</sup>, groups of low dielectric constant (e.g. a hydrocarbon chain) embedded in a medium of high dielectric constant are repelled from the neighbourhood of the charge. This results in a stiffened and extended hydrocarbon chain and a resultant entropy decrease due to the decrease in the number of degrees of freedom of the chain.

For a diamine similar in structure to the daimine-dioxime ligand without the oxime substituents it would be expected that the free energy changes for protonation would be similar to those for N,N'-dimethylethylenediamine.

#### Empirically Calculated Enthalpy Changes

An estimate of the enthalpy changes for such an amine (termed II) can be made using empirical formulae. Christensen and coworkers<sup>124</sup> have reported empirical formulae for the calculation of enthalpy and entropy changes on protonation of both primary and secondary N-alkyl substituted monoamines. A further formula for the prediction of the enthalpies of protonation of some diamines has also been reported<sup>127</sup>. From these formulae and from the enthalpy data for N,N'-dimethylethylenediamine protonation, the  $\Delta H^\circ$  of protonation of the atom N\* in the model compound I can be

estimated



The enthalpy of protonation of dimethylamine is  $-12.04 \text{ kcal mol}^{-1}$  <sup>124</sup>, (The calculation has been performed in  $\text{kcal mol}^{-1}$  for consistency with references 124 and 127) while  $\Delta H_1$  for N,N'-dimethylethylenediamine is  $-10.74 \text{ kcal mol}^{-1}$  <sup>121</sup> (and Table 6.6). Therefore, the effect of a  $\text{CH}_2\text{NHCH}_3$  substituent reduces the  $-\Delta H^\circ$  for protonation of dimethylamine by  $+12.04 - (+10.74) = 1.3 \text{ kcal mol}^{-1} = \delta(\text{CH}_2\text{NHCH}_3)$ . The formula proposed by Paoletti and coworkers <sup>127</sup> for predicting the enthalpy changes for diamine protonation is

$$-\Delta H = \Delta H(\text{NH}_2) + \sum_n \left(\frac{1}{2}\right)^{n-1} \cdot \delta(\text{C}) + \left(\frac{1}{2}\right)^{n-1} \cdot \delta(\text{NH}_2) + \left(\frac{1}{2}\right)^{n-1} \delta(\text{NH}_3^+)$$

where  $n$  is the position of the atom with respect to the amino group being protonated (numbered in I above),  $\Delta H(\text{NH}_2)$  is an empirical value for the protonation of an  $\text{NH}_2$  group,  $\delta(\text{C}) = 0.66 \text{ kcal mol}^{-1}$  represents the effect of a carbon in position 1 on the enthalpy of protonation and  $\delta(\text{NH}_2)$  and  $\delta(\text{NH}_3^+)$  have similar interpretations. For the compound I the formula reduces to

$$-\Delta H = \Delta H(\text{NH}) + \sum_n \left(\frac{1}{2}\right)^{n-1} \cdot \delta(\text{C}) + \delta(\text{CH}_2\text{NHCH}_3)$$



where  $\delta(\text{CH}_2\text{NHCH}_3)$  is the effect of the  $\text{CH}_2\text{NHCH}_3$  group on the enthalpy of protonation of I.  $\Delta\text{H}(\text{NH})$  was reported by Paoletti as  $10.8 \text{ kcal mol}^{-1}$ . The term  $\delta(\text{CH}_2\text{NHCH}_3)$  was obtained as described above. Therefore, by summing the effects of the carbon atoms in the alkyl chain

$$-\Delta\text{H} = 10.8 + (1 + 1 + \frac{3}{2} + \frac{1}{4} + \frac{1}{8})0.66 - 1.3 \text{ kcal mol}^{-1}$$

$$-\Delta\text{H} = 12.06 \text{ kcal mol}^{-1} (50.5 \text{ kJ mol}^{-1})$$

(The formula reported by Christensen<sup>124</sup> gives a value of  $-50.8 \text{ kJ mol}^{-1}$  using the same  $\delta(\text{CH}_2\text{NHCH}_3)$  value.)

Similarly, the second stepwise protonation of the diamine-dioxime ligand without the oxime substituents can be estimated by calculating the enthalpy of protonation of I with a proton on the nitrogen atom labelled (a). The effect of the substituent  $\text{CH}_2\text{N}^+\text{HCH}_3$  is estimated from the  $\Delta\text{H}$  values for  $(\text{CH}_3)_2\text{NH}$  and for the second protonation of N,N'-dimethylethylenediamine. The difference between these values is  $-2.37 \text{ kcal mol}^{-1}$ . Using Paoletti's formula the predicted enthalpy of protonation (of the cation of I) is  $-11.0 \text{ kcal mol}^{-1}$  ( $-46 \text{ kJ mol}^{-1}$ ). If it can be assumed that the effect of a  $\text{CH}_2\text{NHCH}_3$  substituent is not too different from a  $\text{CH}_2\text{NH}-\text{C}(\text{CH}_3)_2\text{CH}_2\text{CH}_2\text{CH}_3$  substituent, then the values of  $-50.5$  and  $-46.0 \text{ kJ mol}^{-1}$  will be approximately representative of the enthalpy changes for the protonation of the model

ligand II. These values could be regarded as upper limit values for the stepwise protonation enthalpies of this compound.

#### Effect of Oxime Substituents

Little information on the base weakening effect of an oxime substituent is available. A recent compilation of Taft  $\sigma^*$  values<sup>128</sup> does not report a value for the C = NOH function. Wang, Bauman and Murmann<sup>8</sup> have determined the free energy and enthalpy changes for protonation of several  $\alpha$ -amine oximes of the form



where R is a hydrogen atom or an alkyl group. A comparison of this data with that for the corresponding amine without the oxime substituents would enable the base weakening effect of the C = NOH group to be estimated. The data for AO (R = H in III) and MeAO (R = CH<sub>3</sub>) and the data for the corresponding monoamines calculated using the empirical formula of Christensen et al.<sup>124</sup> are given in Table 6.7.

Table 6.7

	log k	$-\Delta G(\text{kcal mol}^{-1})$	$-\Delta H(\text{kcal mol}^{-1})$	$\Delta S(\text{e.u.})$
AO	9.09	12.4	12.7	-1
amine	10.74	14.65	14.58	+3
MeAO	9.24	12.6	10.3	8
amine	11.05	15.07	13.3	5.9

The base weakening effect (the difference in the log k values) is 1.65 from the AO data and 1.8 from the MeAO data.

Substituent effects diminish with distance from the basic centre; a transmission factor of 0.50 per carbon atom in the chain has previously been used<sup>123</sup>. Assuming that the log k values for N,N'-dimethylethylenediamine would be similar to those for the diamine-dioxime ligand without the oxime substituents, then using a base weakening effect of 0.8, the predicted log k values for the diamine-dioxime ligand at I = 0.00 M would be 9.2 and 6.0 which agree well with the measured values (see Table 6.4) of 9.35 and 5.89.

#### Enthalpy Changes

For most carbon and nitrogen substituted 1,2-diaminoethanes  $-\Delta H_1$  for the first stepwise protonation of the diamine is larger than  $-\Delta H_2$ , the enthalpy of protonation for the diaminemonocation<sup>5,124</sup>. From a consideration of the electrostatics of protonation, this difference is not

unexpected<sup>129</sup>. Naturally enough, these differences between  $\Delta H_1$  and  $\Delta H_2$  are dependent on the substituents on the amine. For example, for ethylenediamine the difference is 2.8 kJ mol<sup>-1</sup>, for N,N'-dimethylethylenediamine 5.9 kJ mol<sup>-1</sup> (Table 6.6) and for N,N,N',N'-tetramethylethylenediamine 3.2 kJ mol<sup>-1</sup> (0.5 M KNO<sub>3</sub>; ref. 121).

The values calculated for the protonation of the hypothetical diamine-dioxime without the oxime substituents were + 50 and + 46 kJ mol<sup>-1</sup> for  $-\Delta H_1$  and  $-\Delta H_2$  respectively. The enthalpy data for the diamine-dioxime protonation (Table 6.6) shows that the introduction of the oxime groups has caused a decrease in the exothermic enthalpy changes for both of the stepwise protonation reactions relative to those estimated for the hypothetical diamine compound. Also, for this diamine-dioxime ligand the values of the stepwise enthalpy changes for protonation are equal within the estimated experimental error.

In view of the weak basicity of the C = NOH group the solvating properties for this group should not be too dissimilar from those of an OH group. The decrease for  $-\Delta H_2$  from +46 kJ mol<sup>-1</sup> for the hypothetical amine to 39 kJ mol<sup>-1</sup> for the diamine-dioxime appears reasonable on comparison with the differences between the enthalpy of protonation of some  $\beta$ -hydroxyamines<sup>59</sup> and the corresponding parent alkyl amines. However, a difference of 10 kJ mol<sup>-1</sup> between  $-\Delta H_1$  for the

diamine dioxime and hypothetical amine is slightly larger.

Qualitatively, the low exothermic enthalpy change for the first stepwise protonation could be interpreted in terms of an intramolecular hydrogen bonding interaction in the free ligand between the unprotonated amine nitrogen and the oxime function. This would have the effect of decreasing the exothermic enthalpy on protonation, this decrease depending on the strength of the intramolecular interaction. Intramolecular hydrogen bonding has often been proposed to explain anomalies in basicity constants or in thermodynamic properties<sup>130,131</sup>, although for this ligand there are no apparent anomalies in the log *k* values. Clearly it would be desirable to have some independent evidence of hydrogen bond formation, especially in terms of the definition adopted by Pimentel and McClellan<sup>118</sup>: "A hydrogen bond is said to exist when:

- (i) there is evidence of a bond, and
- (ii) there is evidence that this bond specifically involves a hydrogen atom already bonded to another atom."

As it is difficult to accurately assess the hydration enthalpies of the ions and molecules of the type in these protonation reactions no attempt was made to obtain information on the gas phase enthalpy changes.

### Entropy Changes

As discussed in Chapter 1, the main contribution to the overall entropy change for protonation of amines in aqueous solution arises from the effect of the solvent. For the reaction  $L + H^+ \rightleftharpoons LH^+$  the entropy change is dependent on the solvent ordering abilities of the species  $L$ ,  $H^+$  and  $LH^+$ . For the diamine-dioxime ligand the gem dimethyl groups in close proximity to the amine nitrogens will provide a shielding of the solvent, to a certain degree, from the charge on the protonated amine nitrogen. Thus on protonation of the ligand, liberation of water molecules from the field of the proton will contribute a positive entropy change. The contribution to the entropy change from configurational changes in the ligand are difficult to assess. If there was no hydrogen bonding in the free molecule then on protonation a decrease in entropy due to chain stiffening<sup>68</sup> would be expected. However, if the oxime function was intramolecularly hydrogen bonded to the amine then the contribution to the overall entropy change for the first stepwise protonation might be expected to be close to zero. The entropy changes for the two stepwise protonations are shown in Table 6.6. On correcting for the statistical term these changes in Table 6.6 become  $40.5 \text{ J mol}^{-1}\text{K}^{-1}$  and  $-13.6 \text{ J mol}^{-1}\text{K}^{-1}$  for the first and second stepwise protonations respectively. From these entropy changes it is not possible to obtain insight into

the conformational changes on protonation. For the first stepwise protonation the entropy change is similar to that for N,N'-dimethylethylenediamine (Table 6.6).

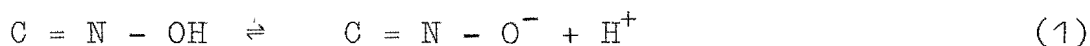
For an ion with two identical charged centres separated by a distance of  $> \text{ca. } 10\text{\AA}^0$  the solvent ordering abilities of the ion would be approximately twice that of each charged centre on the ion. However, it can be readily shown that for an ion with two coincident charged centres the volume of solvent influenced by this centre will be 2.8 times as great as that for a single charged centre<sup>68</sup>. Thus, in the stepwise protonation  $\text{LH}^+ + \text{H}^+ \rightleftharpoons \text{LH}_2^{2+}$  for N,N'-dimethylethylenediamine, where the two charge centres in the dication are separated by only two carbon atoms, the solvent ordering ability of the dication will be greater than twice that of the monocation  $\text{LH}^+$ . The entropy change for this protonation  $\Delta S_2^0$  would be expected to be considerably less positive than that for the protonation  $\text{L} + \text{H}^+ \rightleftharpoons \text{LH}^+$  ( $\Delta S_1^0$ ). The data in Table 6.6 shows a difference between  $\Delta S_1^0$  and  $\Delta S_2^0$  for N,N'-dimethylethylenediamine of ca.  $42 \text{ J mol}^{-1}\text{K}^{-1}$ .

Similarly for the diamine-dioxime protonation reactions  $\Delta S_2^0$  would be expected to be less positive than  $\Delta S_1^0$  as the amine nitrogens are only separated by two carbon atoms. Also, the predominantly hydrophobic substituents on the amine nitrogens will undergo a considerable loss of configurational entropy due to chain stiffening<sup>68,125</sup> when

the amine nitrogens are protonated. Thus, the overall entropy change  $\Delta S_2^0$  for the diamine-dioxime ligand would be expected to be considerably less positive than the  $\Delta S_1^0$  value. The data in Table 6.6 shows that the  $\Delta S_2^0$  value is in fact considerably negative and that the difference between  $\Delta S_1^0$  and  $\Delta S_2^0$  is ca.  $66 \text{ J mol}^{-1} \text{ K}^{-1}$ .

### 6.1.3 Proton Dissociation from an Oxime Group

The proton of an oxime functional group is weakly acidic,



To date, most studies of oxime ionisation have been concerned with the ionisation of vic-dioximes<sup>6,7</sup> or in compounds where the oxime is attached to an aromatic system<sup>5,13c</sup> e.g. in salicylaldoxime. The  $\text{pK}_a$  values for the ionisation (1) of a few of these oximes are given in Table 6.8. The values show that the oxime group is very weakly acidic, the magnitude of the  $\text{pK}_a$  depending on the environment of the oxime grouping. In the first ionisation of vic-dioximes there is a possibility of hydrogen bonding of the oximato group with the unionised oxime function, which would increase the stability of the anion. A similar effect could exist in salicylaldoxime. Thus it might be expected that the  $\text{pK}$  for an isolated monoxime group would be larger than the values found for say, dimethylglyoxime. The  $\text{pK}$  for acetoxime has been reported as ca. 12 although no reference to the



TABLE 6.8

The  $pK_a$  for ionisation of a number of oximes

<u>Compound</u>	<u>Method</u>	<u>Conditions</u>	<u><math>pK_1</math></u>	<u><math>pK_2</math></u>	<u>reference</u>
DMG	UV spectra	0.1M(aq.NaCl), 23°C	10.65	11.9	(a)
DMG	pH	water/dioxan→0% dioxan	10.48	-	(b)
DMG	pH	50% glyoxan, 25°C	12.83	-	(e)
DMG	spectra	?	10.57	-	(d)
DMG	pH	50% dioxan	12.84	-	(c)
Acetoxime	?	?	~12	-	(f)
pyridine-2-aldoxime	spectra	I = 0, 25°C	10.22	-	(g)
pyridine-2-aldoxime	pH	0.1(KNO <sub>3</sub> ), 24°C	10.02	-	(h)
salicylaldoxime	pH	75% dioxan-water, 30°C	11.72	-	(i)

(a) Reference 134.

(b) Reference 6.

(c) R.G. Charles and H. Freiser, *Analyt.Chim.Acta*, 11, 101 (1954).(d) V.M. Sovostina, E.K. Astakhova and V.M. Peshkova, *Chem.Abs.* 59, 1062a (1963).(e) V.M. Bochkova and V.M. Peshkova, *Zhur.Neorg.Khim.*, 3, 1131 (1958).(f) A.A. Grinberg, A.I. Stetsenko and S.G. Strelin, *Russ.J.Inorg.Chem.*, 13, 569 (1968).

(g) Reference 170.

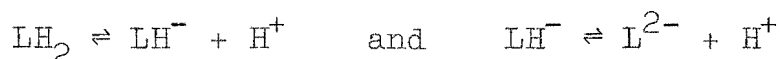
(h) S. Bolton and R.I. Ellin, *J.Pharm.Sci.*, 51, 533 (1962).

(i) Reference 132.

source of this value was given.

### Oxime Ionisation in the Diamine-Dioxime Ligand

For this ligand there are two possible ionisations



with equilibrium constants (for protonation) given by

$$k_2 = \frac{[\text{LH}_2]}{[\text{LH}^-][\text{H}]} \quad \text{and} \quad k_1 = \frac{[\text{LH}^-]}{[\text{L}][\text{H}]} .$$

Attempts were made to obtain an approximate estimate of the possible ionisation constants for the oxime functions of this ligand both by pH and U.V. spectral methods.

### pH Method

In this diamine-dioxime ligand the oxime nitrogen atoms are separated by 10 atoms; thus to a first approximation the ionisations would be independent, i.e.  $k_1 \approx k_2$ . This approximation together with the mass balance equation for  $T_L$  and the electroneutrality equation gives three equations in three unknowns which can be solved to obtain an estimate of the ionisation constant for the oxime function.  $p[\text{H}^+]$  data in the range 10.5 - 12.1 from a titration of a neutral free ligand ( $\text{LH}_2$ ) solution with NaOH were analysed in terms of one constant and no fit to the data could be obtained. A least squares analysis in terms of the constants  $k_1$  and  $k_2$  also did not yield any fit to the data.

### U.V. Spectral Study

The U.V. spectrum of a non-conjugated oxime function is generally centred in the far U.V. below 190 nm, e.g. the  $\lambda_{\text{max}}$  for the  $\Pi \rightarrow \Pi^*$  transition in cyclohexanone oxime is equal to 189 nm ( $\epsilon = 7,800$ )<sup>133</sup>. However, the U.V. spectrum for dimethylglyoxime (conjugated oxime) has an absorption band at ~230 nm which, on the addition of alkali shifts to ~260 nm.<sup>134</sup> This shift has been attributed to the ionisation of one of the oxime groups<sup>134</sup>.

For the diamine-dioxime ligand the tail of an intense absorption band extended to about 240 nm. On the addition of alkali there was a shift in this absorption which caused the tail to extend to ~270 nm. It was assumed that this shift was due to an ionisation of the oxime function. In alkaline solution it was difficult to obtain accurate spectra below ~225 due to the intense absorption of the  $\text{CO}_3^{2-}$  at 218 nm ( $\epsilon \sim 10,000$ )<sup>135</sup>.

The measured pH and the absorption spectrum from ca. 220-270 nm for a number of solutions of the free oxime  $\text{LH}_2$ , NaOH and NaCl ( $I = 0.20 \text{ M}$ ) were recorded. The results are shown in Table 6.9. To ensure that the absorption due to the carbonate ion was small, the spectra for a number of NaOH and NaCl solutions ( $I = 0.20 \text{ M}$ ) were also recorded.

Irving Rossotti and Harris<sup>136</sup> have reported a method for the determination of acid dissociation constants from

TABLE 6.9

Data from UV spectra of the diamine-dioxime

I = 0.20M (NaCl) and at 25°C

<u>pH</u>	<u>p[H<sup>+</sup>]<sup>a</sup></u>	<u>[NaOH]<sub>added</sub></u>	<u>A<sub>240mμ</sub><sup>b</sup></u>	<u>10<sup>12</sup>[H<sup>+</sup>]</u>	<u>10<sup>-3</sup>A/2.T<sub>L</sub></u>
11.603	11.535	0.00674	0.425	2.917	0.865
11.921	11.863	0.01348	0.455	1.371	0.926
12.227	12.175	0.02696	0.518	0.668	1.05 <sub>4</sub>
12.524	12.477	0.05393	0.562	0.333	1.14 <sub>4</sub>
12.618	12.573	0.06741	0.585	0.267	1.19 <sub>0</sub>
12.695	12.652	0.08089	0.597	0.223	1.21 <sub>5</sub>
12.811	12.770	0.10786	0.605	0.170	1.23 <sub>1</sub>

<sup>a</sup> Interpolated from a calibration curve of pH<sub>meas</sub> vs. p[H<sup>+</sup>]  
which was established using NaOH/NaCl solutions.

<sup>b</sup> Concentration of diamine-dioxime is 2.45<sub>7</sub> x 10<sup>-4</sup>M, cell path  
length = 1 cm.

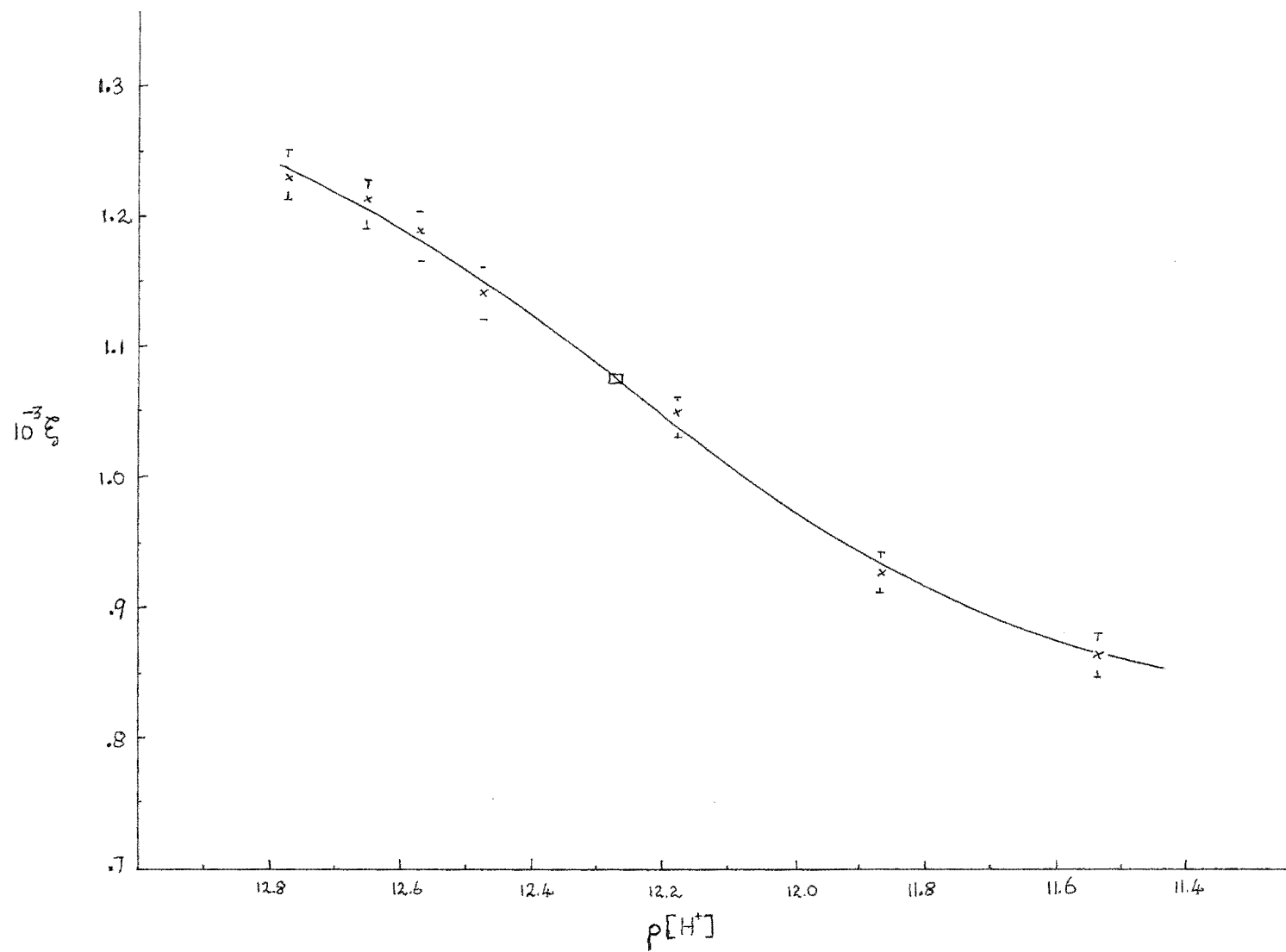


**Fig 6.3** Determination of the  $pK_a$  for proton ionisation

absorbance measurements, without prior knowledge of the extinction coefficients for the species involved. It is assumed that in the ligand the two oxime functions are completely independent. Consider a monooxime species HL which on ionisation gives the species  $L^-$  and  $H^+$ ; the absorbance of the solution is given by  $A_s = \ell(\epsilon_o[L] + \epsilon_1[HL] + \epsilon_H[H])$  where  $\ell$  is the path length and  $\epsilon_o$ ,  $\epsilon_1$ ,  $\epsilon_H$  are the extinction coefficients of the species L, HL and H respectively. A quantity  $\xi$  is now defined

$$\begin{aligned}\xi &= \frac{A_s - \ell\epsilon_H[H]}{T_L \ell} \\ &= \frac{\epsilon_o + \epsilon_1\beta_1[H]}{1 + \beta_1[H]}\end{aligned}$$

where

$$\beta_1 = [HL]/[L][H].$$

The condition that  $d^2\xi/d(pH)^2 = 0$  is that  $\log \beta_1 = pH^{136}$ , i.e. the pH is equal to the pK for the ionisation of HL.

Thus from a plot of  $\xi$  against pH the value of the pH where the slope of the curve is greatest is equal to the pK for the ionisation. Such a plot, along with the estimated point of maximum slope, is shown in Fig. 6.3. Although the data is not particularly accurate, at least a lower limit to the pK can be estimated. The value of  $12.3 \pm 0.2$  is considerably larger than that for DMG and does compare favourably with the value reported for acetoxime.

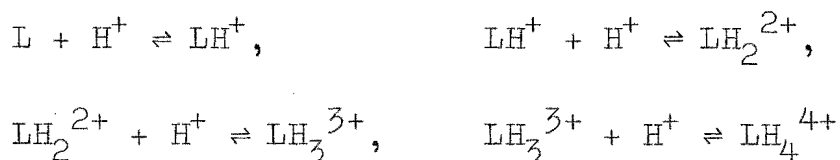
The magnitude of this pK for the oxime function also implies that under the conditions for study of the copper complexes the equilibrium (1) is not important (see Chapter 7).

## 6.2 PROTONATION OF THE TETRAAMINES 3,2,3-tet AND hm-3,2,3-tet

### 6.2.1 Results

Data from the pH titrations of the amines are shown in Tables 6.10 and 6.11. Only one titration from a set of reproducible titrations has been reported. The data are also graphically represented in Figs 6.4 and 6.5. The formation curve for 3,2,3-tet in Fig. 6.4 shows only one marked point of inflexion at  $\bar{n} = 3$  while that for hm-3,2,3-tet in Fig. 6.5 shows two at  $\bar{n} = 3$  and  $\bar{n} = 2$ . The differences between the two formation curves indicate different stepwise basicities for the two ligands.

The protonation of each tetraamine can be represented by four stepwise equilibria;



with concentration quotients given by

$$k_1 = \frac{[\text{LH}]}{[\text{L}][\text{H}]} \quad k_2 = \frac{[\text{LH}_2]}{[\text{LH}][\text{H}]} \quad k_3 = \frac{[\text{LH}_3]}{[\text{LH}_2][\text{H}]} \quad k_4 = \frac{[\text{LH}_4]}{[\text{LH}_3][\text{H}]}$$

The quotients  $k_1$ ,  $k_2$ ,  $k_3$  and  $k_4$  were calculated as described

**Fig 6.4**

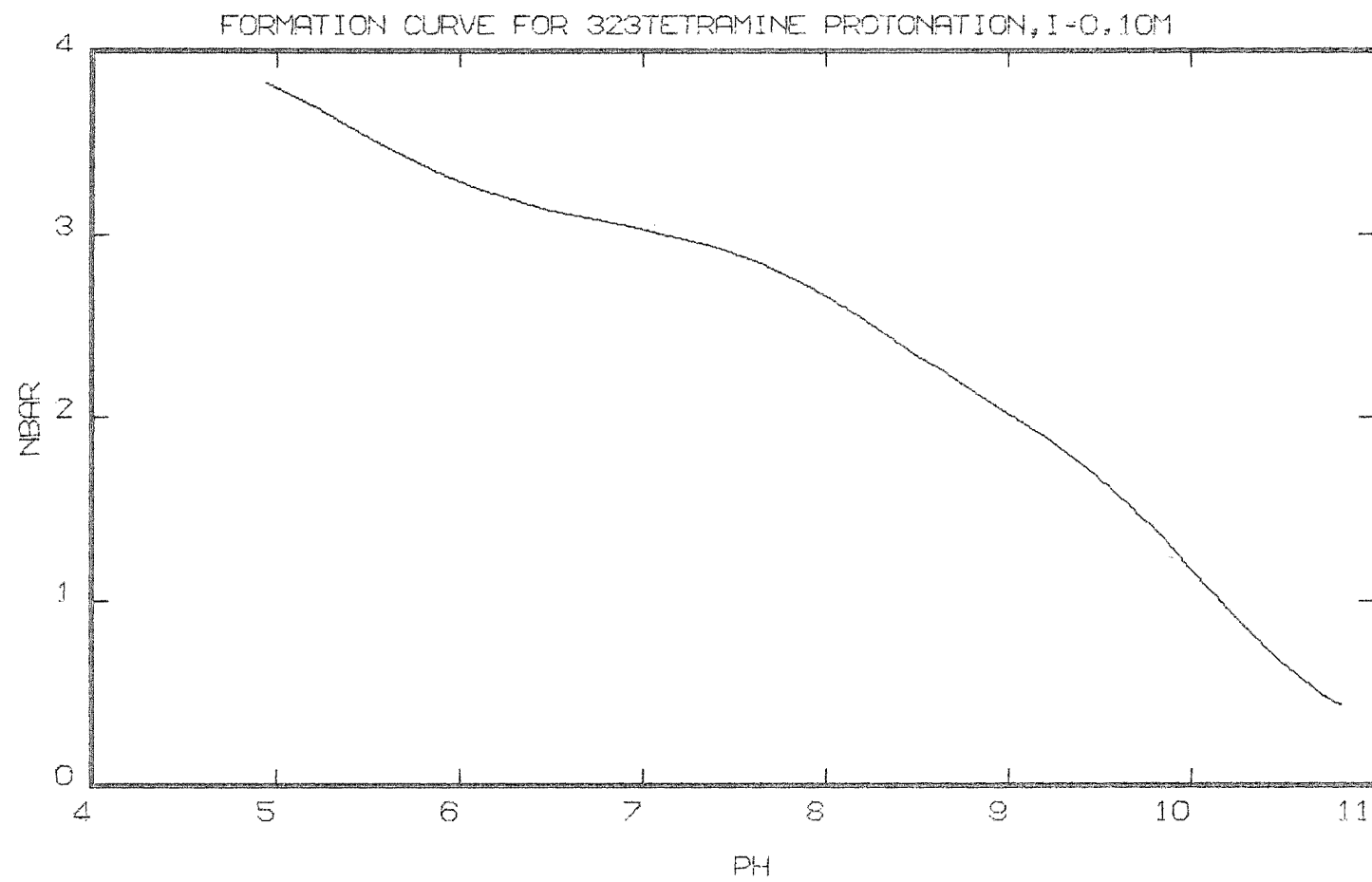




**Fig 6.5**

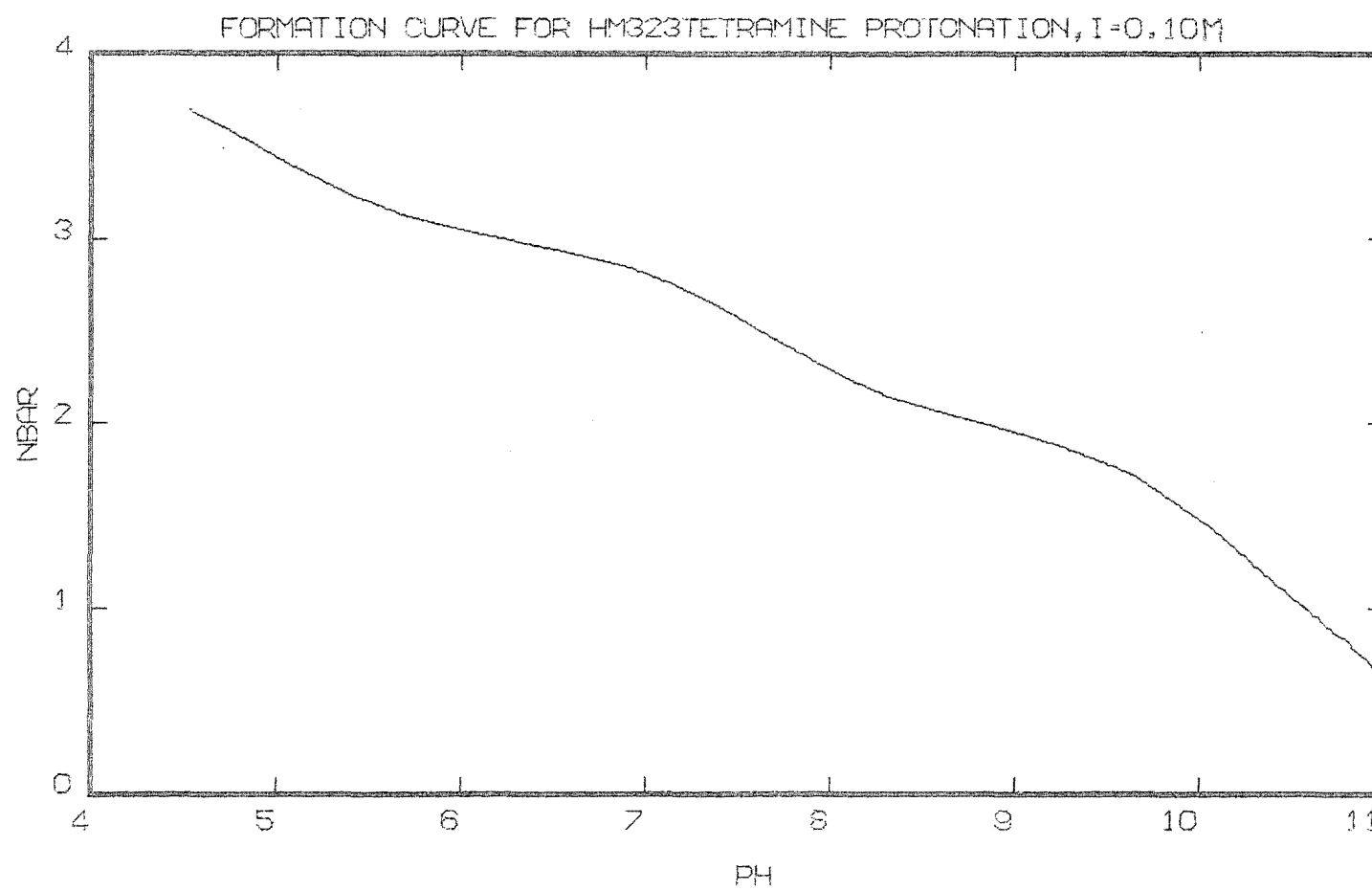


TABLE 6.10

pH titration data<sup>a</sup> from the hm-3,2,3 tet/HCl system  
titrated with NaOH at 25°C and 0.10M (NaCl)

Volume	$\bar{n}$	p[H <sup>+</sup> ]	Volume	$\bar{n}$	p[H <sup>+</sup> ]
0.010	3.852	4.128	0.110	1.957	8.970
0.015	3.782	4.338	0.115	1.873	9.265
0.020	3.699	4.530	0.120	1.793	9.476
0.025	3.610	4.706	0.125	1.717	9.640
0.030	3.517	4.871	0.130	1.643	9.768
0.035	3.422	5.037	0.135	1.573	9.877
0.040	3.326	5.217	0.140	1.505	9.973
0.045	3.229	5.424	0.150	1.378	10.133
0.050	3.132	5.684	0.160	1.265	10.271
0.055	3.034	6.067	0.170	1.166	10.389
0.060	2.935	6.557	0.180	1.077	10.490
0.065	2.836	6.921	0.190	1.002	10.582
0.070	2.736	7.174	0.200	0.937	10.663
0.075	2.637	7.375	0.210	0.881	10.735
0.080	2.538	7.552	0.220	0.833	10.801
0.085	2.439	7.722	0.230	0.778	10.855
0.090	2.340	7.896	0.250	0.687	10.952
0.090	2.241	8.090	0.270	0.608	11.034
0.100	2.143	8.321	0.290	0.539	11.105
0.105	2.048	8.621			

<sup>a</sup> Solution composition:  $T_L = 9.640 \times 10^{-4}M$ ,  $T_H = 3.979 \times 10^{-3}M$ ,  
Initial volume = 49.94 ml and titrant [NaOH] = 0.9569M.

TABLE 6.11

Representative data<sup>a</sup> from the titrations of 1,5,8,12-tetraazadodecane/HCl solutions<sup>b</sup> against NaOH at ionic strengths of 0.20, 0.15, 0.10 and 0.04 M, NaCl media

I = 0.04			I = 0.10			I = 0.15			I = 0.20		
NaOH (ml)	$\bar{n}^c$	$p[H^+]^d$	NaOH (ml)	$\bar{n}$	$p[H^+]$	NaOH (ml)	$\bar{n}$	$p[H^+]$	NaOH (ml)	$\bar{n}$	$p[H^+]$
.215	3.832	4.689	.160	3.826	4.938	.160	3.827	5.000	.160	3.828	5.057
.220	3.723	4.920	.170	3.632	5.329	.170	3.633	5.399	.170	3.634	5.461
.223	3.656	5.048	.175	3.534	5.503	.180	3.436	5.750	.180	3.436	5.816
.226	3.588	5.171	.180	3.435	5.679	.190	3.237	6.173	.190	3.238	6.568
.233	3.427	5.461	.185	3.336	5.876	.200	3.038	6.935	.200	3.038	7.033
.240	3.265	5.808	.190	3.237	6.116	.210	2.840	7.681	.210	2.840	7.745
.250	3.033	6.743	.200	3.038	6.925	.220	2.641	8.082	.220	2.642	8.138
.260	2.800	7.552	.210	2.839	7.637	.230	2.444	8.392	.230	2.444	8.445
.270	2.568	7.979	.215	2.740	7.851	.240	2.248	8.685	.240	2.249	8.734
.280	2.336	8.339	.220	2.641	8.026	.250	2.056	8.978	.250	2.058	9.020
.285	2.220	8.524	.230	2.443	8.338	.260	1.870	9.257	.260	1.873	9.291
.290	2.106	8.714	.235	2.345	8.485	.270	1.691	9.493	.270	1.696	9.521
.300	1.882	9.089	.240	2.247	8.636	.280	1.519	9.688	.280	1.527	9.711
.310	1.665	9.396	.245	2.150	8.789	.290	1.356	9.854	.290	1.366	9.873
.315	1.560	9.525	.250	2.054	8.941	.300	1.200	8.994	.300	1.213	10.014
.320	1.457	9.640	.255	1.959	9.088	.310	1.059	10.129	.310	1.072	10.141
.330	1.259	9.844	.260	1.866	9.227	.320	0.926	10.252	.320	0.945	10.261
.340	1.072	10.020	.270	1.686	9.468	.330	0.810	10.364	.330	0.830	10.369
.350	0.902	10.183	.280	1.512	9.667	.340	0.707	10.465	.340	0.729	10.468
.360	0.753	10.333	.290	1.345	9.836	.350	0.622	10.562	.350	0.645	10.560
.370	0.629	10.473	.300	1.187	9.984	.360	0.550	10.649	.360	0.573	10.644
.380	0.527	10.597	.310	1.041	10.120	.370	0.496	10.730	.370	0.514	10.721
.390	0.451	10.709	.320	0.907	10.245	.380	0.446	10.801	.380	0.466	10.791
.400	0.388	10.806	.330	0.788	10.361				.400	0.392	10.911
			.340	0.684	10.468						
			.350	0.600	10.569						
			.360	0.528	10.659						
			.380	0.428	10.817						

<sup>a</sup> The  $\log K$  values reported in Table 3.6 are the average values obtained from a number of titrations.

<sup>b</sup> Composition of solutions: I = 0.04; [NaOH] = 1.268M,  $T_H = 9.653 \times 10^{-3}M$ ,  $T_B = 1.088 \times 10^{-3}M$ , initial volume = 49.9 mls. I = 0.10, 0.15, 0.20; [NaOH] = 1.269M,  $T_H = 7.752 \times 10^{-3}M$ ,  $T_B = 1.103 \times 10^{-3}M$ , initial volume = 49.9 mls.

<sup>c</sup>  $\bar{n}$  is the degree of formation.

<sup>d</sup>  $p[H^+]$  values were calculated from the calibration curve.

in Chapter 4. The results ( $\log k_1$  values) and their estimated uncertainties are shown in Table 6.15. For 3,2,3-tet thermodynamic constants  $k_n^0$  have also been calculated (Table 3.6), however the data at  $I = 0.10$  M has been used in the discussion as thermodynamic data for related ligands are scarce.

Data from the calorimetric titrations of the amines with standard HCl are shown in Tables 6.12 and 6.13. Tables 6.12 and 6.13 show the solution composition data (calculation procedure Chapter 5) for the titrations of 3,2,3-tet and hm-3,2,3-tet respectively. Tables 6.12a and 6.13a give the heat changes and the differences in solution composition between successive titration points for the titrations of 3,2,3-tet and hm-3,2,3-tet respectively. In these tables  $Q_m$  are the measured heat changes, corrected for the heat of dilution of HCl, and  $Q_{corr}$  are the  $Q_m$  values, corrected for the secondary reaction  $H^+ + OH^- \rightarrow H_2O, \Delta H^0 = -55.84 \text{ kJ mol}^{-1}$  <sup>56</sup>. The  $Q_{calc}$  values are the values calculated from the least squares calculation of the stepwise enthalpy changes (see page 77, Chapter 5).

The enthalpy, entropy and free energy changes for the stepwise protonation reactions at  $I = 0.10$  (NaCl) and  $25^\circ\text{C}$  for the ligands 3,2,3-tet and hm-3,2,3-tet are given in Table 6.15.

TABLE 6.12

Calorimetric data from titrations<sup>a</sup> of 3,2,3-tet with HCl at 25°C

Vol. <sup>b</sup> (ml)	p[H <sup>+</sup> ]	$\bar{n}$	$\underline{L}^c$ (mmol)	$\underline{LH}$ (mmol)	$\underline{LH}_2$ (mmol)	$\underline{LH}_3$ (mmol)	$\underline{LH}_4$ (mmol)
0.000	10.898	0.337	0.26006	0.11137	0.00829	0.00002	0.00000
0.270	10.626	0.536	0.19845	0.15904	0.02215	0.00010	0.00000
0.530	10.352	0.794	0.13064	0.19701	0.05163	0.00046	0.00000
0.805	10.054	1.109	0.06819	0.20382	0.10587	0.00186	0.00000
1.075	9.735	1.439	0.02664	0.16623	0.18025	0.00662	0.00000
1.325	9.371	1.755	0.00696	0.10028	0.25119	0.02132	0.00000
1.605	8.842	2.117	0.00065	0.03181	0.26974	0.07750	0.00004
1.905	8.248	2.510	0.00003	0.00529	0.17584	0.19816	0.00044
2.235	7.227	2.944	0.00000	0.00008	0.02899	0.34276	0.00790
2.585	5.754	3.405	0.00000	0.00000	0.00064	0.22486	0.15425
0.270 <sup>d</sup>	10.626	0.536	0.19845	0.15904	0.02215	0.00010	0.00000
0.530	10.352	0.794	0.13064	0.19701	0.05163	0.00046	0.00000
0.790	10.071	1.091	0.07113	0.20460	0.10228	0.00173	0.00000
1.070	9.741	1.433	0.02721	0.16730	0.17875	0.00647	0.00000
1.330	9.363	1.762	0.00673	0.09883	0.25235	0.02183	0.00000
1.610	8.832	2.124	0.00062	0.03099	0.26899	0.07910	0.00005
1.920	8.217	2.530	0.00002	0.00475	0.16949	0.20500	0.00048
2.250	7.133	2.964	0.00000	0.00005	0.02357	0.34620	0.00991
2.620	5.673	3.451	0.00000	0.00000	0.00049	0.20768	0.17157
0.000 <sup>e</sup>	9.817	1.358	0.03477	0.17933	0.16076	0.00488	0.00000
0.290	9.402	1.732	0.00786	0.10563	0.24673	0.01953	0.00000
0.570	8.864	2.102	0.00073	0.03371	0.27129	0.07397	0.00004
0.860	8.276	2.492	0.00003	0.00583	0.18168	0.19181	0.00039
1.160	7.423	2.896	0.00000	0.00020	0.04393	0.33076	0.00486
1.470	5.921	3.314	0.00000	0.00000	0.00108	0.25824	0.12042

<sup>a</sup> Initial solution composition:- Titrations 1 and 2;  $T_L = 3.842 \times 10^{-3}M$ ,  $T_H = 0.0$ ; initial volume = 98.84 ml, titrant HCl = 0.5002M. Titration 3;  $T_L = 3.842 \times 10^{-3}M$ ,  $T_H = 5.108 \times 10^{-3}M$ , initial volume 98.84 ml, titrant HCl = 0.5128M.

<sup>b</sup> Cumulative volume of HCl added at each titration point.

<sup>c</sup> Values for all ligand species are the number of mmoles of each titration point.

<sup>d</sup> Titration 2.

<sup>e</sup> Titration 3.

TABLE 6.12a

Changes in composition and the heat changes for 3,2,3-tet/HCl  
titrations

R(LH) <sup>a</sup>	S(LH <sub>2</sub> )	T(LH <sub>3</sub> )	U(LH <sub>4</sub> )	Q <sub>m</sub> <sup>b</sup>	Q <sub>corr</sub> <sup>b</sup>	Q <sub>calc</sub> <sup>b</sup>
0.06161	0.01394	0.00008	0.00000	7.233	3.914	3.908
0.06781	0.02984	0.00035	0.00000	6.857	5.067	5.064
0.06245	0.05564	0.00140	0.00000	7.171	6.162	6.170
0.04155	0.07914	0.00476	0.00000	7.000	6.463	6.453
0.01968	0.08564	0.01470	0.00000	6.353	6.072	6.089
0.00631	0.07477	0.05622	0.00004	6.729	6.577	6.626
0.00062	0.02715	0.12105	0.00039	6.725	6.678	6.671
0.00003	0.00523	0.15207	0.00747	7.045	7.030	7.082
0.00000	0.00008	0.02844	0.14635	6.257	6.255	6.210
0.06781	0.02984	0.00035	0.00000	6.842	5.052	5.064
0.05952	0.05193	0.00127	0.00000	6.792	5.824	5.820
0.04391	0.08121	0.00474	0.00000	7.267	6.697	6.681
0.02049	0.08896	0.01537	0.00000	6.648	6.356	6.332
0.00611	0.07394	0.05730	0.00004	6.771	6.622	6.619
0.00060	0.02684	0.12634	0.00044	6.986	6.939	6.884
0.00002	0.00472	0.15064	0.00943	6.993	6.979	7.061
0.00000	0.00005	0.02314	0.16165	6.463	6.462	6.501
0.02691	0.10062	0.01465	0.00000	7.621	7.256	7.236
0.00713	0.07904	0.05448	0.00004	6.967	6.805	6.815
0.00070	0.02858	0.11820	0.00036	6.688	6.639	6.625
0.00003	0.00567	0.14341	0.00446	6.658	6.643	6.630
0.00000	0.00020	0.04305	0.11557	5.876	5.874	5.799

<sup>a</sup> Values are the changes in the number of mmoles between successive titration points (as recorded in Table 6.12; calculations described Chapter 5).

<sup>b</sup> Defined in text.

TABLE 6.13

Calorimetric data from titrations<sup>a</sup> of hm-3,2,3-tet with HCl at 25°C

Vol. <sup>b</sup> (ml)	p[H <sup>+</sup> ]	$\bar{n}$	L <sup>c</sup> (mmol)	LH (mmol)	LH <sub>2</sub> (mmol)	LH <sub>3</sub> (mmol)	LH <sub>4</sub> (mmol)
0.000	11.220	0.470	0.24997	0.18492	0.01276	0.00000	0.00000
0.300	11.037	0.608	0.19916	0.22482	0.02366	0.00001	0.00000
0.580	10.829	0.779	0.14301	0.26040	0.04421	0.00003	0.00000
0.860	10.582	0.994	0.08630	0.27784	0.08341	0.00009	0.00000
1.130	10.301	1.237	0.04198	0.25777	0.14759	0.00030	0.00000
1.400	9.965	1.507	0.01447	0.19273	0.23938	0.00107	0.00000
1.675	9.471	1.799	0.00217	0.09037	0.35023	0.00487	0.00000
1.945	8.465	2.099	0.00002	0.00978	0.38381	0.05402	0.00001
2.220	7.761	2.413	0.00000	0.00131	0.26043	0.18565	0.00026
2.520	7.133	2.756	0.00000	0.00013	0.11074	0.33481	0.00197
Titration 2							
0.000	11.221	0.470	0.24988	0.18456	0.01271	0.00000	0.00000
0.275	11.054	0.594	0.20381	0.22099	0.02234	0.00001	0.00000
0.545	10.858	0.755	0.15031	0.25612	0.04070	0.00002	0.00000
0.820	10.620	0.960	0.09404	0.27697	0.07607	0.00007	0.00000
1.090	10.346	1.199	0.04758	0.26337	0.13595	0.00025	0.00000
1.360	10.021	1.466	0.01748	0.20486	0.22394	0.00088	0.00000
1.630	9.574	1.751	0.00331	0.10852	0.33168	0.00364	0.00000
1.910	8.602	2.059	0.00004	0.01372	0.39301	0.04036	0.00001
2.200	7.800	2.391	0.00000	0.00148	0.26968	0.17576	0.00022
2.510	7.131	2.758	0.00000	0.00013	0.11014	0.33490	0.00198
2.869	5.632	3.147	0.00000	0.00000	0.00390	0.37367	0.06958
3.210	4.822	3.545	0.00000	0.00000	0.00033	0.20264	0.24418
Titration 3							
0.000	11.062	0.588	0.18416	0.19608	0.01947	0.00001	0.00000
0.269	10.856	0.757	0.13380	0.22926	0.03663	0.00002	0.00000
0.540	10.602	0.976	0.08067	0.24792	0.07105	0.00007	0.00000
0.810	10.297	1.241	0.03704	0.22964	0.13275	0.00028	0.00000
1.090	9.903	1.552	0.01038	0.15953	0.22862	0.00117	0.00000
1.360	9.282	1.873	0.00087	0.05606	0.33557	0.00720	0.00000
1.635	8.139	2.219	0.00000	0.00366	0.30493	0.09106	0.00005
1.940	7.422	2.610	0.00000	0.00036	0.15600	0.24261	0.00073
2.250	6.220	3.007	0.00000	0.00000	0.01481	0.36720	0.01770
2.570	5.047	3.416	0.00000	0.00000	0.00063	0.23233	0.16675
Titration 4							
0.000	8.824	2.002	0.00012	0.02257	0.38772	0.02389	0.00000
0.280	7.908	2.331	0.00000	0.00203	0.28668	0.14546	0.00014
0.570	7.305	2.673	0.00000	0.00025	0.14262	0.29028	0.00115
0.870	6.115	3.027	0.00000	0.00000	0.01260	0.39734	0.02436
1.210	5.027	3.427	0.00000	0.00000	0.00064	0.24777	0.18589

<sup>a</sup> Initial solution composition: Titration 1,  $T_L = 4.529 \times 10^{-3}M$ ,  $T_H = -0.591 \times 10^{-3}M$ ; Titration 2,  $T_L = 4.524 \times 10^{-3}M$ ,  $T_H = -0.599 \times 10^{-3}M$ ; Titration 3,  $T_L = 4.044 \times 10^{-3}M$ ,  $T_H = 0.482 \times 10^{-3}M$ ; Titration 4,  $T_L = 4.394 \times 10^{-3}M$ ,  $T_H = 8.788 \times 10^{-3}M$ . For the four titrations; titrant [HCl] = 0.5128 and initial volume = 98.84 ml.

<sup>b</sup> Cumulative volume of HCl added at each titration point.

<sup>c</sup> Values for all ligand species are the number of mmoles at each titration point.

TABLE 6.13a

Changes in composition and the heat changes for hm-3,2,3-tet/HCl titrations

$R(LH)^a$ (mmol)	$S(LH_2)$ (mmol)	$T(LH_3)$ (mmol)	$U(LH_4)$ (mmol)	$Q_m^b$ (J)	$Q_{corr}^b$ (J)	$Q_{calc}^b$ (J)
0.05081	0.01091	0.00001	0.00000	8.381	3.236	3.181
0.05615	0.02057	0.00002	0.00000	7.663	3.926	3.968
0.05671	0.03926	0.00006	0.00000	7.620	4.964	4.990
0.04431	0.06438	0.00021	0.00000	7.381	5.731	5.694
0.02751	0.09256	0.00076	0.00000	7.529	-	-
0.01229	0.11465	0.00380	0.00000	7.476	6.902	6.886
0.00215	0.08274	0.04916	0.00001	6.954	6.709	6.779
0.00002	0.00849	0.13187	0.00024	6.578	6.556	6.576
0.00000	0.00118	0.15087	0.00171	7.080	7.076	7.117
0.04606	0.00964	0.00001	0.00000	7.643	2.877	2.871
0.05350	0.01837	0.00002	0.00000	7.387	3.669	3.715
0.05627	0.03543	0.00005	0.00000	7.459	4.707	4.763
0.04646	0.06006	0.00018	0.00000	7.363	5.589	5.573
0.03010	0.08861	0.00063	0.00000	7.369	6.301	6.270
0.01416	0.11050	0.00276	0.00000	7.335	6.719	6.714
0.00327	0.09807	0.03674	0.00001	7.324	7.016	7.072
0.00004	0.01228	0.13561	0.00021	7.026	6.995	6.950
0.00000	0.00135	0.16090	0.00176	7.589	7.584	7.593
0.00000	0.00013	0.10637	0.06760	6.921	-	-
0.00000	0.00000	0.00357	0.17460	5.967	5.967	5.972
0.05036	0.01718	0.00001	0.00000	7.463	3.531	3.491
0.05313	0.03447	0.00005	0.00000	7.362	4.496	4.552
0.04363	0.06191	0.00020	0.00000	7.405	5.577	5.527
0.02666	0.09677	0.00090	0.00000	7.679	6.603	6.539
0.00951	0.11298	0.00603	0.00000	7.311	6.756	6.758
0.00087	0.05327	0.08391	0.00005	6.876	6.713	6.763
0.00000	0.00331	0.15223	0.00068	7.298	7.288	7.258
0.00000	0.00036	0.14155	0.01696	6.929	-	-
0.00000	0.00000	0.01418	0.14906	5.545	5.545	5.615
0.00012	0.02066	0.12171	0.00014	6.853	6.800	6.752
0.00000	0.00178	0.14583	0.00100	6.968	6.962	6.891
0.00000	0.00025	0.13028	0.02321	6.776	6.774	6.827
0.00000	0.00000	0.01196	0.16153	6.003	6.003	5.926

<sup>a</sup> Tabulated values are the changes in the number of mmoles of each species between successive titration points.

<sup>b</sup> Defined in text.



## 6.2.2 Discussion

### Logk Values

The logk data for stepwise protonation of 3,2,3-tet and hm-3,2,3-tet (Table 6.15) show that the overall basicities ( $\sum_{i=1}^4 (\log k_i)$ ) of the two ligands are similar. However, the data indicates that this similarity in basicity is due to a compensation of the differences between the  $\log k_i$  values for each of the ligands.

The free energy change on protonation of an amine nitrogen in the presence of a charge (or a dipole) elsewhere in the molecule will decrease as the distance of the charge (or dipole) from the protonation centre increases<sup>127</sup>. For the methylenediamines  $\text{NH}_2(\text{CH}_2)_n\text{NH}_2$ , both  $\log k_1$  and  $\log k_2$  increase as n increases from n = 2 (ethylenediamine) to n = 6 (hexamethylenediamine)<sup>127</sup>. Similarly, a comparison of the data for diethylenetriamine (dien) and dipropylenetriamine (dpt)<sup>106</sup> (Table 6.16) shows that the overall basicity for dpt, which has a chain of three methylene groups joining each amine nitrogen is greater than that for dien which has two methylene groups separating each nitrogen atom. Linear tetramines have three methylene chains joining the four amine nitrogen atoms. Thus the predicted basicity sequence ( $\sum_{i=1}^4 \log k_i$ ) for the tetraamines with a combination of two and three membered methylene chains would be

$$3,3,3 > 3,3,2 \sim 3,2,3 > 2,2,3 \sim 2,3,2 > 2,2,2$$

TABLE 6.15

Thermodynamic<sup>a</sup> data for the stepwise protonation of 3,2,3-tet and  
hm-3,2,3-tet in aqueous solution, 25°C, I = 0.10M

1,5,8,12-tetraazadodecane (3,2,3-tet.)

<u>Reaction</u>	<u>log k<sub>n</sub></u>	<u>-ΔG kJmole<sup>-1</sup></u>	<u>-ΔH kJmol<sup>-1</sup></u>	<u>ΔS Jmol<sup>-1</sup>K<sup>-1</sup></u>
1. L + H <sup>+</sup> ⇌ LH <sup>+</sup>	10.53 ± 0.02	60.10 ± 0.1	51.68 ± 0.2 <sub>7</sub>	28.3 ± 1.2
2. LH <sup>+</sup> + H <sup>+</sup> ⇌ LH <sub>2</sub> <sup>2+</sup>	9.77 ± 0.02	55.76 ± 0.1	51.80 ± 0.2 <sub>0</sub>	13.3 ± 1.0
3. LH <sub>2</sub> <sup>2+</sup> + H <sup>+</sup> ⇌ LH <sub>3</sub> <sup>3+</sup>	8.30 ± 0.02	47.37 ± 0.1	43.18 ± 0.1 <sub>4</sub>	14.1 ± 0.8
4. LH <sub>3</sub> <sup>3+</sup> + H <sup>+</sup> ⇌ LH <sub>4</sub> <sup>4+</sup>	<u>5.59 ± 0.01</u>	<u>31.90 ± 0.06</u>	<u>34.16 ± 0.1<sub>3</sub></u>	<u>-7.6 ± 0.6</u>
	34.19	195.13	180.82	48.1

2,11-diamino-4,4,9,9-tetramethyl-5,8-diazadodecane (hm-3,2,3-tet)

<u>Reaction</u>	<u>log k<sub>n</sub></u>	<u>-ΔG kJmol<sup>-1</sup></u>	<u>-ΔH kJmol<sup>-1</sup></u>	<u>ΔS Jmol<sup>-1</sup>K<sup>-1</sup></u>
1. L + H <sup>+</sup> ⇌ LH <sup>+</sup>	11.09 <sub>0</sub> ± 0.03	63.29 ± 0.1 <sub>7</sub>	51.22 ± 0.1 <sub>2</sub>	40.5 ± 1.3
2. LH <sup>+</sup> + H <sup>+</sup> ⇌ LH <sub>2</sub> <sup>2+</sup>	10.05 <sub>9</sub> ± 0.02	57.41 ± 0.1	53.03 ± 0.3 <sub>0</sub>	14.6 ± 1.3
3. LH <sub>2</sub> <sup>2+</sup> + H <sup>+</sup> ⇌ LH <sub>3</sub> <sup>3+</sup>	7.61 <sub>4</sub> ± 0.01	43.45 ± 0.1	46.38 ± 0.2 <sub>5</sub>	-9.8 ± 1.1
4. LH <sub>3</sub> <sup>3+</sup> + H <sup>+</sup> ⇌ LH <sub>4</sub> <sup>4+</sup>	<u>4.90<sub>3</sub> ± 0.01</u>	<u>27.98 ± 0.06</u>	<u>33.25 ± 0.3<sub>0</sub></u>	<u>-17.7 ± 1.2</u>
	33.67	192.13	183.88	27.6

<sup>a</sup> With reference to a standard state of 0.10M NaCl.

TABLE 6.16

Thermodynamic data for the protonation of some polyamines

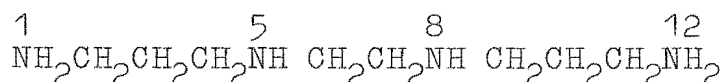
Amine	Chain system	log k	$-\Delta G \text{ kJmol}^{-1}$	$-\Delta H \text{ kJmole}^{-1}$	$\Delta S \text{ Jmol}^{-1}\text{K}^{-1}$	Conditions
trien <sup>a</sup>	(2,2,2)	1 9.78	55.81	46.07	32.7	0.1M KCl 25°C
		2 9.06	51.71	47.15	15.3	
		3 6.55	37.38	39.87	-8.4	
		4 3.24	18.49	28.58	-33.8	
	$\sum_{i=1}^4 (\log k_i) = 28.63$					
tripen <sup>b</sup>	(3,3,3)	1 10.61		-		0.1M NaNO <sub>3</sub> 20°C
		2 9.98		-		
		3 8.69		-		
		4 7.35		-		
	$\sum (\log k_i) = 36.63$					
c	(2,3,2)	1 10.25		-		0.5M KCl 25°C
		2 9.50		-		
		3 7.28		-		
		4 6.02		-		
	$\sum (\log k_i) = 33.05$					
dien <sup>d</sup>	(2,2)	1 9.79	55.86	46.86	30.2	0.10M KCl 25°C
		2 8.98	51.25	50.00	4.2	
		3 4.25	24.27	30.12	-19.6	
dpt <sup>e</sup>	(3,3)	1 10.65	60.79	51.42	31.4	0.1M KCl 25°C
		2 9.57	54.60	54.35	0.8	
		3 7.72	44.06	43.80	0.8	

<sup>a</sup> Triethylenetetramine data from reference 138.<sup>b</sup> Tripropylenetetramine data from reference 14.<sup>c</sup> N,N-bis(2-aminoethyl)-1,3-propanediamine data from reference 15.<sup>d</sup> Diethylenetriamine data from reference 106.<sup>e</sup> Dipropylenetriamine data from reference 106.

where 2,3,2 is the amine  $\text{NH}_2(\text{CH}_2)_2\text{NH}(\text{CH}_2)_3\text{NH}(\text{CH}_2)_2\text{NH}_2$  etc. The available data for these tetraamines (Tables 6.15 and 6.16) shows that this predicted sequence is found.

#### The Empirical Prediction of logk Values

From the macroscopic protonation constants alone possible protonation sites for the tetraamines cannot be predicted. For each cation  $\text{LH}_n^{n+}$  there will be an equilibrium between the possible tautomeric forms; for the monocation there will be two possible structures, for the dication, four and two for the trication. However, by assuming the most likely protonation scheme the protonation constants can be predicted using the empirical rules of Clark and Perrin<sup>123</sup>. These calculations for one possible protonation scheme for 3,2,3-tet are as follows.



#### 1. Addition of the first proton on atom 1 (or 12)

(i) Typical $\text{pK}_a$ for a primary amine	10.77
(ii) Effect of an NHR group 3 carbons away	- .45
(iii) Effect of a NHR 5C and 1N away	- .05
(iv) Statistical effect	+ .3

---

predicted logk      10.57

2.	<u>Addition of the second proton on atom 12 (or 1)</u>	
	(i) + (ii) + (iii) above	10.27
	Statistical effect	- .3
	Effect of $\text{NH}_3^+$ at other end	- .01
		<hr/>
	predicted logk	9.96
3.	<u>Addition of the third proton on atom 5 (or 8)</u>	
	(v) Typical $\text{pK}_a$ for a secondary amine	11.15
	(vi) Effect of $\text{RNH}$ 2 carbons distant	- .9
	(vii) Effect of $\text{NH}_3^+$ 3 carbons distant	-1.8
	Statistical effect	+ .3
	(viii) Effect of $\text{NH}_3^+$ 5C and 1N away	- .22
		<hr/>
	predicted logk	8.53
4.	<u>Addition of the fourth proton on atom 8 (or 5)</u>	
	(v) + (vii) + (viii)	9.13
	Effect of $\text{RNH}^+$ 2 carbons distant	-3.6
	Statistical effect	- .3
		<hr/>
	predicted logk	5.23

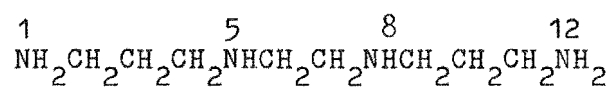
These rules predict the logk values at 20°C\*. The experimental logk values for 3,2,3-tet at 25°C (Table 6.14) were corrected to 20°C using the enthalpy data in Table 6.15.

---

\*There was no mention of ionic strength effects in Clark and Perrin's article<sup>123</sup>.

TABLE 6.14

The predicted  $\log k_i$  for possible protonation  
sequences for 3,2,3-tet.



<u>Protonation sequences</u>				<u>Predicted values</u>			
<u>1</u>	<u>2</u>	<u>3</u>	<u>4</u>	<u><math>\log k_1</math></u>	<u><math>\log k_2</math></u>	<u><math>\log k_3</math></u>	<u><math>\log k_4</math></u>
1	12	5	8	10.6	10.0	8.5	5.2
1	8	12	5	10.6	9.6	8.9	5.2
8	1	12	5	10.1	10.1	8.9	5.2
8	12	1	5	10.1	8.4	10.1	5.2
1	8	5	12	10.6	9.6	5.7	8.5
				<u>Experimental values</u>			
				10.7	9.9	8.4	5.7

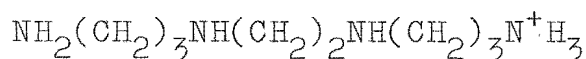
These corrected values and some predicted pK values for different protonation sequences are shown in Table 6.14.

The values predicted from the most probable schemes (first three in Table 6.14) are similar to the experimental values. Although the agreement between the predicted  $\log k_1$ , assuming protonation on a primary nitrogen, and the experimental value is good there is evidence to suggest that protonation on the secondary nitrogen also occurs for this first stepwise protonation (see later discussion). However, for hm-3,2,3-tet the predicted  $\log k_1$  values, which will be identical to those for 3,2,3-tet, do not show very good agreement with the experimental values. The enthalpy and entropy changes which contribute to the overall  $\log k_1$  value indicate that solvation effects are important (see further discussion below). In view of the theory behind Clark and Perrin's empirical rules it is not surprising that the  $\log k_1$  values for hm-3,2,3-tet could not be predicted.

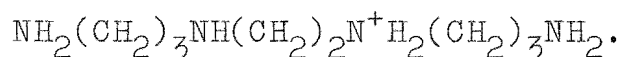
#### Enthalpy Changes

For the protonation of monoamines the free energy changes are slightly more negative for secondary amines than for primary amines but the enthalpy changes are more exothermic for primary amines<sup>124</sup>. Also for ethylenediamine the  $-\Delta H_1$  value at  $I = .10$  M (KCl) and  $25^\circ\text{C}$  is  $49.9 \text{ kJ mol}^{-1}$ <sup>137</sup> and that for piperazine, which has two secondary amine nitrogens, is  $42.6 \text{ kJ mol}^{-1}$ <sup>138</sup>. The enthalpy data (Table 6.15) for

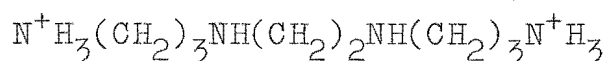
the tetraamines 3,2,3-tet and hm-3,2,3-tet, which have two secondary and two primary amine nitrogens, show that  $\Delta H_1$  is slightly less exothermic than  $\Delta H_2$  (for 3,2,3-tet the difference is not statistically significant). This suggests that in the first stage of protonation there is a slightly larger proportion of the protons residing on the secondary nitrogens, than in the second stage. For the monocation of 3,2,3-tet there are two possible structures which will be in equilibrium,



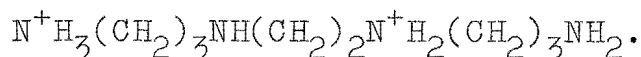
and



For the dication there are four possible structures although it is reasonable to assume that the dominant forms will be



and



These structures can be formed from the monocation structures by protonation of a primary amine nitrogen. Thus, if the proportion of protonation on a secondary nitrogen atom is smaller for the second stepwise protonation than for the first then the value of  $\Delta H_2$  will be more exothermic than  $\Delta H_1$ .



The only other available enthalpy data for a linear tetra-amine (trien) show that  $\Delta H_1$  is less exothermic than  $\Delta H_2$  (see Table 6.16). Similarly, for both the triamines dien and dpt  $\Delta H_2$  is more exothermic than  $\Delta H_1$  (see Table 6.16).

For successive protonations of these tetraamines charge repulsion will lead to a decrease in the exothermic heat of protonation. As the distance between the charges increases this electrostatic interaction will decrease and a more exothermic enthalpy change will result. The  $-\Delta H_3$  and  $-\Delta H_4$  values for trien (Table 6.16) are smaller than those for both 3,2,3-tet and hm-3,2,3-tet.

For the fourth stepwise protonation of 3,2,3-tet protonation of the ion  $N^+H_3(CH_2)_3N^+H_2(CH_2)_2NH(CH_2)_3N^+H_3$  is likely to be the dominant reaction. As the charges of closest proximity to the protonation site will be of greatest importance it might be expected that  $-\Delta H_4$  for 3,2,3-tet would lie between the value for dien and the value for dpt. The data in Tables 6.15 and 6.16 show that  $-\Delta H_4$  increases in the order dien < 3,2,3-tet < dpt.

The enthalpy data for 3,2,3-tet and hm-3,2,3-tet (Table 6.15) show that the differences between the stepwise enthalpy changes for these tetraamines are slight. The enthalpy change for the overall reaction  $L + 4H^+ \rightleftharpoons LH_4^{4+}$  ( $\sum_i \Delta H_i$ ) is only 3 kJ mol<sup>-1</sup> more exothermic for hm-3,2,3-tet than for 3,2,3-tet. As discussed earlier (chapter 1) any

enthalpy change can be separated into a gas phase term and hydration enthalpies of the species involved. The inductive effect of the six methyl substituents on hm-3,2,3-tet will increase the electron density on the nitrogen atoms which would produce more exothermic gas phase enthalpy changes than that for 3,2,3-tet. However, these methyl substituents will also shield the solvent from the charge centres which will lead to a decrease in the hydration enthalpy of the cations. Thus, as there is no marked difference between the stepwise enthalpies for 3,2,3-tet and hm-3,2,3-tet, it would appear that these two effects are largely compensatory. This effect has also been observed for some C4-alkyl-substituted ethylenediamines<sup>87</sup>.

The data in Table 6.15 show that the differences in  $\log k_1$  and  $\log k_4$  for 3,2,3-tet and hm-3,2,3-tet are predominantly the result of the entropy differences while those differences for  $\log k_3$  and  $\log k_2$  result from contributions from both the entropy and enthalpy differences.

#### Entropy Changes

The entropy change for the protonation of alkyl monoamines increases in the order  $\text{RNH}_2 < \text{R}_2\text{NH} < \text{R}_3\text{N}$ ; for R = methyl there is an almost constant increase (ca.  $20 \text{ Jmol}^{-1}\text{K}^{-1}$ ) in passing from primary to secondary to tertiary<sup>126</sup>. A similar trend has also been observed for the diamines ethylenediamine (primary), piperazine (secondary) and

triethylenediamine (tertiary)<sup>139</sup>. This change has been attributed to (i) solvent exclusion from the charge on the amine as amine hydrogens are successively replaced by alkyl groups<sup>126</sup> or (ii) as a decreased ability of the amine cation to hydrogen bond to the solvent as the amine hydrogens are replaced by alkyl groups<sup>140</sup>.

Tables 6.15 and 6.16 show that the first stepwise protonation entropy change  $\Delta S_1$  for the ligands trien, dien, dpt and 3,2,3-tet are all of similar magnitude (the values vary from a smallest of 28.3 to a largest of 32.7 J mol<sup>-1</sup>K<sup>-1</sup>). These values lie between the  $\Delta S_1$  value for ethylenediamine (2 primary nitrogens) of 23.8 J mol<sup>-1</sup>K<sup>-1</sup> and that for piperazine (2 secondary nitrogens) of 43.1 J mol<sup>-1</sup>K<sup>-1</sup><sup>138</sup>. This suggests that for these tri and tetraamines the protonation for the first stepwise process occurs neither exclusively on a primary nor a secondary nitrogen atom. This evidence supports the conclusions drawn from the enthalpy data discussed above.

The  $\Delta S_1$  value for hm-3,2,3-tet is 12.2 J mol<sup>-1</sup>K<sup>-1</sup> higher than that for 3,2,3-tet (Table 6.15). The six methyl substituents of the former amine are in an arrangement (see Fig. 1.1) which is likely to result in shielding of the solvent from any charge on the secondary amines. This will lead to a larger entropy ( $\Delta S_1$ ) change for hm-3,2,3-tet relative to that for 3,2,3-tet due to the decreased

electrostriction of the solvent by the charge on the ion. For subsequent stepwise protonations interpretation of the entropy changes is difficult because of the large number species in tautomeric equilibrium. These entropy changes will be a summation of contributions from configuration entropy changes of the molecules and ions and from changes in the solvent ordering ability of these molecules and ions.

The entropy data in Table 6.15 shows that the changes for the third and fourth protonation reactions for hm-3,2,3-tet are more negative than those for 3,2,3-tet. Relative to 3,2,3-tet the solvent ordering ability of hm-3,2,3-tet will be decreased due to the shielding effect of the six methyl substituents. This will lead to a more positive entropy change. However, the hm-3,2,3-tet molecule has a greater internal entropy than has 3,2,3-tet; a larger number of configurational degrees of freedom arise from the additional six methyl substituents. Successive protonations for hm-3,2,3-tet will thus lead to a greater configurational entropy loss than that for 3,2,3-tet. As the third and fourth entropy changes for hm-3,2,3-tet are more negative than those for 3,2,3-tet it would appear that the loss of configurational entropy is dominant over the decreased solvent ordering ability.

### 6.3 PROTONATION OF THE DIAMINE-DIKETONE LIGAND

#### 6.3.1 Results

This ligand (Fig. 1.1) has two secondary amine functions and two ketone groups. The constants for amine protonation were determined, however no attempt was made to measure the basicity of the very weakly basic ketone functions<sup>141,142</sup>.

$p[H^+]$  data from the titrations of NaOH against solutions of the diamine-diketone ligand and acid are shown in Table 6.17. As solutions of the ligand decomposed quite rapidly (section 6.3.3) the approach used to obtain pH data was slightly different from that previously described. A solution of the ligand dihydroperchlorate salt in water decomposed slowly enough for a stock solution to be used for titrations. Data in the pH range 5 to 6.7 were obtained by the normal titration method. At each titration point the solution pH rapidly attained a constant value, which was readily reproducible to within the usual error limits. However, in the alkaline region (pH 8-10) the solution pH decreased at a rate of approximately 0.005 pH/minute. This drift was associated with a very large increase in the rate of decomposition of the ligand (see section 6.3.3). For any one titration only two or three measurements were made in the alkaline region; the pH value at 30-45 seconds after the addition of the titrant increment was recorded. For the final point from a titration a plot of pH against time (over

TABLE 6.17

pH titration data from titrations<sup>a</sup> of the diamine-diketone  
ligand with NaOH at 25°C and I = 0.10M (NaCl)

<u>Vol.</u>	<u><math>\bar{n}</math></u>	<u>p[H<sup>+</sup>]</u>	<u>Vol.</u>	<u><math>\bar{n}</math></u>	<u>p[H<sup>+</sup>]</u>
0.040	1.772	5.661	0.230	0.738	8.957
0.060	1.662	5.892	0.240	0.689	9.060
0.070	1.607	5.996	0.250	0.641	9.157
0.090	1.495	6.190	0.260	0.593	9.240
0.100	1.440	6.293	0.270	0.547	9.326
0.120	1.328	6.499	0.290	0.460	9.479
0.130	1.273	6.625	0.310	0.380	9.623
0.140	1.217	6.756	0.320	0.345	9.695
0.150	1.161	6.918	0.340	0.280	9.826
0.210	0.840	8.712	0.350	0.255	9.894
0.220	0.788	8.841	0.360	0.230	9.953

<sup>a</sup> Data collected as described in the text. Solution composition:

$T_H = 1.219 \times 10^{-3}M$ ,  $T_L = 6.096 \times 10^{-4}M$ , initial volume =  
49.94 ml and titrant [NaOH] = 0.1702M.

about 5 minutes) was recorded, from which the pH at time of addition was obtained by a short extrapolation. Both of these methods gave identical pH values, within the experimental error. Thus, the titration data in Table 6.17 were obtained from a number of titrations of samples from one stock solution. The reproducibility of this data was checked by comparison with the ( $\bar{n}$ ,  $p[H^+]$ ) data obtained using a different stock solution.

The protonation constants for the ligand, calculated using the least squares procedure (Chapter 4) are shown in Table 6.18. As the ligand solutions were not stable (w.r.t. decomposition), for sufficiently long periods, no calorimetric study was attempted.

### 6.3.2 Discussion of the log $k$ Data

The structure of the diamine-diketone ligand is identical to that of the diamine-dioxime ligand except for the different terminal functional groups. Any difference between the  $\log k_i$  values for the two ligands could be attributed to the change in the functional grouping. There does not appear to be any thermodynamic data available that will enable an assessment of the substituent effects of a C=NOH and a C=O function in aliphatic systems<sup>5</sup>.

A comparison of the  $\log k_i$  data for the diamine-diketone (Table 6.18) with those for the diamine-dioxime (Table 6.5) shows that the overall basicity is slightly

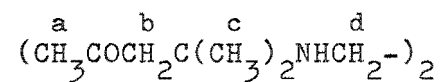
TABLE 6.18

Protonation constants for the diamine-diketone ligand  
at I = 0.10 (NaCl) and 25°C

<u>n</u>	<u>Reaction</u>	<u>log k<sub>n</sub></u>	<u>-ΔG kJmol<sup>-1</sup></u>	<u>-ΔH kJmol<sup>-1</sup></u>	<u>ΔS Jmol<sup>-1</sup>K<sup>-1</sup></u>
1	L + H <sup>+</sup> ⇌ HL <sup>+</sup>	9.41 ± 0.03	53.70 ± 0.1 <sub>7</sub>	-	-
2	HL <sup>+</sup> + H <sup>+</sup> ⇌ H <sub>2</sub> L <sup>2+</sup>	6.19 ± 0.02	35.33 ± 0.1	-	-

TABLE 6.19

NMR data for the ketone ligand in D<sub>2</sub>O



chemical shifts <sup>x</sup> (τppm)				Buffer salt added	Res. Integral a:b:c:d
<u>a</u>	<u>b</u>	<u>c</u>	<u>d</u>		
7.77	6.95	8.62	6.67	-	1.5:0.75:3:1
7.76	-	8.65	6.82	phosphate	1.5: - :3:1
7.78	-	8.80	7.18	borax	ca.1.5: - :3:1

<sup>x</sup> relative to external TMS .



greater for the diamine-dioxime and that this difference arises from the larger  $\log k_4$  for the dioxime ligand.

This slight difference is difficult to assess, especially as the enthalpy changes for the protonation of the diamine-diketone are not available.

### 6.3.3 Decomposition of the Diamine-Diketone Ligand

It has been reported that  $\beta$ -amino-ketones (not to be confused with  $\beta$ -imino ketones  $R_1 - NH - CR_2 = CR_3 - C(=O)R_4$ ) show a tendency to decompose to form an amine and an  $\alpha,\beta$ -unsaturated carbonyl compound<sup>143</sup>. The pH of a solution of the ketone dihydroperchlorate salt in water was stable to within  $\pm 0.006$  pH over eight hours, however the ultraviolet spectrum of a solution of the ligand (pH 4.5,  $T_L = 3.35 \times 10^{-3} M$ ) changed with time. There was an increase in intensity of an absorption band at 244 nm at a rate of 0.36A/hour.

If this change represented the formation of an  $\alpha,\beta$ -unsaturated compound then the product from this ligand would be mesityl oxide  $((CH_3)_2C = CH - C(=O) - CH_3)$ . Mesityl oxide has an absorption at 243 nm<sup>144</sup> with an extinction coefficient of 10,000<sup>144</sup>. Thus, assuming that a decomposition to form only mesityl oxide does occur then the rate of decomposition, was ca. 0.5% per hour. The rate of increase in intensity of the absorption at 244 nm was very dependent on pH. In alkaline solution (pH 9) the rate of decomposition of the ligand was ca. 0.5% decomposition in 5 minutes.

### Enolisation of Nonconjugated Ketones

The enolisation of an aliphatic non-conjugated ketone group is a slow process, which is catalysed by acids and bases<sup>145</sup>. The tautomeric equilibrium constant  $K_t = \frac{[\text{enol}]}{[\text{ketone}]}$  is low for non-conjugated ketones in aqueous solution, e.g. for acetone  $K_t$  ca.  $0.9 \times 10^{-6}$ , for cyclopentanone, ca.  $1.3 \times 10^{-5}$ <sup>145</sup>.

For the diamine-diketone ligand, the  $\alpha$ -methylene protons did undergo deuterium exchange at a rate dependent on the solution pH. This suggests the presence of the enol tautomer. The NMR of the ligand in  $D_2O$  showed a four band spectrum (Table 6.19) which became a three band spectrum after 24 hrs, as the resonance due to protons b slowly decreased in intensity relative to the others. At higher pH (phosphate and borax salts added to  $D_2O$ ) the NMR spectra (Table 6.19) showed three bands which changed with time. The changes indicated that mesityl oxide was formed (by comparison with a spectrum of mesityl oxide in  $D_2O$ ) although it was not the only product formed.

The NMR data did not suggest that an enol tautomer was formed in measurable concentration in acid solution while the data in alkaline solution indicated that appreciable decomposition occurred.

The chemical shifts for the protons c and d (Table 6.19) for the diamine-diketone dihydroperchlorate salt in  $D_2O$

compare favourably with those for the diamine-dioxime dihydrochloride in D<sub>2</sub>O (τ8.58 and 6.65 ppm, Table 6.1).

## CHAPTER 7

### FORMATION OF COPPER(II) COMPLEXES WITH THE LIGANDS

#### 7.1 FORMATION OF COPPER COMPLEXES WITH 3,2,3-tet AND hm-3,2,3-tet

##### 7.1.1 Results for hm-3,2,3-tet

For the pH titrations, the solution pH at each titration point prior to the end point (see Fig. 7.1) did not attain a steady value until about ten minutes after the addition of the titrant NaOH. After the end point, equilibrium was attained almost instantaneously. This suggests that the formation of the metal-ligand complex must be kinetically controlled. Data from the pH titrations at two different total ligand concentrations are shown in Table 7.1. The  $p[H^+]$  data was obtained from the measured pH as described in Chapter 3. Only one titration from a set of reproducible titrations has been tabulated.

The visible spectrophotometric data from ca. 1:1 metal:ligand solutions containing HCl/NaOH indicated that as the solution pH was increased from approximately 3 to 11 there was no change in the position of maximum absorption,  $\lambda_{\max}$  (534 nm,  $I = 0.10 \text{ M}(\text{NaCl})$ ). The visible absorption spectrum for 1:1 metal:ligand solutions in tartrate, phthalate, phosphate and borax buffer solutions also showed no change in  $\lambda_{\max}$  ( $535 \pm 2$ ). This visible spectrophotometric data

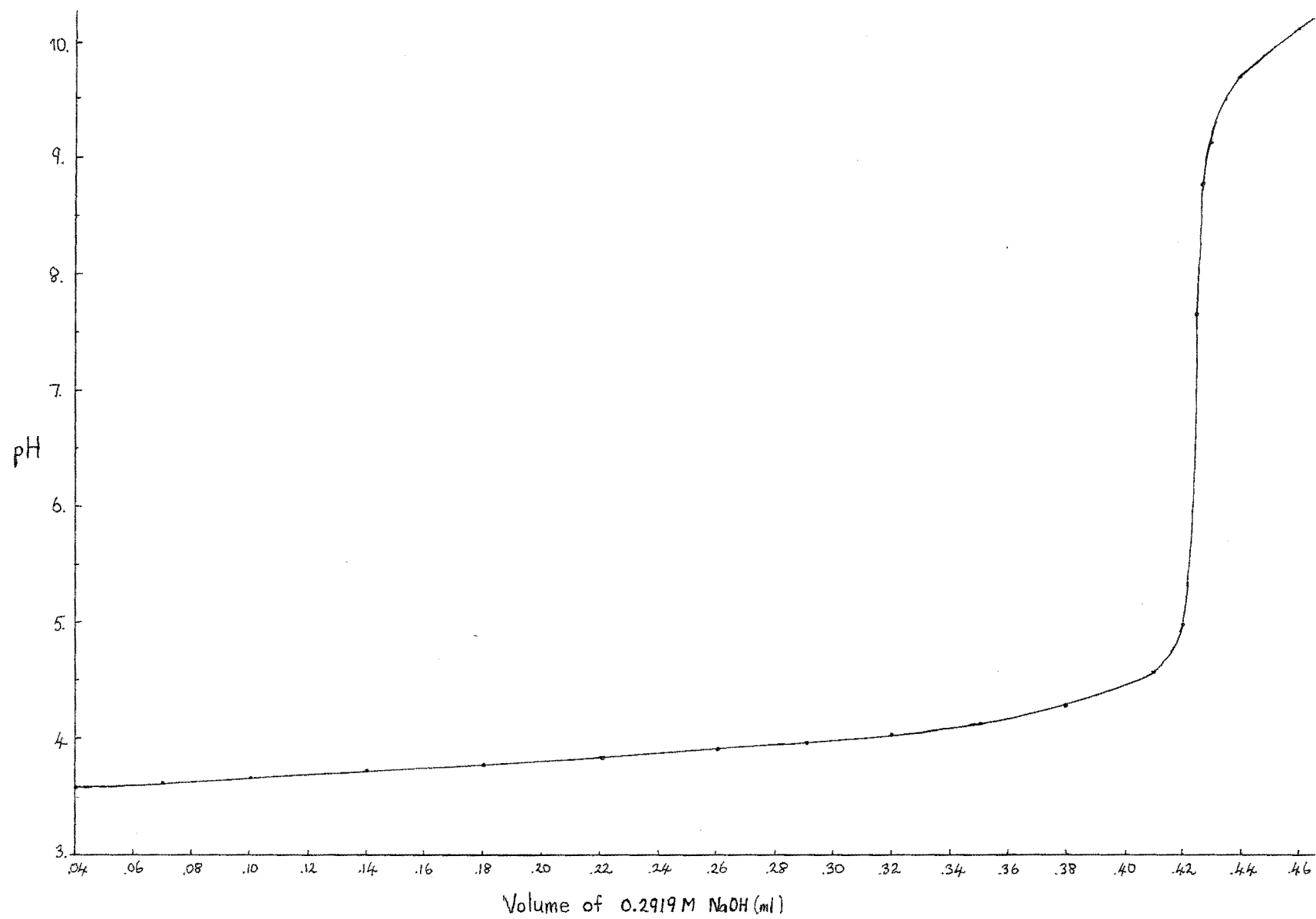


**Fig 7.1** Titration curve for copper/hm-3,2,3-tet  $T_M = 5.957 \times 10^{-4} M$ ,  $T_L = 6.037 \times 10^{-4} M$

TABLE 7.1

pH titration and stability constant data for the copper(II)  
hm-3,2,3-tet complex at 25°C and I = 0.10M (NaCl)

$T_L = 1.205 \times 10^{-3} M, T_M = 1.192 \times 10^{-3} M, T_H = 4.463 \times 10^{-3} M$					$T_L = 6.037 \times 10^{-4} M, T_H = 2.483 \times 10^{-3} M, T_M = 5.957 \times 10^{-4} M$				
<u>VOL<sup>a</sup></u>	<u>p[H<sup>+</sup>]</u>	<u><math>\bar{n}</math></u>	<u><math>10^{22}[L]</math></u>	<u><math>\log K</math></u>	<u>VOL<sup>b</sup></u>	<u>p[H<sup>+</sup>]</u>	<u><math>\bar{n}</math></u>	<u><math>10^{22}[L]</math></u>	<u><math>\log K</math></u>
0.020	3.435	0.226	0.1075	22.434	0.040	3.497	0.196	0.0985	22.392
0.040	3.488	0.297	0.1585	22.426	0.070	3.543	0.256	0.1388	22.393
0.060	3.535	0.371	0.2182	22.431	0.100	3.583	0.319	0.1831	22.407
0.080	3.583	0.445	0.2986	22.429	0.140	3.642	0.403	0.2750	22.390
0.100	3.631	0.520	0.4009	22.431	0.160	3.670	0.446	0.3294	22.388
0.120	3.689	0.594	0.5758	22.405	0.180	3.695	0.490	0.3810	22.402
0.130	3.711	0.632	0.6382	22.431	0.200	3.730	0.533	0.4805	22.375
0.140	3.750	0.669	0.8204	22.392	0.220	3.759	0.577	0.5671	22.381
0.150	3.775	0.708	0.9128	22.424	0.240	3.798	0.620	0.7274	22.351
0.160	3.800	0.746	0.9984	22.469	0.260	3.823	0.666	0.8053	22.394
0.170	3.853	0.783	1.389	22.414	0.290	3.892	0.731	1.220	22.347
0.190	3.946	0.858	2.143	22.452	0.320	3.955	0.798	1.639	22.381
0.210	4.106				0.350	4.053	0.863	2.753	22.358
0.230	4.587				0.380	4.192			
0.235	8.297				0.410	4.512			
0.237	9.314				0.420	4.898			
0.240	9.752				0.425	7.616			
0.245	10.072				0.4275	8.736			
0.250	10.260				0.430	9.105			
0.260	10.489				0.435	9.461			
0.270	10.643				0.440	9.669			
0.280	10.754				0.460	10.084			
0.290	10.844				0.500	10.441			
0.300	10.916								

$\log K$ : mean 22.42<sub>8</sub>  $\sigma$  = 0.02

$\log K$ : mean = 22.38<sub>1</sub>  $\sigma$  = 0.02

<sup>a</sup> Volume of 0.9569M NaOH added to 49.94 ml of a solution of Cu<sup>2+</sup>, ligand and H<sup>+</sup>.

<sup>b</sup> Volume of 0.2919M NaOH added to 49.94 ml.

<sup>c</sup> Calculation of  $\log K$  is described in the text.

indicates that the coordination environment around the central metal ion does not change as the solution pH changes. This suggests that within the pH range 3 - 11 neither a hydroxy complex ( $\text{CuL}(\text{OH})^+$ ) nor a protonated complex ( $\text{Cu}(\text{HL})^{3+}$ ) is formed.

#### Calculations using the $\text{p}[\text{H}^+]$ data

If it is assumed that only one metal-ligand complex,  $\text{CuL}^{2+}$ , is formed then the mass balance equations for  $T_M$ ,  $T_L$  and  $T_H$  are

$$T_L = [\text{L}] + [\text{HL}] + [\text{H}_2\text{L}] + [\text{H}_3\text{L}] + [\text{H}_4\text{L}] + [\text{CuL}] \quad 7.1$$

$$T_M = [\text{Cu}] + [\text{CuL}] \quad 7.2$$

$$T_H = [\text{H}] + [\text{HL}] + 2[\text{H}_2\text{L}] + 3[\text{H}_3\text{L}] + 4[\text{H}_4\text{L}] - K_w/[\text{H}] \quad 7.3$$

and the stability constant  $K$  for the formation of  $\text{CuL}$ , is

$$K = \frac{[\text{CuL}]}{[\text{Cu}][\text{L}]} .$$

As the protonation constants for the ligand were previously determined, at each titration point the concentration of the free ligand  $[\text{L}]$  was determined from equation 7.3. This value of  $[\text{L}]$  was then substituted into equations 7.2 and 7.1 and  $[\text{Cu}]$  and  $[\text{CuL}]$  were calculated. From these quantities the stability constant for the complex was determined using the data at each titration point. The results of these calculations, which were performed using a suitable computer

program, are shown in Table 7.1.  $\bar{n}$ , the degree of formation of the complex  $\text{CuL}$ , was also calculated. For each titration the  $\log K$  values do not show a trend but fluctuate about a mean value. The mean of the  $\log K$  values and the standard deviation of an observation from the mean are shown for each of the titrations. The difference between the two mean  $\log K$  values is not statistically significant. These results indicate that the pH titration data were readily interpretable in terms of one metal ligand complex  $\text{Cu(L)}^{2+}$ .

#### Calorimetric Results

The calorimetric data from the titration of a solution of hm-3,2,3-tet with copper chloride are shown in Table 7.2. pH measurements showed that, for the calorimetric titration conditions (an excess of ligand), the rate of formation of the copper-ligand complex was faster than for titrations where the ratio of M:L was ca. 1:1 (see Table 7.1). However, during a calorimetric run the recorder trace showed that complex formation was occurring to a small extent after the completion of titrant addition. Thus, the uncertainty in the corrected heat change will be higher for this ligand system than for other complexes studied.

#### 7.1.2 Results for 3,2,3-tet

Data from the pH titrations of NaOH against solutions of copper ions, ligand and acid are shown in Table 7.3. For each of the metal:ligand ratios only one titration from a



TABLE 7.2

Calorimetric data from the titration of hm-3,2,3-tet/HCl solution  
with copper chloride at 25°C and I = 0.10M

Vol. <sup>a</sup>	p[H <sup>+</sup> ]	$\frac{L}{b}$ (mmol)	$\frac{HL}{b}$ (mmol)	$\frac{H_2L}{b}$ (mmol)	$\frac{H_3L}{b}$ (mmol)	$\frac{H_4L}{b}$ (mmol)	$\frac{CuL}{b}$ (mmol)
0.000	10.993	0.19631	0.24526	0.02857	0.000012	0.000000	0.000000
0.130	10.916	0.14556	0.21668	0.03008	0.000015	0.000000	0.077818
0.260	10.815	0.09767	0.18437	0.03245	0.000020	0.000000	0.155636
0.390	10.663	0.05468	0.14576	0.03623	0.000032	0.000000	0.233454
0.530	10.363	0.01696	0.09067	0.04518	0.000081	0.000000	0.317258

Changes in composition between successive titration points

$\frac{\Delta(LH)^c}{(mmol)}$	$\frac{\Delta(LH_2)}{(mmol)}$	$\frac{\Delta(LH_3)}{(mmol)}$	$\frac{R(ML)}{(mmol)}$	$\frac{Q^d}{(J)}$	$\frac{Q_{corr}^e}{(J)}$	$\frac{\Delta H(ML)}{(kJ\ mol^{-1})}$
-0.02707 <sup>f</sup>	0.00151	0.000004	0.077818	8.274	8.158	104.8 <sub>4</sub>
-0.02992	0.00238	0.000005	0.077818	8.256	8.086	103.9 <sub>1</sub>
-0.03483	0.00379	0.000012	0.077818	8.277	8.139	104.5 <sub>9</sub>
-0.04609	0.00900	0.000050	0.083804	8.826	8.606	102.6 <sub>9</sub>
						104.0 ± 0.9

<sup>a</sup> Volume of 0.5986M copper chloride added to 98.84ml of ligand/acid solution;  
 $T_L = 4.757 \times 10^{-3}M$ ,  $T_H = 1.449 \times 10^{-3}M$ .

<sup>b</sup> For each species values are the number of mmoles of each titration point. Calculations are described in Chapter 5.

<sup>c</sup> For each species values are the changes in the number of mmoles between each titration point.

<sup>d</sup> Corrected for the heat of dilution of copper chloride. (See Appendix F).

<sup>e</sup> Values of Q have been corrected for the hydrolysis and ligand protonation secondary reactions.

<sup>f</sup> A negative change means LH was dissociating to form L.

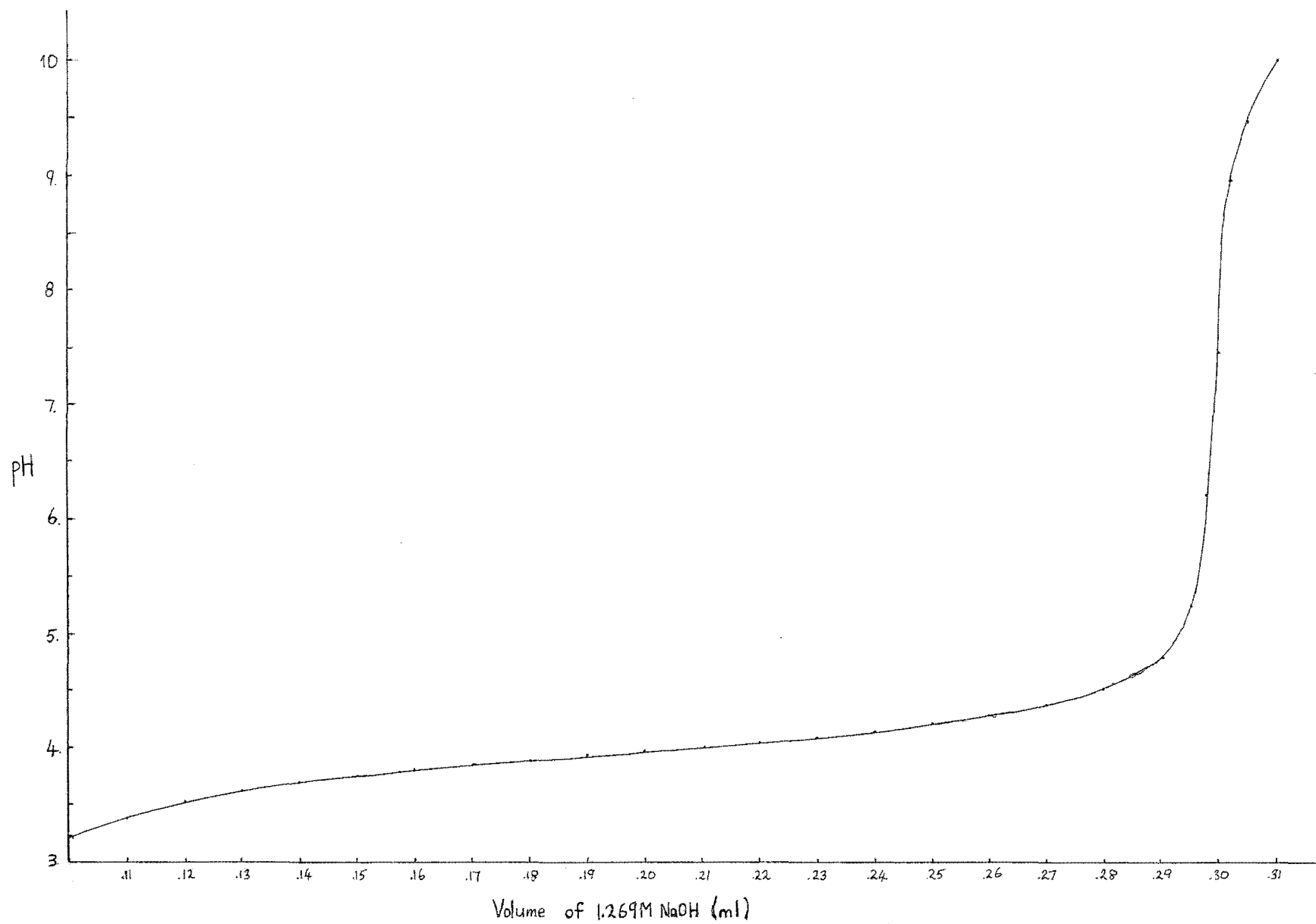


**Fig 7.2** Titration curve for copper/3,2,3-tet system  $T_M = 1.082 \times 10^{-3} \text{ M}$ ,  $T_L = 1.103 \times 10^{-3} \text{ M}$

TABLE 7.3

$p[H^+]$  data from the titrations<sup>c</sup> of NaOH against solutions of copper(II)

ions, 3,2,3-tet and acid at 25°C and I = 0.10M

$T_L = 1.103 \times 10^{-3}M$ ,  $T_M = 1.082 \times 10^{-3}M$   $T_L = 1.098 \times 10^{-3}M$ ,  $T_M = 7.721 \times 10^{-4}M$   $T_L = 1.098 \times 10^{-3}M$ ,  $T_M = 9.651 \times 10^{-3}M$

$T_H = 7.753 \times 10^{-3}M$

$T_H = 7.768 \times 10^{-3}M$

$T_H = 7.778 \times 10^{-3}M$

<u>Volume<sup>a</sup></u>	<u><math>p[H^+]</math></u>	<u>Volume<sup>a</sup></u>	<u><math>p[H^+]</math></u>	<u>Volume<sup>a</sup></u>	<u><math>p[H^+]</math></u>
0.130	3.541	0.130	3.563	0.130	3.309
0.135	3.578	0.140	3.646	0.140	3.361
0.140	3.612	0.150	3.707	0.150	3.404
0.145	3.642	0.160	3.762	0.160	3.441
0.150	3.668	0.170	3.811	0.170	3.475
0.155	3.691	0.180	3.862	0.180	3.506
0.160	3.719	0.190	3.909	0.190	3.537
0.170	3.760	0.200	3.955	0.200	3.565
0.180	3.801	0.210	4.014	0.210	3.596
0.190	3.842	0.220	4.079	0.220	3.626
0.200	3.881	0.230	4.161	0.230	3.658
0.210	3.921	0.240	4.287	0.240	3.693
0.220	3.965	0.250	4.681	0.260	3.784
0.230	4.010	0.255	5.263	0.270	3.852
0.240	4.061	0.260	5.919		
0.250	4.121	0.265	7.148		
0.260	4.195	0.270	8.024		
0.270	4.287	0.275	8.578		
0.280	4.425	0.280	9.079		

<sup>a</sup> Data are the volume of 1.269M NaOH added to 49.90 ml of the copper/ligand solution.

<sup>b</sup>  $p[H^+]$  values were interpolated off the calibration curve (see Chapter 3).

<sup>c</sup> Only one titration from a reproducible set has been tabulated.

reproducible set has been tabulated, For each point during the titrations equilibrium was rapidly attained. Analysis of the 1:1 titration data (Table 7.3) in terms of only one complex species  $\text{CuL}$  (as outlined for hm-3,2,3-tet above) was not satisfactory. The data showed that the  $\log K$  value was not constant throughout the titration but decreased from  $\log K = 21.82$  at  $\bar{n} = 0.18$  to  $\log K = 21.41$  at  $\bar{n} = 0.82$ .

Visible spectrophotometric measurements on 1:1 solutions of copper ions : ligand in aqueous buffers gave the following results:

<u>Buffer solution</u>	<u><math>\lambda_{\text{max}}</math></u>	<u>ca. pH</u>
borax	545	9.2
phosphate	546	6.8
phthalate	568	4.0
tartrate	<u>ca.</u> 575	3.5

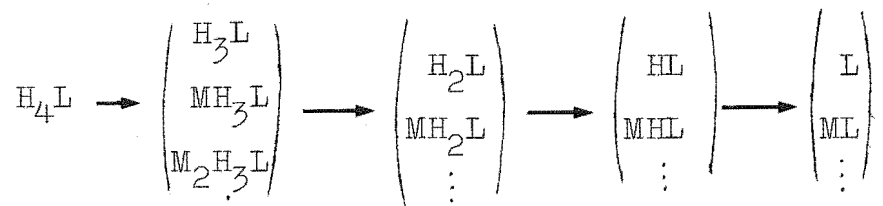
This change in  $\lambda_{\text{max}}$  as the pH of the solution decreased suggested that a protonated complex  $\text{CuHL}^{3+}$  was formed at lower pH values.

#### Calculation of Stability Constants from $p[\text{H}^+]$ Data

#### Analysis of the 10X excess metal ion data (Table 7.3)

Schwarzenbach<sup>146</sup> reported a method for the analysis of  $p[\text{H}^+]$  data from the ten-fold excess metal ion titration curve when protonated complexes were likely. This method as applied to the copper(II)/3,2,3-tet system is as follows:

Consider the scheme



Apparent acid association constants, neglecting polynuclear species, are defined

$$k_1' = \frac{[HL] + [MHL]}{[H]([L] + [ML])} = k_1 \frac{(1 + [M]K_{MHL}^M)}{(1 + [M]K_{ML}^M)}$$

where  $k_1 = \frac{[HL]}{[H][L]}$ ,  $K_{MHL}^M = \frac{[MHL]}{[M][HL]}$  and  $K_{ML}^M = \frac{[ML]}{[M][L]}$ .

Similarly other apparent acid association constants are

$$k_2' = k_2 \frac{(1 + [M]K_{MH_2L}^M)}{(1 + [M]K_{MHL}^M)}$$

$$k_3' = k_3 \frac{(1 + [M]K_{MH_3L}^M)}{(1 + [M]K_{MH_2L}^M)}$$

$$k_4' = k_4 \frac{(1 + [M]K_{MH_4L}^M)}{(1 + [M]K_{MH_3L}^M)}$$

If  $[MH_4L] = 0$  then

$$k_1'k_2'k_3'k_4' = k_1k_2k_3k_4 \frac{1}{(1 + [M]K_{ML}^M)} \quad 7.4$$

therefore as  $[M]$  is approximately equal to  $T_M$  for the titration with a ten fold excess of metal ion an approximate value of  $K_{ML}^M$  can be calculated if the apparent acidity

constants  $k_n'$  can be calculated. From the mass balance equations for  $T_L$  and  $T_H$  equation 7.5 can be derived

$$\bar{n}_H + (\bar{n}_H - 1)k_1'[H] + (\bar{n}_H - 2)\bar{k}_2'[H]^2 + (\bar{n}_H - 3)\bar{k}_3'[H]^3 + (\bar{n}_H - 4)\bar{k}_4'[H]^4 = 0 \quad 7.5$$

where

$$\bar{k}_n' = k_n' \cdot k_{n-1}' \dots k_1'.$$

For the titration of copper ions, ligand and acid with alkali the initial overall reaction is



Thus the contributions from two of the terms in equation 7.5 will be small w.r.t. the other terms and can be neglected. Equation 7.5 reduces to

$$\bar{n}_H + (\bar{n}_H - 1)\bar{k}_1'[H] + (\bar{n}_H - 4)\bar{k}_4'[H]^4 = 0.$$

This equation can be further rearranged to give

$$\frac{1}{k_1'} \frac{\bar{n}_H}{[H](\bar{n}_H - 1)} + 1 + \frac{(\bar{n}_H - 4)[H]^3}{(\bar{n}_H - 1)} k_4'k_3'k_2' = 0 \quad 7.6$$

which is of the form

$$\frac{1}{k_1'} \cdot x + y \cdot k_4'k_3'k_2' = -1.$$

Thus when  $\frac{1}{k_1'} = 0$ ,  $k_4'k_3'k_2' = -\frac{1}{y}$  and when  $k_4'k_3'k_2' = 0$ ,  $\frac{1}{k_1'} = \frac{-1}{x}$ . Therefore for each data point in the titration a line joining graph coordinates  $-1/x$  and  $-1/y$  should

intersect in a point ( $k_1'$ ,  $k_4'k_3'k_2'$ ). In practise this point would be a region as  $x$  and  $y$  are subject to experimental uncertainties. Data from the excess metal ion curve gave  $k_1' = 0.313 \times 10^4$  and  $k_4'k_3'k_2' = 7.45 \times 10^{10}$ .

Substituting these values into equation 7.4 and using

$$[M] = T_M \text{ gave } \log K_{ML}^M = 21.87 \pm 0.1.$$

Similarly an expression for  $K_{MHL}^M$  can be evaluated

$$k_2'k_3'k_4' = k_2k_3k_4 \frac{1}{(1 + [M]K_{MHL}^M)} \quad 7.7$$

From equation 7.7 a value for  $K_{MHL}^M$  can be evaluated. The data gave  $\log K_{MHL}^M = 14.80 \pm 0.1$ .

#### Analysis of the 1 : 1 metal : ligand titration data

Assuming that two copper-ligand complex species  $CuL^{2+}$  and  $CuLH^{3+}$  are formed during the titration of a 1 : 1 metal : ligand solution with alkali then the mass balance equations for  $T_M$ ,  $T_L$  and  $T_H$  are

$$T_M = [Cu] + [CuL] + [CuHL] \quad 7.8$$

$$T_L = [L] + [HL] + [H_2L] + [H_3L] + [H_4L] + [CuL] + [CuHL] \quad 7.9$$

$$T_H = [H] - K_w/[H] + [HL] + 2[H_2L] + 3[H_3L] + 4[H_4L] + [CuHL] \quad 7.10$$

From the equations 7.9 and 7.10 and the approximate complex stability constants calculated from the 10X excess metal ion titration data,  $[Cu]$  was eliminated and a value

for  $[L]$  calculated. This was substituted into equation 7.8 and a value of  $[M]$  was calculated. These values were then used to obtain improved values for the stability constants of the complexes  $CuL^{2+}$  ( $K_1$ ) and  $CuHL^{3+}$  ( $K_2$ ) and the process was repeated. These calculations were performed for each titration point using a suitable computer program. The average log K values and the standard deviations obtained from 1:1 titration data (Table 7.3) were,

$$\log K_1 = 21.68 \pm 0.02 \quad \text{and} \quad \log K_2 = 14.61 \pm 0.02.$$

#### Least Squares analysis of the pH titration data

The stability constants for the complexes  $CuL$  and  $CuHL$  were calculated from a least squares analysis of the titration data in Table 7.3. These calculations were performed using the computer program ORGLS (see Appendix D for a description of the program). For each titration point equation 7.10 can be expressed as

$$T_H - [H] = f(K_1, K_2, [M], [L])$$

i.e. the LHS is a function of the unknowns  $K_1$ ,  $K_2$ ,  $[L]$  and  $[M]$ . However, from equations 7.8 and 7.9  $[L]$  and  $[Cu]$  can be expressed in terms of known quantities and the unknowns  $K_1$  and  $K_2$ . Thus from the three mass balance equations

$$T_H - [H] = f(K_1, K_2)$$



(The hydrolysis term  $K_w/[H]$  was neglected as for each titration point the solution  $pH \ll 7$ .) This equation forms the basis of the least squares process. The LHS was derived in subroutine PRELIM of ORGLS (see Appendix D) and was termed  $Y_{OBS}$ . The RHS which was termed  $Y_{CALC}$ , was calculated from given  $K_1$  and  $K_2$  using subroutine CALC. The least squares process varied the parameters  $K_1$  and  $K_2$  so as to minimise the sum of the squares of the differences between  $Y_{OBS}$  and  $Y_{CALC}$ . Data from the least squares analysis of the 1:1 ligand:metal pH titration data (see Table 7.3) are shown in Table 7.4. The difference between  $Y_{OBS}$  and  $Y_{CALC}$  is generally less than 1% of  $Y_{OBS}$ . The precision with which  $p[H^+]$  can be determined using the calibration curve is  $\pm 0.005$  pH units. A change in the value of  $p[H^+]$  by 0.005 pH for a few data points caused a change in  $Y_{CALC}$  by ca. 0.5%. This change was of the same order as the difference between each  $Y_{OBS}$  and  $Y_{CALC}$ .

The results from least squares analyses of the titration data in Table 7.3 are shown in Table 7.5. For all the least squares analyses and for the analysis of the 10:1 metal:ligand pH titration data using Schwarzenbach's method it was assumed that only  $CuL^{2+}$  and  $CuHL^{3+}$  metal-ligand complex species were formed. The agreement between the results for the different metal:ligand ratios suggests that the data should be interpreted in terms of two complexes. The

TABLE 7.4

Data from the least squares<sup>a</sup> analysis of the 1:1  
ligand:metal  $p[H^+]$  titration data<sup>b</sup> (Table 7.3)

$p[H^+]$	$Y_{OBS}(x10^2)$	$Y_{CALC}(x10^2)$
3.578	0.4044	0.3998
3.612	0.3937	0.3898
3.642	0.3826	0.3796
3.668	0.3712	0.3695
3.691	0.3596	0.3597
3.719	0.3481	0.3467
3.760	0.3244	0.3258
3.801	0.3006	0.3029
3.842	0.2766	0.2789
3.881	0.2525	0.2556
3.921	0.2282	0.2318
3.965	0.2040	0.2064
4.010	0.1797	0.1819
4.061	0.1555	0.1563
4.121	0.1313	0.1297

<sup>a</sup>  $Y_{OBS}$  and  $Y_{CALC}$  data are from the final cycle of ORGLS

<sup>b</sup> Each data point was weighted at unity.

TABLE 7.5

Stability constants for the copper 3,2,3-tet complexes  
at  $I = 0.10M$  and  $25^{\circ}C$  calculated from the  
titration data in Table 7.3

Reaction	$\underline{T_L \approx T_M}$	$\underline{T_L > T_M}$	$\underline{T_M \gg T_L}$
$Cu^{2+} + L \rightleftharpoons CuL^{2+}; \log K_1$	$21.68_7 \pm 0.08$	$21.67_8 \pm 0.08$	$21.72_5 \pm 0.08$
$Cu^{2+} + HL^+ \rightleftharpoons CuHL^{3+}; \log K_2$	$14.69_0 \pm 0.08$	$14.68_5 \pm 0.09$	$14.70_1 \pm 0.10$

agreement between the  $\log K_1$  and  $\log K_2$  values obtained from a least squares analysis and from the Schwarzenbach analysis is satisfactory. The slightly higher values obtained from the analysis of the  $p[H^+]$  data from the 10:1 metal:ligand data are not statistically significant.

#### Distribution Curves

The % distribution of the metal-ligand complex species as a function of the solution  $p[H^+]$  is shown in Fig. 7.3. The calculations were performed using the computer program DIST (see Appendix D). The values of  $T_L$  and  $T_M$  used in the calculations were  $1.103 \times 10^{-3}$  and  $1.082 \times 10^{-3}$  M respectively. The curves indicate that the concentration of the protonated complex  $CuHL^{3+}$  is at a maximum at ca.  $p[H^+] = 4.0$ .

#### Calorimetric Results

The solution composition at each point in the calorimetric titrations is shown in Table 7.6. The calculation of these data has been described in section 5.1. The changes in the solution composition between successive titration points and the corresponding heat changes are shown in Table 7.7. The experimental exothermic heat changes  $Q$  have been corrected for the heat of dilution of HCl. The  $Q_{corr}$  values are the experimental  $Q$  values, corrected for the heat of protonation of the ligand species  $LH_1$ . The calculation of this correction has been described in section 5.1.

**Fig 7.3**

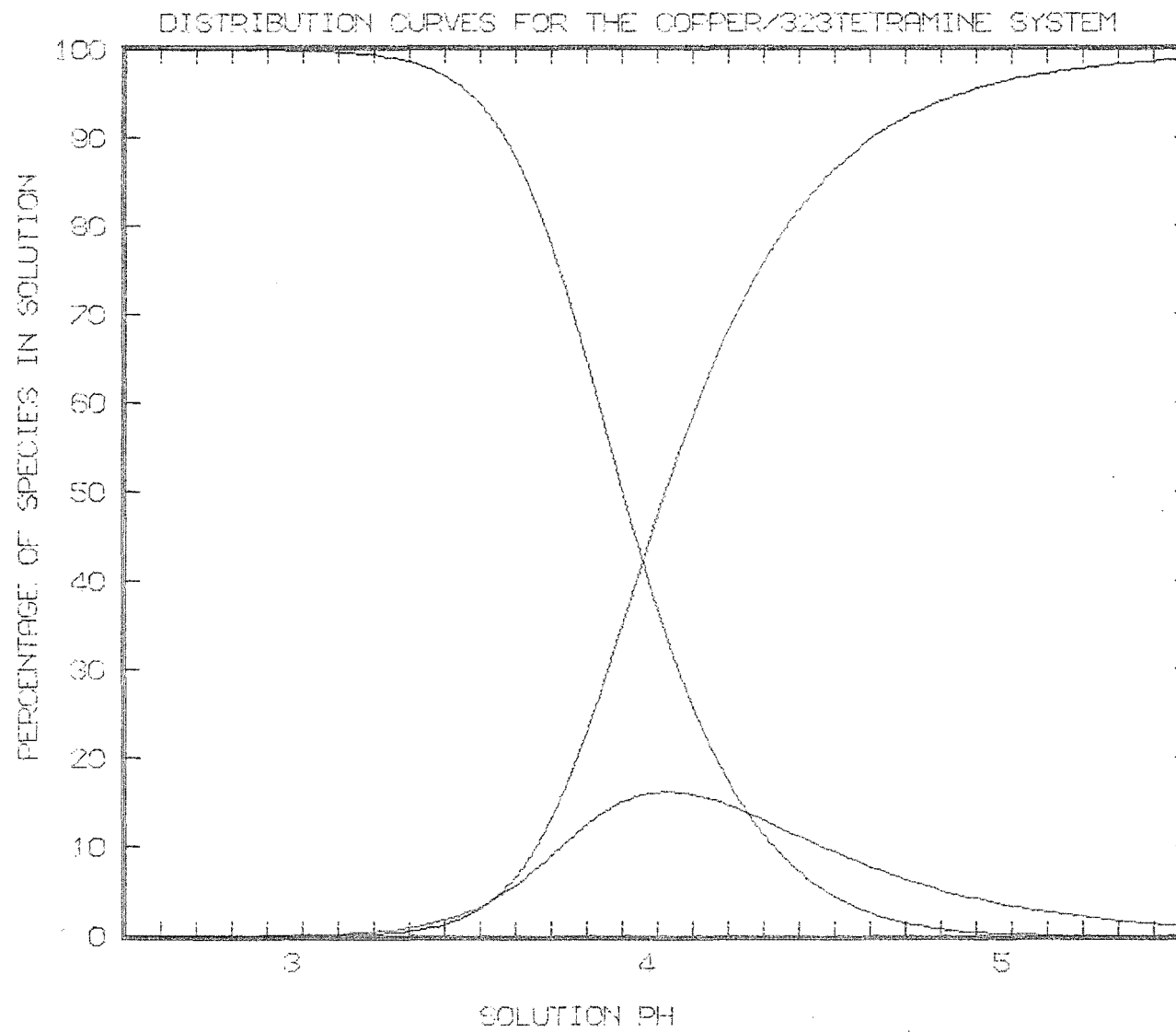


TABLE 7.6

Calorimetric data<sup>a</sup> from the titrations of the copper (3,2,3-tet)  
complex with HCl at 25°C and I = 0.10M

Vol. (ml)	p[H <sup>+</sup> ]	<u>L</u> <sup>b</sup> (mmol)	<u>HL</u> (mmol)	<u>H<sub>2</sub>L</u> (mmol)	<u>H<sub>3</sub>L</u> (mmol)	<u>H<sub>4</sub>L</u> (mmol)	<u>ML</u> (mmol)	<u>MHL</u> (mmol)
0.320	4.197	0.00000	0.00000	0.00000	0.00196	0.04846	0.47687	0.10329
0.650	3.979	0.00000	0.00000	0.00000	0.00291	0.11872	0.37467	0.13429
0.980	3.844	0.00000	0.00000	0.00000	0.00350	0.19519	0.29011	0.14179
1.330	3.732	0.00000	0.00000	0.00000	0.00389	0.28032	0.21223	0.13417
1.680	3.631	0.00000	0.00000	0.00000	0.00405	0.36842	0.14358	0.11456
2.030	3.524	0.00000	0.00000	0.00000	0.00395	0.45935	0.08279	0.08449
2.430	3.350	0.00000	0.00000	0.00000	0.00325	0.56432	0.02497	0.03806
Titration 2								
0.330	4.196	0.00000	0.00000	0.00000	0.00201	0.04974	0.49683	0.10793
0.660	3.982	0.00000	0.00000	0.00000	0.00296	0.11979	0.39373	0.14002
1.000	3.846	0.00000	0.00000	0.00000	0.00358	0.19840	0.30580	0.14871
1.330	3.743	0.00000	0.00000	0.00000	0.00396	0.27849	0.23137	0.14267
1.660	3.651	0.00000	0.00000	0.00000	0.00415	0.36122	0.16513	0.12598
2.000	3.555	0.00000	0.00000	0.00000	0.00413	0.44829	0.10457	0.09951
2.330	3.443	0.00000	0.00000	0.00000	0.00381	0.53476	0.05286	0.06508

<sup>a</sup> Solution composition: Titration 1: [CuL]<sub>initial</sub> = 6.380x10<sup>-3</sup>M. Titration 2: [CuL]<sub>initial</sub> = 6.642x10<sup>-3</sup>M. For both titrations the initial volume of complex = 98.84ml and the titrant HCl concentration = 0.9670M.

<sup>b</sup> For each species, values are the number of mmoles at each titration point.

TABLE 7.7

Changes in composition and the heat changes between successive titration points for the titrations of copper(3,2,3-tet) complex with HCl at 25°C and I = 0.10M

$\Delta(\text{HL})^a$ (mmol)	$\Delta(\text{H}_2\text{L})$ (mmol)	$\Delta(\text{H}_3\text{L})$ (mmol)	$\Delta(\text{H}_4\text{L})$ (mmol)	$\Delta(\text{CuL})^b$ (mmol)	$\Delta(\text{CuHL})^c$ (mmol)	$Q^d$ —	$Q_{\text{corr}}^d$	$Q_{\text{calc}}^d$
0.10220	0.07119	0.07119	0.07025	0.10220	-0.03100	5.973	-8.470	-8.452
0.08457	0.07706	0.07706	0.07646	0.08457	-0.00751	6.016	-8.286	-8.271
0.07788	0.08550	0.08550	0.08512	0.07788	0.00763	6.410	-8.643	-8.638
0.06866	0.08826	0.08826	0.08810	0.06866	0.01961	6.366	-8.574	-8.520
0.06079	0.09085	0.09085	0.09096	0.06079	0.03007	6.361	-8.517	-8.437
0.05782	0.16426	0.10426	0.10496	0.05782	0.04644	7.164	-9.312	-9.278
0.10310	0.07100	0.07100	0.07005	0.10310	-0.03209	6.024	-8.441	-8.471
0.08793	0.07925	0.07925	0.07862	0.08793	-0.00869	6.228	-8.529	-8.538
0.07443	0.08048	0.08048	0.08009	0.07443	0.00604	6.068	-8.158	-8.168
0.06624	0.08293	0.08293	0.08274	0.06624	0.01669	6.079	-8.047	-8.064
0.06056	0.08702	0.08702	0.08704	0.06056	0.02646	6.233	-8.136	-8.160
0.05171	0.08615	0.08615	0.08647	0.05171	0.03444	6.139	-7.669	-7.799

<sup>a</sup> For the  $\text{H}_i\text{L}$  species the tabulated values are the number of mmoles of each species formed on the addition of the titration increment.

<sup>b</sup> These values are the number of mmoles of  $\text{CuL}$  that dissociate on the addition of titrant acid.

<sup>c</sup> These values are the number of mmoles of  $\text{CuHL}$  that dissociate on the addition of titrant HCl.

<sup>d</sup> See Text.

(Negative  $Q_{\text{corr}}$  values imply endothermic heat changes.) The values of  $Q_{\text{calc}}$  are those calculated from the least squares process (see chapter 5). The differences between  $Q_{\text{corr}}$  and  $Q_{\text{calc}}$  values give an indication of the refinement in the least squares process.

The thermodynamic data ( $I = 0.10 \text{ M}$ ) for the formation of the copper-ligand complexes for 3,2,3-tet and hm-3,2,3-tet are shown in Table 7.8.

$\log K_n^0$  data for the formation of copper-3,2,3-tet complexes were determined from the concentration quotient data at  $I = 0.20, 0.15, 0.10$  and  $0.04$  as described in Chapter 1. However, only the data at  $I = 0.10$  has been used in the discussion as there are few available thermodynamic  $K_n^0$  data for related reactions.

The results at the other ionic strengths and the  $K_n^0$  values are given in Appendix E.

### 7.1.3 Discussion

#### $\log K$ values for the $\text{CuL}^{2+}$ complexes

The copper complexes of 3,2,3-tet and hm-3,2,3-tet both have two six membered and one five membered chelate rings. It is well known that for labile complexes six membered chelate rings are less stable than five membered rings<sup>35,148</sup>. For example, the free energy change for the formation of the 1:1 copper complex with 1,3-diaminopropane is less negative than that for 1,2-diaminoethane<sup>147</sup>. For the triamines

TABLE 7.8

Thermodynamic<sup>a</sup> data for the formation of some copper(II) complexes  
with 3,2,3-tet and hm-3,2,3-tet at 25°C and I = 0.10M

<u>1,5,8,12-tetraazadodecane(3,2,3-tet)</u>				
<u>Reaction</u>	<u>logK<sub>n</sub></u>	<u>-ΔG kJmol<sup>-1</sup></u>	<u>-ΔH kJmol<sup>-1</sup></u>	<u>ΔS Jmol<sup>-1</sup>K<sup>-1</sup></u>
1. Cu <sup>2+</sup> + L ⇌ CuL <sup>2+</sup>	21.68 <sub>7</sub> ± 0.08	123.7 <sub>7</sub> ± 0.46	104.0 ± 0.9	66.3 ± 5
2. Cu <sup>2+</sup> + HL <sup>+</sup> ⇌ CuHL <sup>3+</sup>	14.69 <sub>0</sub> ± 0.08	83.8 <sub>4</sub> ± 0.4 <sub>6</sub>	70.2 <sub>7</sub> ± 1.2	45.5 ± 5

2,11-diamino-4,4,9,9-tetramethyl-5,8 diazadodecane (hm-3,2,3-tet)

<u>Reaction</u>	<u>logK<sub>1</sub></u>	<u>-ΔG kJmol<sup>-1</sup></u>	<u>-ΔH kJmol<sup>-1</sup></u>	<u>ΔS Jmol<sup>-1</sup>K<sup>-1</sup></u>
Cu <sup>2+</sup> + L ⇌ CuL <sup>2+</sup>	22.41 ± 0.06	127.8 <sub>9</sub> ± 0.3	104.0 ± 0.9	80.2 ± 4

<sup>a</sup> With reference to a standard state of 0.10M NaCl.



TABLE 7.9

Thermodynamic data for the formation of the copper(II) complexes with some polyamines

<u>Amine, Reaction</u>	<u>Ring System</u>	<u>log K</u>	<u>-ΔG kJmol<sup>-1</sup></u>	<u>-ΔH kJmol<sup>-1</sup></u>	<u>ΔS Jmol<sup>-1</sup>K<sup>-1</sup></u>	<u>Conditions</u>
$\text{Cu}^{2+} + 2,3,2\text{-tet} \rightarrow \text{Cu}(2,3,2\text{tet})^{2+}$	5,6,5	23.9 <sup>a</sup>	136.4	-	-	0.5M KCl, 25°C
$\text{Cu}^{2+} + \text{tripen} \rightarrow \text{Cu}(\text{tripen})^{2+}$	6,6,6	17.3 <sup>b</sup>	98.7 <sub>3</sub>	-	-	0.1 NaNO <sub>3</sub> , 20°C
$\text{Cu}^{2+} + \text{trien} \rightarrow \text{Cu}(\text{trien})^{2+}$	5,5,5	20.0 <sub>8</sub> <sup>c</sup>	114.6 <sub>4</sub>	90.1 <sub>6</sub>	81.6	0.1M KCl, 25°C
$\text{Cu}^{2+} + \text{dien} \rightarrow \text{Cu}(\text{dien})^{2+}$	5,5	15.8 <sup>d</sup>	90.1 <sub>6</sub>	75.3	50.2	0.1M KCl, 25°C
$\text{Cu}^{2+} + \text{dpt} \rightarrow \text{Cu}(\text{dpt})^{2+}$	6,6	14.2 <sup>d</sup>	81.0 <sub>9</sub>	67.3 <sub>2</sub>	46.0	0.1M KCl, 25°C
$\text{Cu}^{2+} + 2\text{en} \rightarrow \text{Cu}(\text{en})_2^{2+}$	5 and 5	20.0 <sup>e</sup>	114.1 <sub>4</sub>	105.2 <sub>7</sub>	29.7	0.1M KCl, 25°C
$\text{Cu}^{2+} + \text{Htrien}^+ \rightarrow \text{Cu}(\text{Htrien})^{2+}$	5,5	13.8 <sup>c</sup>	78.66	66.1	41.8	0.1M KCl, 25°C

<sup>a</sup> Datum from reference 15.<sup>b</sup> Datum from reference 14.<sup>c</sup> All the thermodynamic data from reference 16.<sup>d</sup> From reference 106.<sup>e</sup> From reference 137.

dien  $(\text{NH}_2\text{CH}_2\text{CH}_2)_2\text{NH}$  and dpt  $(\text{NH}_2\text{CH}_2\text{CH}_2\text{CH}_2)_2\text{NH}$  the 1:1 copper complex of dien is more stable than that for dpt (see Table 7.9), even though dpt is a stronger base. The crystal structures of the nickel complexes,  $\text{NiL}_2^{2+}$ , with L dien and dpt have been reported<sup>148,149</sup>. The data show that the metal-secondary nitrogen bonds are  $0.16 \text{ \AA}$  longer for  $\text{Ni}(\text{dpt})_2^{2+}$  than for  $\text{Ni}(\text{dien})_2^{2+}$ . It was suggested that the more endothermic enthalpy changes, for the formation of the nickel complexes of dpt, relative to those of dien was due (in part) to this difference in the strength of the metal-secondary nitrogen bond. For the tetraamines triethylenetetramine (trien) and tripropylenetetramine (tripen) the stability constant data show that the copper complex with three five membered chelate rings (trien) is more stable than that with three six membered chelate rings (tripen) (see Table 7.9).

It has been reported<sup>150</sup> that, for the coordination of trien with copper(II) ions in a planar configuration, the chelate rings cannot all adopt the favoured gauche form without very considerable strain (distortion of bond angles).

In cobalt(III) complexes trien achieves the favoured gauche form by adopting a cis configuration<sup>150</sup>. For tripen, models show that each chelate ring can be formed in the favoured chair configuration<sup>151</sup> but there is considerable strain in the metal-secondary nitrogen bonds. However, the data in Tables 7.8 and 7.9 indicate that when the ligand

enables the formation of a mixture of five and six membered chelate rings, as in the complexes with 2,3,2-tet and 3,2,3-tet, the complexes formed are more stable than those with either five or six membered rings alone. From models of the ligands 3,2,3-tet and 2,3,2-tet<sup>150</sup> in square coordination it is apparent that the five membered ring can adopt the favoured gauche form and the six membered ring can readily adopt the favoured chair configuration. For both ligands in a planar coordination these configurations result in an apparent strain-free system. That the copper complex of 2,3,2-tet is more stable than the complex for 3,2,3-tet (see Tables 7.8 and 7.9) indicates that five membered chelate rings are more stable than six membered rings.

The log K data in Table 7.8 shows that the copper complex with hm-3,2,3-tet is only slightly more stable than the complex of 3,2,3-tet (a difference of ca. 0.7 log units).  
Enthalpy changes for the  $\text{CuL}^{2+}$  complexes

The enthalpy changes for coordination reactions are the quantities most readily related to the changes in the number and strength of bonds. It is convenient to express the free energy on the coordination of a ligand to a metal ion in terms of two parts; the free energy change which involves long range electrostatic interactions (which depend on the solvent and which will be temperature dependent) and a term representing the short range covalent forces which will be

temperature independent<sup>152,153</sup>, i.e.

$$\Delta G = \Delta G_c + \Delta G_e - \Delta_n RT \ln 55.5$$

where  $\Delta G_c$  is the covalent (temperature independent) term,  $\Delta G_e$  is the electrostatic (temperature dependent) term and  $\Delta_n RT \ln 55.5$  is the quantity which renders the equilibrium constant dimensionless.  $\Delta_n$  is the increase in the number of solute species on coordination and 55.5 is the number of moles contained in 1000g of water. This term is called the cratic term as first defined by Gurney<sup>36</sup>. For purely electrostatic interactions the free energy will be inversely proportional to the dielectric constant  $\epsilon$ , which can be expressed<sup>36</sup>,

$$1/\epsilon = \alpha' e^{T/\nu}$$

where  $\alpha'$  is a constant and  $\nu$  is a temperature characteristic of the solvent (219°K for water). Thus

$$\Delta G = \Delta G_c - \Delta_n RT \ln 55.5 - \alpha e^{T/\nu}$$

and the entropy change is given by

$$\Delta S = -\partial(\Delta G)/\partial T = \frac{\alpha}{\nu} e^{T/\nu} + \Delta_n R \ln 55.5$$

and

$$\Delta H = \Delta G_c - \alpha e^{T/\nu} (1 - T/\nu).$$

The electrostatic components  $\Delta G_e$  and  $\Delta H_e$  can be calculated by equations 7.11 and 7.12

$$\Delta G_e = -\alpha e^{T/v} = -v(\Delta S - \Delta_n R \ln 55.5) \quad 7.11$$

$$\Delta H_e = (T - v)(\Delta S - \Delta_n R \ln 55.5) \quad 7.12$$

The temperature independent part of the enthalpy  $\Delta H_c$  is given by the difference  $\Delta H_c = \Delta H - \Delta H_e$ . If it is assumed that the major contribution of  $\Delta H_c$  arises from the formation of the metal-ligand bonds then an approximate value can be calculated for each bond. The temperature dependent and temperature independent contributions to the enthalpy data for the formation of the copper complexes of some amines are shown in Table 7.10.

Structural features in addition to the formation of a metal-nitrogen bond make a contribution to the  $\Delta H_c$  values. The more endothermic values for dien and trien compared with en indicate the increased strain in the formation of additional chelate rings. The value of  $-\Delta H_c/p$  for 3,2,3-tet is very similar to that for ethylenediamine. This evidence supports the conclusion that the copper complex with 3,2,3-tet is almost strain free, as discussed earlier.

From the enthalpy data in Tables 7.8 and 7.9, the enthalpy changes for the reaction



where L is trien and 3,2,3-tet, are  $15.1 \text{ kJ mol}^{-1}$  and  $1.3 \text{ kJ mol}^{-1}$  respectively. It has been suggested<sup>16</sup> that the large

TABLE 7.10

Temperature independent enthalpy data for the formation  
of some copper(II) amine complexes

Amine, Reaction	$-\Delta H \text{ kJmol}^{-1}$	$\Delta n$	$\Delta H_e \text{ kJmol}^{-1}$	$-\Delta H_c \text{ kJmol}^{-1}$	$-\Delta H_c^a / p \text{ kJmol}^{-1}$
$\text{Cu} + 2\text{en} \rightarrow \text{Cu}(\text{en})_2^{2+}$	105.3 <sup>b</sup>	2	7.6	112.9	28.2
$\text{Cu} + 323\text{tet} \rightarrow \text{Cu}(323\text{tet})^{2+}$	104.0 <sup>d</sup>	1	7.9	111.9	28.0
$\text{Cu} + \text{trien} \rightarrow \text{Cu}(\text{trien})^{2+}$	80.16 <sup>b</sup>	1	7.0 <sub>8</sub>	97.2	24.8
$\text{Cu} + \text{dien} \rightarrow \text{Cu}(\text{dien})^{2+}$	75.3 <sup>b</sup>	1	6.6	81.9	27.3
$\text{Cu} + \text{dpt} \rightarrow \text{Cu}(\text{dpt})^{2+}$	67.3 <sup>b</sup>	1	6.2 <sub>7</sub>	73.6	24.5
$\text{Cu} + \text{NH}_3 \rightarrow \text{Cu}(\text{NH}_3)^{2+}$	24.68 <sup>c</sup>	1	2.5	27.2	27.2

<sup>a</sup> p is the number of nitrogens bonded to the central copper ion.

<sup>b</sup> Data from Table 7.9.

<sup>c</sup> Data from reference 153.

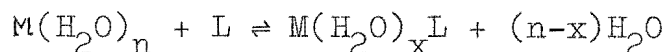
<sup>d</sup> Data from Table 7.8.

endothermic  $\Delta H$  for reaction I when  $L = \text{trien}$  is due to both the increase in internal strain in the chelate rings of  $\text{CuL}$  and to the probable lower heat of formation of a metal-secondary nitrogen bond compared with a metal-primary nitrogen bond. However, as both  $\text{trien}$  and  $\beta,2,\beta\text{-tet}$  have two primary and two secondary nitrogen atoms and as the  $\Delta H$  change for reaction I when  $L = \beta,2,\beta\text{-tet}$  is only  $1.3 \text{ kJ mol}^{-1}$  it would appear that the increase in internal strain in the chelate rings is the cause of the large  $\Delta H$  value for  $\text{trien}$ .

The data in Table 7.8 show that the enthalpy changes for the formation of  $\text{Cu}(\beta,2,\beta\text{-tet})^{2+}$  and  $\text{Cu}(\text{hm-}\beta,2,\beta\text{-tet})^{2+}$  are identical within the experimental error. As noted earlier, the stability of the latter complex is slightly greater than for the former, therefore the difference in stability must arise from the entropy difference.

#### Entropy Changes for the $\text{CuL}^{2+}$ Complexes

The factors which contribute to the entropy change for the reaction



have been discussed in Chapter 1. The data in Tables 7.8 and 7.9 show that the entropy change for the formation of the complexes  $\text{Cu}(\text{hm-}\beta,2,\beta\text{-tet})^{2+}$  and  $\text{Cu}(\beta,2,\beta\text{-tet})^{2+}$  are positive and the value for  $\text{Cu}(\beta,2,\beta\text{-tet})^{2+}$  is smaller (by  $15.3 \text{ J mol}^{-1}\text{K}^{-1}$ ) than that for  $\text{Cu}(\text{trien})^{2+}$ . This difference of  $15.3 \text{ J mol}^{-1}\text{K}^{-1}$  suggests that the expected greater loss

in ligand configurational entropy for 3,2,3-tet compared with trien, on coordination to copper(II) ions, is not entirely compensated by the expected decreased solvent orientation of the  $\text{Cu}(3,2,3\text{-tet})^{2+}$  complex compared with  $\text{Cu}(\text{trien})^{2+}$ .

The  $\Delta S$  value for the formation of  $\text{Cu}(\text{hm-3,2,3-tet})^{2+}$  is ca.  $12 \text{ J mol}^{-1}\text{K}^{-1}$  greater than that for  $\text{Cu}(3,2,3\text{-tet})^{2+}$ . The six methyl substituents would be expected to shield the solvent from the influence of the charge on the complex ion  $\text{Cu}(\text{hm-3,2,3-tet})^{2+}$  and this will produce a larger entropy change than for  $\text{Cu}(3,2,3\text{-tet})^{2+}$  formation. Models indicate that, when the hm-3,2,3-tet ligand is coordinated in a planar configuration, there would be considerable interaction between the axial members of the gem-dimethyl groups and the water molecules weakly coordinated in the trans-planar sites. This interaction would result in a weaker binding of these water molecules to the copper ion. Visible absorption spectral data (see section below) do suggest that the tetragonal distortion in  $\text{Cu}(\text{hm-3,2,3-tet})^{2+}$  is greater than that for  $\text{Cu}(3,2,3\text{-tet})^{2+}$ . Any such tetragonal distortion will lead to a slightly larger entropy change for the formation of the complex.

#### Visible Electronic Spectra and Bonding

The ligand field splitting diagram for copper(II) is shown in Fig. 7.4. When copper is in a tetragonal



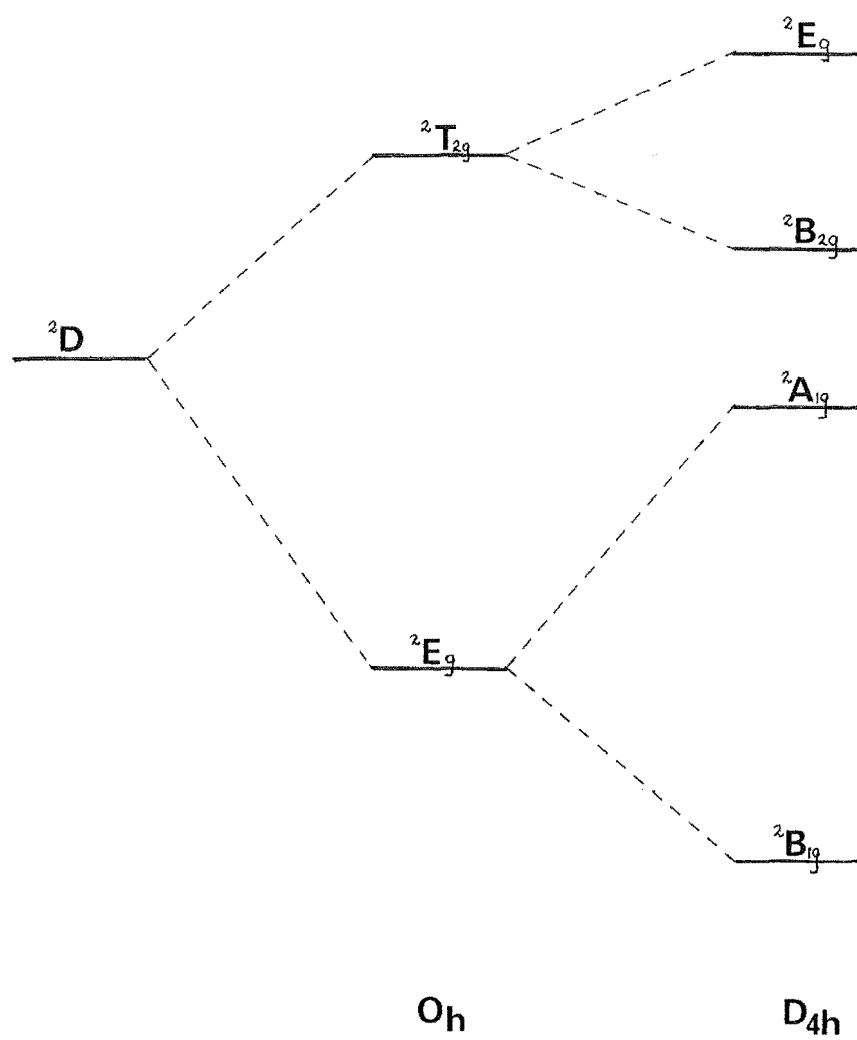


Fig. 7·4

environment the symmetry approximates to  $D_{4h}$ <sup>154</sup>. The energy level diagram predicts that there will be three electronic transitions, however the energies of the  ${}^2E_g$ ,  ${}^2B_{2g}$  and  ${}^2A_{1g}$  states are similar enough so that a single band is obtained in the observed absorption spectrum<sup>154</sup>. As the tetragonal distortion is increased the splitting of the energy states is increased resulting in a higher ligand field strength as measured by  $\lambda_{\max}$ . The visible spectrophotometric data for the copper complexes of a number of amines are shown in Table 7.11. The value of  $\lambda_{\max}$  will depend on the donor strength of the in-plane donor atoms and on the degree of tetragonal distortion. The thermodynamic quantity that would be expected to relate most closely to  $\lambda_{\max}$  is the temperature independent enthalpy term  $-\Delta H_c$ . A comparison of the enthalpy data in Table 7.10 with the  $\lambda_{\max}$  data in Table 7.11 shows that both the ligand field strength and the  $-\Delta H_c$  increase in the order  $Cu(dien)^{2+} < Cu(trien)^{2+} < Cu(en)_2^{2+} \sim Cu(3,2,3-tet)^{2+}$ , in fact the correlation is linear as shown in Fig. 7.5. The point for hm-3,2,3-tet does not lie very close to the line of best fit through the other data. However, the value of  $\lambda_{\max}$  will be more sensitive to slight changes in the degree of tetragonal distortion than will the change in  $-\Delta H_c$ , when solvent water molecules occupy the trans-planar sites. Thus the deviation for hm-3,2,3-tet is not surprising. No enthalpy data for

TABLE 7.11

Visible spectrophotometric data for a number of  
copper-amine complexes in aqueous solution

<u>Complex</u>	<u><math>\lambda_{\max}</math> nm</u>	<u><math>\nu</math> cm<sup>-1</sup></u>	<u><math>\epsilon</math></u>
Cu(3,2,3-tet) <sup>2+</sup>	545	18,350	90
Cu(hm-3,2,3-tet) <sup>2+</sup>	534	18,700	110
Cu(en) <sub>2</sub> <sup>2+</sup>	549 <sup>a</sup>	18,200	63
Cu(trien) <sup>2+</sup>	575 <sup>b</sup>	17,400	150
Cu(2,3,2-tet) <sup>2+</sup>	524 <sup>c</sup>	19,100	66
Cu(dien) <sup>2+</sup>	611 <sup>a</sup>	16,300	74
Cu(tn) <sub>2</sub> <sup>2+</sup>	568 <sup>a</sup>	17,600	111

<sup>a</sup> Data from reference 164.

<sup>b</sup> Data from reference 16.

<sup>c</sup> Data from reference 155.

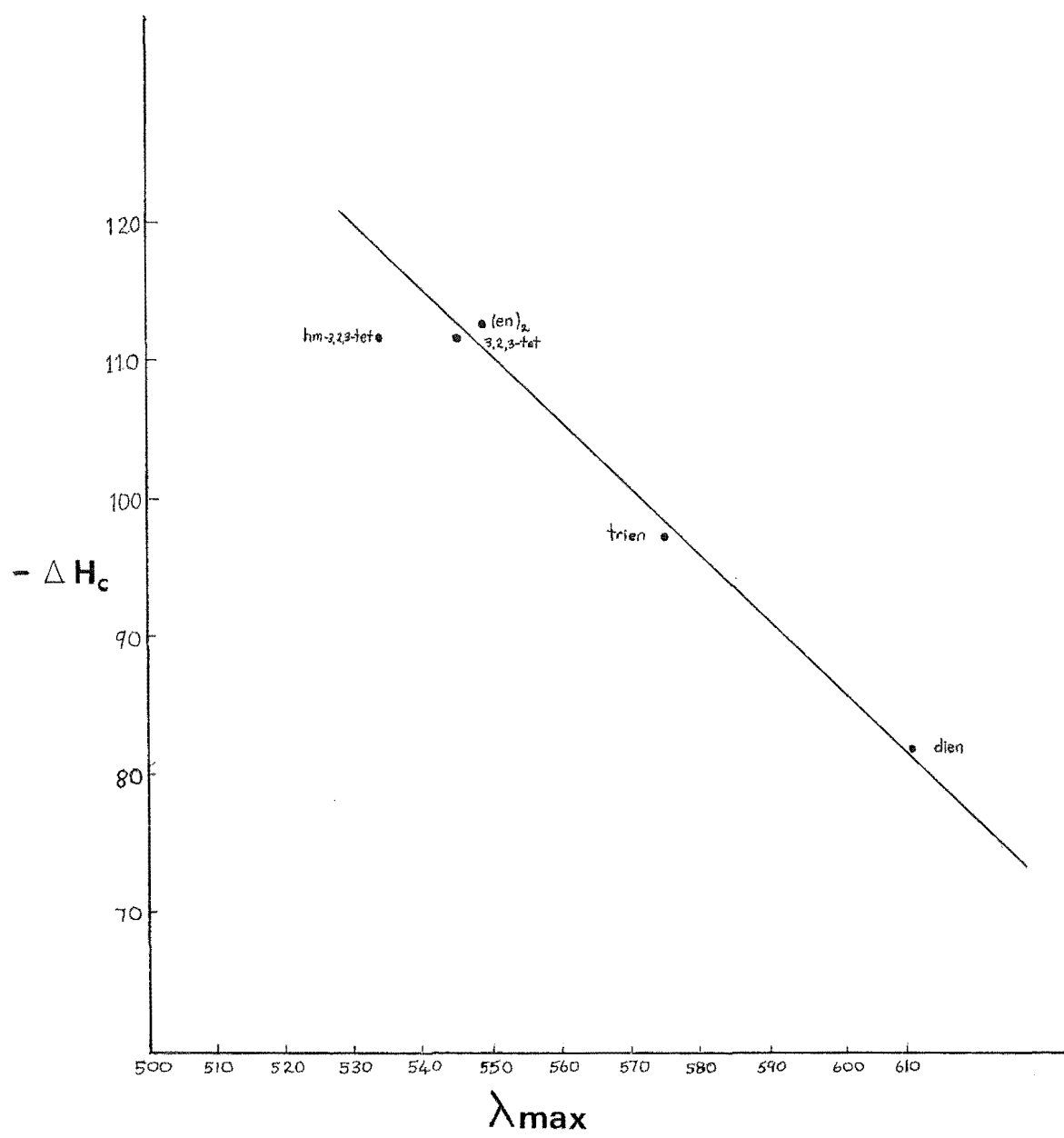


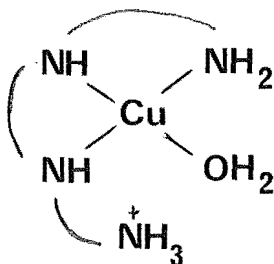
Fig 7.5

the formation of the copper-2,3,2-tet complex are available.

The covalent bonding parameters from the epr spectra for  $\text{Cu(en)}_2(\text{H}_2\text{O})_2^{2+}$ ,  $\text{Cu}(3,2,3\text{-tet})(\text{H}_2\text{O})_2^{2+}$  and  $\text{Cu}(2,3,2\text{-tet})(\text{H}_2\text{O})_2^{2+}$  imply<sup>155</sup> that the covalent bonding is nearly the same in all three complexes but is slightly stronger in the 2,3,2-tet case. This result is consistent with the visible spectral data in Table 7.11. It might be expected therefore, that the  $-\Delta H_c$  for  $\text{Cu}(2,3,2\text{-tet})^{2+}$  will be greater than that for the formation of  $\text{Cu}(3,2,3\text{-tet})^{2+}$ .

#### Protonated complex $\text{CuHL}^{3+}$

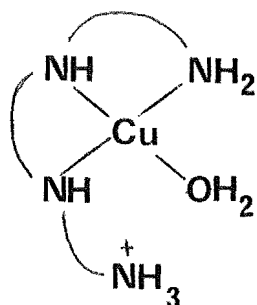
The most likely structure of the protonated complex  $\text{CuHL}^{3+}$  for 3,2,3-tet is



where one primary and two secondary nitrogen atoms are coordinated to the metal ion and the remaining nitrogen atom is protonated. There will be one five membered and one six membered chelate ring. The formation of a protonated complex was also found for the ligand trien<sup>16</sup>. Thermodynamic data for the formation of the protonated complexes for trien and 3,2,3-tet ligands are shown in Tables 7.8 and 7.9.

The enthalpy data for the formation of  $\text{Cu}(\text{dien})^{2+}$  (Table 7.9) and for  $\text{Cu}(\text{Htrien})^{3+}$  show that the  $\Delta H$  of formation for the latter complex is less exothermic by ca.  $9 \text{ kJ mol}^{-1} \text{K}^{-1}$ . Presumably, this difference is due to the inductive and electrostatic effects associated with the terminal  $-\text{NH}_3^+$  group. No thermodynamic data for the formation of the copper complex with the ligand 2,3-tri  $(\text{NH}_2(\text{CH}_2)_3\text{NH}(\text{CH}_2)_2\text{NH}_2)$  are available. Margerum et al.<sup>15</sup> found that the 1:1 nickel complex with 2,3-tri was of closely similar stability to that with dien. Thus it might be expected that the thermodynamic data for the formation of  $\text{Cu}(2,3\text{-tri})^{2+}$  would be similar to that for dien (see Table 7.9). The enthalpy change for the formation of  $\text{Cu}(\text{H } 3,2,3\text{-tet})^{3+}$  is ca.  $4 \text{ kJ mol}^{-1}$  greater than  $\Delta H$  for  $\text{Cu}(\text{H trien})^{3+}$ . This is consistent with the greater distance between the two positively charged centres in the protonated complex  $\text{Cu}(\text{H } 3,2,3\text{-tet})^{3+}$ .

No protonated complex was observed for the ligand tripen ((3,3,3-tet)). This was due to the copper ligand complex being formed in a pH range of 5.3-6.2<sup>14</sup>. For the ligands 3,2,3-tet and hm-3,2,3-tet the complexes were formed in the pH range 3.5-4.2 and yet no protonated complex for hm-3,2,3-tet was detected. This implies that for hm-3,2,3-tet the species



in the pH range 3.5 - 4.2, very readily loses a proton to form the 1:1 copper ligand complex.

### Hydroxy-Complexes

It has been shown<sup>157</sup> that the degree of formation of soluble metal ion hydroxy species decreases as the metal-ligand stability increases and as the number of donor groups increases. Hydroxy complexes  $\text{CuL}(\text{OH})^+$  have been well characterised for dien and dpt<sup>103</sup>. A hydroxy complex has also been reported for  $\text{Cu}(\text{trien})^{2+}$ <sup>157</sup> ( $\text{pK}_a$  for  $\text{Cu}(\text{trien})(\text{H}_2\text{O})_2^{2+}$  is 10.8). However, spectrophotometric data from solutions of pH 4-11 showed no evidence for the formation of hydroxy species for either hm-3,2,3-tet or 3,2,3-tet.

## 7.2 FORMATION OF COPPER COMPLEXES WITH THE DIAMINE-DIOXIME LIGAND

### 7.2.1 Results

#### p[H<sup>+</sup>] titration data

Solutions of copper(II) ions and protonated ligand  $\text{LH}_4^{2+}$  (both the  $\alpha$ .2HCl and  $\gamma$ .2HClO<sub>4</sub> isomers were used) were

titrated with both standard NaOH and HCl.  $p[H^+]$  titration data were obtained for a number of different metal : ligand ratios and at different total metal ion concentrations.

Data from titrations at  $T_M : T_L$  of ca. 1 : 3 and 1 : 2 are shown in Table 7.12, data at  $T_M : T_L$  of ca. 1 : 1.5 are shown in Table 7.13 and data at  $T_M : T_L$  of ca. 1 : 1 are shown in Table 7.14. Only one titration from a reproducible set of titrations has been tabulated in each case. Representative titration curves, using the data from Tables 7.12-7.14, are shown in Fig. 7.6. For comparison purposes the titration data have all been plotted on the same titrant scale. The 1 : 1 data are anomalous and will be discussed separately.

The ca. 1 : 1.5 metal : ligand data shows that the titrations with the  $\alpha$  or  $\gamma$  isomers are identical up to pH ca. 6. The deviation after this point is due to the different  $T_L$  values for the two sets of data (see Table 7.13). The first end point (1) for the 1 : 1.5 and 1 : 2 titrations corresponds to the addition of 3 moles of titrant per mole of metal ion, while the second end points (2) can be ascribed to the neutralisation of one proton from the excess ligand,  $LH_4^{2+}$ . The agreement of the experimental end points with those calculated from this interpretation is within the experimental error of ca. 0.5%.



TABLE 7.12

p[H<sup>+</sup>] data from the titrations of NaOH or HCl against solutions of copper(II) ions, diamine-dioxime ligand and acid at 25°C,

I = 0.10M (NaCl)

$T_L = 4.905 \times 10^{-4} M$ ,  $T_M = 1.531 \times 10^{-4} M$

$T_L = 7.647 \times 10^{-4} M$ ,  $T_M = 3.812 \times 10^{-4} M$

used $\gamma.2HClO_4$				used $\gamma.2HClO_4$			
<u>Vol.</u> <sup>a</sup>	<u>p[H<sup>+</sup>]</u> <sup>b</sup>	<u>Vol.</u> <sup>c</sup>	<u>p[H<sup>+</sup>]</u>	<u>Vol.</u> <sup>d</sup>	<u>p[H<sup>+</sup>]</u> <sup>b</sup>	<u>Vol.</u> <sup>c</sup>	<u>p[H<sup>+</sup>]</u>
0.000	3.404	0.000	3.404	0.000	3.121		
0.010	3.439	0.005	3.359	0.020	3.149	0.010	3.085
0.020	3.474	0.010	3.322	0.040	3.179	0.020	3.050
0.030	3.516	0.015	3.285	0.060	3.212	0.030	3.015
0.040	3.560	0.020	3.253	0.080	3.249	0.040	2.986
0.050	3.611	0.030	3.192	0.100	3.285	0.060	2.931
0.060	3.667	0.040	3.140	0.120	3.327	0.080	2.881
0.070	3.735	0.050	3.094	0.140	3.372	0.100	2.837
0.080	3.814	0.060	3.052	0.150	3.397	0.140	2.756
0.090	3.910	0.070	3.012	0.170	3.451	0.180	2.680
0.095	3.968	0.080	2.978	0.180	3.481	0.220	2.615
0.100	4.031	0.100	2.913	0.190	3.514	0.280	2.527
0.105	4.106	0.120	2.855	0.200	3.548		
0.110	4.201	0.140	2.805	0.210	3.588		
0.115	4.312	0.160	2.762	0.220	3.629		
		0.190	2.698	0.230	3.675		
		0.220	2.643	0.240	3.730		
				0.250	3.790		
				0.260	3.861		
				0.270	3.942		
				0.280	4.047		
				0.290	4.176		
				0.300	4.361		

<sup>a</sup> Volume of 0.1740M NaOH added to 49.94ml of solution.

<sup>b</sup> All p[H<sup>+</sup>] data were obtained using the calibration curve (see Chapter 3).

<sup>c</sup> Volume of 0.4979M HCl added to 49.94ml of the titrated solution.

<sup>d</sup> Volume of 0.1779M NaOH added to 49.94ml of the titrated solution.

TABLE 7.13

p[H<sup>+</sup>] data from the titrations of NaOH (and HCl) against solutions of copper(II) ions, diamine-dioxime ligand and acid at 25°C, I = 0.10M (NaCl)

$$T_L = 5.939 \times 10^{-4} M, T_M = 3.812 \times 10^{-4} M$$

$$T_L = 5.844 \times 10^{-4} M, T_M = 3.812 \times 10^{-4} M$$

used $\alpha$ .2HCl				used $\gamma$ .2HClO <sub>4</sub>			
Vol. <sup>b</sup>	p[H <sup>+</sup> ] <sup>a</sup>	Vol. <sup>c</sup>	p[H <sup>+</sup> ]	Vol. <sup>d</sup>	p[H <sup>+</sup> ]	Vol. <sup>c</sup>	p[H <sup>+</sup> ]
0.000	3.145	0.000	3.146	0.000	3.153	0.000	3.152
0.020	3.185	0.010	3.109	0.010	3.171	0.020	3.080
0.030	3.205	0.020	3.075	0.020	3.191	0.040	3.015
0.040	3.229	0.030	3.042	0.030	3.211	0.050	2.985
0.050	3.252	0.040	3.010	0.040	3.232	0.060	2.258
0.060	3.276	0.060	2.953	0.050	3.256	0.080	2.902
0.070	3.300	0.080	2.900	0.060	3.277	0.100	2.855
0.080	3.328	0.120	2.809	0.070	3.301	0.120	2.810
0.090	3.356	0.160	2.730	0.080	3.326	0.150	2.753
0.100	3.386	0.200	2.658	0.090	3.353	0.170	2.717
0.110	3.419	0.240	2.595	0.100	3.379	0.200	2.661
0.120	3.452	0.280	2.538	0.110	3.410	0.230	2.612
0.130	3.489			0.120	3.439		
0.140	3.530			0.130	3.473		
0.150	3.574			0.140	3.510		
0.160	3.623			0.150	3.549		
0.170	3.680			0.160	3.595		
0.180	3.749			0.170	3.642		
0.190	3.826			0.180	3.692		
0.200	3.920			0.190	3.757		
0.210	4.053			0.200	3.830		
0.220	4.240			0.210	3.920		
				0.220	4.040		
				0.230	4.202		
				0.240	4.459		
				0.245	4.666		
				0.250	4.969		

<sup>a</sup> All p[H<sup>+</sup>] data was obtained using the calibration curve (see Chapter 3).

<sup>b</sup> Volume of 0.2389M NaOH added to 49.94ml of the titrated solution.

<sup>c</sup> Volume of 0.4979M HCl added to 49.94ml of the copper/oxime solution.

<sup>d</sup> Volume of 0.2261M NaOH added to 49.94ml.

TABLE 7.14

$p[H^+]$  data from the titrations of NaOH against solutions  
of copper(II) ions, diamine-dioxime ligand and acid at

25°C and I = 0.10M

$T_L = 1.557 \times 10^{-4} M$		$T_L = 3.821 \times 10^{-4} M$		$T_L = 3.755 \times 10^{-4} M$		$T_L = 3.840 \times 10^{-4} M$	
$T_M = 1.531 \times 10^{-4} M$		$T_M = 3.812 \times 10^{-4} M$		$T_M = 3.820 \times 10^{-3} M$		$T_M = 3.812 \times 10^{-4} M$	
$\gamma$ isomer used		$\gamma$ isomer used		$\gamma$ isomer used		$\alpha$ isomer used	
Vol. <sup>a</sup>	$p[H^+]^b$	Vol. <sup>c</sup>	$p[H^+]$	Vol. <sup>d</sup>	$p[H^+]$	Vol. <sup>e</sup>	$p[H^+]$
0.000	2.952	0.000	3.227	0.000	3.105	0.000	3.220
0.020	2.978	0.010	3.251	0.020	3.136	0.020	3.268
0.040	3.003	0.020	3.274	0.040	3.175	0.030	3.294
0.060	3.032	0.030	3.300	0.060	3.218	0.040	3.322
0.080	3.063	0.040	3.326	0.080	3.264	0.060	3.382
0.100	3.095	0.050	3.353	0.100	3.315	0.080	3.451
0.120	3.131	0.060	3.382	0.120	3.371	0.090	3.490
0.140	3.167	0.070	3.412	0.130	3.401	0.100	3.531
0.160	3.209	0.080	3.447	0.140	3.445	0.110	3.577
0.180	3.255	0.090	3.483	0.150	3.470	0.120	3.626
0.200	3.303	0.100	3.522	0.160	3.510	0.130	3.684
0.220	3.356	0.110	3.562	0.170	3.551	0.140	3.746
0.240	3.415	0.120	3.610	0.180	3.599	0.150	3.820
0.260	3.484	0.130	3.660	0.190	3.650	0.160	3.898
0.270	3.522	0.140	3.716	0.200	3.707	0.170	3.993
0.280	3.563	0.150	3.778	0.210	3.775	0.180	4.101
0.290	3.610	0.160	3.848	0.220	3.861	0.190	4.248
0.300	3.659	0.170	3.925	0.230	3.946	0.200	4.435
0.310	3.719	0.180	4.020	0.240	4.067		
0.320	3.780	0.185	4.068	0.250	4.215		
0.330	3.855	0.190	4.124	0.260	4.419		
0.340	3.943	0.195	4.188				
0.350	4.050	0.200	4.255				
0.360	4.185	0.205	4.331				
0.370	4.358	0.210	4.421				
0.380	4.610	0.215	4.529				
		0.220	4.653				

<sup>a</sup> Volume of 0.1779M NaOH added to 49.94ml of solution.

<sup>b</sup>  $p[H^+]$  data obtained using the calibration curve (see Chapter 3).

<sup>c</sup> Volume of 0.2261M NaOH added to 49.94ml of solution.

<sup>d</sup> Volume of 0.1915M NaOH added to 49.94ml.

<sup>e</sup> Volume of 0.2389M NaOH added to 49.94ml.

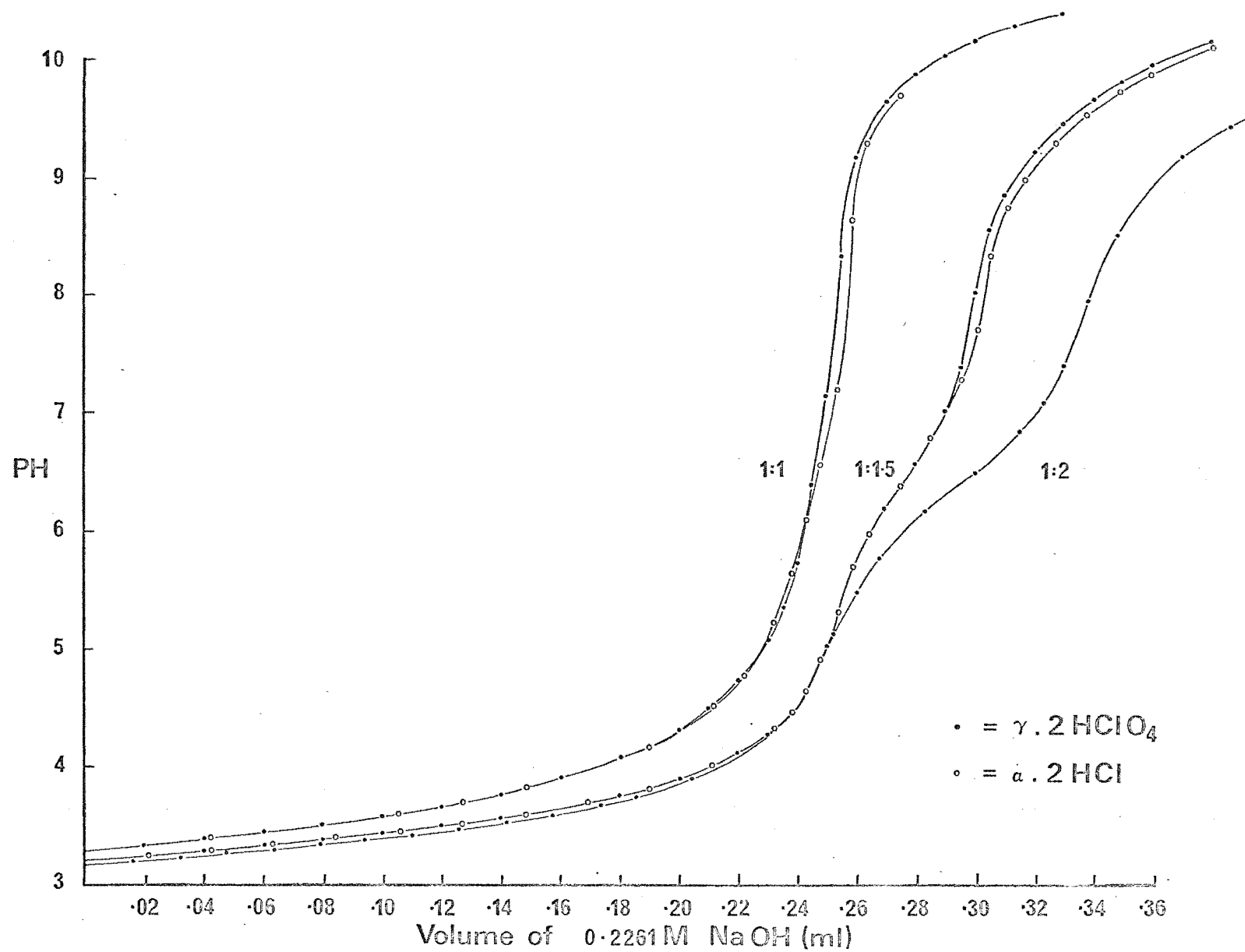
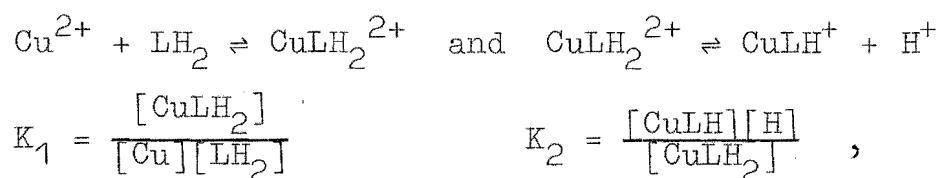


Fig.7-6 Representative titration curves for copper/oxime system  $T_M = 3.812 \times 10^{-4} \text{M}$

Calculations from 1:1.5 and 1:2 p[H<sup>+</sup>] titration data

The end point analysis of the titration curves suggested that either a proton was removed from the oxime function of the ligand or that a 1:1 metal-ligand hydroxy species  $\text{CuLH}_2(\text{OH})^+$  was formed. Spectroscopic evidence (see section below) and solid state evidence<sup>158</sup> suggested that two complexes were formed during a p[H<sup>+</sup>] titration, a 1:1 metal:ligand species  $\text{CuLH}_2^{2+}$  and a 1:1 deprotonated species  $\text{CuLH}^+$ , the proton having been removed from one of the oxime functions.

Assuming that only these two complexes are formed, with formation constants given by



then the two mass balance equations for  $T_M$  and  $T_L$ , valid at  $\text{pH} < 11$ , are

$$T_M = [\text{Cu}] + [\text{CuLH}_2] + [\text{CuLH}] \quad 7.14$$

$$T_L = [\text{LH}_2] + [\text{LH}_3] + [\text{LH}_4] + [\text{CuLH}_2] + [\text{CuLH}] \quad 7.15$$

The electroneutrality equation is

$$[\text{Na}^+] + [\text{H}^+] + 2[\text{Cu}^{2+}] + 2[\text{CuLH}_2^{2+}] + [\text{CuLH}^+] + [\text{LH}_3^+] + 2[\text{LH}_4^{2+}]$$

$$= T_{\text{Cl}^-} + [\text{OH}^-] \quad 7.16$$

where  $T_{Cl^-}$  is the total concentration of anion added as copper chloride and as ligand dihydrochloride (or dihydroperchlorate), and  $[Na^+]$  is the concentration of sodium ions from titrant NaOH. For titrations against HCl,  $[Na^+] = 0$  and an additional term  $[Cl_{ADD}^-]$  was added to the RHS of equation 7.16. Upon the elimination of  $[Cu^{2+}]$  from equations 7.14 and 7.15 and by using the protonation concentration quotients for the ligand species and the formation constants above, a quadratic equation in  $LH_2$  was formed,

$$[LH_2]^2 \cdot (D) \left( K_1 + \frac{K_1 K_2}{[H]} \right) + [LH_2] \left( D + K_1 + \frac{K_2 K_1}{[H]} \right) - T_L = 0$$

where  $D = 1 + k_3[H] + k_4 k_2 [H]^2$ . Given values for  $K_1$  and  $K_2$ , the free ligand concentration  $[LH_2]$  was calculated. This value was then substituted into a rearranged electroneutrality equation

$$\begin{aligned} T_{Cl^-} - [Na^+] - [H^+] &= [LH_2] (k_3[H] + 2k_4 k_3 [H]^2) \\ &+ (T_M - T_L + [LH_2] \cdot D) \left( 2 + 2K_1 [LH_2] + \frac{K_2 K_1 [LH_2]}{[H]} \right) \end{aligned} \quad 7.17$$

and a least squares procedure was used to calculate values of  $K_1$  and  $K_2$ . These were then used to calculate improved values for  $[LH_2]$  and the process was repeated until convergence was obtained. Four or five cycles of the computer program ORGLS were usually required. The computer

output from the final cycle for one of the titration data sets is shown in Table 7.15.  $Y_{OBS}$  is the LHS of equation 7.17 and  $Y_{CALC}$  is the RHS calculated using the 'parameters of best fit' (these are given in Table 7.16). The data in Table 7.15 were calculated using the  $p[H^+]$  data from both the titrations with NaOH and HCl. The agreement factor (see footnote, Table 7.15 and Appendices C and D) shows that the least squares refinement was satisfactory.

The results from least squares analyses on the pH titration data at various  $T_M:T_L$  ratios are shown in Table 7.16. In the analysis for each data set the differences in  $Y_{OBS} - Y_{CALC}$  were generally in the range 0.1 - 0.7%. The estimated uncertainty in  $Y_{OBS}$  was ca. 0.5%. For the  $T_M:T_L$  data of 1:1.5 identical results, within the estimated uncertainty, were obtained for the  $\alpha$  and  $\gamma$  isomers. The results for the ca. 1:3 data are slightly different from those at the other ratios.

#### Calculations from the 1:1 metal:ligand titration data

The end point of the titration curve, although not being well defined, suggested that a proton was being removed from one of the oxime groups. However, a least squares analysis of the pH titration data in terms of the complexes  $CuLH_2^{2+}$  and  $CuLH^+$  did not give satisfactory results. For the data at  $T_M = 3.812 \times 10^{-4}$  (Table 7.14),  $\gamma$  isomer, the parameters obtained were  $\log K_1 = 13.8_0$  and  $\log K_2 = -4.1_3$ ;

TABLE 7.15

Data from the least squares analysis<sup>a</sup> of the 1:2 metal:ligand p[H<sup>+</sup>]titration data<sup>b</sup> (Table 7.12) for the copper/oxime system

<u>p[H<sup>+</sup>]</u>	<u>Y<sub>OBS</sub>(x10<sup>2</sup>)</u>	<u>Y<sub>CALC</sub>(x10<sup>2</sup>)</u>	<u>p[H<sup>+</sup>]</u>	<u>Y<sub>OBS</sub>(x10<sup>2</sup>)</u>	<u>Y<sub>CALC</sub>(x10<sup>2</sup>)</u>
2.527	0.2083	0.2095	3.372	0.1363	0.1363
2.615	0.2039	0.2031	3.397	0.1351	0.1351
2.680	0.1982	0.1976	3.423	0.1339	0.1339
2.756	0.1923	0.1903	3.451	0.1326	0.1327
2.837	0.1827	0.1820	3.481	0.1314	0.1315
2.881	0.1769	0.1774	3.514	0.1303	0.1302
2.931	0.1714	0.1721	3.548	0.1290	0.1291
2.986	0.1656	0.1665	3.588	0.1279	0.1279
3.015	0.1623	0.1636	3.629	0.1267	0.1267
3.050	0.1599	0.1602	3.675	0.1254	0.1255
3.085	0.1569	0.1569	3.730	0.1244	0.1243
3.121	0.1535	0.1537	3.790	0.1232	0.1231
3.149	0.1510	0.1513	3.861	0.1221	0.1218
3.179	0.1485	0.1488	3.942	0.1209	0.1206
3.212	0.1462	0.1463	4.047	0.1197	0.1193
3.249	0.1440	0.1436	4.176	0.1185	0.1179
3.285	0.1413	0.1412	4.361	0.1172	0.1163
3.327	0.1389	0.1387			

$$\text{agreement factor } (\sum (\omega_i (O-C)^2) / (NO-NV))^{\frac{1}{2}} = 0.6 \times 10^{-5}$$

<sup>a</sup> Output from the computer program ORGLS.

<sup>b</sup> Each data point was weighted at unity.



TABLE 7.16

Stability constants for the copper/diamine-dioxime complexes  
at I = 0.10 and 25°C calculated<sup>a</sup> from the  
titration data in Tables 7.12 and 7.13.

<u>Reaction</u>	<u>Ratio T<sub>L</sub>:T<sub>M</sub> (isomer used)</u>			
	<u>ca. 3:1(γ)</u>	<u>ca. 2:1(γ)</u>	<u>ca. 1.5:1(α)</u>	<u>ca. 1.5:1(γ)</u>
$\text{Cu}^{2+} + \text{LH}_2 \rightleftharpoons \text{CuLH}_2^{2+}; \log K_1$	$13.30_9 \pm 0.06$	$13.24_6 \pm 0.05$	$13.22_1 \pm 0.07$	$13.19_4 \pm 0.08$
$\text{CuLH}_2^{2+} \rightleftharpoons \text{CuLH}^+ + \text{H}^+; \log K_2$	$-3.11_9 \pm 0.08$	$-3.24_7 \pm 0.07$	$-3.26_3 \pm 0.08$	$-3.27_8 \pm 0.08$

<sup>a</sup> Each data point was weighted at unity in the least squares.

<sup>b</sup> Errors were estimated from a consideration of the differences in the  $\log K_i$   
produced from reproducible data and from the uncertainties in analytical concentration.

however the differences between  $Y_{OBS}$  and  $Y_{CALC}$  were large (5-15%). The data was recollected using a different ligand sample. The same results were obtained. (The results were also independent of which solid isomer was used, Fig. 7.6.) The 1:1 titration data at  $T_M = 1.531 \times 10^{-4}M$  (Table 7.14) also could not satisfactorily be interpreted in terms of two constants  $K_1$  and  $K_2$ . Österberg's graphical method<sup>159</sup>, as applied to this 1:1 titration data, also did not yield a satisfactory result when the only complexes assumed were  $CuLH_2^{2+}$  and  $CuLH^+$ .

#### Spectrophotometric Results

Visible and ultraviolet spectrophotometric data obtained using copper-oxime solutions from the pH titrations are shown in Table 7.17. A few U.V. spectra are also shown in Fig. 7.7. For the visible spectra the solution ionic strength was 0.10 M (NaCl) while for the ultraviolet spectra the ionic strength was 0.05 M (NaCl). The extinction coefficients were calculated with respect to the concentration of metal ion available for coordination, for even in the 1:1 copper:ligand solution there was a slight excess of ligand.

The spectrophotometric data for the  $(Cu(LH))_2Cl_2$  solid (prepared by J.W. Fraser<sup>158</sup>) in a number of non-aqueous solvents are also tabulated in Table 7.17. The extinction coefficients were calculated from the known concentration of the complex.

TABLE 7.17

Visible-Ultraviolet spectra for the copper/diamine-dioxime system

<u>Visible</u>				
<u>Solution</u> <sup>a</sup>	<u>ca. ratio T<sub>M</sub>:T<sub>L</sub></u>	<u>ca. pH</u>	<u>λ(nm)</u>	<u>ε</u>
γ isomer, T <sub>M</sub> =3.812x10 <sup>-4</sup> M	1:2	9.42	579	219
α isomer, T <sub>M</sub> =3.812x10 <sup>-4</sup> M	1:1.5	9.7	580	214
γ isomer, T <sub>M</sub> =3.812x10 <sup>-4</sup> M	1:1	5.7	582	189
α isomer, T <sub>M</sub> =3.812x10 <sup>-4</sup> M	1:1	10.0	579	192
γ isomer, T <sub>M</sub> =1.531x10 <sup>-4</sup> M	1:1	10.1	578	190
α isomer, T <sub>M</sub> =3.812x10 <sup>-4</sup> M	1:1	3.3	592	-
γ isomer, T <sub>M</sub> =3.812x10 <sup>-4</sup> M	1:1	3.3	593	-
<u>Ultraviolet</u>				
<u>Solution</u> <sup>b</sup>	<u>ca. ratio T<sub>M</sub>:T<sub>L</sub></u>	<u>ca. pH</u>	<u>λ(nm; ε in parenthesis)</u>	
α isomer, T <sub>M</sub> =1.906x10 <sup>-4</sup> M	1:1	3.3	277(-)	
		4.3	273(-), 325(-)	
		10.0	272(4200), 330sh(2620)	
α isomer, T <sub>M</sub> =1.906x10 <sup>-4</sup> M	1:1.5	3.2	277(-)	
		10.8	271(4600), 328	
		3.2	277(-)	
γ isomer, T <sub>M</sub> =1.906x10 <sup>-4</sup> M	1:1.5	10.7	269(4650), 330(2800)	
γ isomer, T <sub>M</sub> =1.531x10 <sup>-4</sup> M	1:3	8.7	272(4600), 325(2830)	
γ isomer, T <sub>M</sub> =1.906x10 <sup>-4</sup> M	1:2	5.4	271(4590), 325(2810)	
		3.2	277(-)	
		10.1	271(4180), 330(2610)	
γ isomer, T <sub>M</sub> =1.531x10 <sup>-4</sup> M	1:1			

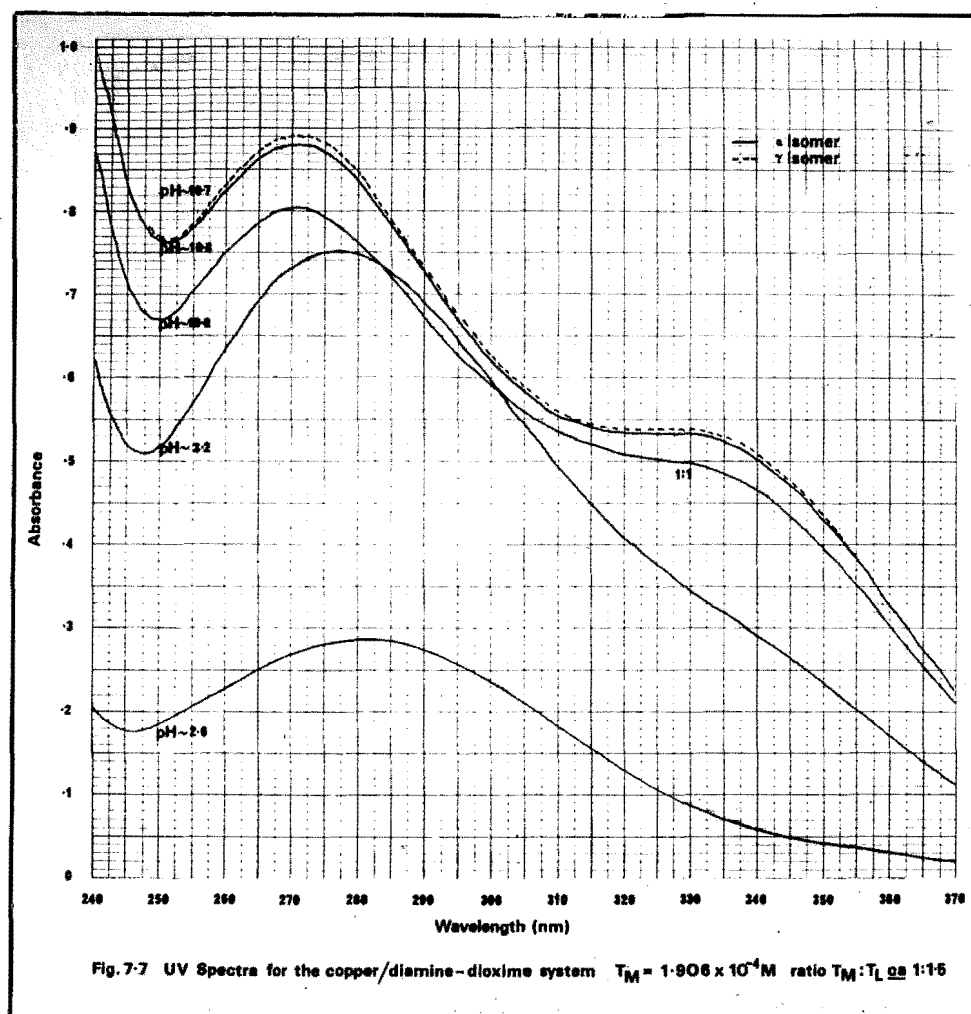
Visible-Ultraviolet spectra in non-aqueous solvents

<u>Complex</u>	<u>Solvent</u>	<u>λ(nm; ε in parentheses)</u>
(Cu(LH)) <sub>2</sub> Cl <sub>2</sub>	C <sub>2</sub> H <sub>5</sub> OH	580(220), 363(2180), 269(4360)
	DMF	590(195), 376(2120), 272(4560)
	HCONH <sub>2</sub>	585(193), 350(2270), 272(4280)
	DMSO <sup>c</sup>	596(234), 373(1800), 270(4300)
	MeCN <sup>c</sup>	622(250), 382(1760), 280(4150)

<sup>a</sup> The spectrophotometric data were obtained using solutions identical in composition to those used in the pH titrations.

<sup>b</sup> Some titration solutions were diluted.

<sup>c</sup> Data from J.W. Fraser, M.Sc. Thesis, University of Canterbury 1970.



### Calorimetric data

Data from the calorimetric titrations of solutions of copper ions, diamine-dioxime dihydrobromide and NaOH against standard HCl are shown in Table 7.18. The measured heat change, which was the difference between the endothermic heat of dissociation of the complex and the exothermic heat of protonation of the ligand, was exothermic and small. Only one or two titration points could be measured for each run. At the end of some of the runs NaOH was added to the calorimetric solution using a Gilmont micrometer syringe. This solution was then used for the next calorimetric run. The calculation of the data in Table 7.18 was described in section 5.3. The enthalpy changes for the formation of  $\text{CuLH}_2^{2+}$  and  $\text{CuLH}^+$  were calculated using the least squares procedure as described previously (see chapter 5). The results are shown in Table 7.20.

These results ( $\Delta H_1$ ,  $\Delta H_2$ ) were confirmed by experimentally determining the enthalpy change ( $\Delta H_1 + \Delta H_2$ ) by titrating an alkaline solution of the diamine-dioxime ligand with copper chloride. The calculations are described in section 5.4. The result in Table 7.19 shows good agreement with the data in Table 7.20. The free energy, enthalpy and entropy changes for the formation of the complexes  $\text{CuLH}_2^{2+}$  and  $\text{CuLH}^+$  are shown in Table 7.20.

TABLE 7.18

Calorimetric data from the titrations of the copper oxime complex ( $\text{CuLH}^+$ )  
with  $\text{HCl}^b$  at  $25^\circ\text{C}$  and  $I = 0.10\text{M}$

Vol.	$p[\text{H}^+]$	$\text{LH}_2^d$	$\text{LH}_3$	$\text{LH}_4$	$\text{M}(\text{LH}_2)$	$\text{M}(\text{LH})$	$\Delta\text{M}(\text{LH}_2)$	$\Delta\text{M}(\text{LH})^e$	$Q$	$Q_{\text{corr}}$	$Q_{\text{calc}}$
$T_L = 3.890 \times 10^{-3}\text{M}$ , $T_M = 2.989 \times 10^{-3}\text{M}$ , $[\text{NaOH}]_a = 7.298 \times 10^{-3}\text{M}$ , INITIAL VOLUME = 100.0ml, $[\text{HCl}]_a = 0.0$											
0.000	3.434	0.00000	0.00012	0.09516	0.11457	0.17917					
							0.08793	0.13020	5.294	-1.735	-1.737
0.470	2.735	0.00000	0.00005	0.18316	0.15685	0.04897					
							0.06401	0.02721	2.275	-2.840	-2.865
0.770	2.498	0.00000	0.00004	0.24717	0.12005	0.02176					
$T_L = 3.995 \times 10^{-3}\text{M}$ , $T_M = 3.020 \times 10^{-3}\text{M}$ , $[\text{NaOH}]_a = 9.140 \times 10^{-3}\text{M}$ , INITIAL VOLUME = 99.0ml, $[\text{HCl}]_a = 0.0^a$											
0.340	3.090	0.00000	0.00007	0.12345	0.15921	0.11281					
							0.10706	0.08360	4.652	-3.904	-3.891
0.840	2.573	0.00000	0.00004	0.23054	0.13575	0.02921					
$T_L = 3.929 \times 10^{-3}\text{M}$ , $T_M = 2.969 \times 10^{-3}\text{M}$ , $[\text{NaOH}]_a = 10.097 \times 10^{-3}\text{M}$ , INITIAL VOLUME = 100.67ml, $[\text{HCl}]_a = 8.069 \times 10^{-3}\text{M}$											
0.320	3.113	0.00000	0.00007	0.11917	0.15502	0.12127					
							0.10556	0.08965	4.833	-3.604	-3.665
0.820	2.597	0.00000	0.00004	0.22476	0.13910	0.03163					
$T_L = 4.063 \times 10^{-3}\text{M}$ , $T_M = 3.020 \times 10^{-3}\text{M}$ , $[\text{NaOH}]_a = 9.338 \times 10^{-3}\text{M}$ , INITIAL VOLUME = 99.0ml, $[\text{HCl}]_a = 0.0$											
0.330	3.137	0.00000	0.00008	0.12433	0.15540	0.12243					
							0.10540	0.09067	4.789	-3.635	-3.632
0.830	2.594	0.00000	0.00004	0.22976	0.14067	0.03176					
$T_L = 3.995 \times 10^{-3}\text{M}$ , $T_M = 2.969 \times 10^{-3}\text{M}$ , $[\text{NaOH}]_a = 17.485 \times 10^{-3}\text{M}$ , INITIAL VOLUME = 100.68ml, $[\text{HCl}]_a = 7.972 \times 10^{-3}\text{M}$											
0.340	3.184	0.00000	0.00008	0.12040	0.14995	0.13180					
							0.10357	0.09747	4.897	-3.381	-3.371
0.840	2.618	0.00000	0.00004	0.22401	0.14385	0.03433					
$T_L = 4.233 \times 10^{-3}\text{M}$ , $T_M = 3.050 \times 10^{-3}\text{M}$ , $[\text{NaOH}]_a = 9.153 \times 10^{-3}\text{M}$ , INITIAL VOLUME = 98.0ml, $[\text{HCl}]_a = 0.0$											
0.350	3.049	0.00000	0.00007	0.14440	0.16453	0.10585					
							0.10699	0.07819	4.506	-4.045	-4.015
0.850	2.549	0.00000	0.00004	0.25142	0.13572	0.02766					
$T_L = 4.161 \times 10^{-3}\text{M}$ , $T_M = 2.999 \times 10^{-3}\text{M}$ , $[\text{NaOH}]_a = 17.286 \times 10^{-3}\text{M}$ , INITIAL VOLUME = 99.69ml, $[\text{HCl}]_a = 8.245 \times 10^{-3}\text{M}$											
0.340	3.074	0.00000	0.00008	0.14173	0.16224	0.11079					
							0.10627	0.08172	4.580	-3.913	-3.892
0.840	2.564	0.00000	0.00004	0.24804	0.13770	0.02906					

<sup>a</sup>  $[\text{HCl}]_a$  is the concentration of titrant  $\text{HCl}$  added from the previous run (see p.79).

<sup>b</sup> Titrant  $\text{HCl}$  concentration was 0.9670M.

<sup>c</sup> These concentration data are for the initial composition, the volume of added titrant was zero.

<sup>d</sup> Data are the number of mmoles of each species at the particular titration point.

<sup>e</sup> These data are the changes in the number of mmoles of the metal complex species between successive titration points.

TABLE 7.19

Calorimetric data<sup>c</sup> from the titration of the diamine-dioxime  
ligand with  $\text{CuCl}_2$  at  $25^\circ\text{C}$  and  $I = 0.10\text{M}$

<u>VOLUME</u> <sup>b</sup>	<u>p[H<sup>+</sup>]</u>	<u>LH<sub>2</sub></u> <sup>a</sup>	<u>LH<sub>3</sub></u>	<u>LH<sub>4</sub></u>	<u>CuLH<sub>2</sub></u>	<u>CuLH</u>
0.000 <sup>c</sup>	10.120	0.45682	0.08759	0.00002	0.00000	0.00000
0.271	9.218	0.15171	0.23168	0.00031	0.00000	0.16222
0.421	7.307	0.00212	0.26396	0.02865	0.00002	0.25200

Changes in the number of mmoles and the heat changes

<u><math>\Delta(\text{LH}_3)</math></u>	<u><math>\Delta(\text{LH}_4)</math></u>	<u><math>R(\text{CuLH}_2)</math></u>	<u><math>S(\text{CuLH})</math></u>	<u>Q</u>	<u>Q<sub>corr</sub></u>	<u><math>\Delta H_1 + \Delta H_2</math></u>
0.14289	0.00032	0.00000	0.16222	not measured	-	-
0.05982	0.02753	0.00002	0.08977	6.410	2.784	31.02

<sup>a</sup> Values are the number of mmoles for each species of each titration point.

<sup>b</sup> Volume of 0.5986M  $\text{CuCl}_2$  added.

<sup>c</sup> Initial solution composition:  $T_L = 5.508 \times 10^{-3}$ ,  $T_H = 0.670 \times 10^{-3}\text{M}$ ;  
Initial volume = 98.84 ml.

TABLE 7.20

Thermodynamic data<sup>a</sup> for the formation of copper(II) complexes  
with the diamine-dioxime ligand at 25°C and I = 0.10M

	<u>Reaction</u>	<u>logK<sub>i</sub></u>	<u>-ΔG kJmol<sup>-1</sup></u>	<u>-ΔH kJmol<sup>-1</sup></u>	<u>ΔS Jmol<sup>-1</sup>K<sup>-1</sup></u>
1	$\text{Cu}^{2+} + \text{LH}_2 \rightleftharpoons \text{CuLH}_2^{2+}$	$13.24 \pm 0.05$	$75.56 \pm 0.3$	$54.84 \pm 0.3$	$69.5 \pm 2$
2	$\text{CuLH}_2^{2+} \rightleftharpoons \text{CuLH}^+ + \text{H}^+$	$-3.23 \pm 0.08$	$-18.43 \pm 0.5$	$-23.69 \pm 0.3$	$17.6 \pm 3$
	$\text{Cu}^{2+} + \text{LH}_2 \rightleftharpoons \text{CuLH}^+ + \text{H}^+$	$10.00 \pm 0.13$	$57.07 \pm 0.8$	$31.15 \pm 0.6$	$87.0 \pm 5$

<sup>a</sup> With reference to a standard state of 0.10M NaCl



## 7.2.2 Discussion

### 7.2.2a Coordination of the ligand to copper ions

The diamine-dioxime ligand has six potential donor atoms; two amine nitrogens, two oxime nitrogens and two oxime oxygens. Coordination in a planar configuration to copper(II) ions could occur in three possible forms:

(i) Through the amine and oxime nitrogen atoms. The isomeric configuration for each oxime group would lie syn (methyl). Models show that the two six membered chelate rings can readily adopt the favoured pseudo-chair formation and the five membered ring can adopt the favoured gauche configuration. In this form the distance between the two oxime oxygen atoms is ca.  $2.1\text{\AA}$ . This distance is shorter than most hydrogen bonding distances involving oxygen atoms in the crystalline state<sup>118</sup>. The hydrogen bond lengths OH---O in  $\text{Ni}(\text{dmg})_2^{2+}$  are  $2.40\text{\AA}$ <sup>160</sup>.

(ii) Coordination through the two amine nitrogens and the two oxime oxygens. The configuration of each oxime function will be anti. This coordination results in the formation of two seven membered chelate rings and one five membered ring. No intramolecular hydrogen bonding is possible in this form.

(iii) Coordination through two amine nitrogens, one oxime nitrogen and one oxime oxygen. This results in the formation of one five, one six and one seven membered chelate

ring, with no obvious strain in the structure. The distance between the two oxime oxygens is ca.  $3\overset{\circ}{\text{\AA}}$ .

Oxygen donors are termed hard<sup>161</sup> and do not form strongly covalent interactions with soft acceptor transition metal ions, e.g.  $\text{Cu}^{2+}$ . Nitrogen donors, as in amines, are softer than oxygen donors and form stronger covalent bonding with copper ions<sup>161</sup>. These properties are reflected in the visible absorption spectrophotometric data for the copper complexes with a number of N and O donors.

The  $\lambda_{\text{max}}$  value for  $\text{Cu}(\text{en})(\text{H}_2\text{O})_2^{2+}$  is 660 nm<sup>162</sup> while that for  $\text{Cu}(\text{en})_2^{2+}$  is 550 nm<sup>163</sup>. The  $\lambda_{\text{max}}$  for bis(glycinato) copper(II) in aqueous solution is 633 nm<sup>164</sup> and for bis(picolinato) copper(II)  $\lambda_{\text{max}}$  is 645 nm<sup>165</sup>. These data show that, while there are slight variations due to the different donor strengths, the  $\lambda_{\text{max}}$  values for the coordination of two nitrogens and two oxygens are about 100 nm larger than those for the coordination of four nitrogen atoms. The data in Table 7.17 show that the  $\lambda_{\text{max}}$  for the copper diamine-dioxime complex is 580 nm. Comparison with the above data suggests that the coordination of the diamine-dioxime ligand is as described in (i) above. If the coordination was through three nitrogens and one oxygen (iii above)  $\lambda_{\text{max}}$  would be expected at ca. 620 nm ( $\lambda_{\text{max}}$  for  $\text{Cu}(\text{dien})(\text{H}_2\text{O})^{2+}$  611, Table 7.11) and if the

coordination was through two nitrogens and two oxygens (ii above)  $\lambda_{\max}$  would be ca. 640 nm.

#### 7.2.2b Electronic Absorption Spectra

##### Aqueous Solution

In the visible region, there is a slight shift in the  $\lambda_{\max}$  value to higher energy as the pH of the solution is increased. At pH ca. 3.3  $\lambda_{\max}$  is 592 nm while at pH > 6  $\lambda_{\max}$  is 580 nm (Table 7.17). This change is interpreted as a slight increase in the basicity of the oxime nitrogen when a proton is removed from an oxime function to form the complex  $\text{CuLH}^+$ , viz.  $\text{C}=\text{N}-\text{O}^-$ . At a pH > 5 (complete formation of  $\text{CuLH}^+$ ) the position of  $\lambda_{\max}$  and the shape of the absorption band are identical for each metal:ligand ratio however the extinction coefficient is about 9% lower for the 1:1 data, independent of isomer type or total metal ion concentration (Table 7.17).

The ultraviolet spectrum for a copper/diamine-dioxime solution shows a more marked change with pH (Table 7.17 and Fig. 7.7). As the pH increases there is an increase in the intensity of the shoulder at 325-330 nm which reaches a maximum at ca. pH 5 where the formation of  $\text{CuLH}^+$  from  $\text{CuLH}_2^{2+}$  is complete. The molar extinction coefficient of this band is large (Table 7.17) and it is assigned to a charge transfer transition between the  $\text{C}=\text{N}-\text{O}^-$  group and the metal ion. At complete formation of  $\text{CuLH}^+$ , the shoulder position is

insensitive to the ratio of metal:ligand in the solution. However, the extinction coefficient for the 1:1 data is ca. 6.6% lower than for the data at other metal:ligand ratios (Table 7.17).

There is a further band in the U.V. centred at ca. 270 nm. The  $\lambda_{\text{max}}$  for this band is slightly altered as the pH changes. At pH = 3.3 ( $\text{CuLH}^+$  and  $\text{CuLH}_2^{2+}$  present) the  $\lambda_{\text{max}}$  value is 277 and at complete formation of  $\text{CuLH}^+$  the band is centred at 271 nm. As above the  $\lambda_{\text{max}}$  value is insensitive to the metal:ligand ratio, however the extinction coefficient for the 1:1 data is ca. 9% lower than for the other metal:ligand ratios (Table 7.17).

This band is characteristic in energy and intensity of the metal reduction ( $\text{L}_\sigma \rightarrow \text{M}$ ) charge transfer transition which has been observed for copper(II)-polyamine complexes and polyamine-imine complexes<sup>107</sup>. The oxime complexes also show the side of an intense absorption centred below 200 nm. This may arise from an intraligand absorption (see section 6.1.3) or possibly from a metal to ligand charge transfer.

#### Non-aqueous Solvents

The data in Table 7.17 show that the charge transfer transition which was at 330 nm in water is variable in other solvents. There is no apparent relationship between the band energy and the solvent dielectric constant or donicity<sup>166</sup>. However, the data do show that the band energy is higher

in the protic than in the aprotic solvents; the band energy order for the protic solvents is  $\text{H}_2\text{O}(330) > \text{HCONH}_2(350) > \text{C}_2\text{H}_5\text{OH}(363)$ .

The hydrogen bonding potentials of these solvents are in the order  $\text{H}_2\text{O} > \text{HCONH}_2 > \text{C}_2\text{H}_5\text{OH}$ <sup>167</sup>. It is possible that oximato ( $\text{C}=\text{N}-\text{O}^-$ )-solvent hydrogen bonding occurs, and this affects the energy of the charge transfer transition.

#### 7.2.2c Thermodynamic Data

##### Stability Constants, $\log K_i$

The agreement between the stability constants calculated from the 1:1.5 and 1:2 data indicates that under the particular titration conditions the data was correctly interpreted in terms of the two species  $\text{CuLH}_2^{2+}$  and  $\text{CuLH}^+$ . A visual indication of the least squares fit of the two parameters  $K_1$  and  $K_2$  was shown by using the constants to reproduce the titration curve. The difference  $\text{pH}_{\text{calc}} - \text{pH}_{\text{obs}}$  was to within  $\pm 0.005$  pH. For the 1:3 data the constants obtained from the least squares were slightly different from the 1:2 data. This difference may indicate the presence of a small amount of another metal-ligand species. However, using the constants from the 1:2 data the 1:3 titration curve could still be reproduced to about 0.01 pH. The  $\log K_i$  values in Table 7.20 are the mean values calculated from the data in Table 7.16.

The stability constants for a ligand EnAO,  $(\text{CH}_3(\text{C}=\text{NOH})\text{C}(\text{CH}_3)_2\text{NHCH}_2-)_2$  which is analogous to the diamine-dioxime in this study (EnAO is an  $\alpha$ -amine-oxime), have been reported<sup>168</sup>. The value of  $\log K$  for  $\text{Cu} + \text{EnAO} \rightleftharpoons \text{CuEnAO}$  was 13.0 at  $I = 0.27 \text{ M}$  ( $\text{Ba}(\text{NO}_3)_2$ ,  $\text{KNO}_3$ ),  $24.2^\circ\text{C}$ . The  $\text{pK}$  for the reaction  $\text{CuEnAO} \rightleftharpoons \text{Cu}(\text{EnAO}-\text{H}) + \text{H}^+$  was 4.3. These data were determined using spectrophotometric methods. The ratio of the stability to the ligand basicity is greater for EnAO than for the diamine-dioxime  $\text{LH}_2$ , in this study (13.0/13.92 for EnAO, 13.24/15.77 for  $\text{LH}_2$ ). This result is surprising in view of the apparent ring strain involved in the formation of the  $\text{CuEnAO}$  complex. No enthalpy data are available for the copper/EnAO reactions.

The data in Table 7.20 show that the formation of the complex  $\text{CuLH}_2^{2+}$  is accompanied by an exothermic enthalpy change and a large positive entropy change, while the formation of  $\text{CuLH}_2^{2+}$  is accompanied by an endothermic enthalpy change and a small positive entropy change.

Enthalpy change for the formation of  $\text{CuLH}_2^{2+}$

It would be useful to be able to compare the enthalpy data for the formation of the complex  $\text{CuLH}_2^{2+}$  with the formation of the 1:1 complex with a N,N' substituted ethylenediamine, however no accurate data are available. The data for the formation of the 1:1 complex with en are shown in Table 7.21.

TABLE 7.21

Reaction	$\log k$	$-\Delta G \text{ kJmol}^{-1}$	$-\Delta H \text{ kJmol}^{-1}$	$\Delta S \text{ Jmol}^{-1}\text{K}^{-1}$
$\text{Cu}^{2+} + \text{en} \rightarrow \text{Cu(en)}^{2+}$	10.54 <sup>a</sup>	60.13	52.6 <sup>b</sup>	25.1
$\text{en} + 2\text{H}^+ \rightarrow \text{enH}_2^{2+}$	17.01 <sup>a</sup>		95.6 <sup>c</sup>	

<sup>a</sup>Data from reference 169<sup>b</sup>from reference 137; assume<sup>c</sup>From Ref. 137.

$$\Delta H_1 = \Delta H_2.$$

If the diamine-dioxime formed a 1:1 complex with only the amine nitrogens coordinated then the ratio of the enthalpy change to the overall enthalpy change for the protonation reactions would be similar to the ratio for ethylenediamine. From the en data and the overall enthalpy for the diamine-dioxime protonation ( $79.77 \text{ kJ mol}^{-1}$ , see section 6.1.2) the enthalpy for the formation of  $\text{CuLH}_2^{2+}$  would be approximately  $43.8 \text{ kJ mol}^{-1}$ . The difference between this value and the observed enthalpy of  $54.8 \text{ kJ mol}^{-1}$  (Table 7.20) suggests that the oxime groups are coordinated to the copper ion. This evidence supports the conclusions drawn from a consideration of the visible spectra.

#### Entropy change for the formation of $\text{CuLH}_2^{2+}$

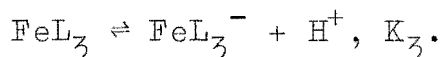
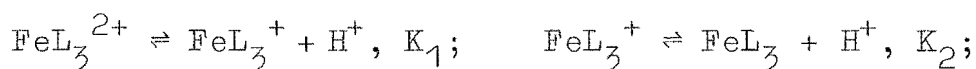
For the formation of  $\text{CuLH}_2^{2+}$  without the oximes coordinated the entropy change would be expected to approximate that for the formation of  $\text{Cu(en)}^{2+}$ . The data in Tables 7.20 and 7.21 show that the formation of  $\text{CuLH}_2^{2+}$  is

accompanied by a positive entropy change which is larger than that for  $\text{Cu(en)}^{2+}$  by ca.  $44 \text{ kJ mol}^{-1}$ . This difference also suggests that the oxime functions are coordinated. This would result in the liberation of two further water molecules from the inner coordination sphere of the copper ion.

The effect of coordination on acid ionisation

Hanania and co-workers<sup>170,171</sup> have shown that the ionisation of side groups ( $= \text{NOH}, \gg \text{N}^+\text{H}, -\text{NH}_3^+$ ) in certain ligands is influenced by the formation of a metal-ligand bond. In general it was shown<sup>170,171</sup> that the effect of complex formation was to increase the acid strength (a reduction in the positive  $\Delta G$  of ionisation) of the groups.

The coordination of pyridine-2-aldoxime to iron(II) results in the formation of a tris complex which undergoes three acid dissociations from the oxime groups;



These ionisations were studied spectrophotometrically by Hanania<sup>170</sup>;  $\text{p}K_1$  was not measurable,  $\text{p}K_2$  was 3.4 and  $\text{p}K_3$  was 7.13 ( $\text{p}K$  for the ligand 10.02). Enthalpy data were obtained from the dependence of the  $\text{p}K$  on temperature. A comparison of the thermodynamic data for ionisation from the complex

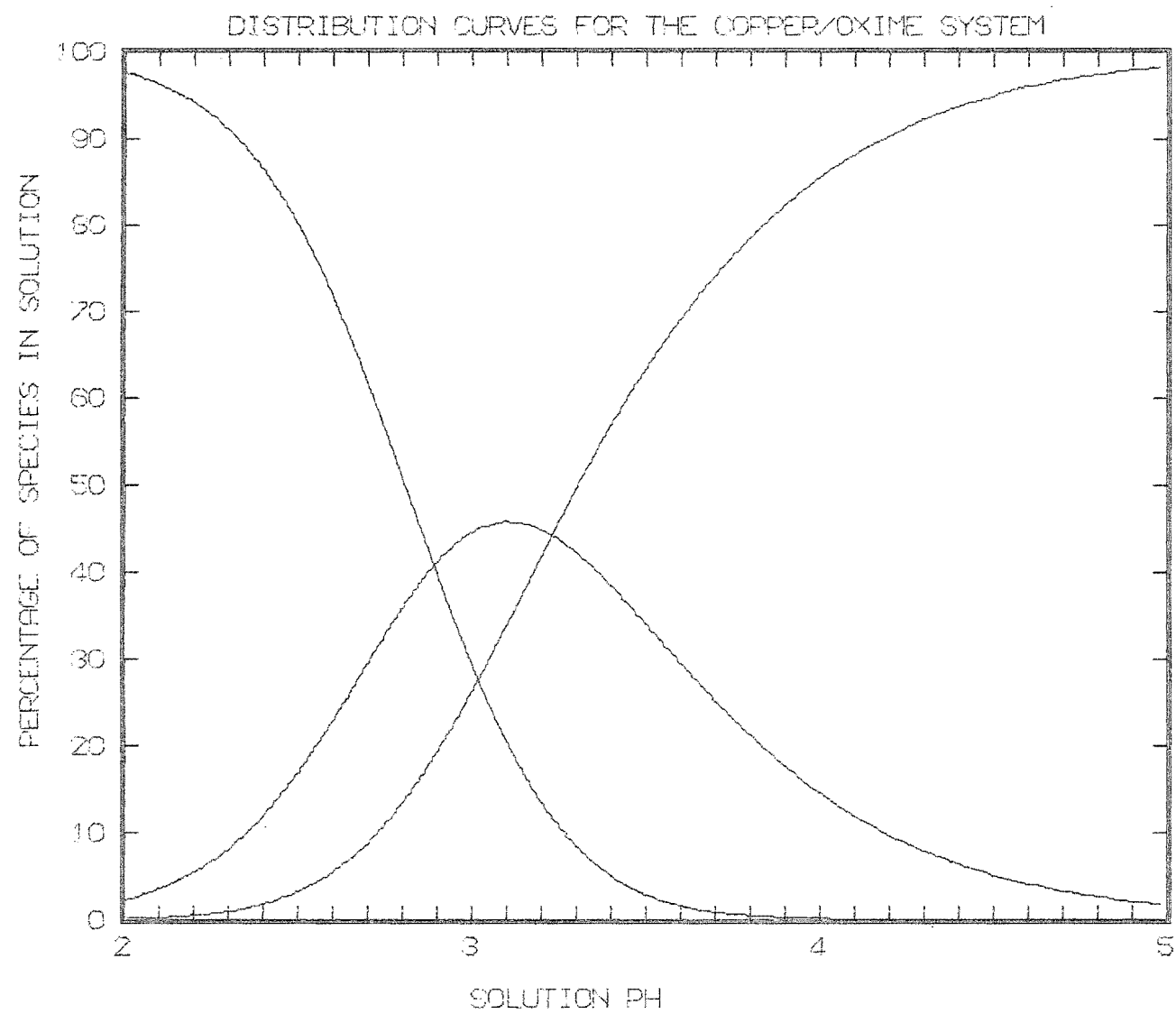


with that of the free ligand showed that the greater acid strength was due to more favourable enthalpy changes<sup>170</sup>. The authors attribute the greater acid strength of the oxime function on coordination as being due to a greater stabilisation, through conjugation, of the anionic form.

Two ionisations of the oxime protons from the bis(pyridine-2-aldoxime) copper(II) complex have also been reported<sup>172</sup>;  $\text{CuL}_2^{2+} \rightleftharpoons \text{CuL}_2 - \text{H}^+ + \text{H}^+$ ,  $\text{pK}_1 = 2.77$  and  $\text{CuL}_2 - \text{H}^+ \rightleftharpoons \text{CuL}_2 - 2\text{H} + \text{H}^+$ ,  $\text{pK}_2 = 6.7$  ( $\text{pK}$  for the ligand is 10.04).

Data for the proton ionisation of the  $\text{CuLH}_2^{2+}$  complex are shown in Table 7.20. Unfortunately no enthalpy data for the ionisation of the ligand  $\text{LH}_2$  or related compounds are available. The  $\text{pK}$  for the free oxime group was estimated as 12.3 (section 6.1.3). The extremely large change in  $\text{pK}$  when the oxime is coordinated to copper(II) ions is presumably associated with the increased stabilisation of the oximate group via the metal ion. This suggests that the ultraviolet absorption occurring at ca. 330 nm (see above) is associated with a ligand to metal charge transfer. The formation of an intraligand oxime-oximate hydrogen bond would also contribute to the stabilisation of  $\text{CuLH}^+$ . The entropy change for the ionisation will have a contribution from a cratic term (an increase in the number of solute particles) and a term associated with the changes

**Fig 7.8**



in solvation of the ions.

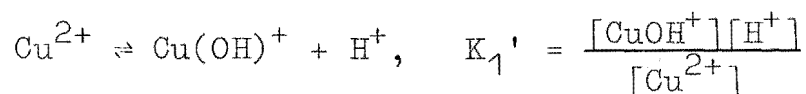
From the pH titration data there was no evidence that a further ionisation to form a neutral CuL species occurred below pH 10.

### Distribution Curves

The distribution of the metal ion species as a function of the solution pH is shown in Fig. 7.8. The stability constants given in Table 7.20 were used in the calculation. The metal:ligand ratio is 1:2 (concentrations given in Table 7.12). The curves show that the species  $\text{CuLH}_2$  is at a maximum concentration at pH = 3.1. (Fraser<sup>158</sup> found that to isolate  $\text{CuLH}_2^{2+}$  complexes uncontaminated with  $\text{Cu(LH)}^+$  species, it was necessary to acidify the reaction mixture to a pH of about 3.)

### Anomalous 1:1 titration data

Data analysis of the 1:1 pH titrations suggested that there must be a further complex species in addition to  $\text{CuLH}_2^{2+}$  and  $\text{CuLH}^+$ . The low extinction coefficients for the 1:1 visible and ultraviolet spectra suggested that perhaps soluble copper hydroxy species were formed, e.g.  $\text{Cu(OH)}^+$  or  $\text{Cu}_2(\text{OH})_2^{2+}$ . Perrin<sup>173</sup> has reported a concentration quotient  $K_1'$  for the reaction



of  $1 \times 10^{-8}$ . Assuming this species  $\text{Cu(OH)}^+$  is present in

solution then the electroneutrality equation 7.17 becomes

$$T_{Cl} - [Na^+] - [H^+] = [LH_2](k_3[H] + 2k_4k_3[H]^2) \\ + (T_M - T_L - [LH_2]D) \left( 2 + \frac{K_1'}{[H]} + 2K_1[LH_2] + \frac{K_2K_1}{[H]}[LH_2] \right) \quad 7.18$$

and, as the pH titration data lies in the range 3-4 the term  $K_1'[H]$  is very small compared with 2. The introduction of a species  $Cu_2(OH)_2^{2+}$  will have a similar negligible effect.

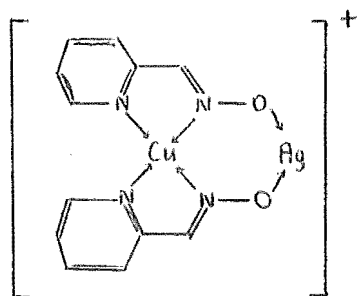
The solubility product of  $Cu(OH)_2$  is ca.  $10^{-19.5}$ . Thus for a  $[Cu^{2+}] = 1 \times 10^{-4} M$  the solution pH would have to be ca. 6.5 before precipitation did occur. Thus hydroxide precipitation in the region of the titration end point will be slight (in the 1:1 titrations there is a slight excess of ligand present, Table 7.14).

The work of Martell and coworkers<sup>174</sup> suggests that the formation of hydroxy complexes  $CuL(OH)^{n+}$  in a pH range 3-4 is not likely (see section 7.3.2).

The complex  $Cu(LH)Br$  has been shown by X-ray analysis<sup>158</sup> to consist of dimeric  $(Cu(LH))_2^{2+}$  cations. The coordinate environment around each copper is a slightly distorted trigonal bipyramid with an oxime nitrogen and an amine nitrogen in the axial positions and the equatorial plane occupied by the other two nitrogens and an oxime oxygen from the other  $CuLH^+$  unit. Oxime bridging, in the solid state, has also been observed for  $Cu(dmgl)_2$ <sup>175</sup> and in a pyridine-2-carbaldehyde oximate copper(II) trimer<sup>176</sup>.

If a dimeric species was formed in aqueous solution it is unlikely that its formation would be confined to 1:1 pH titrations and therefore the postulation of such a species is not likely to explain the apparent difference for the 1:1 titration data.

The species that is formed must (i) cause a decrease in the free hydrogen ion concentration in solution compared with that expected if only  $\text{CuLH}_2^{2+}$  and  $\text{CuLH}^+$  were formed, (ii) be decomposed in the presence of excess ligand. A species  $\text{Cu}_3(\text{LH})_2$  where a copper ion links two  $\text{CuLH}^+$  cations by coordination through the oximato oxygens might be formed. A similar complex  $[\text{Cu}(\text{pyral})_2\text{Ag}]^+$ , where pyral is pyridine-2-aldoxime, has been reported<sup>177</sup>. In this species the  $\text{Ag}^+$  ion is bonded to the two oximato oxygen atoms



The determination of stability constants of polynuclear species requires a rigorous mathematical analysis of extremely accurate data<sup>178</sup> and is further complicated when mixed complexes are also present. No further analysis of the data was attempted.

### 7.3 FORMATION OF THE COPPER COMPLEX WITH THE DIAMINE- DIKETONE LIGAND

#### 7.3.1 Results

##### p[H<sup>+</sup>] titration data

Solutions of copper(II) ions and protonated ligand,  $\text{LH}_2(\text{ClO}_4)_2$ , were titrated with standard NaOH. Data obtained using different ratios of  $T_M:T_L$  are shown in Table 7.22. Only one titration from a reproducible set of titrations has been tabulated in each case. One titration is shown graphically in Fig. 7.9. The end point in the titration curve corresponds to the neutralisation of two protons from the coordinated ligand and one proton from the excess ligand. The intensity of the blue colour of alkaline solutions of the metal-ligand complex decreased with time. This was presumably due to the decomposition of the ligand (see section 6.3.3). Addition of further NaOH to the titration solution at ca. pH 7.5 ultimately resulted in the formation of  $\text{Cu}(\text{OH})_2$ .

##### Calculations from the p[H<sup>+</sup>] data.

The end point in the titrations suggested the formation of a 1:1 metal:ligand complex  $\text{CuL}$ . Assuming only one such species, the three mass balance equations for  $T_M$ ,  $T_L$  and  $T_H$  are

$$T_M = [\text{Cu}] + [\text{CuL}] \quad 7.19$$

TABLE 7.22

pH titration and stability constant data for the copper(II)  
diamine-diketone complex at 25°C and I = 0.10M (NaCl)

$T_L = 6.094 \times 10^{-4} M$ , $T_H = 1.218 \times 10^{-3} M$ , $T_M = 3.812 \times 10^{-4} M$					$T_L = 7.882 \times 10^{-4} M$ , $T_H = 1.576 \times 10^{-3} M$ , $T_M = 7.629 \times 10^{-4} M$				
<u>VOL</u> <sup>a</sup>	<u>p[H<sup>+</sup>]</u>	<u><math>\bar{n}</math></u>	<u><math>10^8[L]</math></u>	<u>log K</u> <sup>c</sup>	<u>VOL</u> <sup>b</sup>	<u>p[H<sup>+</sup>]</u>	<u><math>\bar{n}</math></u>	<u><math>10^8[L]</math></u>	<u>log K</u>
0.060	4.927	0.249	0.0868	8.583	0.060	4.825	0.206	0.0675	8.584
0.080	5.030	0.329	0.1296	8.579	0.070	4.877	0.239	0.0816	8.585
0.090	5.081	0.370	0.1569	8.572	0.080	4.927	0.272	0.0980	8.581
0.100	5.126	0.410	0.1853	8.575	0.090	4.975	0.305	0.1162	8.578
0.110	5.174	0.451	0.2214	8.569	0.100	5.019	0.339	0.1350	8.580
0.120	5.221	0.491	0.2628	8.565	0.110	5.067	0.373	0.1585	8.574
0.130	5.268	0.532	0.3097	8.565	0.120	5.109	0.407	0.1812	8.578
0.140	5.318	0.572	0.3707	8.557	0.130	5.157	0.441	0.2121	8.570
0.150	5.368	0.612	0.4425	8.553	0.140	5.200	0.475	0.2417	8.573
0.160	5.419	0.652	0.5287	8.550	0.150	5.250	0.609	0.2828	8.564
0.170	5.476	0.692	0.6435	8.542	0.160	5.299	0.543	0.3261	8.562
0.180	5.536	0.730	0.7939	8.533	0.170	5.349	0.577	0.3769	8.559
0.190	5.600	0.768	0.9918	8.525	0.180	5.403	0.612	0.4401	8.554
0.200	5.670	0.805	1.264	8.515	0.190	5.459	0.646	0.5137	8.500
					0.200	5.523	0.680	0.6115	8.541
					0.220	5.665	0.749	0.8878	8.527
					0.230	5.752	0.784	1.105	8.516

log K: mean = 8.55<sub>6</sub>  $\sigma$  = 0.02

log K: mean = 8.56<sub>3</sub>  $\sigma$  = 0.02

<sup>a</sup> Volume of 0.1702M NaOH added to 49.94 ml of solution.

<sup>b</sup> Volume of 0.2702M NaOH added to 49.94 ml of solution.

<sup>c</sup> Calculation procedure is described in text.

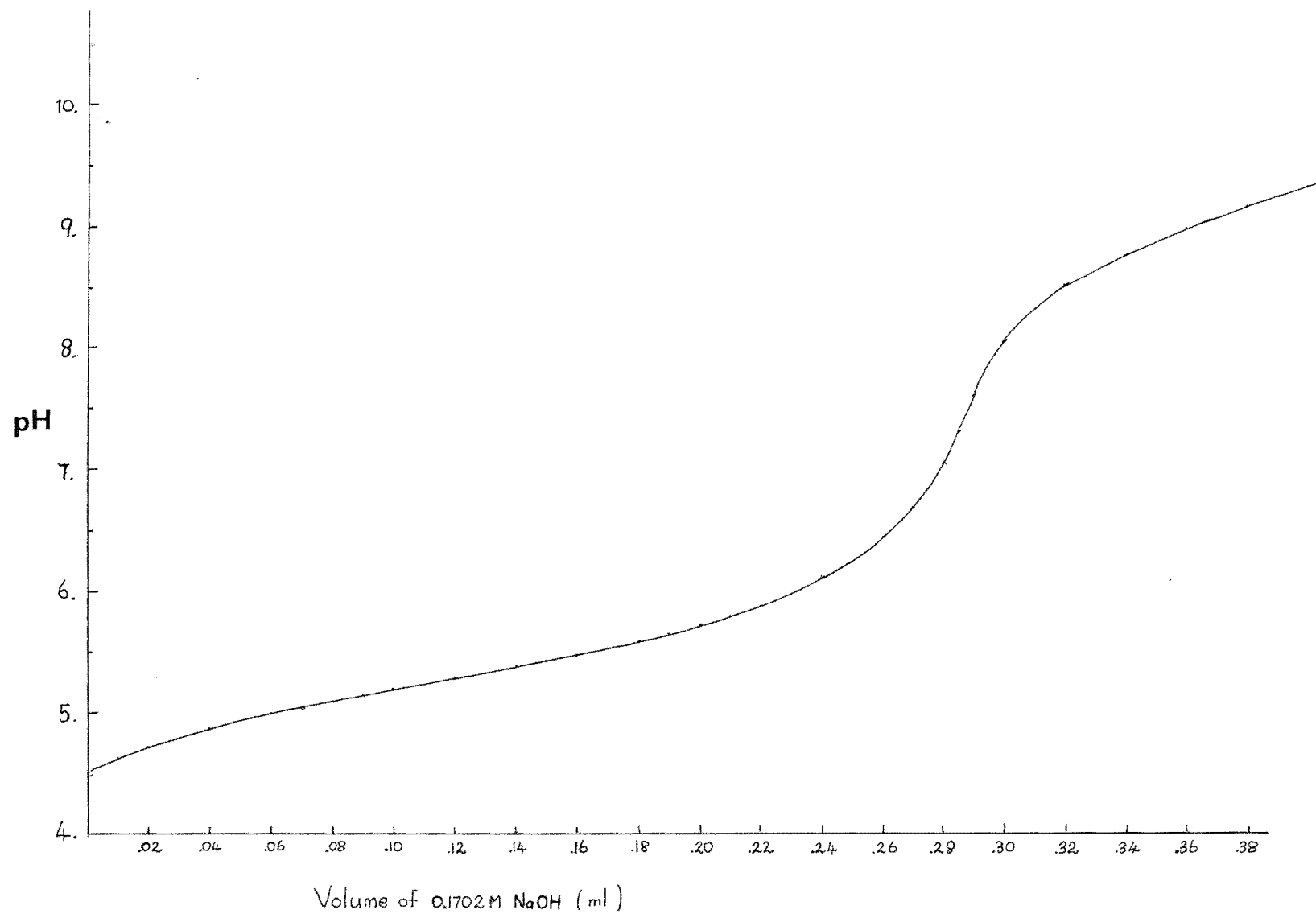


**Fig 7.9** Titration curve for copper/diamine-diketone system  $T_M = 3.812 \times 10^{-4} M$ ,  $T_L = 6.092 \times 10^{-4} M$ .



$$T_L = [L] + [LH] + [LH_2] + [CuL] \quad 7.20$$

$$T_H = [H] + [HL] + 2[LH_2] - K_w/[H] \quad 7.21$$

Using the protonation constants of the ligand (section 6.3), the free ligand concentration  $[L]$  can be calculated, at each titration point, from equation 7.21. From equations 7.19 and 7.20,  $T_M - T_L = [Cu] - [L] - [LH] - [LH_2]$ , thus using the value of  $[L]$ ,  $[Cu]$  can be calculated. The value for  $K_1$ , the stability constant for the 1:1 copper diamine-diketone complex, can be calculated

$$K_1 = \frac{[CuL]}{[Cu][L]} = \frac{T_M - [Cu]}{[Cu][L]} \quad .$$

The results of these calculations for the two titrations are shown in Table 7.22. The mean of the  $\log K_1$  values and the standard deviation for each titration are also shown. The agreement between the mean values for each titration is satisfactory. This agreement of  $\log K$  values from titrations at a different  $T_L:T_M$  ratio and also at a different  $T_M$  concentration implies that the formation of polynuclear species is negligible. However, the  $\log K$  values in Table 7.22 do not show a random distribution about a mean value. There is a steady decrease from ca. 8.58 at  $\bar{n} = 0.2$  to ca. 8.53 at  $\bar{n} = 0.7$ . The introduction of a soluble metal hydroxy species  $Cu(OH)^+$ , for which a formation constant has been determined<sup>173</sup>, into equation 7.19 did not alter the

trend in the  $\log K$  values (or even the magnitude of the constant). The total change of 0.05 in  $\log K$  is not really statistically significant and probably arises from a small systematic error in one of the fixed quantities, e.g.  $T_M$  or the protonation constant of the ligand,  $\log k_i$ .

As the ligand decomposed in alkaline solutions (see section 6.3.3) no enthalpy data for the formation of the copper-diamine-diketone complex could be obtained.

#### Spectrophotometric data

In aqueous solution the visible spectrum of the copper ligand complex showed a broad absorption band centred at 648 nm ( $\epsilon$  163). The ultraviolet spectrum in aqueous solution showed an absorption at 287 nm ( $\epsilon$  ca. 4900) and the tail of an intense band centred below 200 nm. The spectrum was observed to change with time. Within two hours there was a distinct shoulder appearing on the high energy side of the band at 287 nm and a decrease in the intensity of this latter absorption. After 26 hours there was a well defined absorption at 245 nm and the absorption at 287 now formed a shoulder at 285 nm. These changes with time were interpreted as indicating the formation of mesityl oxide from the decomposition of the ligand (section 6.3.3).

### 7.3.2 Discussion

#### Coordination of the ligand

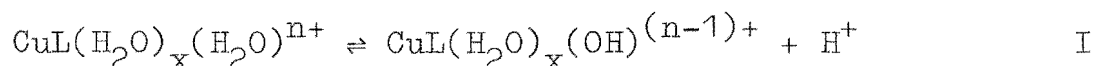
This diamine-diketone has four potential donor atoms, two secondary amine nitrogens and two weakly basic ketone functions. The energy of the d-d transition (648 nm) is similar to that for other copper complexes with two nitrogen and two oxygen donors coordinated in the plane (two solvent molecules in the trans planar positions) (see 7.2.2). In view of the weak basicity of the ketone function the question that does arise is: are the ketone functions coordinated to the copper ion in aqueous solution?

The stability constant of the 1:1 copper ethylene-diamine complex is 10.54 (Table 7.21) while that for the copper diamine-diketone complex is 8.56 (Table 7.22). The basicities ( $\log k_1 + \log k_2$ ) for the two ligands ethylene-diamine and the diamine-diketone are 17.01 (Table 7.21) and 15.60 (Table 6.18) respectively. The ratio of the complex stability to the ligand basicity for the ketone (8.56/15.60) is smaller than that for ethylenediamine (10.54/17.01).

However, similar observations were found when the ratios of the stabilities of the copper complexes to the ligand basicities of a number of N-alkyl substituted ethylenediamines were compared with ethylenediamine<sup>179</sup>. (Data in 0.5 M  $\text{KNO}_3/\text{Ba}(\text{NO}_3)_2$  at 25°C.)

A comparison of the ratio of the copper complex stability of NN'-di-n-propylethylenediamine to the ligand basicity (8.79/17.80, reference 179) with that for the diamine-diketone ligand (8.56/15.60) may indicate that the copper complex with the diamine diketone is more stable than expected on the basis of the basicity alone, and perhaps indicates that the ketone functions are coordinated.

Martell and coworkers<sup>174</sup> have shown that the pK's for the proton dissociation of the 1:1 copper chelates of a number of carbon and nitrogen substituted ethylenediamines were in the range 7.1 - 7.5. The narrow range of values obtained suggested that the reaction



was relatively independent of the stability of the 1:1 chelate.

For the copper diamine-diketone, reaction I would be important towards the end of a pH titration (pH 5.5 - 6.5, see Fig. 7.9) if the ketone functions were not coordinated. This would cause a detectable difference between the observed end point and that calculated assuming coordination of the ketone groups. No such difference was found; this indirect evidence supports the coordination of the ketone functions.

### Spectrophotometric data

The absorption band in the U.V. spectrum at 287 nm is assigned as a  $L_{\sigma} \rightarrow M$  charge transfer associated with the secondary amine nitrogens. The energy of this absorption is slightly lower than that for the similarly assigned charge transfer for the copper-diamine-dioxime complex,  $CuLH_2$ , 277 nm (see section 7.2.2b).

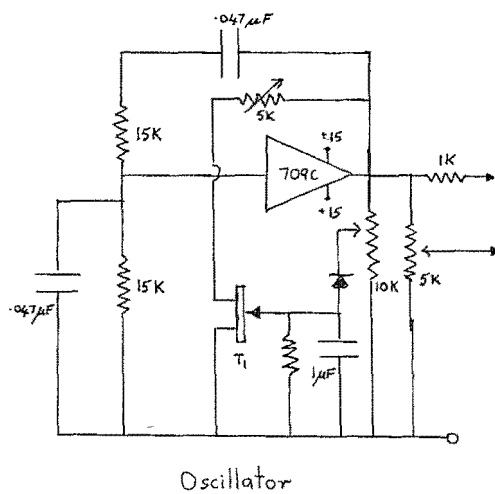
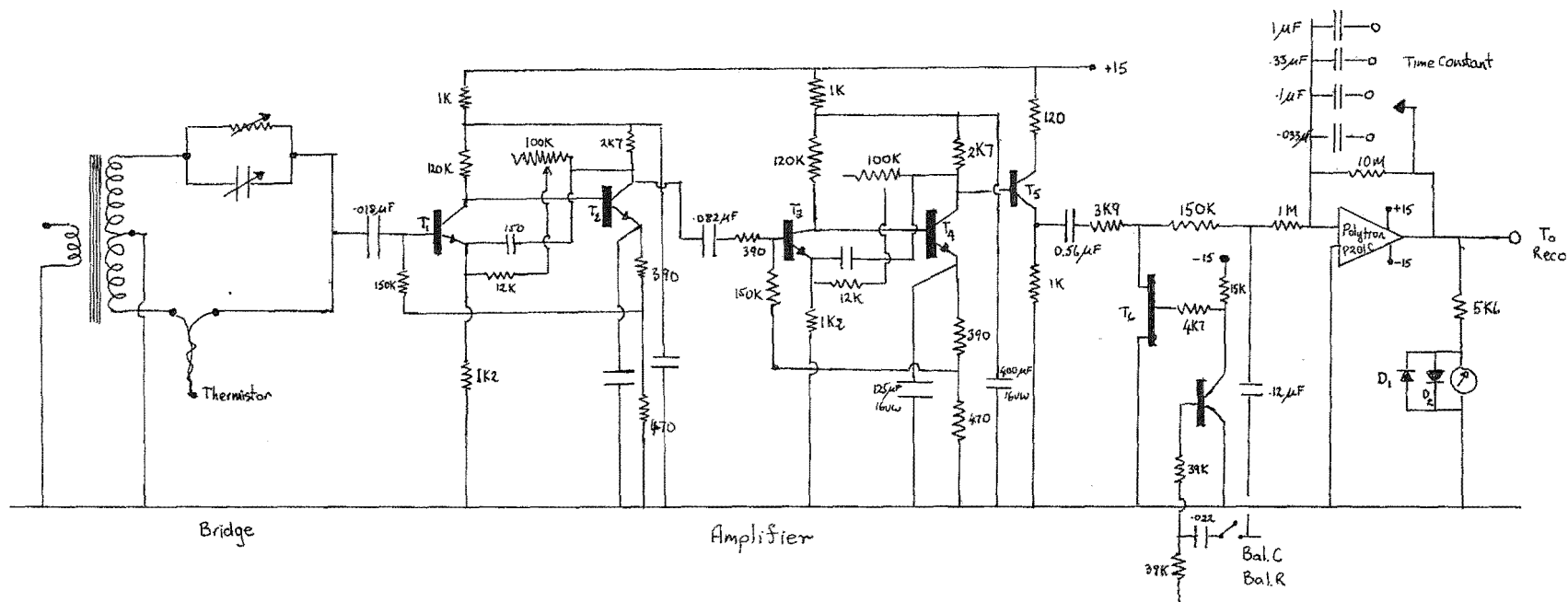
The band centred below 200 nm is possibly associated with a ligand  $\pi \rightarrow \pi^*$  transition<sup>180</sup>, or a metal  $\rightarrow \pi^*$  transition if the ketone groups are coordinated.

### 7.4 COPPER COMPLEXES - A BRIEF SUMMARY

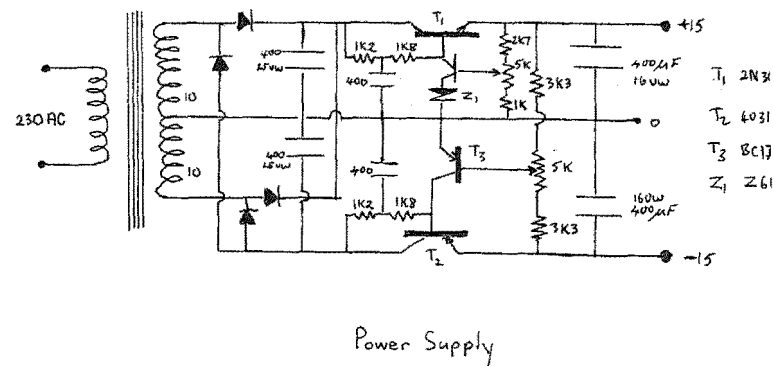
The slightly greater stability of the  $Cu(hm-3,2,3-tet)^{2+}$  complex compared with  $Cu(3,2,3-tet)^{2+}$  is due to a more favourable entropy change. This greater entropy change for the formation of  $Cu(hm,3,2,3-tet)^{2+}$  is associated with decreased solvation in the trans-planar sites due to the interaction with the axial methyl groups. The visible absorption spectrophotometric data support this interpretation.

A comparison of the enthalpy and entropy changes shows that the difference in stability between  $Cu(hm-3,2,3-tet)^{2+}$  and  $Cu(LH_2)^{2+}$  (diamine-dioxime ligand) is due almost entirely to the difference in the enthalpy terms;  $\Delta H$  is the term most closely associated with bonding of the ligands.

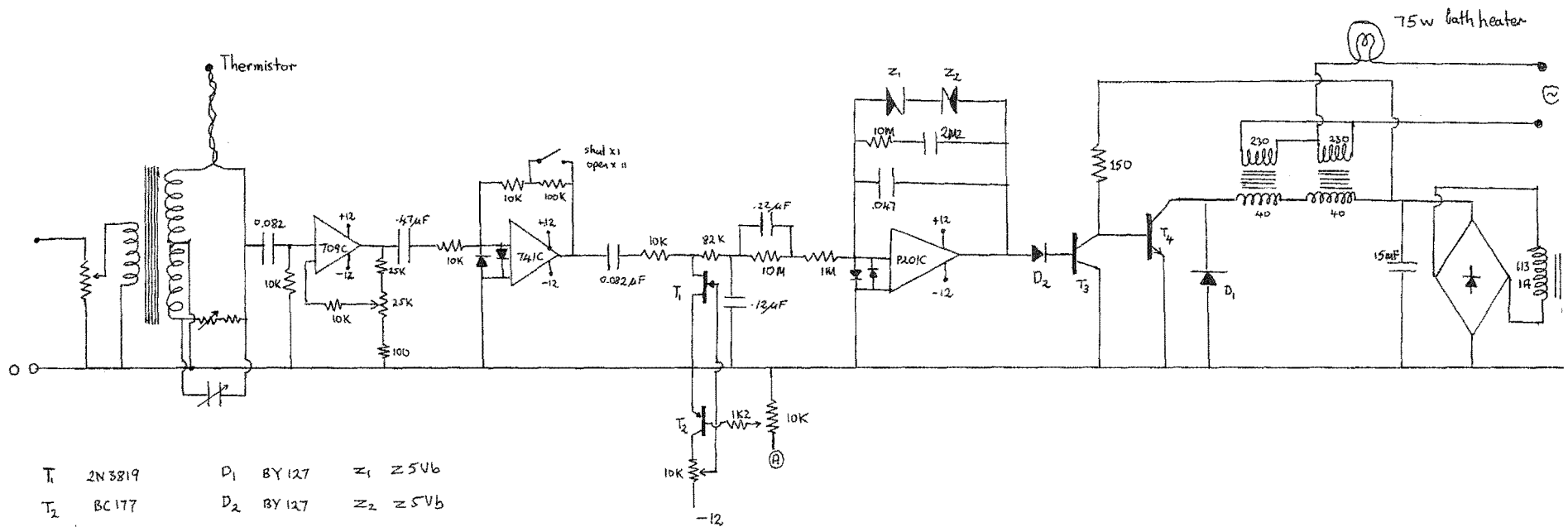
$T_1$  2N2586  
 $T_2$  BC109  
 $T_3$  BC109  
 $T_4$  BC109  
 $T_5$  BC109  
 $T_6$  2N3819  
 $D_1$  1N914  
 $D_2$  1N914



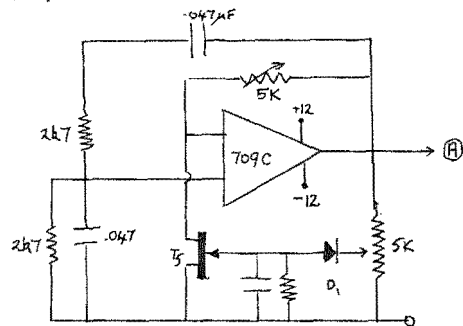
$T_1$  2N3819



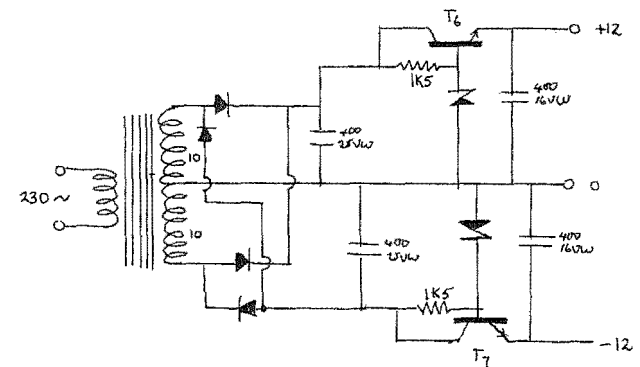
# Appendix A. Calorimeter Bridge Circuit



$T_1$  2N3819       $D_1$  BY127       $Z_1$  5V6  
 $T_2$  BC177       $D_2$  BY127       $Z_2$  5V6  
 $T_3$  2N3053  
 $T_4$  2N3054



$T_5$  2N3819  
 $D_1$  1N914



$T_6$  2N3053  
 $T_7$  40319

Water Bath Temperature Controller

## APPENDIX B

### Determination of End Points in Potentiometric Titrations

In a potentiometric titration the end point of the reaction will be revealed by an increase in the slope of the plot of pH (or EMF) against titre; the actual end point being at a titre value where the slope of the plot is greatest, i.e. where the derivative of pH with respect to titre is a maximum or where the second derivative is zero. The accuracy with which the end point can be found using derivative methods depends on the magnitude of the change in pH in the region of the end point which, in acid-base neutralisation reactions depends on the strength of the acid and base.

Generally, the derivative method for the determination of titration end points was found to be adequate in this study. However, in some cases (where the magnitude of the change in pH in the end point region was slight), for example in the titration of 3,2,3-tet and excess HCl with standard alkali, the end point for the neutralisation of the excess acid could be more accurately assessed by the use of a Gran plot<sup>181</sup>. The application of this technique has been more recently reviewed by Rossotti<sup>182</sup>. An outline of how a Gran plot is used, as applicable to the 3,2,3-tet titration, is as follows:



Let  $v_{e_1}$  be the volume of alkali required to neutralise the excess acid and  $v_{e_2}$  be the volume of alkali required to neutralise the excess acid plus one equivalent of acid from the tetraprotonated ligand. At any point in the titration ( $v$ ,  $p[H^+]$ ) before the first end point,

$$H^+ = T_H - C_{NaOH}$$

where  $T_H$  is the total available excess acid and  $C_{NaOH}$  is the concentration of alkali added. If  $V$  is the total initial volume of solution then,

$$[H^+] = \frac{V \cdot T_H}{(V + v)} - \frac{v \cdot B}{(V + v)}$$

where  $B$  is concentration of base. Now at the equivalence point  $V \times T_H = v_{e_1} \times B$ , thus

$$[H^+] = \frac{(v_{e_1} - v)B}{(V + v)}.$$

Now multiplying by the activity coefficient for the hydrogen ion  $\gamma_{H^+}$ ,

$$(V + v)[H^+]\gamma_{H^+} = (v_{e_1} - v)B \cdot \gamma_{H^+}$$

$$\text{i.e. } \tau_1 = (V + v)10^{-pH} = (v_{e_1} - v)B \cdot \gamma_{H^+}.$$

Thus if  $\gamma_{H^+}$  and the liquid junction potential are constant then a plot of  $\tau_1$  against  $v$  is linear and when extrapolated to  $\tau = 0$  gives  $v = v_{e_1}$ . After the first end point, the equilibrium

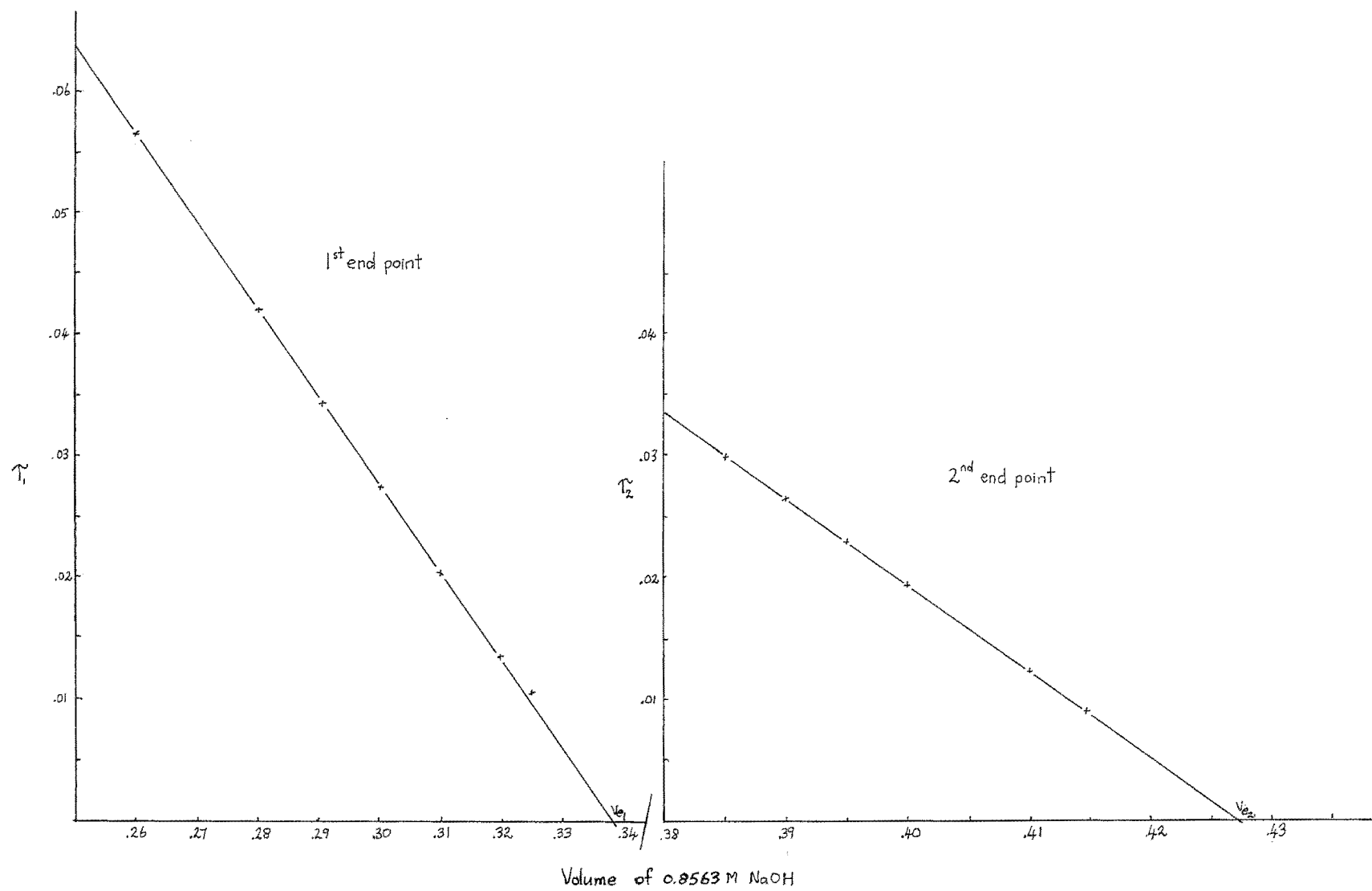
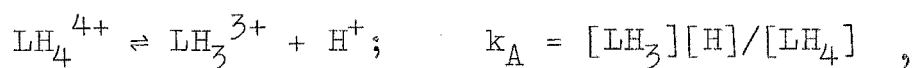


Fig 1 Gran Plots for 3,2,3-tet Standardisation



has to be considered. The equation

$$k_A = \left[ \frac{(v - v_{e1}) \cdot B}{(V + v)} \right] [\text{H}^+] / \left[ \frac{V \times H_c}{V + v} - \frac{(v - v_{e1}) \cdot B}{V + v} \right] \quad (1)$$

is valid if the free acid concentration is small compared with  $[\text{LH}_3]$  and  $[\text{LH}_4]$ ,  $H_c$  is the concentration of protonated 3,2,3-tet. Rearranging equation (1) gives

$$V \cdot H_c - (v - v_{e1})B = (v - v_{e1}) \cdot B \cdot [\text{H}^+] / k_A$$

and at the second end point

$$V \cdot H_c = (v_{e2} - v_{e1}) \cdot B \quad (2)$$

From the rearranged form of equation (1) and from (2)

$$k_A(v_{e2} - v) = (v - v_{e1})[\text{H}^+] ;$$

multiplying both sides of this equation by  $\gamma_{\text{H}^+}$  gives

$$\tau_2 = (v - v_{e1})10^{-\text{pH}} = k_A \cdot \gamma_{\text{H}^+} \cdot (v_{e2} - v) ,$$

where pH is the experimental pH value. If the liquid junction potential,  $\gamma_{\text{H}^+}$  and  $k_A$  are constant then a plot of  $\tau_2$  against  $v$  will be linear and, when extrapolated to  $\tau = 0$ , will give the value of  $v_{e2}$ .

Gran plots for the two equivalence points in a 3,2,3-tet/acid titration with standard NaOH are shown in Fig. 1.

## APPENDIX C

### The Algebra of Least Squares

Consider a set of  $n$  equations which are linear in some unknown parameters  $x_1, x_2, \dots, x_m$ ,  $n > m$

$$\begin{aligned} b_1 &= a_{11}x_1 + a_{12}x_2 + \dots + a_{1m}x_m \\ b_2 &= a_{21}x_1 + a_{22}x_2 + \dots + a_{2m}x_m \\ &\vdots \\ b_n &= a_{n1}x_1 + a_{n2}x_2 + \dots + a_{nm}x_m \end{aligned} \tag{1}$$

where  $b_i$  and  $a_{ij}$  arise from experimental observations. These equations (1) are more readily expressed in matrix notation

$$A X = b$$

As the elements  $b_i$  and  $a_{ij}$  are subject to experimental error, a method is required whereby the 'best' solution of the set of  $m$  parameters is found. A vector of residuals is defined

$$r = b - AX,$$

the best solution being that which minimises the sum of weighted residuals, i.e. minimising

$$M = r^T r$$

where  $r^T$  is the transpose of the vector  $r$ . The minimising condition  $\partial M / \partial X = 0$  gives rise to the expression<sup>183</sup>

$$A^T A X = A^T b$$

These are called the normal equations<sup>183</sup> which can be solved directly to obtain the required estimates of  $X$  by pre-multiplying  $A^T b$  by  $(A^T A)^{-1}$ ,

$$X = (A^T A)^{-1} A^T b$$

The equations (1) are linear in the unknown parameters  $x_i$ . A non-linear problem can also be solved by a least squares procedure by the use of the Taylor expansion.

Consider a set of observable functions  $f_i$  of  $m$  parameters  $x_j$ ;  $f_i = f_i(x_1, x_2, \dots, x_m)$ . The function can be expanded in a Taylor series about the point  $(x_1^0 \dots x_m^0)$  and neglecting terms of order higher than one<sup>184</sup>

$$f_i \approx f_i(x_1^0 \dots x_m^0) + \frac{\partial f_i}{\partial x_1} (x_1 - x_1^0) + \frac{\partial f_i}{\partial x_2} (x_2 - x_2^0) + \dots$$

or

$$f_i - f_i^0 \approx \sum_{j=1}^m \frac{\partial f_i}{\partial x_j} (x_j - x_j^0)$$

or

$$\Delta f_i \approx \sum_{j=1}^m \frac{\partial f_i}{\partial x_j} \cdot \Delta x_j, \quad (2)$$

thus the problem has now been reduced to a linear one of the form  $b = AX$  as above. For given approximate values of the parameters  $x_j$ , the corrections  $\Delta x_j$  can be calculated. As the non-linear terms in the Taylor expansion are ignored, it is necessary to repeat the solution of (2) until convergence of each  $x_j$  is obtained.

### Matrix Inversion - The Choleski Process

A symmetric matrix A can be factorised<sup>185</sup>

$$A = LL^T$$

where L is the lower triangular matrix. The inverse of A is  $A^{-1} = (LL^T)^{-1} = (L^T)^{-1}(L^{-1})$  and  $(L^T)^{-1} = (L^{-1})^T$ , therefore to form the inverse of matrix A the three steps in the process are

- (i) factorise the matrix into its lower triangular matrix
- (ii) invert the lower triangular matrix
- (iii) premultiply this matrix by its transpose.

This process was used in the least squares program ORGLS.

The matrix inversion is carried out in SUBROUTINE MATINV (see Appendix D).

### Errors in Least Squares Analysis

Errors in the parameters  $x_j$  are calculated during the least squares analysis. It can be shown<sup>186</sup> that the variance-covariance matrix of the parameter estimates is given by the inverse of the normal equations matrix multiplied by an unbiased estimate of  $\sigma^2$ , the variance of an observation of unit weight, an unbiased estimate of which can be obtained from the weighted sum of squares of residuals. In general the e.s.d. of parameter i is given by

$$\sigma_i^2 = (a_{ii}) \sum w(\Delta r_i)^2 / (n-m) \quad (3)$$

where n is number of observations, m is the number of

parameters,  $a_{ii}$  is an element from the inverse matrix of the normal equations and  $\sum w(\Delta r_i)^2$  is the sum of weighted squares of residuals. The dependence of the magnitude of each  $\sigma_i$  on the weighting scheme is evident from equation (3).

## APPENDIX D

### Computer Programs

The Fortran computer programs listed below were used on an IBM System 360/Model 44 computer. Graphs were plotted on an IBM 1620 computer, with a 1627 X-Y plotter attachment, using the PLOTA subroutine package<sup>187</sup>.

#### Program ORGLS

This program was modified from the program ORGLS of W.R. Busing and H.A. Levy<sup>188</sup>. The listing below shows the program adapted to calculate the  $\log k_1$  data for the protonation of the ligand hm-3,2,3-tet. (The program ORGLS was also adapted to enable copper/ligand stability constants and enthalpy data to be calculated. The appropriate changes to subroutine PRELIM and CALC have not been shown).

The program consists of five sections; the four subroutines PRELIM, CALC, TEST and MATINV and the MAIN LINE program. PRELIM enables preliminary calculations on the initial data, e.g. calculation of  $\bar{n}$  from pH titration data. In CALC a value of the observed quantity YO is calculated from the parameters P and the variable X (hydrogen ion concentration in the program below). MATINV incorporates the matrix inversion process (see Appendix C). TEST is used to apply checks on the parameters at the end of each least squares cycle. The various sections of the program are described within the program below.

The programs FORM, THERM, DIST and CUTHERM are described within the listings below.



```

C      ORGLS
C      LEAST SQUARES ANALYSIS OF THE HM323TET PH DATA
C
C
C      SUBROUTINE PRELIM(YO,X,NO,SIGYO)
C      TO CALCULATE NBAR AND THE STANDARD DEVIATION OF NBAR
C      DIMENSION X(2,100),YO(100)
C      DIMENSION SIGYO(100)
C      INPUT DATA ---- SOLUTION COMPOSITION TOTAL ACID TH, TOTAL LIG. SL
C      TITRANT NAOH ALK, IONIC ACTIVITY FUNCTION OF WATER GAMA,
C      VOLUME OF TITRANT YO, SOLUTION PH X -----
C      READ(5,43) TH,SL,ALK,GAMA
C      DO 11 I=1,NO
C      IF(X(1,I).GE.10.84) GO TO 3
C      X(1,I)=(X(1,I)-0.0862)/.9953
3    PH=X(1,I)+0.003
C      X(1,I)=10.**(-X(1,I))
C      H=10.**(-PH)
C      DELH=X(1,I)-H
C      Q=49.94/(49.94+YO(I))
C      TL=SL*Q
C      ACID=TH*Q
C      ALKA=YO(I)*ALK/(49.94+YO(I))
C      CALCULATE THE STANDARD DEVIATION FOR YO SIGYO
C      CONST=(ACID-ALKA)*0.30E-2/TL
C      SIGYO(I)=SQRT(((1.+1.007E-14/(GAMA*X(1,I)**2))*DELH/TL)**2+CONST**
12)
C      STORE NBAR AS YO
C      11 YO(I)=(ACID-X(1,I)+1.007E-14/(GAMA*X(1,I))-ALKA)/TL
C      43 FORMAT(2(E10.3),F10.4,F10.3)
C      RETURN
C      END
C
C      SUBROUTINE CALC(I,X,Y,P)
C      DIMENSION X(2,100),YO(100),P(20)
C      Y=(P(1)*X(1,I)+2.*P(2)*P(1)*X(1,I)**2+3.*P(3)*P(2)*P(1)*X(1,I)**3+
14.*P(4)*P(3)*P(2)*P(1)*X(1,I)**4)/(1.+P(1)*X(1,I)+P(2)*P(1)*X(1,I)
2.**2+P(3)*P(2)*P(1)*X(1,I)**3+P(4)*P(3)*P(2)*P(1)*X(1,I)**4)
C      RETURN
C      END
C
C      SUBROUTINE TEST(ISTOP,P,SQSIG,NP)
C      DIMENSION P(10),SQSIG(2)
C      I=1
C      5 IF(P(I)) 3,3,4
C      3 ISTOP=1
C      GO TO 8
C      4 I=I+1
C      IF(I-NP) 5,5,6
C      6 A=ALOG10(SQSIG(2))-ALOG10(SQSIG(1))
C      IF(A) 11,12,12
C      11 A=-A

```

```

12 IF (A.LT.0.0005) GO TO 7
   GO TO 8
7  ISTOP=2
8  CONTINUE
   RETURN
   END

```

```

SUBROUTINE MATINV(AM,N,NFAIL)
DIMENSION AM(700)
C ***** SEGMENT 1 OF CHOLESKI INVERSION *****
C ***** FACTOR MATRIX INTO LOWER TRIANGLE X TRANSPOSE *****
K=1
IF (N-1) 10,8,9
8  AM(1)=1.0/AM(1)
   GO TO 204
C ***** LOOP M OF A(L,M) *****
9  DO 7 M=1,N
   IMAX=M-1
C ***** LOOP L OF A(L,M) *****
   DO 6 L=M,N
   SUMA=0.0
   KLI=L
   KMI=M
   IF (IMAX) 23,23,1
C ***** SUM OVER I=1,M-1 A(L,I)*A(M,I) *****
   DO 2 I=1,IMAX
   SUMA=SUMA+AM(KLI)*AM(KMI)
   J=N-I
   KLI=KLI+J
   KMI=KMI+J
C ***** TERM=C(L,M)-SUM *****
23  TERM=AM(K)-SUMA
   IF (L-M) 3,3,5
   IF (TERM) 10,10,4
C ***** A(M,M)=SQRT(TERM) *****
4  DENOM= SQRT(TERM)
   AM(K)=DENOM
   GO TO 6
10  NFAIL= K
   GO TO 300
C ***** A(L,M)=TERM/A(M,M) *****
5  AM(K)=TERM/DENOM
6  K=K+1
7  CONTINUE
C ***** SEGMENT 2 OF CHOLESKI INVERSION *****
C ***** INVERSION OF TRIANGULAR MATRIX *****
100 AM(1)=1.0/AM(1)
   KDM=1
C ***** STEP L OF B(L,M) *****
   DO 104 L=2,N
   KDM=KDM+N-L+2
C ***** RECIPROCAL OF DIAGONAL TERM *****
   TERM = 1.0/AM(KDM)
   AM(KDM)=TERM
   KMI=0
   KLI=L
   IMAX=L-1
C ***** STEP M OF B(L,M) *****
   DO 103 M=1,IMAX
   K=KLI
C ***** SUM TERMS *****
   SUMA=0.0
   DO 102 I=M,IMAX
   II=KMI+I
   SUMA=SUMA-AM(KLI)*AM(II)
102 KLI=KLI+N-I

```

```

C ***** MULT SUM * RECIP OF DIAGONAL *****
AM(K)=SUMA*TERM
J=N-M
KLI=K+J
103 KMI=KMI+J
104 CONTINUE
C ***** SEGMENT 3 OF CHOLESKI INVERSION *****
C *****PREMULTIPLY LOWER TRIANGLE BY TRANSPOSE*****
200 K=1
DO 203 M=1,N
KLI=K
DO 202 L=M,N
KMI=K
IMAX=N-L+1
SUMA=0.0
DO 201 I=1,IMAX
SUMA=SUMA+AM(KLI)*AM(KMI)
KLI=KLI+1
201 KMI=KMI+1
AM(K)=SUMA
202 K=K+1
203 CONTINUE
204 NFAIL=0
300 RETURN
END

C GENERAL LEAST-SQUARES (WITH FORTRAN MATRIX INVERTER). 5
C OR GLS, GENERAL FORTRAN LEAST SQUARES
C
C DIMENSIONS FOR NV(MAX)=100,NP(MAX)=200,NO(MAX)=1000,NX(MAX)=5
C
C DIMENSION AM(700)
C DIMENSION TITLE(18),P(20),X(2,100),YD(100),SIGYD(100),KI(20)
C DIMENSION ZP(20),SUBT(18)
C DIMENSION DP(20),SQSIG(2), V(50),DC(20),DV(50),DD(200)
C DIMENSION DIAG(50),PD(50),ROW(50)
C COMMON AM,V,DC,DV,DP,YC,P,X
C COMMON NC,NV,NX,ID,IW,IP,IT,NP,ISENT,NO,NM,NCY,IC
C COMMON SQRTW, DPK,PSAVE,YD,JK,ISING,II,IID,PDI,IJ,IJD,POLD
C COMMON SIGP,ISTOP,NT,NPCD
C COMMON TITLE, O,SIGYO,KI, SQSIG, DD,DIAG,PD,ROW

C
C FORMAT STATEMENTS
C
20 FORMAT(8X,I2)
21 FORMAT('D',5X,I1,5X,E10.4,5X,F8.4)
29 FORMAT('D',I,P LOG(P) ')
41 FORMAT(F10.2,8X,I2)
40 FORMAT('D',10NIC STRENGTH',F5.2,5X,'TITRATION NUMBER B',I2)
51 FORMAT(18A4)
52 FORMAT(///1H018A4)
53 FORMAT(7I3)
54 FORMAT(32H0NUMBER OF CYCLES IN THIS JOB ISI2/37H0NUMBER OF PARAMET
1ERS TO BE VARIED ISI3/51H0NUMBER OF INDEPENDENT VARIABLES PER OBSE
2RVATION ISI2)
58 FORMAT(31H0DERIVATIVES PROGRAMMED BY USER)
59 FORMAT(57H0NUMERICAL DERIVATIVES UNLESS PARAMETER INCREMENT IS ZER
10)
61 FORMAT(31H0WEIGHTS TO BE SUPPLIED BY USER)
62 FORMAT(34H0UNIT WEIGHTS TO BE SET BY PROGRAM)
63 FORMAT(36H0PARAMETERS TO BE READ AS INPUT DATA)
64 FORMAT(34H0PARAMETERS TO BE TAKEN FROM CYCLEI2,16H OF PREVIOUS JOB
1)
66 FORMAT(I3,77X/(8E9.3,8X))
67 FORMAT(29H0NUMBER OF PARAMETERS READ ISI3)
68 FORMAT(I1,F8.3,F9.3,F9.4)
69 FORMAT(31H0NUMBER OF OBSERVATIONS READ ISI4)
70 FORMAT(72I1)
71 FORMAT(8E9.3)
72 FORMAT(46H0CALCULATED Y BASED ON PARAMETERS BEFORE CYCLEI2)
73 FORMAT('D',Y(OBS) Y(CALC) OBS-CALC SIG(O)

```

```

1      (O-C)/SIG(O)          X(I)    ')
79 FORMAT(1H 6(E10.3,5X))
80 FORMAT(51H)AGREEMENT FACTORS BASED ON PARAMETERS BEFORE CYCLE 12/
120H)SUM(W*(O-C)**2) IS E11.3/35H)SQRTF(SUM(W*(O-C)**2)/(NO-NV)) IS
2 E11.4)
81 FORMAT(60H)ESTIMATED AGREEMENT FACTORS BASED ON PARAMETERS AFTER C
1YCLE 12/20H)SUM(W*(O-C)**2) IS E11.3/35H)SQRTF(SUM(W*(O-C)**2)/(NO
2-NV)) IS E11.4)
83 FORMAT(62H MATRIX HAS A ZERO DIAGONAL ELEMENT CORRESPONDING TO PAR
1AMETER I3,16H OF THOSE VARIED)
85 FORMAT(40H SINGULARITY RETURN FROM MATRIX INVERTER)
86 FORMAT(37H)PARAMETERS AFTER LEAST SQUARES CYCLE 12/58H)          OLD
1      CHANGE          NEW          ERROR/1H )
88 FORMAT(1H I3,5X,E10.4,15X,E10.4)
89 FORMAT(1H I3,4(5X,E10.4))
90 FORMAT(66H)SUBROUTINE TEST INDICATES THAT JOB IS TO BE TERMINATED
1FOR REASON I2)
91 FORMAT('0' ' REASON 2 -- PARAMETER INCREMENTS SMALL ENOUGH FOR
1ADEQUATE REFINEMENT ')
92 FORMAT(11H)INPUT DATA/40H) I          P(I)          KI(I)          DP(I)/
11H )
93 FORMAT(1H I3,5X,E10.4,5X,I4,3X,E11.3)
94 FORMAT(51H)CORRECTED PARAMETERS NOT TO BE SAVED FOR LATER USE)
95 FORMAT(51H)CORRECTED PARAMETERS TO BE WRITTEN ON PRIVATE TAPE)
96 FORMAT(51H)CORRECTED PARAMETERS TO BE WRITTEN FOR CARD OUTPUT)
97 FORMAT(19H)CORRELATION MATRIX)
98 FORMAT(1H)I3,10F9.4/(1H 3X,10F9.4))
99 FORMAT('0' ' REASON 1 -- NEGATIVE OR ZERO PARAMETER FOUND ')
INTEGER RDR,PTR,PCH
PCH=7
RDR=5
PTR=6

C
C READ TITLE AND CONTROL DATA ---- IONIC STRENGTH AISTR ,
C TITRATION NUMBER TN , NO. OF CYCLES IN JOB NC , NO. OF PARAS. TO
C BE VARIED NV , NO. OF DETERMINATIONS OF THE VARIABLE X ,
C DERIVATIVE INDICATOR ID, WEIGHT INDICATOR IW , IP AND IT ARE
C OUTPUT CONTROL PARAMETERS
C
INTE=0
READ(RDR,20) KODE
30 READ(RDR,51)(TITLE(I),I=1,18)
WRITE(PTR,52)(TITLE(I),I=1,18)
READ(RDR,41) AISTR,TN
WRITE(PTR,40) AISTR,TN
READ(RDR,53) NC,NV,NX,IO,IW,IP,IT
WRITE(PTR,54) NC,NV,NX
IF(IO)205,204,206
204 WRITE(PTR,58)
GO TO 207
206 WRITE(PTR,59)
207 IF(IW)210,208,210
208 WRITE(PTR,61)
GO TO 211
210 WRITE(PTR,62)
211 IF(IP)212,212,214
212 WRITE(PTR,63)
GO TO 215
214 WRITE(PTR,64)IP
215 IF(IT-1)216,218,221
216 WRITE(PTR,94)
GO TO 301
218 WRITE(PTR,95)
GO TO 301
221 WRITE(PTR,96)
C
C READ TRIAL PARAMETERS P , AND NO. OF PARAS. NP
C
301 IF(IP)401,401,501
401 READ(RDR,66)NP,(P(I),I=1,NP)

```

```

      GO TO 601
501   DO 503 J=1,IP
503   CONTINUE
601   WRITE(PTR,67)NP
C
C   READ OBSERVATIONS TO SENTINEL
C
      J=0
801   J=J+1
      READ(RDR,68) ISENT,YO(J),SIGYO(J),X(1,J)
      IF(ISENT)801,801,1101
1101  NO=J-1
      WRITE(PTR,69)NO
C   READ KEY INTEGERS AND PARAMETER INCREMENTS IF SPECIFIED
      IF(NC)1601,1601,1301
1301  READ(RDR,70)(KI(I),I=1,NP)
601   IF(ID)1501,1611,1501
1501  READ(RDR,71)(DP(I),I=1,NP)
      GO TO 1621
1601  DO 1602 I=1,NP
1602  KI(I)=0
1611  DO 1612 I=1,NP
1612  DP(I)=0.0
C
C   INITIALIZE PROBLEM AND ENTER SUBROUTINE PRELIM IF PROVIDED
C
1621  NM=(NV*(NV+1))/2
      SQSIG(1)=1.0
      CALL PRELIM(YO,X,NO,SIGYO)
C   PUT OUT TRIAL PARAMETERS, KEY INTEGERS, AND PARAMETER INCREMENTS
      WRITE(PTR,92)
      DO 1653 I=1,NP
1653  WRITE(PTR,93)I,P(I),KI(I),DP(I)
C
C   START LOOP TO PERFORM NC CYCLES AND ONE FINAL CALCULATION OF Y
C
      NCY=NC+1
      DO 8501 IC=1,NCY
C   CLEAR ARRAYS AM AND V EXCEPT ON LAST CYCLE
      IF(IC-NCY)1851,2001,2001
1851  DO 1852 I=1,NM
1852  AM(I)=0.0
      DO 1902 I=1,NV
1902  V(I)=0.0
C
C   INITIALIZE FOR CYCLE IC AND PUT OUT CAPTION FOR LIST OF Y(CALC)
C
2001  SQSIG(2)=SQSIG(1)
      SIG=0.0
      WRITE(PTR,52)(TITLE(I),I=1,18)
      WRITE(PTR,40) AISTR,TN
      WRITE(PTR,72)IC
      WRITE(PTR,73)
C
C   START LOOP THROUGH NO OBSERVATIONS
C
2201  DO 5101 I=1,NO
C
C   ENTER USERS SUBROUTINE TO COMPUTE Y(CALC) AND DERIVATIVES
C
      CALL CALC(I,X,YC,P)
C   OBTAIN WEIGHT AND CALCULATE QUANTITIES FROM Y(OBS)-Y(CALC)
      IF(IW)2501,2501,2601
2501  SQRTW=1.0/SIGYO(I)
      GO TO 2701
2601  SIGYO(I)=1.0
      SQRTW=1.0
2701  DY=YO(I)-YC
      WDY=SQRTW*DY
      SIG=SIG+WDY*WDY

```

```

C
C      PUT OUT Y(CALC) AND OTHER INFORMATION FOR ONE OBSERVATION
C
2070 WRITE(PTR,79) YO(I),YC,DY,SIGYO(I),WDY,X(1,I)
C      BY-PASS DERIVATIVE AND MATRIX SET-UP ON FINAL CALC OF Y
      IF(IC-NCY)3001,5101,5101
C
C      START LOOP TO STORE AN ARRAY OF NV DERIVATIVES
C
3001      J=1
      DO 4101 K=1,NP
        IF(KI(K))4101,4101,3201
        IF(ID)3401,3301,3401
        OBTAIN DERIVATIVE FROM THOSE PROGRAMMED BY USER
3201      DV(J)=SQRTW*DC(K)
        GO TO 4001
        OBTAIN DERIVATIVE NUMERICALLY UNLESS PARAMETER
        INCREMENT IS ZERO
3401      DPK=DP(K)
        IF(DPK)3601,3301,3601
3601      PSAVE=P(K)
        P(K)=PSAVE+DPK
      CALL CALC(I,X,YD,P)
      DV(J)=SQRTW*(YD-YC)/DPK
      P(K)=PSAVE
4001      J=J+1
4101      CONTINUE
      END LOOP TO OBTAIN DERIVATIVES
C
C      START LOOP TO STORE MATRIX AND VECTOR.
      1604 OR GLS STORAGE SCHEME IS REVERSE OF 7090 OR GLS
C
      JK=1
      DO 5001 J=1,NV
4301      TEMP=DV(J)
        IF(TEMP)4501,4401,4501
        BY-PASS IF DERIVATIVE IS ZERO
4401      JK=JK+NV+1-J
        GO TO 5001
4501      DO 4801 K=J,NV
        AM(JK)=AM(JK)+TEMP*DV(K)
        JK=JK+1
        CONTINUE
4801      V(J)=V(J)+TEMP*WDY
        CONTINUE
5001      END LOOP TO STORE MATRIX AND VECTOR
5101      CONTINUE
      END LOOP THROUGH NO OBSERVATIONS
C
C      COMPUTE AND PUT OUT AGREEMENT FACTORS
C
      SQSIG(1)= SQRT(SIG/FLOAT(NO-NV))
      WRITE(PTR,80)IC,SIG,SQSIG(1)
      BY-PASS MATRIX INVERSION AND PARAMETER OUTPUT ON FINAL CYCLE
      IF(IC-NCY)5401,8701,8701
C
C      START LOOP TO TEST FOR ZERO DIAGONAL ELEMENT
C
5401      ISING=0
      II=1
      IID=NV
      DO 5801 I=1,NV
        IF(AM(II))5701,5601,5701
5601      ISING=1
        WRITE(PTR,83)I
5701      II=II+IID
        IID=IID-1
5801      CONTINUE
      END LOOP TO TEST FOR ZERO DIAGONAL ELEMENT
      TERMINATE JOB IF ZERO DIAGONAL ELEMENT WAS FOUND
C

```

```

IF(ISING)10301,6001,10301
C
C
C
6001    CALL MATINV(AM,NV,ISING)
C        IF(ISING)6201,6301,6201
6201    TERMINATE JOB IF SINGULAR MATRIX WAS FOUND
C        WRITE(PTR,85)
C        GO TO 10301
C
C        START LOOP FOR MATRIX VECTOR MULTIPLICATION FOR
C        PARAMETER CHANGES
6301    DO 7201 I=1,NV
C        PDI=0.0
C        IJ=I
C        IJD=Nv-1
C        DO 7001 J=1,NV
C        PDI=PDI+AM(IJ)*V(J)
6701    IF(J-I)6701,6801,6901
C        IJ=IJ+IJD
C        IJD=IJD-1
C        GO TO 7001
C
C        SAVE DIAGONAL ELEMENTS OF INVERSE MATRIX
6801    DIAG(I)=AM(IJ)
6901    IJ=IJ+1
7001    CONTINUE
C        PD(I)=PDI
C        SIG=SIG-PDI*V(I)
7201    CONTINUE
C        END LOOP FOR MATRIX VECTOR MULTIPLICATION
C
C        RECOMPUTE AGREEMENT FACTOR USING MODIFIED SIG
3655    Sqsig(1)= SQRT(SIG/float(Nv-NV))
C        PUT OUT CAPTION FOR LIST OF CORRECTED PARAMETERS
3666    WRITE(PTR,52)(TITLE(I),I=1,18)
C        WRITE(PTR,86)IC
C
C        START LOOP TO CORRECT AND PUT OUT PARAMETERS
C
C        J=1
C        DO 8001 I=1,NP
7601    IF(KI(I))7601,7601,7701
C        WRITE(PTR,88)I,P(I),P(I)
C        GO TO 8001
7701    POLD=P(I)
C        P(I)=POLD+PD(J)
8111    SIGP=SQRT(DIAG(J))*Sqsig(1)
C        WRITE(PTR,89)I,POLD,PD(J),P(I),SIGP
C        J=J+1
8001    CONTINUE
C        END LOOP TO CORRECT AND PUT OUT PARAMETERS
C
C        PUT OUT ESTIMATED AGREEMENT FACTORS
C        WRITE(PTR,81)IC,SIG,Sqsig(1)
C
C        ENTER USERS SUBROUTINE TO TEST AND MODIFY PARAMETERS
C        OR END JOB
8112    ISTOP=0
C        CALL TEST(ISTOP,P,Sqsig,NP)
C        WRITE CORRECTED PARAMETERS ON AUXILIARY TAPE IF
C        DESIRED
8204    IF(IT-1) 8403,8204,8204
C        NT=7
8205    NPCD=8*((NP-1)/8+1)

```

```

      WRITE(PCH,66)NP,(P(I),I=1,NPCD)
8403 IF(ISTOP) 8501,8501,8401
8401 WRITE(PTR,90)ISTOP
      IF(ISTOP-1) 8410,8410,8411
8410 WRITE(PTR,99)
      GO TO 8701
8411 WRITE(PTR,91)
      GO TO 8701
8501 CONTINUE
      C      END LOOP THROUGH NC CYCLES AND FINAL CALC OF Y
      C
      C      TERMINATE JOB
8701 IF(NC)10501,10501,8801
      C
      C      CONVERSION OF THE CONSTANTS TO LOG VALUES
      C
8801 WRITE(PTR,29)
      DO 8522 I=1,NP
      IF(P(I)) 18,18,19
      18 ZP(I)=1.0
      GO TO 8522
      19 ZP(I)=ALOG10(P(I))
8522 WRITE(PTR,21) I,P(I),ZP(I)
      C      CALCULATE AND PUT OUT CORRELATION MATRIX
      WRITE(PTR,52)(TITLE(I),I=1,18)
      WRITE(PTR,97)
      DO 9101 I=1,NV
      DIAG(I)=1.0/SQRT(DIAG(I))
9101 CONTINUE
      IJ=1
      DO 10201 I=1,NV
      DO 9601 J=1,NV
      ROW(J)=0.0
9601 CONTINUE
      DO 10001 J=I,NV
      ROW(J)=AM(IJ)*DIAG(I)*DIAG(J)
      IJ=IJ+1
10001 CONTINUE
      WRITE(PTR,98)I,(ROW(J),J=1,NV)
10201 CONTINUE
10301 CONTINUE
      INTE=INTE+1
      IF(INTE-KODE) 30,10501,10501
10501 STOP
      END

```



# FORM

```

C *****
C *
C * TO CALCULATE THE FORMATION CURVE FOR THE KETONE LIGAND *
C *
C *****
C DIMENSION PH(100),V(100)
C INTE=0
C READ(5,80) NKODE
8 READ(5,72) TA,TL,ALK,GAMA,AISTR,TN,CORR
C J=0
C J=J+1
C READ(5,71) ISENT,V(J),PH(J)
C IF(ISENT) 2,2,3
3 NO=J-1
C WRITE(6,78) TA,TL,ALK
C WRITE(6,73) AISTR,TN
C WRITE(6,74)
C WRITE(6,75)
C DO 6 I=1,NO
C KODE=0
C
C APPLY DAVIES CORRECTION TO THE MEASURED PH DATA
C
C PCH=PH(I)-CORR
C Q=49.94/(49.94+V(I))
C ACID=TA*Q
C ALKA=V(I)*ALK/(49.94+V(I))
C ZLIG=TL*Q
7 H=10.**(-PCH)
C ALKH=1.007E-14/(GAMA*H)
C ZNBAR=(ACID-ALKA+ALKH-H)/ZLIG
C IF(KODE) 4,4,5
4 WRITE(6,76) V(I),ZNBAR,PCH
C KODE=1
C
C APPLY CALIBRATION CURVE CORRECTION TO THE MEASURED PH DATA
C
C PCH=(PH(I)-.9862)/.9953
C GO TO 7
5 WRITE(6,77) V(I),ZNBAR,PCH
6 CONTINUE
C INTE=INTE+1
C IF(INTE-NKODE) 8,9,9
9 STOP
71 FORMAT(11,F8.3,9X,F9.4)
72 FORMAT(2(E10.3),F10.4,F10.3,F10.2,8X,I2,F10.4)
73 FORMAT('0' ' IONIC STRENGTH',F4.2,5X,' TITRATION NUMBER B',I2)
74 FORMAT('0' ' DAVIES CORRECTIONS
1 CALIBRATION CURVE CORRECTIONS ')
75 FORMAT('0' ' VOLUME NBAR CAL PH
1 VOLUME NBAR CAL PH ')
76 FORMAT('0' 3(F10.3,5X))
77 FORMAT('+ ' 55X,(3F10.3,5X))
78 FORMAT('0' 'TOTAL ACID CONCENTRATION IS',E9.4,3X,'TOTAL LIGAND CO
INCENTRATION IS',E9.4,3X,'ALKALI CONCENTRATION IS',F6.4)
80 FORMAT(I2)
C END

```

```

C          DIST
C *****
C *
C *   DISTRIBUTION CURVES FOR COPPER OXIME AS A FUNCTION OF THE
C *                               SOLUTION PH
C *   ALSO PLOT OUTPUT USING THE IBM PLOTTER
C *
C *****
C DIMENSION PH(200),H(200),PM(200,3),Z(200),N(200),LINE(101)
C DIMENSION Y1(200),Y2(200),Y3(200)
C LOGICAL*1 ILABEL(11)
C LOGICAL*1 JLABEL(33)
C LOGICAL*1 KLABEL(54)
C REAL MLH2,MLH,M,LH2
C INTEGER DOT,BLANK,AST,X,PLUS
C DATA DOT/' ','/',BLANK/' ','/',AST/'*','/',X/'*','/',PLUS/'+'/'
C NK=1
C READ(5,79) NKODE
2 READ(5,73) TL,TM,TN,AISTR,KODE
C READ(5,72) Z4,Z3,P1,P2
C WRITE(6,61) AISTR,TN,TL,TM
C WRITE(6,67)
C WRITE(6,62) Z4,Z3
C WRITE(6,75)
C WRITE(6,76) P1,P2
C WRITE(6,63)
C WRITE(6,66)
C READ(5,80) ILABEL,JLABEL,KLABEL
C I=1
C
C DRAW Y AXIS
C
C DO 11 J=1,101
11 LINE(J)=DOT
C WRITE(6,64) LINE
C
C CALCULATE THE PERCENT COMPOSITION FOR A GIVEN PH
C
C PH(I)=2.0
1 H(I)=10.0*(-PH(I))
D=1.0+Z3*H(I)+Z3*Z4*H(I)**2
A=D*P1+D*P1*P2/H(I)
B=D+(TM-TL)*(P1+P2*P1/H(I))
LH2=(-B+SQRT(B**2+4.0*TL*A))/(2.0*A)
M=TM/(1.0+P1*LH2+P2*P1*LH2/H(I))
MLH2=P1*M*LH2
MLH=P2*P1*M*LH2/H(I)
PM(I,1)=M*100.0/TM
PM(I,2)=MLH2*100.0/TM
PM(I,3)=MLH*100.0/TM
C
C CONVERSION TO FIXED POINT MODE ---- PLOT ONE LINE OF DATA
C
C DO 13 L=1,3
C Z(L)=PM(I,L)
C N(L)=Z(L)
C IF((Z(L)-N(L)).GE.0.50) GO TO 7
C GO TO 13
7 N(L)=N(L)+1
13 CONTINUE
C DO 12 K=1,101
12 LINE(K)=BLANK
C DO 14 J=1,3
C IF(N(J).GT.100) GO TO 15
C GO TO 14
15 N(J)=99
14 CONTINUE
C LINE(N(1)+1)=X
C LINE(N(2)+1)=AST
C LINE(N(3)+1)=PLUS
C LINE(1)=DOT

```

```

WRITE(6,65) PH(I),LINE
C
IF(I-KODE) 3,4,4
3 I=I+1
  PH(I)=PH(I-1)+.02
  GO TO 1
4 WRITE(6,78)
C
C PUT OUT PERCENTAGE CONCENTRATION DATA
C
DO 6 I=1,KODE
  Y1(I)=PM(I,1)
  Y2(I)=PM(I,2)
  Y3(I)=PM(I,3)
6 WRITE(6,74) PH(I),Y1(I),Y2(I),Y3(I)
C
PUNCH OUTPUT FOR IBM 1620/27 PLOTTER USING PLOTA
C
CALL AINIT(1000)
CALL AORIG(200,200)
CALL AGRID(0,0,30,10,20,50,1,3)
CALL ASCA(-45,-20,200,0,2,1,4,1,2)
CALL ASCA(-60,-5,0,50,0,10,11,1,2)
CALL ALAB(200,-50,ILABEL,11,1,2)
CALL ALAB(-50,100,JLABEL,33,1,4)
CALL ALAB(60,510,KLABEL,54,1,2)
CALL ALINEX(0,4,Y1,KODE,0.0,20.0)
CALL ALINEX(0,4,Y2,KODE,0.0,20.0)
CALL ALINEX(0,4,Y3,KODE,0.0,20.0)
CALL AEND
IF(NKODE.LE.NK) GO TO 31
GO TO 2
31 STOP
61 FORMAT('1 IONIC STRENGTH IS ',F10.2,5X,'TITRATION NUMBER IS ',I2
1/'E TOTAL LIGAND CONCENTRATION IS ',E10.3/'E TOTAL METAL CONCENTR
2ATION IS ',E10.3)
62 FORMAT('0' 2(E11.4,3X),10X,'LIGAND PROTONATION')
63 FORMAT('0' PERCENTAGE OF SPECIES IN S
1OLUTION ')
64 FORMAT('0'10X,101A1)
65 FORMAT('0' 4X,F5.2,1X,101A1)
66 FORMAT('0' 0 10 20 30 100 40
1 50 60 70 80 90
67 FORMAT('0 CONSTANTS'/'0 K4 K3')
72 FORMAT(4(E10.3))
73 FORMAT( 2(E10.3),8X,I2,F10.2,7X,I3)
74 FORMAT('0' 3X,F10.3,4X,E13.5,4X,E13.5,4X,E13.5)
75 FORMAT('0' p1 p2)
76 FORMAT('0' 2(E10.4,3X),10X,'METAL LIGAND FORMATION')
78 FORMAT('0' PH M MLH2 MLH ')
79 FORMAT(I2)
80 FORMAT(11A1/33A1/54A1)
END

```

# THERM

```

C   TO CALCULATE THE COMPOSITION OF THE CALORIMETER SOLUTION FOR
C   HEXAMETHYL323TETRAMINE PROTONATION REACTION USING NEWTON RAPSON
C   METHOD
C   DIMENSION YO(50),SIGYO(50),R(50),S(50),T(50),U(50)
C   J=0
801  J=J+1
    READ(5,68) ISENT,YO(J),SIGYO(J)
    IF(ISENT)801,801,1101
1101 ND=J-1
C   ENTER PRELIM TO CALCULATE SOLUTION COMPOSITION
C   CALL PRELIM(YO,R,S,T,U)
C   PUT OUT CHANGES IN CONCENTRATION OF SPECIES
    WRITE(6,75)
    WRITE(6,76)
C   PUNCH OUTPUT FOR THE LEAST SQUARES PROGRAM THERM(ADAPTED ORGLS)
C   DO 100 I=1,ND
    WRITE(7,69) YO(I),R(I),S(I),T(I),U(I)
100  WRITE(6,77) R(I),S(I),T(I),U(I)
    77  FORMAT('0',4(F9.5,5X))
    75  FORMAT('// '0 CHANGES IN COMPOSITION BETWEEN ADJACENT TITRATION POIN
    ITS (IN MMOLES)')
    76  FORMAT('0',R(LH)          S(LH2)          T(LH3)          U(LH4) ')
    68  FORMAT(11,F9.3,F10.2)
    69  FORMAT(F10.3,4(F10.6))
    END

SUBROUTINE PRELIM(YO,R,S,T,U)
C   TO CALCULATE THE CHANGES IN THE SOLUTION COMPOSITION
C   REAL K1,K2,K3,K4,KW,NBAR,L
    REAL LH(50),LH2(50),LH3(50),LH4(50),FL(50)
    DIMENSION PH(50),VOL(50)
    DIMENSION R(50),S(50),T(50),U(50),OH(50),YO(50)
    READ(5,41) K1,K2,K3,K4,KW,DELHH
    WRITE(6,51)
    WRITE(6,52) K1,K2,K3,K4
    WRITE(6,46)
    INTE=1
    NM=0
    READ(5,37) KODE
2    READ(5,38) NO
    READ(5,40) ACID,TL,THI
    WRITE(6,50) ACID,TL
    READ(5,35) (VOL(J),PH(J),J=1,NO)
    BETA1=K1
    BETA2=K2*K1
    BETA3=K3*K2*K1
    BETA4=K4*K3*K2*K1
    DO 11 I=1,NO
    TVOL=98.84+VOL(I)
    Q=98.84/TVOL
    H=10.**(-PH(I))
    N=1
    ACIDA=THI*Q
    TH=ACID*VOL(I)/(98.84+VOL(I))+ACIDA
    YH=H
    B=BETA3+4.*TL*Q*BETA4-TH*BETA4
    C=3.*TL*Q*BETA3-KW*BETA4+BETA2-TH*BETA3
    D=2.*TL*Q*BETA2-KW*BETA3+BETA1-TH*BETA2

```

```

E=BETA1*TL*Q-KW*BETA2+1.-TH*BETA1
F=-KW*BETA1-TH
C
C CALCULATE AN IMPROVED VALUE FOR H
C
7 FX=BETA4*YH**6+B*YH**5+C*YH**4+D*YH**3+E*YH**2+F*YH-KW
FXP=6.*BETA4*YH**5+5.*B*YH**4+4.*C*YH**3+3.*D*YH**2+2.*E*YH+F
XH=YH-FX/FXP
IF(XH) 8,8,9
9 PYH=-ALOG10(YH)
PXH=-ALOG10(XH)
G=PXH-PYH
IF(ABS(G)-0.0005) 5,5,6
6 N=N+1
YH=XH
GO TO 7
4 WRITE(6,45) N,PYH,PXH
GO TO 11
8 WRITE(6,42) N,I
GO TO 11
C
C CALCULATE THE SOLUTION COMPOSITION(IN MMOLES) FROM THE REFINED PH
C
5 H=XH
OH(I)=TVOL*KW/H
NBAR=(TH-H+KW/H)/(TL*Q)
L=TL*Q/(1.+BETA1*H+BETA2*H**2+BETA3*H**3+BETA4*H**4)
FL(I)=TVOL*L
LH(I)=TVOL*BETA1*L*H
LH2(I)=TVOL*BETA2*L*H**2
LH3(I)=TVOL*BETA3*L*H**3
LH4(I)=TVOL*BETA4*L*H**4
WRITE(6,47) VOL(I),PXH,NBAR,FL(I),LH(I),LH2(I),LH3(I),LH4(I),N
11 CONTINUE
C
C CALCULATION OF THE CHANGE IN COMPOSITION( IN MMOLES)
C AND APPLY HYDROLYSIS CORRECTION TO Y0
C
NN=NO-1
DO 12 J=1,NN
L=NM+J
CORR=(OH(J+1)-OH(J))*DELHH
Y0(L)=Y0(L)+CORR
R(L)=FL(J)-FL(J+1)
S(L)=LH(J)+R(L)-LH(J+1)
T(L)=S(L)+LH2(J)-LH2(J+1)
12 U(L)=LH4(J+1)-LH4(J)
NM=NN+NM
INTE=INTE+1
IF(INTE,LE,KODE) GO TO 2
CONTINUE
36 FORMAT(2(F10.3))
38 FORMAT(I2)
37 FORMAT(I2)
40 FORMAT(F10.4,2(E10.3))
41 FORMAT(5(E10.3),F10.2)
42 FORMAT('0 THE SOLUTION IS NEGATIVE OR ZERO FOR CYCLE NUMBER',I2 '
1 FOR DATA POINT NUMBER ',I2)
45 FORMAT('0 NO CONVERGENCE WITHIN',I2,'CYCLES. VALUE OF PH ON PENUL
1 TIMATE CYCLE=',F7.3,' VALUE ON LAST CYCLE=',F7.3)
46 FORMAT('0 COMPOSITION(IN MMOLES) OF CALORIMETER SOLUTION AS A FUN
1 CTION OF VOLUME AND PH'//0 VOL HCL CAL PH CAL NBAR L
2 LH LH2 LH3 LH4 NO OF CYCLES')
47 FORMAT('0' F6.3,3X,F7.3,3X,F6.3,2X,5(F7.5,3X),3X,I2)
50 FORMAT('0 CONCENTRATION OF TITRANT ACID =',F6.4/'0' 'TOTAL LIGAND
1 CONCENTRATION =',E10.4)
51 FORMAT('0 K1 K2 K3 K4')
52 FORMAT('0' 4(E10.4,3X))
RETURN
END

```

# CUTHERM

```

C *****
C *
C *   CALCULATION OF THE CHANGE IN COMPOSITION IN THE COPPER
C * 323TETRAMINE CALORIMETRIC TITRATION
C *   TITRATION OF COPPER COMPLEX WITH ACID
C *
C *****
REAL M,L,K1,K2,K3,K4,MLI
REAL LSAVE
REAL LH(30),LH2(30),LH3(30),LH4(30),ML(30),MHL(30)
DIMENSION VOL(30),PH(30),OH(30),FL(30)
DIMENSION TITLE(18)
DIMENSION YO(30)
READ(5,74) NKODE
INTE=1

C READ INPUT DATA ----- LIGAND PROTONATION CONSTANTS K,
C COPPER/LIGAND STAB. CONST. P, LIGAND ENTHALPIES OF PROTONATION
C DELH, TITRANT ACID CONCENTRATION ACID, CONC. OF COMPLEX MLI,
C CUMULATIVE VOLUME INCREMENT VOL, APPROX. SOLUTION PH PH,
C THE OBSERVED HEAT CHANGE YO, NUMBER OF TITRATION POINTS NO -----
C
READ(5,71) K1,K2,K3,K4,P1,P2
WRITE(6,72) K1,K2,K3,K4
WRITE(6,73) P1,P2
READ(5,69) DELH1,DELH2,DELH3,DELH4,DELH5
READ(5,90) DELH5
WRITE(6,68) DELH1,DELH2,DELH3,DELH4
1 READ(5,83) (TITLE(I),I=1,18)
WRITE(6,84) (TITLE(I),I=1,18)
READ(5,70) ACID,MLI
WRITE(6,82) ACID,MLI
READ(5,74) NO
NM=NO-1
DO 3 J=1,NO
3 READ(5,75) VOL(J),PH(J)
READ(5,85) (YO(I),I=1,NM)
BETA1=K1
BETA2=K2*K1
BETA3=K3*K2*K1
BETA4=K4*K3*K2*K1
WRITE(6,80)
WRITE(6,79)
DO 11 I=1,NO
TVOL=98.84+VOL(I)
Q=98.84/TVOL
H=10.**(-PH(I))
TH=ACID*VOL(I)/TVOL
TM=MLI*Q
TL=MLI*Q
HSAVE=H
KODE=1
NN=0
LSAVE=0.0
N=1

C SOLVE FOR L AND M FROM THE GIVEN VALUE OF H
C
C J=1
6 B1=1.+BETA1*H+BETA2*H**2+BETA3*H**3+BETA4*H**4
A1=B1+P1*(TM-TL)+P2*K1*H*(TM-TL)
C1=(P1+P2*K1*H)*B1
L=(-A1+SQRT(A1**2+4.*C1*TL))/(2.*C1)
M=TM/(1.+P1*L+P2*K1*H*L)
IF(ABS(L-LSAVE).LE.0.0005*L) GO TO 12
CMHL=P2*M*H*K1*L
LSAVE=L

C CALCULATE AN IMPROVED VALUE FOR H
C
C

```

```

A=4.*BETA4*L
B=3.*BETA3*L
C=2.*BETA2*L
D=1.*BETA1*L+P2*BETA1*M*L
14 FX=A*H**4+B*H**3+C*H**2+D*H-TH
FXP=4.*A*H**3+3.*B*H**2+2.*C*H+D
XH=H-FX/FXP
C
C TEST FOR CONVERGENCE
C
IF(XH) 8,8,9
9 PPH=-ALOG10(H)
PXH=-ALOG10(XH)
G=ABS(PXH-PPH)
IF(G.LE,0.0003) GO TO 5
N=N+1
IF(N.GE,60) GO TO 4
H=XH
GO TO 14
5 H=XH
NN=NN+1
IF(NN-50) 6,15,15
15 WRITE(6,91) LSAVE,L
GO TO 11
C
C CALCULATE THE SOLUTION COMPOSITION FROM REFINED VALUES OF H,L ANDM
C
12 OH(I)=TVOL*1.6374E-14/H
FL(I)=TVOL*L
LH(I)=TVOL*BETA1*L*H
LH2(I)=TVOL*BETA2*L*H**2
LH3(I)=TVOL*BETA3*L*H**3
LH4(I)=TVOL*BETA4*L*H**4
ML(I)=P1*M*L*TVOL
MHL(I)=CMHL*TVOL
WRITE(6,77) VOL(I),PXH,FL(I),LH(I),LH2(I),LH3(I),LH4(I),ML(I),MHL(
11),N
GO TO 11
2 PXH=-ALOG10(H)
GO TO 12
4 WRITE(6,45) N,PPH,PXH
GO TO 11
8 IF(KODE.EQ,0) GO TO 10
H=HSAVE+0.50*HSAVE
J=J+1
IF(J.LE,20) GO TO 6
KODE=0
J=1
10 H=HSAVE-0.50*HSAVE
J=J+1
IF(J.LE,20) GO TO 6
WRITE(6,76) I
11 CONTINUE
C
C CALCULATION OF THE CHANGE IN COMPOSITION BETWEEN SUCCESSIVE
C TITRATION POINTS --- ALSO APPLY CORRECTIONS TO Y0
C
WRITE(6,81)
WRITE(6,87)
DO 13 J=1,NM
C HCORR IS THE HYDROLYSIS CORRECTION FOR Y0
HCCORR=(OH(J)-OH(J+1))*DELHH
R=ML(J)-ML(J+1)
S=MHL(J)-MHL(J+1)
CORR1=R+FL(J)-FL(J+1)
CORR2=LH(J)+CORR1-LH(J+1)+S
CORR3=CORR2+LH2(J)-LH2(J+1)
CORR4=CORR3+LH3(J)-LH3(J+1)
Y0(J)=Y0(J)-CORR1*DELH1-CORR2*DELH2-CORR3*DELH3-CORR4*DELH4-HCCORR
YPL=Y0(J)/R

```

```

XPL=S/R
C
C PUNCH OUTPUT FOR THE ADAPTED LEAST SQUARES PROGRAM ORGLS
C
WRITE(7,93) YO(J),R,S
13 WRITE(6,86) YO(J),H CORR,CORR1,CORR2,CORR3,CORR4,R,S,YPL,XPL
  INTE=INTE+1
  IF(INTE.LE.NKODE) GO TO 1
  STOP
45 FORMAT('0 NO CONVERGENCE WITHIN',I2,'CYCLES. VALUE OF PH ON PENUL
  TIMATE CYCLE=',F7.3,' VALUE ON LAST CYCLE=',F7.3)
68 FORMAT('0 ENTHALPY OF PROTONATION OF 323TETRAMINE '/'0 DELH1
  1 DELH2 DELH3 DELH4 '/'0' 4(F5.2,8X))
69 FORMAT(5(F10.2))
70 FORMAT(F10.4,E10.3)
71 FORMAT(6(E10.3))
72 FORMAT('1 PK'S FOR THE LIGAND ARE ',4(E11.4,3X))
73 FORMAT('0 STABILITY CONSTANTS FOR THE TWO METAL COMPLEXES ARE ',
  12(E11.4,3X))
74 FORMAT(I2)
75 FORMAT(2(F10.3),2(F10.2))
76 FORMAT('0 A NEGATIVE OR ZERO SOLUTION WAS FOUND FOR DATA POINT ',
  1I2)
77 FORMAT('0' F5.3,3X,F8.4,3X,7(F8.6,3X),3X,I2)
79 FORMAT('0 VOLUME CAL PH L LH LH2 LH3
  1 L4 ML MHL NO OF CYCLES')
80 FORMAT('0 COMPOSITION(IN MMOLES) AT EACH TITRATION POINT ')
81 FORMAT('0 CHANGE IN COMPOSITION(IN MMOLES) BETWEEN SUCCESSIVE T
  1ITRATION POINTS')
82 FORMAT('0 TITRANT ACID CONCENTRATION =',F7.4,' INITIAL CONCENTRA
  1TION OF COMPLEX=',E10.4)
83 FORMAT(18A4)
84 FORMAT('0' 18A4)
85 FORMAT(F10.3)
86 FORMAT('0' F6.3,3X,F6.3,3X,6(F9.6,3X),F8.3,3X,F8.4)
87 FORMAT('0' YO HYD CORR CORR(LH) CORR(LH2) CORR(LH3)
  1 CORR(LH4) R(ML) S(MHL) YO/R S/R ')
88 FORMAT(' ' 4(E11.4,5X))
90 FORMAT(F10.2)
91 FORMAT('0 NO CONVERGENCE FOR L---- LAST VALUES OF L WERE ',2(E1
  11.4,3X))
92 FORMAT('0' 20X,E11.4)
93 FORMAT(F10.3,2(F10.6))
  END

```



# APPENDIX E

p[H<sup>+</sup>] titration<sup>a</sup> and log K<sub>n</sub> data for the formation  
of copper/3,2,3-tet complexes

I = 0.20M		I = 0.150M		I = 0.04M	
Vol.	p[H <sup>+</sup> ] <sup>b</sup>	Vol.	p[H <sup>+</sup> ]	Vol.	p[H <sup>+</sup> ]
0.130	3.593	0.100	3.141	0.100	3.120
0.135	3.638	0.110	3.300	0.120	3.373
0.140	3.671	0.120	3.460	0.130	3.461
0.145	3.705	0.130	3.573	0.135	3.495
0.150	3.732	0.140	3.648	0.140	3.526
0.155	3.760	0.150	3.703	0.145	3.551
0.160	3.782	0.155	3.729	0.150	3.579
0.170	3.830	0.160	3.753	0.155	3.601
0.180	3.870	0.170	3.800	0.160	3.624
0.190	3.909	0.180	3.840	0.170	3.665
0.200	3.950	0.190	3.880	0.180	3.704
0.210	3.990	0.200	3.918	0.190	3.746
0.220	4.034	0.210	3.958	0.200	3.785
0.230	4.081	0.215	3.981	0.210	3.824
0.240	4.134	0.220	4.002	0.220	3.865
0.250	4.195	0.230	4.050	0.230	3.912
0.260	4.269	0.240	4.100	0.240	3.960
0.270	4.360	0.245	4.129	0.250	4.021
0.280	4.499	0.250	4.160	0.260	4.093
		0.260	4.232	0.270	4.190
		0.270	4.323	0.275	4.250
		0.280	4.460	0.280	4.326
		0.290	4.723	0.290	4.615

<sup>a</sup> Solution composition: I = 0.20, 0.15, 0.04M, T<sub>L</sub> = 1.103x10<sup>-3</sup>M, T<sub>M</sub> = 1.082x10<sup>-3</sup>M, T<sub>H</sub> = 7.753x10<sup>-3</sup>M, titrant [NaOH] = 1.269M, initial volume = 49.90ml.

<sup>b</sup> p[H<sup>+</sup>] data obtained as described in Chapter 3.

<u>Ionic strength (M/l)</u>	<u>log K<sub>1</sub></u>	<u>log K<sub>2</sub></u>
0.20	21.81 ± 0.05	14.80 ± 0.07
0.15	21.69 ± 0.05	14.73 ± 0.07
0.04	21.53 ± 0.05	14.50 ± 0.07
0.00	21.22 <sup>a</sup> ± 0.1	14.18 <sup>b</sup> ± 0.1

<sup>a</sup> From a plot of log K<sub>1</sub> - 1√I/(1+√I) vs. I <sup>b</sup>  
from a plot of log K<sub>2</sub> - 2√I/(1+√I) vs. I.

APPENDIX F

Heat of dilution<sup>c</sup> of copper chloride

<u>Vol.</u> <sup>a</sup>	<u>CuCl<sub>2</sub></u> <sup>b</sup>	<u>Q</u>	<u><math>\Delta H_{dil}</math></u>	<u>ca. mole ratio</u> <sup>d</sup>
(ml)	(mmol)	(J)	(kJmol <sup>-1</sup> )	
0.400	.23944	1.234	5.1 <sub>5</sub>	1:23,100
0.400	.23944	1.214	5.0 <sub>7</sub>	1:23,100
0.480	.28733	1.445	5.0 <sub>3</sub>	1:19,400
0.450	.26937	1.356	5.0 <sub>3</sub>	1:20,800
0.350	.20951	1.026	4.9 <sub>0</sub>	1:27,000
0.350	.20951	1.007	4.8 <sub>1</sub>	1:27,000

<sup>a</sup> Volume of 0.5986M CuCl<sub>2</sub> added to 0.1M NaCl.

<sup>b</sup> Number of mmoles of titrant added.

<sup>c</sup> Reproducibility of  $Q_H/\Delta R$ ,  $Q_H \sim 1.7J$  was  $\pm 2\%$ .

<sup>d</sup> Mole ratio of CuCl<sub>2</sub>:H<sub>2</sub>O.

## REFERENCES

1. N.F. Curtis, Y.M. Curtis and H.K.J. Powell, J. Chem. Soc. (A), 1015 (1966).
2. J.L. Love and H.K.J. Powell, Chem. Commun., 39 (1968).
3. M.W. Morgan, B.Sc.(Hons) report, University of Canterbury (1968).
4. M. Burgess and H.K.J. Powell, unpublished work, University of Canterbury.
5. L.G. Sillén and A.E. Martell, "Stability Constants", Chem. Soc. spec. Publs. No.17 and No.25 (Chemical Society: London, 1964 and 1971).
6. C.V. Banks and S. Anderson, Inorg. Chem., 2, 112 (1963).
7. C.V. Banks, Record of Chem. Prog., 25, 85 (1964).
8. J.C. Wang, J.E. Bauman, Jr., and R.K. Murmann, J. Phys. Chem., 68, 2296 (1964).
9. R.M. Izatt, W.C. Fernelius and B.P. Block, J. Phys. Chem., 59, 235 (1955).
10. M. Honda and G. Schwarzenbach, Helv. Chim. Acta, 40, 27 (1957).
11. D.F. Martin, G.A. Janusonis and B.B. Martin, J. Amer. Chem. Soc. 83, 73 (1961).
12. G.W. Everett, Jr., and R.H. Holm, Inorg. Chem., 7, 776 (1968).

13. J. Bjerrum, "Metal Ammine Formation in Aqueous Solution", Hasse, Copenhagen (1957).
14. P. Teyssié, G. Anderegg and G. Schwarzenbach, Bull. Soc. chim. belges, 71, 177 (1962).
15. D.C. Weatherburn, E.J. Billo, J.P. Jones and D.W. Margerum, Inorg. Chem., 9, 1557 (1970).
16. L. Sacconi, P. Paoletti and M. Ciampolini, J. Chem. Soc., 5115 (1961).
17. F.J.C. Rossotti and H. Rossotti, "The Determination of Stability Constants", McGraw Hill Book Co. Inc., London, 1961, p.1.
18. R.G. Bates, "Determination of pH Theory and Practice", John Wiley and Sons Inc., New York, 1964, p.7.
19. R.A. Robinson and R.H. Stokes, "Electrolyte Solutions", Butterworths Pub. Ltd., 2nd Ed., 1959.
20. G.N. Lewis and M. Randall, J. Amer. Chem. Soc., 43, 1140 (1921).
21. G.H. Nancollas, "Interactions in Electrolyte Solutions", Elsevier Publishing Co., London, 1966, p.74.
22. Reference 17, p.32.
23. G.G. Manov, R.G. Bates, W.J. Hamer and S.F. Acree, J. Amer. Chem. Soc., 65, 1765 (1943).
24. Reference 17, p.33.
25. J.J. Christensen, R.M. Izatt and L.D. Hansen, Rev. Sci. Instr., 36, 779 (1965).

26. S. Johansson, Arkiv Kemi, 24, 189 (1965).
27. P. Gerding, I. Leden and S. Sunner, Acta Chem. Scand., 17, 2190 (1963) and references therein.
28. I. Wadsö, Acta Chem. Scand., 22, 927 (1968).
29. A. Vacca and P. Paoletti, J. Chem. Soc. (A), 2378 (1968).
30. H.J.V. Tyrrell and G.L. Hollis, Trans. Faraday Soc., 48, 893 (1952).
31. H.S. Harned and B.B. Owen, "The Physical Chemistry of Electrolytic Solutions", 2nd Ed., Am. Chem. Soc. Monograph Series, No. 95, Reinhold, New York, 1950, p.39.
32. J.J. Christensen and R.M. Izatt in "Physical Methods in Advanced Inorganic Chemistry", (Eds., H.A.O. Hill and P. Day), Interscience, New York, 1968, p.546.
33. S.J. Ashcroft and C.T. Mortimer, "Thermochemistry of Transition Metal Complexes", Academic Press, London, 1970, p.9.
34. J. Konicek and I. Wadsö, Acta Chem. Scand., 25, 1541 (1971).
35. F.J.C. Rossotti in "Modern Coordination Chemistry", (Eds., J. Lewis and R.G. Wilkins), Interscience Pub. Inc., New York, 1960, p.17.
36. R.W. Gurney, "Ionic Processes in Solution", McGraw-Hill, New York, 1953.

37. A.E. Martell in "Werner Centennial", Advances in Chemistry, Series 62, Amer. Chem. Soc. Pub., 1967, p.275.
38. A.W.J. Adamson, J. Amer. Chem. Soc., 76, 1578 (1954).
39. Reference 33, p.5.
40. F.A. Cotton and G. Wilkinson, "Advanced Inorganic Chemistry", 2nd Ed., William Clowes and Sons Ltd, London, 1966, p.664.
41. Reference 21, p.124.
42. Reference 33, p.7.
43. A.I. Vogel, "A Textbook of Quantitative Inorganic Analysis", Longmans, London, 3rd Ed., 1962.
44. G. Schwarzenbach and H. Flaschka, "Complexometric Titrations", 2nd English Ed., Methuen and Co. Ltd, p.256.
45. Reference 18, p.124.
46. D.J. Alner, J.J. Creczek and A.G. Smeeth, J. Chem. Soc. (A), 1205 (1967).
47. Reference 43, p.200.
48. R.C. Weast ed., "Handbook of Chemistry and Physics", 48<sup>th</sup> Ed., Chemical Rubber Co., Cleveland, Ohio, 1967, p.D-131.
49. Reference 18, p.315.
50. Reference 18, p.316 and 333.
51. D.D. Perrin and I.G. Sayce, Chem. and Ind., 661 (1966).
52. H.J.V. Tyrell and A.E. Beezer, "Thermometric Titrimetry", Franklin Printing House, Hungary, 1968, p.19.

53. S. Sunner and I. Wadsö, Acta Chem. Scand., 13, 97 (1959).
54. Reference 52, p.24.
55. J.M. Sturtevant in "Technique of Organic Chemistry", Part I, "Physical Methods", Ed. A. Weissberger, Vol.I, p.523.
56. I. Grenthe, H. Ots and O. Ginstруп, Acta Chem. Scand., 24, 1067 (1970).
57. D.D. Wagman, W.H. Evans, V.B. Parker, I. Halow, S.M. Bailey and R.H. Schumm, "Selected Values of Chemical Thermodynamic Properties", NBS Technical Note 270-3, Jan. 1968.
58. L.D. Hansen and E.A. Lewis, J. Chem. Thermo., 3, 35 (1971), and references therein.
59. G. Ojelund and I. Wadsö, Acta Chem. Scand., 22, 2691 (1968).
60. Reference 48, p.F-4.
61. Reference 18, p.33-34.
62. Reference 18, p.31.
63. Reference 18, p.75.
64. R.G. Bates and E.A. Guggenheim, Pure Appl. Chem., 1, 163 (1960).
65. Reference 18, p.77.
66. C.W. Davies, "Ion Association", Butterworths, London, 1962, p.41.

67. H.S. Harned and F.C. Hickey, J. Amer. Chem. Soc., 59, 1284 (1937) and references therein.
68. D.H. Everett and B.R.W. Pinsent, Proc. Roy. Soc. (Lond.), A215, 416 (1952).
69. Reference 31, p.523.
70. Reference 18, p.87.
71. W.H. Beck, A.E. Bottom and A.K. Covington, Analyt. Chem., 40, 501 (1968).
72. Reference 18, p.76, 88-90.
73. W.A.E. McBryde, The Analyst, 94, 337 (1969).
74. Reference 31, p.578 and p.485.
75. N.I. Vilenkin, "Successive Approximations", Pergamon Press, Oxford, 1964.
76. H.S. Harned, J. Amer. Chem. Soc., 48, 329 (1926).
77. Reference 18, p.58.
78. I. Feldman, Analyt. Chem., 28, 1859 (1956).
79. Reference 19, 465.
80. Reference 18, p.60.
81. C.W. Childs, Inorg. Chem., 9, 2465 (1970).
82. A. Vacca and D. Arenare, J. Phys. Chem., 71, 1495 (1967).
83. W.A.E. McBryde, communication to H.K.J. Powell, 1971.
84. G. Schwarzenbach, E. Kampitsch and R. Steiner, Helv. Chim. Acta, 28, 828 (1945).



85. K.S. Rajan and A.E. Martell, J. Inorg. Nuclear Chem., 26, 789 (1964).
86. D.D. Perrin and C.W. Childs, J. Chem. Soc. (A), 1039 (1969).
87. H.K.J. Powell and N.F. Curtis, J. Chem. Soc. (B), 1205 (1966).
88. E.A. Guggenheim and J.C. Turgeon, Trans. Faraday Soc., 51, 747 (1955).
89. Reference 66, p.40.
90. J. Kielland, J. Amer. Chem. Soc., 59, 1675 (1937).
91. Reference 17, p.40.
92. B. Sen, Analyt. Chim. Acta, 27, 515 (1962).
93. K.H. Schrøder, Acta Chem. Scand., 20, 1401 (1966).
94. F.J.C. Rossotti and H.S. Rossotti, Acta Chem. Scand., 9, 1166 (1955).
95. Reference 17, p.110.
96. Scatchard quoted, J.T. Edsall, G. Felsenfeld, D.S. Goodman and F.R.N. Gurd, J. Amer. Chem. Soc., 76, 3054 (1954).
97. C.W. Childs, P.S. Hallman and D.D. Perrin, Talanta, 16, 629 (1969).
98. F.J.C. Rossotti, H.S. Rossotti and R.J. Whewell, J. Inorg. Nuclear Chem., 33, 2051 (1971) and references therein.

99. J.S. Rollet Ed., "Computing Methods in Crystallography", Pergamon Press, 1965.
100. P.C. Jurs, *Analyt. Chem.*, 42, 747 (1970).
101. Z.Z. Hugus in "Advances in the Chemistry of Coordination Compounds", Ed. S. Kirschner, 1961, p.388.
102. D.D. Perrin and I.G. Sayce, *J. Chem. Soc. (A)*, 82 (1967).
103. A. Vacca, D. Arenare and P. Paoletti, *Inorg. Chem.* 5, 1384 (1966).
104. L.G. Sillen, *Acta Chem. Scand.*, 16, 159 (1962); 18, 1085 (1965).
105. Reference 17, p.58.
106. P. Paoletti, F. Nuzzi and A. Vacca, *J. Chem. Soc. (A)*, 1385 (1966).
107. G.R. Hedwig, J.L. Love and H.K.J. Powell, *Austral. J. Chem.*, 23, 981 (1970).
108. S. Patai Ed., "The Chemistry of the Carbon-Nitrogen Double Bond", Interscience, 1970, p.235.
109. Reference 108, p.384.
110. W.Z. Heldt and L.G. Donaruma, *Org. Reactions*, 11, 1 (1960).
111. E. Lustig, *J. Phys. Chem.*, 65, 491 (1961).
112. A.C. Huitrig, D.B. Roll and J.R. De Boer, *J. Org. Chem.*, 32, 1661 (1967).

113. H. Saito and K. Nukada, J. Mol. Spectroscopy 18, 1 (1965) and references therein.
114. W.F. Trager and A.C. Huitrig, Tetrahedron Letters, 825 (1966).
115. R.K. Norris and S. Sternhell, Austral. J. Chem., 22, 935 (1969) and references therein.
116. Reference 108, p.390-392.
117. G.W. Wheland, "Advanced Organic Chemistry", 2nd Ed., J. Wiley, N.Y., 1949, p.344.
118. G.C. Pimentel and A.L. McClellan, "The Hydrogen Bond", Freeman and Co. Ltd., 1960.
119. R. Näsänen, M. Koskinen, L. Anttila, and M.L. Korvola, Suomen Kem., B39, 122 (1966).
120. R. Näsänen and P. Merilainen, Suomen Kem., B37, 1, 54 (1964).
121. P. Paoletti, R. Barbucci, A. Vacca and A. Dei, J. Chem. Soc. A, 310 (1971).
122. F. Basolo, R.K. Murmann and Y.T. Chen, J. Chem. Soc., 75, 1478 (1953).
123. J. Clark and D.D. Perrin, Quart. Rev., 18, 295 (1964).
124. J.J. Christensen, R.M. Izatt, D.P. Wrathall and L.D. Hansen, J. Chem. Soc. (A), 1212 (1969).
125. M.C. Cox, D.H. Everett, D.A. Landsman and R.J. Munn, J. Chem. Soc. (B), 1373 (1968).

126. A.G. Evans and S.D. Hamann, Trans. Faraday Soc., 47, 34 (1951) and references therein.
127. R. Barbucci, P. Paoletti and A. Vacca, J. Chem. Soc. (A), 2202 (1970).
128. C.D. Ritchie and W.F. Sager, "Progress in Physical Organic Chemistry", Vol.II Eds, S. Cohen, A. Streitwieser Jr. and R.W. Taft, Interscience, N.Y., 1964.
129. G. Schwarzenbach, "Electrostatic and Non-electrostatic Contributions to Ion Association in Solution", in Plenary Lectures, XII<sup>th</sup> International Conference on Coordination Chemistry, Sydney, 1969, Butterworths, London, 1969.
130. E.J. King, 'Acid-Base Equilibria', Pergamon Press, 1965, p.174.
131. A.K. Covington and P. Jones Ed., "Hydrogen-Bonded Solvent Systems", Taylor and Francis Ltd, 1968, p.5.
132. K.E. Jabalpurwala, K.A. Venkatachalam and M.B. Kabadi, J. Inorg. Nuclear Chem., 26, 1011 (1964).
133. P.J. Orenski and W.D. Closson, Tetrahedron Letters, 37, 3629 (1967).
134. C.V. Banks and A.B. Carlson, Analyt. Chim. Acta, 7, 291 (1952).
135. H. McConnell, J. Chem. Phys., 20, 700 (1952).
136. H. Irving, H.S. Rossotti and G. Harris, Analyst, 80, 83 (1955).

137. T. Davies, S.S. Singer and L.A.K. Stavely, J. Chem. Soc., 2304 (1954).
138. P. Paoletti, M. Ciampolini and A. Vacca, J. Phys. Chem., 67, 1065 (1963).
139. P. Paoletti, J.H. Stern and A. Vacca, J. Phys. Chem., 69, 3759 (1965).
140. A.F. Trotman-Dickenson, J. Chem. Soc., 1293 (1949).
141. G.C. Levey, J.D. Cargioli and W. Racela, J. Amer. Chem. Soc., 92, 6238 (1970).
142. G.A. Olah, M. Calin and D.H. O'Brien, J. Amer. Chem. Soc., 89, 3586 (1967).
143. N.H. Cromwell, Chem. Rev., 38, 83 (1946).
144. S. Nagakura, A. Moniyeshi and K. Stanfield, J. Amer. Chem. Soc., 79, 1035 (1957).
145. J. Zabicky Ed., "The Chemistry of the Carbonyl Group", Vol. 2, Interscience, 1970, chapter 3.
146. G. Schwarzenbach, Helv. Chim. Acta, 33, 947 (1950).
147. I. Poulsen and J. Bjerrum, Acta Chem. Scand., 9, 1407 (1955).
148. P. Paoletti, S. Biagini and M. Cannas, Chem. Commun., 513 (1969).
149. S. Biagini and M. Cannas, J. Chem. Soc. (A), 2398 (1970).
150. B. Bosnich, R.D. Gillard, E.D. McKenzie and G.A. Webb, J. Chem. Soc., (A), 1331 (1966).

151. R.D. Gillard and H.M. Irving, Chem. Rev., 65, 603 (1965).
152. G. Degisher and G.H. Nancollas, J. Chem. Soc. (A), 1125 (1970).
153. G. Anderegg, Helv. Chim. Acta, 51, 1856 (1968).
154. I.M. Procter, B.J. Hathaway and P. Nicholls, J. Chem. Soc. (A), 1678 (1968).
155. M.D. Alexander, P.C. Harrington and A. Van Heuvelen, J. Phys. Chem., 75, 3355 (1971).
156. G. Schwarzenbach, Helv. Chim. Acta, 33, 974 (1950).
157. R.C. Courtney, R.L. Gustafson, S. Chaberek, Jr., and A.E. Martell, J. Amer. Chem. Soc., 81, 519 (1959).
158. J.W. Fraser, M.Sc. Thesis, University of Canterbury, 1970.
159. Reference 17, p.400.
160. D.E. Williams, G. Wohlauser and R.E. Rundle, J. Amer. Chem. Soc., 81, 755 (1959).
161. S. Ahrland, in "Structure and Bonding", Springer-Verlag, N.Y., 1968, Vol. 5, p.118.
162. J. Bjerrum and E.J. Nielson, Acta Chem. Scand., 2, 297 (1948).
163. C.K. Jorgensen, Acta Chem. Scand., 10, 887 (1956).
164. C.K. Jorgensen, Acta Chem. Scand., 9, 1362 (1955).
165. R.D. Gillard and S.H. Laurie, J. Inorg. Nuclear Chem., 33, 947 (1971).

166. V. Gutman, Chem. in Brit., 7, 102 (1971).
167. R.P. Bell, "The Proton in Chemistry", Cornell University Press, Ithaca, N.Y., 1959, Chapter 4.
168. R.K. Murmann, J. Amer. Chem. Soc., 80, 4174 (1958).
169. R. Näsänen and P. Merilainen, Suomen Kem., B36, 97 (1963).
170. G.I.H. Hanania and D.H. Irvine, J. Chem. Soc., 2745 (1962).
171. G.I.H. Hanania and D.H. Irvine, J. Chem. Soc., 2750 (1962).
172. C.H. Liu and C.F. Liu, J. Amer. Chem. Soc. 83, 4169 (1961).
173. D.D. Perrin, J. Chem. Soc., 3189 (1960).
174. A.E. Martell, S. Chaberek Jr, R.C. Courtney, S. Westerbäck and H. Hyytiäinen, J. Amer. Soc., 79, 3036 (1957).
175. A. Vaciago and L. Zambonelli, J. Chem. Soc. (A), 218 (1970).
176. R. Beckett and B.F. Hoskins, J. Chem. Soc. Dalton, 291 (1972).
177. C.H. Liu and C.F. Liu, J. Amer. Chem. Soc. 83, 4167 (1961).
178. Reference 17, chapter 17.
179. F. Basolo and R.K. Murmann, J. Amer. Chem. Soc., 74, 2373 (1952); 74, 5243 (1952).

180. S. Patai Ed., "The Chemistry of the Carbonyl Group",  
Vol. I, Interscience, N.Y., 1966, p. 28.
181. G. Gran, Analyst, 77, 661 (1952).
182. F.J.C. Rossotti and H. Rossotti, J. Chem. Educ., 42,  
375 (1965).
183. Reference 99, p.33.
184. W.C. Hamilton, "Statistics in Physical Science",  
Ronald Press Co., N.Y., 1964, p.154.
185. Reference 99, p.20.
186. Reference 184, p.129.
187. A. Causer, "Plot A subroutines for the 1627 plotter",  
Memo. University of Canterbury Computer Centre, 1970.
188. W.R. Busing and H.A. Levy, "General Least Squares  
Program", ORNL-TM-271, Chemistry Division, Oak Ridge  
National Laboratory, Oak Ridge, Tennessee, 1962.